Polarimetry of Early Emission Line Stars

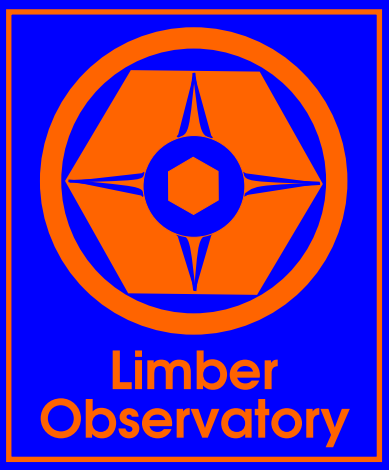

David McDavid

Polarimetry of Early Emission Line Stars

Polarimetrie van vroeg-type sterren met emissielijnen

Academisch Proefschrift

ter verkrijging van de graad van doctor
aan de Universiteit van Amsterdam,
op gezag van de Rector Magnificus
Prof. Dr. J.J.M. Franse,
ten overstaan van een door het college voor promoties ingestelde commissie,
in het openbaar te verdedigen in de Aula der Universiteit
op
dinsdag 29 mei 2001, te 10:00 uur

door

David Andrew McDavid
geboren te San Antonio, Texas, USA

Promotiecommissie:

Promotor:	prof. dr E.P.J. van den Heuvel	
Co-Promotor:	dr H.F. Henrichs	
Overige leden:	prof. dr M. Breger	Universität Wien, Oostenrijk
	prof. dr J.C. Brown	University of Glasgow, Schotland
	prof. dr J.W. Hovenier	Vrije Universiteit, UvA
	prof. dr A. Lagendijk	
	dr G.J. Savonije	
	dr J. Tinbergen	ASTRON/Universiteit Leiden
	prof. dr L.B.F.M. Waters	

Sterrenkundig Instituut "Anton Pannekoek"
Faculteit der Natuurwetenschappen, Wiskunde en Informatica
Universiteit van Amsterdam

ISBN 90-9014848-5

Proem:

> But leave the Wise to wrangle, and with me
> The Quarrel of the Universe let be:
> And, in some corner of the Hubbub coucht,
> Make Game of that which makes as much of Thee.

RUBÁIYÁT of Omar Khayyám

for my beloved Judy...

Contents

Chapter 1

Overview

1. Introduction and Background

A Be star is a non-supergiant B-type star whose spectrum has, or had at some time, one or more Balmer lines in emission (Collins 1987). The transition from a normal B-type absorption spectrum to a Be-type emission spectrum and back again on a time scale of years to decades is known as "the Be phenomenon". Beginning with the hypothesis of Struve (1931) it has been generally attributed to rotationally enhanced mass loss from the star leading to the formation of a circumstellar envelope in which the emission lines are produced, followed by a gradual dissipation of the envelope. However, the fundamental mechanism behind the process has remained a mystery from the first (visual) observation of the Hβ emission line in the spectrum of γ Cas (B0.5 IVe) (Secchi 1866) up to and including the present day.

The historical development of the field can be traced through the published proceedings of five IAU meetings devoted wholly or largely to Be stars (Slettebak 1976; Jaschek & Groth 1982; Slettebak & Snow 1987; Balona, Henrichs, & Le Contel 1994; Smith, Henrichs, & Fabregat 2000). Two general review articles by Slettebak (1979, 1988) and a detailed introduction (Underhill & Doazan 1982) are also recommended to the unfamiliar reader.

Figure 1 (Peters 1986) illustrates the difference between the B and Be phases at Hα, which is the most common spectral feature of interest. A more subtle mode of variability taking place within many of the emission line profiles which show a double peak during the Be phase is a change in the intensity ratio of the V (violet) to R (red) peaks which is sometimes quasi-cyclic, as shown in Figure 2 (Guo 1994).

About 10% of all non-supergiant B-type stars may be classified as Be stars, with a maximum of about 20% around B2 (Jaschek & Jaschek 1983) and dropping sharply toward earlier spectral types but including the analogous Oe stars (Frost & Conti 1978). The highest rotation rates of normal stars are also found among the early B stars. Although the maximum observed equatorial rotation velocities are less than 85% of the "critical" velocity for centrifugal force to balance gravity at the equator (Slettebak 1987), rapid rotation clearly plays an important role in the mass loss process. However,

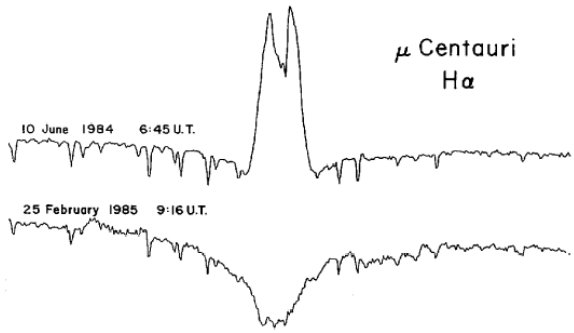

Fig. 1.— Hα line profiles showing the transition within 8 months from Be (emission) to B (absorption) phase for the Be star μ Cen (B2 IV-Ve) (Peters 1986).

a further triggering mechanism is apparently required, which has led to a bewildering variety of hypotheses including nonradial pulsation, radiatively driven winds, flarelike magnetic activity, and binary interaction. None of these has been demonstrably verified to work for all Be stars, but none of them can be excluded either. Interestingly, for two Be stars the outbursts have been found to be triggered by constructive interference of two nonradial pulsation modes (Rivinius et al. 1998; Tubbesing et al. 2000).

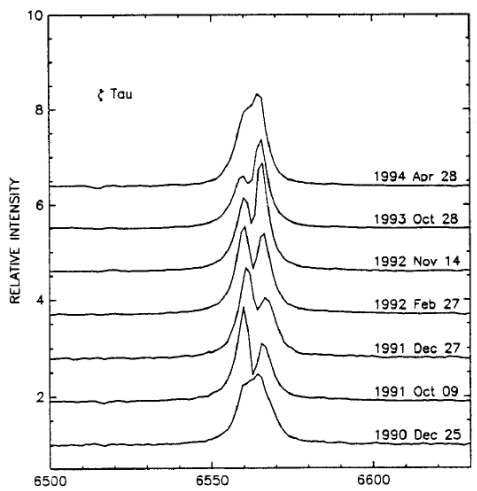

Fig. 2.— Hα line profiles showing the V/R variations of the Hα emission line of the Be star ζ Tau (B1 IVe-shell) (Guo 1994).

The intrinsic polarization of Be stars was discovered as soon as astronomical stellar polarimetry became an exact observational technique through the adaptation of polaroid analyzers to early photoelectric photometers. (See Shurcliff 1962, Gehrels 1974, Serkowski 1974, Tinbergen 1996, and Leroy 2000 for discussions of polarized light and the history of its applications in astronomy, including the development of astronom-

ical instrumentation for the measurement of polarization.) Although Be stars were included in the beginning surveys which led to the discovery of the Galactic interstellar polarization (Hiltner 1949, Hall 1949), the first evidence of their intrinsic polarization was the polarimetric variability observed by Behr (1959) and Coyne & Gehrels (1967). Serkowski (1968) called attention to the unusual wavelength dependence of the polarization of Be stars as additional evidence that it must be at least partially intrinsic. (The high ratio of blue to ultraviolet polarization was distinctly different from the normal pattern established by the earliest multiwavelength broad band *UBVRI* measurements.) The work of Poeckert, Bastien, & Landstreet (1979) is a good introduction to methods which have since been used to separate the intrinsic and interstellar components of the polarization, including results with various degrees of confidence for 70 stars.

The fact that the light from Be stars is up to 2% linearly polarized is strong evidence that some fundamental asymmetry is present. Coyne & Kruszewski (1969), Capps, Coyne, & Dyck (1973), and Gehrz, Hackwell, & Jones (1974) explained the intrinsic polarization as due to scattering of light from the central star by free electrons in the rotationally flattened equatorial circumstellar envelope or disk where the spectral emission lines originate, with the wavelength dependence being caused by neutral hydrogen opacity. If the plane of the disk is not perpendicular to the line of sight, the scattering region has an apparent asymmetry, leading to a net polarization at a position angle parallel to the projection of the stellar rotation axis onto the plane of the sky, which should be perpendicular to the direction of the apparent elongation of the disk. Thus the polarization and its wavelength dependence are still being studied very profitably as indicators of the density, temperature, and geometry of Be-star envelopes, and polarization observations are generally accepted as some of the strongest evidence that the envelopes must be equatorially flattened (or at least considerably asymmetric). An outstanding modern verification of the rotational flattening model is the interferometric imaging of the circumstellar disk of ζ Tau by Quirrenbach et al. (1994), as shown in Figure 3 below.

The basic disk model was quantified in analytical detail in a series of theoretical papers by Brown & McLean (1977), Brown, McLean, & Emslie (1978), McLean & Brown (1978), and McLean (1979). Poeckert & Marlborough (1978) produced a detailed model for the circumstellar envelope of γ Cas using a numerical approach to match observations of both the emission line profiles and the broad band polarization. Another series of theoretical papers (Brown & Fox 1989, Fox & Brown 1991, Fox 1991, and Fox 1994) addressed the depolarizing effect of the finite size of the star (see also Cassinelli, Norsieck, & Murison 1987 and Brown, Carlaw, & Cassinelli 1989) and the effect of occultation of the scattering disk by the star. An interesting theoretical discussion by Fox & Henrichs (1994) explored the possibility of polarimetric detection of clumps or condensations in the outflowing winds of early type stars. Such density enhancements might be expected to exist in correspondence with the discrete absorption components (DACs) commonly observed in the winds of early type stars by UV spectroscopy, but none have ever been clearly observed.

On the observational front, Coyne (1975) monitored the polarization of several Be stars over periods of five to eight years and found variability on a time scale of hundreds of days, with superimposed changes on a time scale of days. For stars with known radial velocity or binary light-curve variations, he found no correlations with the polarization. Huang, Hsu, & Guo (1989) closely monitored 14 Be stars for about six months with similar results, except for an indication of possible orbital periodicity in the polarization of the Be binary CX Dra (B4 IV(e)). A spectacular observation of short term changes in the polarization of a Be star was the outburst of ω Ori (B2 IIIe) (Hayes & Guinan 1984; Brown & Henrichs 1987; Sonneborn et al. 1988), in which the onset and decline of a major mass loss event were covered continuously over an interval of about 100 days.

Beginning with Clarke & McLean (1974), who used a tilted narrow band interference filter to scan the polarization across the Hβ lines of several bright Be stars, polarimetry of Be stars has been done with increasing spectral resolution in order to derive more detailed information about the envelope characteristics (Poeckert & Marlborough 1977). McLean et al. (1979) improved the technique of emission line scanning with a high resolution spectropolarimeter using a Digicon detector, which led to detailed maps of the velocity structure of Be disks, indicating a complicated combination of rotation and expansion. A low resolution optical spectropolarimeter (Nordsieck et al. 1992) has been in operation since 1989 to monitor the polarization of Be stars and to provide support for a similar space-based ultraviolet spectropolarimeter. Combining the data from these two instruments resulted in the discovery of an unexpected decrease in the polarization of Be stars in the near ultraviolet, which has been attributed to heavy circumstellar blanketing by Fe lines (Bjorkman et al. 1991).

Analysis of the modern spectropolarimetric observations requires more sophisticated theoretical treatments of polarization by electron scattering with neutral hydrogen opac-

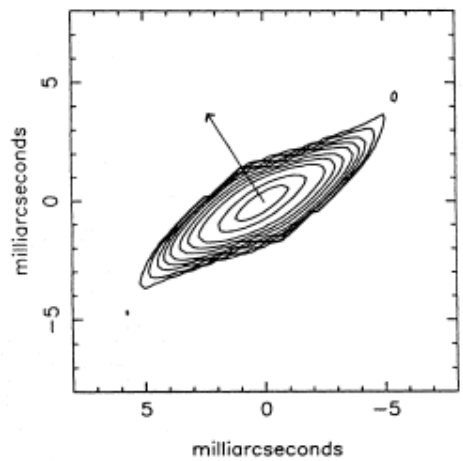

Fig. 3.— Maximum-entropy reconstruction of ζ Tau in the Hα emission line (Quirrenbach et al. 1994). The arrow indicates the position angle of the linear polarization.

ity. Hillier (1994) developed a numerical method to solve the polarized radiation transfer equation, while Wood, Bjorkman, Whitney, & Code (1996) applied a Monte Carlo computational scheme to simulate the polarization by tracing stellar photons in their interactive paths through the circumstellar envelope. Wood, Bjorkman, & Bjorkman (1997) were able to use their Monte Carlo code to model successfully the spectropolarimetry of ζ Tau, with the conclusion that the disk appears to be optically thick but geometrically thin, and the surprising discovery that multiple scattering actually increases the polarization over the degree predicted by the single scattering approximation.

2. Outline

This thesis is focused on the observational approach of continuum linear polarimetry to compile data characterizing the long term variability of a representative sample of Be stars which can be used together with other forms of observational data to constrain the changes in physical stellar and circumstellar parameters involved in the Be phenomenon.

The scientific results presented here cover about 15 years of continuous annual monitoring, which has considerable archival value in itself. Careful attention to detail in maintaining a consistent observational system has shown that significant variability in polarization on all time scales is far less common than was widely claimed at the time the project began. Some interesting cases of clearly variable polarization are only beginning to become apparent, while theoretical methods are being developed for the physical interpretation of the variability. Specifically, the correlation between variations in polarization and V/R variability in the Hα line profiles favors Keplerian rotation of the circumstellar disks, and parameters derived from the fitting of a model to the *UBVRI* wavelength dependence of the polarization gives evidence that Be disks are geometrically thin. These results may eventually be brought to bear on the disk formation process.

Chapter 2 describes the beginning of an observational program at The University of Texas McDonald Observatory, intended to document the long term changes in polarization of a representative sample of bright and well-studied Be stars corresponding to the growth and decay of their circumstellar envelopes in transitions from normal B to active Be phases and the reverse. A *UBVRI* filter system was chosen in order to make the best use of existing observations, which were mostly broad band. Comparison of the new measurements with the preceding 20 years of data taken from the literature revealed significant long term changes in ζ Tau and π Aqr (B1 III-IVe).

Chapter 3 summarizes the next four years of annual monitoring. It is primarily devoted to devising a statistical scheme to identify both night-to-night and year-to-year variability based on the small samples of data acquired in annual observing runs covering about one week each for summer and winter objects. Once again ζ Tau and π Aqr showed variable polarization on a time scale of years. However, no convincing evidence was found for short term night-to-night variations of any of the program stars.

Chapter 4 continues the annual monitoring program with a report on the next four years and a cumulative summary of all the data back to the beginning of the project. The only compelling case of variability was π Aqr, which had declined from nearly the highest polarization of any Be star to an almost completely unpolarized state over the full eight-year time period. The wavelength dependence of the polarization had become steadily weaker, as expected since neutral hydrogen absorption is proportional to the square of the electron density N_e^2 while electron scattering is proportional to N_e.

Chapter 5 serves to document the transfer of the monitoring project from McDonald Observatory, where the 0.9 m telescope was taken out of service, to the 0.4 m telescope at Limber Observatory, where a new polarimeter was custom-built to continue the program. A careful comparison of standard star measurements verified that the two instrumental systems are well matched. No variability was formally detected for any of the program stars over this four-year time period, but the colinear distribution of data points in cumulative Stokes parameter plots strongly suggests small but real changes in polarization for several of the stars being studied. A brief discussion is given for each individual star.

Chapter 6 explains a polarimetric test of the hypothesis that the commonly observed long term quasi-periodic cycles in the amplitude ratio of the V (violet, or blue) to the R (red) component of double-peaked emission line profiles in some Be stars are caused by a slowly precessing "one-armed" density perturbation in the circumstellar disk. We used numerically generated perturbation models for the line profile variations as input to a Monte Carlo electron scattering simulation to calculate the expected behavior of the polarization and found results consistent with the observations of two typical Be shell stars, ζ Tau and 48 Lib (B3:IV:e-shell). An important implication of this theory, if it is correct, is that the circumstellar disks of Be stars are in a state of Keplerian orbital motion.

Chapter 7 is devoted to a theoretical model for the approximate calculation of the polarization of Be stars, using a spherical sector geometry to represent the circumstellar disk. Details of the computational method are shown, with consideration of electron scattering, correction for the finite apparent size of the central star, wavelength dependence of the polarization due to absorption by neutral hydrogen in the disk, and convolution with the instrumental system, subject to the fundamental limiting aasumption that the disk is optically thin. Application of the model to observational data for eight Be stars gives good fits, and the results favor the idea that Be disks are geometrically thin.

Chapter 8 presents the polarimetry results from an extended series of coordinated multiwavelength campaigns undertaken to investigate short term variability of OB emission line stars, with emphasis on *IUE* UV and ground-based optical spectroscopy. A major goal of these campaigns was to observationally distinguish between two proposed models for variable mass loss: nonradial pulsations and photospheric active regions (spots). At the time the campaigns began, there was so much published evidence for short term polarization variations that the prospects for correlation with simultaneous spectro-

scopic variations seemed good. Surprisingly, however, no polarization variations could be independently identified out of the entire sample of eight Be stars and seven O stars. In some cases weak correspondence appears when the polarimetry data are matched against the observed spectroscopic cycles (see Chapter 9), so it is possible that there are polarization effects which are simply too small to measure with current instrumentation.

Chapter 9 concerns new survey polarimetry of a sample of bright emission line O stars, which in some respects are high luminosity counterparts of the Be stars. Most of the program stars were observed intensively for polarization along with UV and optical spectroscopy during a series of campaigns to investigate the origins of short term wind variability and mass loss (see thesis papers of Kaper (1993) and de Jong (2000)). Two stars, 68 Cyg (O7.5 III:n((f))) and ξ Per (O7.5 III(n)((f))), showed marginal correlations between polarization and Hα emission that are consistent with wind models based on the idea of corotating interaction regions. For the most part, though, it is demonstrated that the observed polarization may be readily accounted for as completely interstellar. Apparently the strong radiation-driven winds of O stars do not allow the formation of Be-type equatorial disks, even for the most rapid rotators.

Chapter 10 is a summary of this thesis written in the Dutch language.

Appendix A is a detailed description of AnyPol, a generic Glan prism photopolarimeter which was built in order to continue the monitoring program on the 0.4 m telescope at Limber Observatory after the 0.9 m telescope of McDonald Observatory was taken out of service. The design and construction of the polarimeter are explained by subsystem, including the physical and mechanical characteristics, the optical system, the electronics, and the computer control and data acquisition functions. Statistical analysis of standard star observations and comparison with the McDonald results validate the performance of the instrument.

Appendix B is a complete list of papers published in refereed journals by the author.

REFERENCES

Balona, L., Henrichs, H., & Le Contel, J.M. 1994, ed., IAU Symp. 162, Pulsation, Rotation and Mass Loss in Early-Type Stars (Dordrecht: Kluwer)

Behr, A. 1959, Nach. Akad. Wiss. Göttingen, 2, Math-Phys. Kl., No. 7, 185 (Veröff. Göttingen, No. 126)

Bjorkman, K.S., Nordsieck, K.H., Code, A.D., Anderson, C.M., Babler, B.L., Clayton, G.C., Magalhaes, A.M., Meade, M.R., Nook, M.A., Schulte-Ladbeck, R.E., Taylor, M., & Whitney, B.A. 1991, ApJ, 383, 67

Brown, J.C., Carlaw, V.A., & Cassinelli, J.P. 1989, ApJ, 344, 341

Brown, J.C. & Fox, G.K. 1989, ApJ, 347, 468

Brown, J.C. & Henrichs, H.F. 1987, A&A, 182, 107

Brown, J.C. & McLean, I. 1977, A&A, 57, 141

Brown, J.C., McLean, I.S., & Emslie, A.G. 1978, A&A, 68, 415

Capps, R.W., Coyne, G.V., & Dyck, H.M. 1973, ApJ, 184, 173

Cassinelli, J.P., Nordsieck, K.H., & Murison, M.A. 1987, ApJ, 317, 290

Clarke, D. & McLean, I.S. 1974, MNRAS, 167, 27

Collins, G.W., II 1987, in IAU Coll. 92, Physics of Be Stars, ed. Slettebak, A. & Snow, T.P. (Cambridge: Cambridge University Press), 5

Coyne, G.V. 1975, Specola Vatic. Ric. Astron., 8, 533

Coyne, G. V. & Gehrels, T. 1967, AJ, 72, 887

Coyne, G.V. & Kruszewski, A. 1969, AJ, 74, 1969

de Jong, J.A. 2000, Thesis, University of Amsterdam

Fox, G.K. 1991, ApJ, 379, 663

Fox, G.K. 1994, ApJ, 435, 372

Fox, G.K. & Brown, J.C. 1991, ApJ, 375, 300

Fox, G.K. & Henrichs, H.F. 1994, MNRAS, 266, 945

Frost, S.A. & Conti, P.S. 1978, in IAU Coll. 70, Be and Shell Stars, ed. Slettebak, A. (Dordrecht: Reidel), 139

Gehrels, T. 1974, ed., Planets, Stars and Nebulae Studied With Photopolarimetry (Tucson: Arizona University Press)

Gehrz, R.D., Hackwell, J.A., & Jones, T.W. 1974, ApJ, 191, 675

Guo, Y. 1994, IBVS 4112

Hall, J.S. 1949, Science, 109, 166

Hayes, D.P. & Guinan, E.F. 1984, ApJ, 279, 721

Hillier, D.J. 1994, A&A, 289, 492

Hiltner, W.A. 1949, Science, 109, 165

Huang, L., Hsu, J.C., & Guo, Z.H. 1989, A&AS, 78, 431

Jaschek, M., & Groth, H. 1982, ed., IAU Symp. 98, Be Stars (Dordrecht: Reidel)

Jaschek, C. & Jaschek, M. 1983, A&A, 117, 357

Kaper, L. 1993, Thesis, University of Amsterdam

Leroy, J. 2000, Polarization of Light and Astronomical Observation (London: Gordon and Breach)

McLean, I.S. 1979, MNRAS, 186, 265

McLean, I.S. & Brown, J.C. 1978, 69, 291

McLean, I.S., Coyne, G.V., Frecker, J.E., & Serkowski, K. 1979, ApJ, 228, 802

Nordsieck, K.H., Babler, B., Bjorkman, K.S., Meade, M.B., Schulte-Ladbeck, B.F., & Taylor, M.J. 1992, in Nonisotropic and Variable Outflows from Stars, ASP Conference Series, Vol. 22, ed. Drissen, L., Leitherer, C., & Nota, A. (San Francisco: ASP), 114

Peters, G.J. 1986, ApJ, 301, 61

Poeckert, R., Bastien, P., & Landstreet, J.D. 1979, AJ, 84, 812

Poeckert, R. & Marlborough, J.M. 1977, ApJ, 218, 220

Poeckert, R. & Marlborough, J.M. 1978, ApJ, 220, 940

Quirrenbach, A., Buscher, D.F., Mozurkewich, D., Hummel, C.A., & Armstrong, J.T. 1994, A&A, 283, 13

Rivinius, Th., Baade, D., Stefl, S., Stahl, O., Wolf, B., & Kaufer, A. 1998, A&A, 336, 177

Secchi, A. 1866, Astron. Nachr., 68, 63

Serkowski, K. 1968, ApJ, 154, 115

Serkowski, K. 1974, in Methods of Experimental Physics, Volume 12: Astrophysics (Part A) (New York: Academic Press), 361

Shurcliff, W.A. 1962, Polarized Light: Production and Use (Cambridge: Harvard University Press)

Slettebak, A. 1976, ed., IAU Symp. 70, Be and Shell Stars (Dordrecht: Reidel)

Slettebak, A. 1979, Space. Sci. Rev., 23, 541

Slettebak, A. 1987, in IAU Coll. 92, Physics of Be Stars, ed. Slettebak, A. & Snow, T.P. (Cambridge: Cambridge University Press), 24

Slettebak, A. 1988, PASP, 100, 770

Slettebak, A. & Snow, T.P. 1987, ed., IAU Coll. 92, Physics of Be Stars (Cambridge: Cambridge University Press)

Smith, M.A., Henrichs, H.F., & Fabregat, J. 2000, ed., IAU Coll. 175, The Be Phenomenon in Early-Type Stars (San Francisco: ASP), 384

Sonneborn, G., Grady, C.A., Wu, Chi-Chao, Hayes, D.P., Guinan, E.F., Barker, P.K., & Henrichs, H.F. 1988, ApJ, 325, 784

Struve, O. 1931, ApJ, 73, 94

Tinbergen, J. 1996, Astronomical Polarimetry (Cambridge: Cambridge University Press)

Tubbesing, S., Rivinius, Th., Wolf. B., & Kaufer, A. 2000, in IAU Coll. 175, The Be Phenomenon in Early-Type Stars, ed. Smith, M.A., Henrichs, H.F., & Fabregat, J. (San Francisco: ASP), 232

Underhill, A. & Doazan, V. 1982, Be Stars With and Without Emission Lines (Washington: NASA)

Wood, K., Bjorkman, K.S., & Bjorkman, J.E. 1997, ApJ, 477, 926

Wood, K., Bjorkman, J.E., Whitney, B.A., & Code, A.D. 1996, ApJ, 461, 828

Wood, K., Bjorkman, J.E., Whitney, B.A., & Code, A.D. 1996, ApJ, 461, 847

Chapter 2

Multicolor Polarimetry of Selected Be Stars: A Long Term Analysis

(originally published in 1986 PASP, 98, 572)

ABSTRACT

New observations of linear polarization in the *UBVRI* system for six bright northern Be stars are combined with existing measurements from two previous epochs in an analysis of long term variation over nearly two decades. No indication of large short term variability is found within the individual data sets, but ζ Tau and π Aqr have shown steady change on the longer time scale.

1. Introduction

The intrinsic polarization of Be stars was suspected in the course of early studies of interstellar polarization by University of Arizona astronomers (Coyne & Gehrels 1967; Coyne & Kruszewski 1969; hereinafter collectively CGK) when it became apparent that the wavelength dependence of the wide band optical linear polarization of many of them did not match the average interstellar pattern. The observed variability of the polarization with time over intervals of one to 30 days (Coyne 1976) provides additional evidence that it is at least partially intrinsic, since any interstellar component is expected to be constant. Several possible approaches to isolating the intrinsic component are exemplified by the work of Poeckert, Bastien, & Landstreet (1979, hereinafter PBL), who gave comprehensive results for 70 stars. The theory of scattering and absorption in an ionized hydrogen disk or envelope has been widely used to explain the origin of the polarization (McLean 1979), and recently developed high resolution scanning techniques have revealed variations of the polarization with wavelength in and around the hydrogen emission lines which may give clues to the details of the envelope and wind structure (Coyne & McLean 1982). Slettebak (1979) gives an excellent review and bibliography on the Be stars in general.

2. Observations

Stars for which complete data are available in both CGK and PBL were chosen for this analysis from a larger group currently being monitored. Observations denoted DM were made in December 1984 and May 1985 using the polarimeter described by Breger (1979) on the 36 inch (0.9 m) telescope of McDonald Observatory with a filter system specified in Table 1. A neutral density filter was used for all measurements in order to restrict the brightness to a tolerable level for the photomultiplier. Tables 2–7 give the mean and standard deviation of the polarization and position angle for at least three observations of each star over a period of about one week.

3. Discussion

The McDonald filter system and those of CGK and PBL as specified in Table 1 are far from identical, but they are close enough in effective wavelength and bandwidth to be useful for this study. The data in Tables 2–7 were compiled from the sets of repeated measurements published by CGK and PBL. If less than three measurements were available in a single filter, the average of the instrumental errors for all measurements in all filters for the same star was calculated as a reasonable estimate of the standard deviation σ_p in the percent polarization. An estimate of the accompanying standard deviation σ_θ in the position angle (exactly valid only for 1.00% polarization) was calculated from $\sigma_\theta = 28.^\circ65(\sigma_p)$.

The criterion for variability used by Coyne (1976) is a polarization change of more than 0.15%, justified as a value greater in general than three times the standard deviation of a single observation. Since the references CGK and PBL list probable errors of 0.05% for many of the single observations, and since this level of precision is also typical of the DM data, Coyne's criterion, although it might be considered conservative, can be quite reasonable applied here for the purpose of identifying large short term variability. McLean (1979) suggests that time variations leave the relative wavelength dependence of the polarization virtually unaltered, so any real variability should be present in all filters, although in somewhat different amounts. For these reasons the criterion $\sigma_A > 0.15\%$,

Table 1. Summary of Filter Systems

Observer	Bandwidth	Effective Wavelength (nm)				
		U	*B*	*V*	*R*	*I*
CGK	wide	360	425	515	650	840
PBL	intermediate	345	405	510	665	850
DM	wide	365	440	550	640	830

where σ_A is the average of σ_p over all filters, was chosen to test for variable polarization. As may be seen from Tables 2–7, no such variability appears for any star in the individual data of CGK, PBL, or DM. The existence of short term changes is certainly not ruled out by this analysis, but it is not verified at the 3 σ level.

The sections labeled AVERAGE in Tables 2–7 give the mean and standard deviation of the results of CGK, PBL, and DM for each of the program stars. Only ζ Tauri and π Aquarii show $\sigma_A > 0.15\%$ over the period of time spanned by these observations (almost two decades). Table 8 illustrates how the considerable variation in position angle for π Aqr disappears when the interstellar polarization given by PBL (maximum 0.46% at 498 nm with position angle 116°) is removed from the individual data sets by the method of Stokes vectors before averaging.

4. Conclusions

The data presented here document the presence of large and monotonic long-term changes in the polarization of two Be stars. Zeta Tau shows a gradual decrease, while π Aqr shows a rapid increase. It should be of interest to theoreticians to use these observations to test current hypotheses about the astrophysical processes involved.

I would like to thank the administration of McDonald Observatory for making observing time available for this project. I also thank Michel Breger for his comments on an early version of the manuscript, as well as an anonymous referee who made helpful suggestions.

REFERENCES

Breger, M. 1979, ApJ, 233, 97

Coyne, G.V. 1976, in IAU Symp. 70, Be and Shell Stars, ed. Slettebak, A. (Dordrecht: Reidel), 233

Coyne, G.V. & Gehrels, T. 1967, AJ, 72, 887

Coyne, G.V. & Kruszewski, A. 1969, AJ, 74, 528

Coyne, G.V. & McLean, I.S. 1982, in IAU Symp. 98, Be Stars, ed. Jaschek, M. and Groth, H. (Dordrecht: Reidel), 77

McLean, I.S. 1979, MNRAS, 186, 265

Poeckert, R., Bastien, P., & Landstreet, J.D. 1979, AJ, 84, 812

Slettebak, A. 1979, Space Sci. Rev., 23, 541

Table 2. ϕ Per Polarization

	U	B	V	R	I
CGK 1966-67					
$p \pm \sigma_p$(%)	0.70± 0.11	1.06± 0.11	0.99± 0.03	0.78± 0.10	0.74± 0.09
$\theta \pm \sigma_\theta$(°)	54.5 ± 4.8	41.4 ± 0.7	42.3 ± 0.9	43.1 ± 2.6	36.6 ± 2.1
σ_A(%)					0.09
PBL 1975-76					
$p \pm \sigma_p$(%)	0.40± 0.02	1.22± 0.03	1.10± 0.02	0.82± 0.02	0.74± 0.02
$\theta \pm \sigma_\theta$(°)	56.8 ± 1.6	35.3 ± 0.9	36.4 ± 0.6	39.9 ± 0.6	35.3 ± 0.6
σ_A(%)					0.02
DM 1984					
$p \pm \sigma_p$(%)	0.68± 0.08	1.12± 0.03	1.06± 0.01	0.89± 0.11	0.72± 0.08
$\theta \pm \sigma_\theta$(°)	43.5 ± 3.2	33.9 ± 2.7	36.4 ± 3.0	35.3 ± 2.3	38.6 ± 5.0
σ_A(%)					0.06
AVERAGE					
$p \pm \sigma_p$(%)	0.59± 0.17	1.13± 0.08	1.05± 0.06	0.83± 0.06	0.73± 0.01
$\theta \pm \sigma_\theta$(°)	51.6 ± 7.1	36.9 ± 4.0	38.4 ± 3.4	39.4 ± 3.9	36.8 ± 1.7
σ_A(%)					0.08

Table 3. 48 Per Polarization

	U	B	V	R	I
CGK 1966-67					
$p \pm \sigma_p$(%)	0.44± 0.03	0.69± 0.03	0.80± 0.03	0.84± 0.08	0.73± 0.05
$\theta \pm \sigma_\theta$(°)	173.9 ± 0.9	173.5 ± 0.9	169.4 ± 0.9	171.7 ± 1.6	171.6 ± 3.1
σ_A(%)					0.04
PBL 1976-77					
$p \pm \sigma_p$(%)	0.61± 0.05	0.82± 0.05	0.85± 0.02	0.88± 0.02	0.78± 0.02
$\theta \pm \sigma_\theta$(°)	171.7 ± 4.4	171.9 ± 3.6	172.6 ± 0.6	172.5 ± 0.6	172.9 ± 0.6
σ_A(%)					0.03
DM 1984					
$p \pm \sigma_p$(%)	0.83± 0.02	0.88± 0.08	0.92± 0.17	0.89± 0.12	0.83± 0.11
$\theta \pm \sigma_\theta$(°)	167.0 ± 5.1	165.7 ± 3.0	172.4 ± 3.5	170.2 ± 1.1	169.1 ± 4.9
σ_A(%)					0.10
AVERAGE					
$p \pm \sigma_p$(%)	0.63± 0.20	0.80± 0.10	0.86± 0.06	0.87± 0.03	0.78± 0.05
$\theta \pm \sigma_\theta$(°)	170.9 ± 3.5	170.4 ± 4.1	171.5 ± 1.8	171.5 ± 1.2	171.2 ± 1.9
σ_A(%)					0.09

Table 4. ζ Tau Polarization

	U	B	V	R	I
CGK 1964-67					
$p \pm \sigma_p(\%)$	1.04± 0.07	1.57± 0.08	1.49± 0.04	1.37± 0.05	1.20± 0.12
$\theta \pm \sigma_\theta(^\circ)$	29.1 ±10.0	31.7 ± 4.9	29.2 ± 5.4	32.9 ± 1.4	30.7 ± 2.5
$\sigma_A(\%)$					0.07
PBL 1975-77					
$p \pm \sigma_p(\%)$	0.54± 0.06	1.40± 0.09	1.32± 0.10	1.12± 0.07	1.04± 0.14
$\theta \pm \sigma_\theta(^\circ)$	32.4 ± 1.3	31.7 ± 1.8	32.8 ± 1.0	32.2 ± 0.5	32.7 ± 1.9
$\sigma_A(\%)$					0.09
DM 1984					
$p \pm \sigma_p(\%)$	0.89± 0.08	1.20± 0.11	1.22± 0.12	1.11± 0.13	0.97± 0.11
$\theta \pm \sigma_\theta(^\circ)$	30.5 ± 1.6	28.0 ± 2.9	30.3 ± 1.9	28.6 ± 4.1	29.6 ± 4.1
$\sigma_A(\%)$					0.11
AVERAGE					
$p \pm \sigma_p(\%)$	0.82± 0.26	1.39± 0.19	1.34± 0.14	1.20± 0.15	1.07± 0.12
$\theta \pm \sigma_\theta(^\circ)$	30.7 ± 1.7	30.5 ± 2.1	30.8 ± 1.8	31.2 ± 2.3	31.0 ± 1.6
$\sigma_A(\%)$					0.17

Table 5. 48 Lib Polarization

	U	B	V	R	I
CGK 1967-68					
$p \pm \sigma_p(\%)$	0.73± 0.04	0.93± 0.09	0.90± 0.14	0.65± 0.04	0.71± 0.04
$\theta \pm \sigma_\theta(^\circ)$	120.7 ± 1.2	120.3 ± 2.4	118.3 ± 3.3	112.4 ± 1.2	113.8 ± 1.2
$\sigma_A(\%)$					0.07
PBL 1975-76					
$p \pm \sigma_p(\%)$	0.54± 0.03	0.72± 0.04	0.77± 0.02	0.70± 0.02	0.68± 0.02
$\theta \pm \sigma_\theta(^\circ)$	109.3 ± 3.3	117.7 ± 0.9	116.4 ± 0.6	113.5 ± 0.6	118.3 ± 3.6
$\sigma_A(\%)$					0.03
DM 1985					
$p \pm \sigma_p(\%)$	0.64± 0.07	0.79± 0.02	0.86± 0.03	0.82± 0.04	0.64± 0.14
$\theta \pm \sigma_\theta(^\circ)$	115.7 ± 5.5	122.4 ± 4.3	117.7 ± 4.1	114.9 ± 2.7	117.1 ± 1.8
$\sigma_A(\%)$					0.06
AVERAGE					
$p \pm \sigma_p(\%)$	0.64± 0.10	0.81± 0.11	0.84± 0.07	0.72± 0.09	0.68± 0.04
$\theta \pm \sigma_\theta(^\circ)$	115.2 ± 5.7	120.1 ± 2.4	117.5 ± 1.0	113.6 ± 1.3	116.4 ± 2.3
$\sigma_A(\%)$					0.08

Table 6. χ Oph Polarization

	U	B	V	R	I
CGK 1966-68					
$p \pm \sigma_p$(%)	0.49± 0.11	0.52± 0.20	0.57± 0.20	0.45± 0.06	0.42± 0.06
$\theta \pm \sigma_\theta$(°)	144.3 ±16.6	126.7 ±20.9	126.3 ±18.1	128.2 ± 1.7	127.0 ± 1.7
σ_A(%)					0.13
PBL 1975-76					
$p \pm \sigma_p$(%)	0.31± 0.02	0.42± 0.02	0.53± 0.03	0.47± 0.03	0.36± 0.03
$\theta \pm \sigma_\theta$(°)	132.4 ± 3.0	133.1 ± 2.3	134.8 ± 0.9	137.4 ± 0.9	134.4 ± 0.9
σ_A(%)					0.03
DM 1985					
$p \pm \sigma_p$(%)	0.46± 0.03	0.52± 0.05	0.46± 0.02	0.50± 0.02	0.46± 0.11
$\theta \pm \sigma_\theta$(°)	134.9 ± 3.1	136.8 ± 1.4	131.5 ± 0.3	134.2 ± 1.3	131.7 ± 2.7
σ_A(%)					0.05
AVERAGE					
$p \pm \sigma_p$(%)	0.42± 0.10	0.49± 0.06	0.52± 0.06	0.47± 0.03	0.41± 0.05
$\theta \pm \sigma_\theta$(°)	137.2 ± 6.3	132.2 ± 5.1	130.9 ± 4.3	133.3 ± 4.7	131.0 ± 3.7
σ_A(%)					0.06

Table 7. π Aqr Polarization

	U	B	V	R	I
CGK 1966-68					
$p \pm \sigma_p$(%)	0.62± 0.06	1.00± 0.17	0.90± 0.10	0.74± 0.13	0.63± 0.08
$\theta \pm \sigma_\theta$(°)	141.7 ± 4.7	152.2 ± 2.3	152.0 ± 4.1	145.3 ± 3.5	148.2 ± 3.0
σ_A(%)					0.11
PBL 1975-76					
$p \pm \sigma_p$(%)	0.57± 0.02	1.66± 0.17	1.40± 0.03	0.92± 0.03	0.86± 0.01
$\theta \pm \sigma_\theta$(°)	145.5 ± 1.1	158.8 ± 1.8	158.3 ± 0.9	154.2 ± 0.9	157.3 ± 2.6
σ_A(%)					0.05
DM 1985					
$p \pm \sigma_p$(%)	1.20± 0.09	1.88± 0.02	1.53± 0.03	1.30± 0.06	0.95± 0.13
$\theta \pm \sigma_\theta$(°)	157.9 ± 2.7	162.1 ± 2.1	158.8 ± 2.4	157.4 ± 1.3	155.4 ± 3.2
σ_A(%)					0.07
AVERAGE					
$p \pm \sigma_p$(%)	0.80± 0.35	1.51± 0.46	1.28± 0.33	0.99± 0.29	0.81± 0.17
$\theta \pm \sigma_\theta$(°)	148.4 ± 8.5	157.7 ± 5.0	156.4 ± 3.8	152.3 ± 6.3	153.6 ± 4.8
σ_A(%)					0.32

Table 8. π Aqr Intrinsic Polarization

	U	B	V	R	I
CGK 1966-68					
$p(\%)$	0.49	0.96	0.87	0.63	0.57
$\theta(^\circ)$	162.5	165.5	166.8	162.9	164.4
PBL 1975-76					
$p(\%)$	0.50	1.69	1.43	0.92	0.88
$\theta(^\circ)$	167.8	166.5	167.5	157.7	168.5
DM 1985					
$p(\%)$	1.23	1.95	1.56	1.32	0.94
$\theta(^\circ)$	167.7	168.8	167.2	166.8	165.8
AVERAGE					
$\theta(^\circ)$	166.0	166.9	167.2	165.8	166.2
$\sigma_\theta(^\circ)$	3.0	1.7	0.4	2.6	2.1

Chapter 3

Multicolor Polarimetry of Selected Be Stars: 1986–89

(originally published in 1990 PASP, 102, 773)

ABSTRACT

Annual monitoring of the broad band visible continuum linear polarization of a sample of the brightest northern Be stars over a period of three years demonstrates that large and readily identifiable variations in polarization are most commonly detected on a year-to-year time scale. No clear cases of night-to-night variability were found at the level of precision on which the polarizations of the standard stars could be assumed constant. Because of the complexity of the Be phenomenon, any model-dependent interpretation of polarimetry data by itself may be misleading. It is therefore hoped that theoreticians will be able to use the data presented here in combination with observations obtained by other techniques and in other spectral regions to develop a more general understanding of the processes at work in Be stars.

1. Introduction

Beginning with the pioneering work of Coyne & Gehrels (1967), the intrinsic linear polarization of Be stars at visible wavelengths has been recognized as one of their most distinctive characteristics. The generally accepted theoretical explanation for the polarization, as outlined by McLean (1979), is electron scattering in an equatorially flattened circumstellar envelope (CE) surrounding the star. Within the framework of this model, polarimetric observations become a useful diagnostic of the CE conditions, including density, temperature, and geometry. The series of papers by Brown and McLean (1977), Brown et al. (1978), and McLean and Brown (1978) showed, however, that it is difficult to place unique constraints on these conditions by polarimetry alone, because there are too many model parameters. A more productive approach is the formulation of models

which reproduce the observed emission line profiles as well as the polarization in the visible (Poeckert and Marlborough 1978), but the incorporation of infrared and ultraviolet data into the interpretation process is an absolute necessity. The unfamiliar reader is referred to a recent review article on Be stars by Slettebak (1988).

Like most observational characteristics of Be stars, the polarization is variable on time scales ranging from hours to years (Coyne 1976). Although the first detections of variable polarization were made with wide band filters, more recent polarimetric observations have emphasized higher wavelength resolution in order to obtain more detailed information about the envelope conditions (Coyne & McLean 1982). This shift in technique away from wide band measurements, which had provided the most uniform coverage of variable polarization over the longest period of time, motivated the annual *UBVRI* polarization monitoring program first described in Paper I (McDavid 1986). That paper linked the new observations of a group of six bright northern Be stars with previous data taken from the literature, showing that the largest changes in polarization of Be stars occur on time scales of years to decades.

The purpose of the present paper is to report the continuing progress of the monitoring program. Section 2 describes the observational system, while Sections 3 and 4 are devoted to evaluation of night-to-night and year-to-year variability, respectively. Section 5 is a discussion of the results, including some suggestions for future work.

2. Observations

The eight bright northern Be stars selected for observation are listed in Table 1. The visual magnitudes are taken from Hoffleit & Jaschek (1982), while the spectral types and $v \sin i$ values are from Slettebak (1982). Linear polarization measurements were made during week-long observing runs with the polarimeter described by Breger (1979), attached to the 36 inch (0.9 m) telescope of McDonald Observatory. A *UBVRI* filter set followed by a neutral density filter of 10% transmission and an EMI 9658 AR-S20 photomultiplier tube determined the wavelength characteristics of the system, which are given approximately in Table 2. It may be noted that the effective wavelength of the *I* passband has been revised since Paper I, although this does not significantly affect any of the conclusions drawn there.

In addition to the groups of four winter Be stars and four summer Be stars, two polarized standard stars from the list of Hsu & Breger (1982) were also systematically observed as checks on the consistency of the observations: 2H Camelopardalis with the winter group and o Scorpii with the summer group. All measurements were corrected for instrumental polarizations on the order of 0.10% determined by repeated observations of unpolarized standard stars during each run. Measurements were also corrected for background sky polarization.

The data are presented in Tables 3–12, where the columns give (1): approximate date (month/year) of the observing run, filter designation, and number (n) of repeated obser-

vations, (2) and (3): mean and standard deviation of the normalized Stokes parameters q and u, (4) and (5): mean and standard deviation of the polarization amplitude p and position angle θ, with no debiasing corrections (Clarke & Stewart 1986), and (6): mean instrumental error dpi in polarization amplitude for each set of measurements according to photon statistics, unless photon statistics gives a value less than 0.02%, in which case the error is approximated as 0.02% due to atmospheric scintillation for the 200-second integration time (Young 1967), and the corresponding mean instrumental error in polarization position angle, based on the relation $d\theta i = 28.^{\circ}65(dpi/p)$.

The data tabulated here should be useful to those interested in investigating possible correlations between polarization and other observational characteristics of this group of stars. The observations provide information on variability over two different time scales: night-to-night and year-to-year. (Although there are several cases of multiple observations per night during some observing runs, no attempt is made here to distinguish between hour-to-hour and night-to-night variability.) It should be noted that the intermediate time scale of weeks to months is not covered, since there is no way to determine the time elapsed during a change in polarization observed from one year to the next. This missing time scale may be significant, because it corresponds to the orbital periods of some Be star systems, such as ϕ Persei and ζ Tauri, which are spectroscopic binaries (Coyne 1976).

3. Analysis of Night-to-Night Variability

Since repeated observations were usually made on different nights during individual observing runs, comparison of dq and du with dpi for each line of Tables 3–12 should reveal any night-to-night variations which might be present. Following the suggestion of Clarke and Stewart (1986), the normalized Stokes parameters are considered rather than the statistically biased quantities p and θ. However, dp and $d\theta$ are presented in the data tables because they may at least roughly indicate whether variability of q and u is an effect of variable amplitude or position angle.

Table 1. Program Be Stars

Name	HD	HR	V	Spectral Type	$v \sin i$ (km s^{-1})
γ Cas	5394	264	2.47	B0.5 IVe	230
ϕ Per	10516	496	4.07	B1.5 (V:)e-shell	400
48 Per	25940	1273	4.04	B4 Ve	200
ζ Tau	37202	1910	3.00	B1 IVe-shell	220
48 Lib	142983	5941	4.88	B3:IV:e-shell	400
χ Oph	148184	6118	4.42	B1.5 Ve	140
π Aqr	212571	8539	4.66	B1 III-IVe	300
o And	217675	8762	3.62	B6 III	260

Table 2. Filter System Parameters

Filter	Effective Wavelength (nm)	Bandpass (fwhm) (nm)
U	365	70
B	440	100
V	550	90
R	640	150
I	790	150

Table 3. 2H Cam (Standard Star)

Date(Mo/Yr) Filter(n)	q/dq (%)	u/du (%)	p/dp (%)	$\theta/d\theta$ (°)	$dpi/d\theta i$ (%) (°)
01/86					
$U(2)$	-1.98/0.08	-2.37/0.09	3.09/0.02	115.0/ 1.1	0.06/ 0.6
$B(40)$	-1.92/0.08	-2.62/0.06	3.25/0.05	116.9/ 0.8	0.03/ 0.3
$V(6)$	-2.03/0.05	-2.83/0.04	3.48/0.06	117.2/ 0.3	0.03/ 0.2
$R(1)$	-1.90/ -	-2.61/ -	3.23/ -	117.0/ -	0.02/ 0.2
$I(1)$	-1.73/ -	-2.45/ -	3.00/ -	117.4/ -	0.04/ 0.4
01/87					
$U(4)$	-1.87/0.07	-2.44/0.04	3.07/0.08	116.2/ 0.3	0.06/ 0.6
$B(3)$	-2.02/0.10*	-2.57/0.02	3.27/0.07	115.9/ 0.6	0.03/ 0.2
$V(25)$	-2.07/0.04	-2.77/0.04	3.46/0.04	116.6/ 0.3	0.03/ 0.2
$R(4)$	-2.02/0.02	-2.70/0.03	3.37/0.03	116.6/ 0.2	0.02/ 0.2
$I(4)$	-1.71/0.06	-2.38/0.06	2.93/0.07	117.2/ 0.4	0.04/ 0.4
01/88					
$U(5)$	-1.80/0.10	-2.23/0.10	2.86/0.08	115.6/ 1.2	0.06/ 0.6
$B(4)$	-1.99/0.08	-2.60/0.08	3.27/0.06	116.3/ 0.8	0.03/ 0.2
$V(9)$	-2.13/0.10*	-2.68/0.06	3.42/0.04	115.7/ 1.0	0.03/ 0.2
$R(5)$	-1.93/0.07*	-2.62/0.05	3.25/0.03	116.8/ 0.7	0.02/ 0.2
$I(5)$	-1.74/0.06	-2.28/0.08	2.87/0.06	116.4/ 0.8	0.04/ 0.4
12/88					
$U(5)$	-2.08/0.09	-2.48/0.14	3.24/0.12	115.0/ 1.0	0.08/ 0.7
$B(5)$	-2.16/0.08	-2.60/0.05	3.38/0.02	115.2/ 0.8	0.04/ 0.3
$V(5)$	-2.24/0.07	-2.78/0.04	3.57/0.05	115.6/ 0.5	0.03/ 0.3
$R(5)$	-2.16/0.06	-2.61/0.07*	3.39/0.07	115.2/ 0.4	0.02/ 0.2
$I(5)$	-1.86/0.04	-2.28/0.04	2.95/0.04	115.4/ 0.3	0.05/ 0.4

Table 4. o Sco (Standard Star)

Date(Mo/Yr) Filter(n)	q/dq (%)	u/du (%)	p/dp (%)	$\theta/d\theta$ (°)	$dpi/d\theta i$ (%) (°)
06/86					
$U(5)$	1.28/0.25	2.68/0.28	2.97/0.35	32.4/ 1.3	0.14/ 1.4
$B(5)$	1.57/0.12	3.06/0.04	3.44/0.08	31.4/ 0.9	0.05/ 0.4
$V(17)$	1.90/0.04	3.74/0.06	4.20/0.06	31.5/ 0.3	0.04/ 0.2
$R(5)$	2.00/0.04	3.93/0.04	4.41/0.03	31.5/ 0.3	0.02/ 0.1
$I(4)$	1.92/0.07	3.92/0.01	4.36/0.03	32.0/ 0.4	0.04/ 0.2
08/87					
$U(4)$	1.33/0.13	2.63/0.25	2.95/0.26	31.6/ 1.1	0.14/ 1.4
$B(4)$	1.48/0.06	3.11/0.05	3.45/0.06	32.2/ 0.5	0.04/ 0.4
$V(4)$	1.79/0.04	3.78/0.02	4.18/0.02	32.4/ 0.2	0.03/ 0.2
$R(4)$	1.89/0.06	3.96/0.04	4.39/0.02	32.2/ 0.4	0.02/ 0.1
$I(4)$	1.82/0.03	3.84/0.03	4.25/0.03	32.3/ 0.2	0.03/ 0.2
07/88					
$U(5)$	1.19/0.16	2.45/0.09	2.73/0.07	32.1/ 1.8	0.15/ 1.6
$B(4)$	1.54/0.04	3.05/0.04	3.41/0.04	31.6/ 0.3	0.04/ 0.4
$V(5)$	1.82/0.05	3.72/0.08	4.14/0.05	32.0/ 0.5	0.03/ 0.2
$R(5)$	1.90/0.04	3.91/0.03	4.35/0.02	32.0/ 0.3	0.02/ 0.1
$I(5)$	1.93/0.04	3.84/0.02	4.30/0.01	31.7/ 0.3	0.04/ 0.2
06/89					
$U(3)$	1.42/0.46	2.55/0.20	2.94/0.31	30.6/ 3.8	0.25/ 2.4
$B(3)$	1.56/0.08	3.04/0.06	3.42/0.06	31.4/ 0.6	0.07/ 0.6
$V(3)$	1.84/0.03	3.72/0.05	4.15/0.06	31.8/ 0.0	0.05/ 0.3
$R(3)$	2.01/0.02	3.94/0.03	4.42/0.03	31.5/ 0.0	0.03/ 0.2
$I(3)$	1.95/0.08	3.84/0.02	4.31/0.04	31.5/ 0.5	0.04/ 0.3

Table 5. γ Cas

Date(Mo/Yr) Filter(n)	q/dq (%)	u/du (%)	p/dp (%)	$\theta/d\theta$ (°)	$dpi/d\theta i$ (%) (°)
01/86					
$U(4)$	-0.46/0.06	-0.29/0.13*	0.56/0.08	105.6/ 6.5	0.02/ 0.7
$B(4)$	-0.66/0.02	-0.45/0.06	0.80/0.05	107.1/ 1.7	0.02/ 0.3
$V(4)$	-0.65/0.06	-0.36/0.04	0.75/0.05	104.6/ 2.0	0.02/ 0.4
$R(4)$	-0.58/0.04	-0.21/0.09*	0.62/0.06	99.9/ 3.7	0.02/ 0.4
$I(4)$	-0.48/0.05	-0.18/0.08*	0.52/0.06	100.2/ 3.9	0.02/ 1.1
01/87					
$U(4)$	-0.57/0.06	-0.33/0.04	0.66/0.05	105.0/ 1.8	0.02/ 0.6
$B(4)$	-0.75/0.07*	-0.49/0.05	0.90/0.08	106.6/ 1.0	0.02/ 0.3
$V(4)$	-0.70/0.09*	-0.41/0.06	0.81/0.10	105.2/ 0.8	0.02/ 0.4
$R(4)$	-0.60/0.10*	-0.28/0.06	0.67/0.08	102.6/ 3.4	0.02/ 0.4
$I(4)$	-0.47/0.12*	-0.24/0.03	0.53/0.11	103.6/ 2.2	0.02/ 1.0
01/88					
$U(5)$	-0.40/0.04	-0.22/0.04	0.46/0.05	104.4/ 2.2	0.02/ 0.8
$B(5)$	-0.64/0.04	-0.43/0.05	0.77/0.05	106.8/ 1.5	0.02/ 0.3
$V(5)$	-0.62/0.04	-0.37/0.03	0.72/0.04	105.2/ 1.4	0.02/ 0.4
$R(5)$	-0.51/0.04	-0.22/0.06	0.55/0.04	101.5/ 3.2	0.02/ 0.4
$I(5)$	-0.47/0.04	-0.20/0.04	0.52/0.04	101.6/ 2.1	0.02/ 1.0
12/88					
$U(5)$	-0.57/0.04	-0.32/0.07*	0.66/0.04	104.5/ 3.2	0.02/ 1.0
$B(5)$	-0.72/0.07*	-0.36/0.02	0.80/0.06	103.3/ 1.5	0.02/ 0.5
$V(5)$	-0.59/0.04	-0.35/0.05	0.69/0.04	105.4/ 2.2	0.02/ 0.6
$R(5)$	-0.55/0.05	-0.21/0.04	0.59/0.05	100.6/ 2.0	0.02/ 0.5
$I(5)$	-0.54/0.05	-0.18/0.06	0.57/0.05	99.2/ 2.8	0.02/ 1.2

Table 6. ϕ Per

Date(Mo/Yr) Filter(n)	q/dq (%)	u/du (%)	p/dp (%)	$\theta/d\theta$ (°)	$dpi/d\theta i$ (%) (°)
01/86					
$U(5)$	0.08/0.09	0.86/0.08	0.86/0.09	42.4/ 2.9	0.04/ 1.2
$B(5)$	0.45/0.05	1.22/0.08*	1.30/0.08	34.8/ 0.9	0.02/ 0.5
$V(5)$	0.33/0.11*	1.09/0.08	1.14/0.10	36.8/ 2.2	0.03/ 0.7
$R(5)$	0.29/0.04	1.05/0.07*	1.09/0.08	37.2/ 0.8	0.02/ 0.6
$I(4)$	0.16/0.12	0.83/0.05	0.86/0.05	39.7/ 4.1	0.04/ 1.4
01/87					
$U(4)$	0.12/0.05	0.79/0.06	0.80/0.05	40.4/ 2.0	0.04/ 1.2
$B(4)$	0.54/0.07*	1.24/0.04	1.35/0.03	33.3/ 1.5	0.02/ 0.4
$V(4)$	0.39/0.06	1.04/0.11*	1.11/0.08	34.5/ 2.4	0.02/ 0.6
$R(4)$	0.38/0.10*	1.01/0.05	1.08/0.02	34.6/ 2.9	0.02/ 0.5
$I(4)$	0.19/0.06	0.78/0.03	0.80/0.02	38.1/ 2.4	0.04/ 1.5
01/88					
$U(5)$	0.23/0.03	0.86/0.07	0.90/0.08	37.5/ 0.8	0.03/ 1.0
$B(5)$	0.53/0.05	1.28/0.05	1.38/0.05	33.8/ 1.0	0.02/ 0.4
$V(5)$	0.42/0.05	1.14/0.06	1.22/0.06	34.8/ 1.4	0.02/ 0.5
$R(5)$	0.44/0.06	1.10/0.06	1.19/0.04	34.0/ 1.8	0.02/ 0.4
$I(5)$	0.29/0.07	0.78/0.08	0.83/0.09	34.8/ 2.0	0.04/ 1.4
12/88					
$U(5)$	0.03/0.08	0.66/0.11	0.66/0.11	43.9/ 3.0	0.05/ 2.2
$B(5)$	0.42/0.10*	1.14/0.09	1.22/0.10	34.8/ 1.9	0.03/ 0.7
$V(5)$	0.40/0.08	1.00/0.07	1.08/0.08	34.0/ 1.8	0.03/ 0.8
$R(5)$	0.35/0.07*	1.00/0.04	1.07/0.05	35.4/ 1.8	0.02/ 0.7
$I(5)$	0.16/0.08	0.75/0.06	0.77/0.06	39.1/ 2.8	0.05/ 2.0

Table 7. 48 Per

Date(Mo/Yr) Filter(n)	q/dq (%)	u/du (%)	p/dp (%)	$\theta/d\theta$ (°)	$dpi/d\theta i$ (%) (°)
01/86					
$U(4)$	0.75/0.04	-0.15/0.09	0.77/0.05	174.5/ 3.2	0.04/ 1.6
$B(4)$	0.81/0.03	-0.23/0.07*	0.84/0.03	172.0/ 2.2	0.02/ 0.8
$V(4)$	0.87/0.05	-0.19/0.10*	0.90/0.04	174.0/ 3.1	0.03/ 0.8
$R(4)$	0.89/0.05	-0.15/0.10*	0.90/0.05	175.1/ 3.4	0.02/ 0.7
$I(4)$	0.87/0.09	-0.17/0.08	0.89/0.08	174.2/ 3.2	0.04/ 1.4
01/87					
$U(4)$	0.69/0.02	-0.21/0.03	0.72/0.01	171.6/ 1.5	0.04/ 1.6
$B(4)$	0.85/0.03	-0.17/0.02	0.86/0.03	174.3/ 0.8	0.02/ 0.7
$V(4)$	0.93/0.04	-0.25/0.10*	0.97/0.04	172.5/ 3.1	0.03/ 0.8
$R(4)$	0.97/0.02	-0.23/0.00	1.00/0.02	173.4/ 0.1	0.02/ 0.6
$I(4)$	0.92/0.08	-0.20/0.07	0.94/0.07	173.7/ 2.3	0.04/ 1.3
01/88					
$U(5)$	0.83/0.05	-0.14/0.03	0.84/0.06	175.4/ 0.9	0.04/ 1.3
$B(5)$	0.85/0.03	-0.28/0.06	0.90/0.03	171.0/ 1.8	0.02/ 0.6
$V(5)$	0.94/0.03	-0.26/0.05	0.97/0.04	172.4/ 1.4	0.02/ 0.7
$R(5)$	0.98/0.04	-0.21/0.06	1.01/0.03	174.0/ 1.9	0.02/ 0.6
$I(5)$	0.90/0.11	-0.18/0.08	0.92/0.10	174.2/ 2.7	0.08/ 2.3
12/88					
$U(5)$	0.65/0.08	-0.33/0.07	0.73/0.07	166.4/ 2.9	0.05/ 2.1
$B(5)$	0.76/0.04	-0.31/0.04	0.82/0.05	169.0/ 0.9	0.03/ 0.9
$V(5)$	0.90/0.01	-0.30/0.07	0.95/0.02	170.8/ 2.1	0.03/ 0.9
$R(5)$	0.92/0.04	-0.22/0.04	0.95/0.04	173.3/ 1.2	0.02/ 0.7
$I(5)$	0.79/0.04	-0.18/0.01	0.81/0.04	173.6/ 0.6	0.05/ 1.8

Table 8. ζ Tau

Date(Mo/Yr) Filter(n)	q/dq (%)	u/du (%)	p/dp (%)	$\theta/d\theta$ (°)	$dpi/d\theta i$ (%) (°)
01/86					
$U(4)$	0.50/0.02	1.08/0.10*	1.19/0.09	32.5/ 1.1	0.02/ 0.5
$B(55)$	0.68/0.03	1.37/0.05	1.53/0.04	31.7/ 0.8	0.02/ 0.2
$V(4)$	0.58/0.05	1.29/0.04	1.42/0.03	32.8/ 1.1	0.02/ 0.3
$R(4)$	0.52/0.12*	1.31/0.11*	1.42/0.08	34.2/ 2.9	0.02/ 0.3
$I(4)$	0.50/0.11*	1.05/0.08	1.17/0.05	32.3/ 3.1	0.03/ 0.8
01/87					
$U(4)$	0.43/0.07*	0.94/0.06	1.04/0.08	32.7/ 1.3	0.02/ 0.6
$B(4)$	0.54/0.06	1.30/0.04	1.41/0.04	33.6/ 1.3	0.02/ 0.2
$V(28)$	0.54/0.04	1.16/0.04	1.28/0.04	32.6/ 0.8	0.02/ 0.3
$R(4)$	0.50/0.03	1.08/0.06	1.19/0.07	32.5/ 0.5	0.02/ 0.3
$I(4)$	0.37/0.06	0.89/0.04	0.96/0.06	33.8/ 1.4	0.03/ 0.9
01/88					
$U(5)$	0.47/0.05	0.94/0.08	1.06/0.06	31.6/ 1.8	0.04/ 0.9
$B(5)$	0.59/0.06	1.23/0.10*	1.37/0.08	32.1/ 1.6	0.02/ 0.4
$V(5)$	0.53/0.06	1.14/0.09	1.26/0.10	32.6/ 1.1	0.03/ 0.7
$R(5)$	0.54/0.06	1.11/0.07*	1.23/0.08	32.1/ 0.8	0.02/ 0.4
$I(5)$	0.42/0.08	0.84/0.10	0.95/0.07	31.6/ 3.4	0.04/ 1.1
12/88					
$U(5)$	0.35/0.04	1.04/0.13*	1.09/0.13	35.6/ 1.3	0.03/ 0.7
$B(5)$	0.65/0.05	1.55/0.16*	1.68/0.16	33.6/ 0.8	0.02/ 0.3
$V(5)$	0.62/0.08*	1.40/0.12*	1.53/0.13	33.2/ 1.0	0.02/ 0.4
$R(5)$	0.53/0.07*	1.32/0.11*	1.42/0.11	34.0/ 1.6	0.02/ 0.3
$I(5)$	0.40/0.05	1.06/0.04	1.14/0.05	34.7/ 1.2	0.04/ 0.9

Table 9. 48 Lib

Date(Mo/Yr) Filter(n)	q/dq (%)	u/du (%)	p/dp (%)	$\theta/d\theta$ (°)	$dpi/d\theta i$ (%) (°)
06/86					
$U(5)$	-0.38/0.09	-0.51/0.17	0.64/0.16	116.1/ 4.1	0.08/ 3.6
$B(5)$	-0.46/0.07	-0.77/0.04	0.90/0.02	119.4/ 2.4	0.04/ 1.2
$V(67)$	-0.54/0.06	-0.70/0.05	0.88/0.04	116.1/ 1.9	0.04/ 1.3
$R(5)$	-0.52/0.06	-0.62/0.03	0.81/0.03	115.1/ 2.1	0.03/ 1.1
$I(5)$	-0.51/0.07	-0.61/0.07	0.79/0.10	115.2/ 0.9	0.07/ 2.5
08/87					
$U(5)$	-0.44/0.09	-0.63/0.07	0.77/0.08	117.5/ 2.9	0.06/ 2.2
$B(5)$	-0.38/0.07	-0.82/0.04	0.90/0.02	122.5/ 2.4	0.03/ 1.0
$V(5)$	-0.52/0.03	-0.77/0.04	0.93/0.04	118.1/ 0.9	0.04/ 1.1
$R(5)$	-0.50/0.06	-0.68/0.04	0.84/0.06	117.0/ 1.5	0.03/ 1.0
$I(5)$	-0.53/0.05	-0.68/0.07	0.86/0.06	116.1/ 1.8	0.06/ 2.1
07/88					
$U(5)$	-0.28/0.06	-0.46/0.06	0.54/0.04	119.2/ 3.6	0.06/ 3.4
$B(5)$	-0.41/0.03	-0.71/0.06	0.82/0.04	119.9/ 1.9	0.03/ 1.1
$V(5)$	-0.58/0.05	-0.63/0.07	0.86/0.06	113.9/ 1.9	0.04/ 1.2
$R(5)$	-0.54/0.05	-0.58/0.04	0.79/0.04	113.7/ 1.8	0.03/ 1.1
$I(5)$	-0.44/0.07	-0.49/0.07	0.66/0.08	114.2/ 2.1	0.07/ 3.3
06/89					
$U(4)$	-0.50/0.14	-0.31/0.21	0.63/0.07	106.3/11.1	0.10/ 4.8
$B(4)$	-0.44/0.05	-0.59/0.04	0.74/0.06	116.6/ 1.0	0.05/ 1.8
$V(4)$	-0.58/0.07	-0.58/0.14	0.83/0.06	112.0/ 5.1	0.05/ 1.8
$R(4)$	-0.57/0.07	-0.46/0.07	0.74/0.09	109.5/ 1.3	0.04/ 1.6
$I(4)$	-0.68/0.13	-0.53/0.04	0.86/0.10	109.2/ 3.0	0.09/ 3.0

Table 10. χ Oph

Date(Mo/Yr) Filter(n)	q/dq (%)	u/du (%)	p/dp (%)	$\theta/d\theta$ (°)	$dpi/d\theta i$ (%) (°)
06/86					
$U(5)$	-0.03/0.07	-0.38/0.06	0.38/0.06	133.4/ 5.5	0.06/ 4.6
$B(5)$	-0.09/0.06	-0.48/0.04	0.49/0.04	129.6/ 3.6	0.03/ 1.9
$V(37)$	-0.08/0.05	-0.48/0.04	0.49/0.04	130.2/ 2.7	0.03/ 1.8
$R(5)$	0.05/0.05	-0.36/0.09*	0.37/0.08	139.7/ 6.1	0.02/ 1.7
$I(5)$	0.03/0.06	-0.51/0.02	0.52/0.02	136.4/ 3.2	0.04/ 2.2
08/87					
$U(5)$	-0.13/0.05	-0.43/0.07	0.45/0.06	126.6/ 3.6	0.06/ 3.8
$B(5)$	-0.04/0.05	-0.49/0.06	0.49/0.06	132.4/ 3.1	0.03/ 1.8
$V(5)$	-0.07/0.06	-0.51/0.03	0.52/0.03	131.1/ 3.5	0.03/ 1.7
$R(5)$	0.02/0.03	-0.40/0.04	0.40/0.04	136.5/ 2.0	0.02/ 1.5
$I(5)$	-0.08/0.03	-0.58/0.06	0.58/0.06	131.0/ 1.7	0.04/ 1.9
07/88					
$U(5)$	0.00/0.04	-0.41/0.04	0.42/0.04	134.8/ 2.8	0.06/ 4.2
$B(5)$	-0.08/0.03	-0.53/0.05	0.54/0.05	130.8/ 1.6	0.03/ 1.6
$V(5)$	-0.10/0.06	-0.53/0.04	0.54/0.05	129.5/ 3.0	0.03/ 1.6
$R(5)$	0.02/0.02	-0.40/0.04	0.40/0.04	136.4/ 1.7	0.02/ 1.5
$I(5)$	-0.01/0.06	-0.50/0.09	0.50/0.08	134.2/ 3.4	0.04/ 2.4
06/89					
$U(3)$	-0.02/0.02	-0.30/0.09	0.31/0.09	132.9/ 1.7	0.09/ 9.1
$B(3)$	-0.02/0.02	-0.50/0.07	0.50/0.07	133.7/ 1.4	0.04/ 2.5
$V(3)$	-0.07/0.07	-0.51/0.02	0.52/0.03	131.2/ 3.4	0.04/ 2.3
$R(3)$	0.01/0.05	-0.39/0.02	0.39/0.02	135.5/ 3.6	0.03/ 2.2
$I(3)$	-0.06/0.14	-0.48/0.11	0.50/0.08	130.5/ 9.6	0.05/ 2.9

Table 11. π Aqr

Date(Mo/Yr) Filter(n)	q/dq (%)	u/du (%)	p/dp (%)	$\theta/d\theta$ (°)	$dpi/d\theta i$ (%) (°)
06/86					
$U(5)$	0.92/0.03	-0.75/0.07	1.19/0.05	160.4/ 1.4	0.05/ 1.2
$B(5)$	1.21/0.09	-1.09/0.04	1.63/0.06	159.0/ 1.2	0.03/ 0.5
$V(5)$	1.09/0.08	-0.98/0.12	1.47/0.02	159.1/ 2.8	0.04/ 0.7
$R(5)$	1.00/0.02	-0.89/0.04	1.34/0.01	159.1/ 1.0	0.03/ 0.6
$I(5)$	0.72/0.06	-0.82/0.07	1.09/0.04	155.7/ 2.2	0.06/ 1.5
08/87					
$U(7)$	0.75/0.08	-0.84/0.11	1.14/0.09	155.9/ 2.6	0.05/ 1.2
$B(7)$	1.24/0.06	-1.12/0.09	1.68/0.07	159.0/ 1.4	0.03/ 0.5
$V(7)$	1.05/0.07	-1.06/0.06	1.50/0.05	157.4/ 1.4	0.03/ 0.6
$R(5)$	0.97/0.03	-0.89/0.07	1.32/0.03	158.7/ 1.4	0.03/ 0.6
$I(5)$	0.70/0.09	-0.82/0.08	1.08/0.04	155.3/ 3.0	0.05/ 1.4
07/88					
$U(4)$	0.62/0.04	-0.65/0.03	0.90/0.04	156.9/ 0.8	0.04/ 1.4
$B(20)$	0.70/0.05	-0.81/0.04	1.08/0.04	155.4/ 1.3	0.03/ 0.8
$V(4)$	0.67/0.06	-0.79/0.04	1.04/0.06	155.0/ 1.1	0.03/ 0.9
$R(4)$	0.69/0.01	-0.71/0.02	0.99/0.01	157.1/ 0.5	0.03/ 0.8
$I(4)$	0.59/0.07	-0.66/0.11	0.89/0.13	155.9/ 0.7	0.06/ 1.9
06/89					
$U(3)$	0.53/0.13	-0.70/0.11	0.89/0.04	153.5/ 5.2	0.08/ 2.5
$B(3)$	0.86/0.08	-0.94/0.06	1.28/0.05	156.3/ 2.0	0.04/ 0.9
$V(3)$	0.55/0.05	-0.80/0.02	0.97/0.04	152.1/ 1.2	0.05/ 1.3
$R(3)$	0.52/0.04	-0.70/0.04	0.88/0.05	153.4/ 0.5	0.04/ 1.2
$I(3)$	0.38/0.15	-0.68/0.03	0.79/0.05	149.4/ 5.4	0.08/ 2.9

Table 12. o And

Date(Mo/Yr) Filter(n)	q/dq (%)	u/du (%)	p/dp (%)	$\theta/d\theta$ (°)	$dpi/d\theta i$ (%) (°)
06/86					
$U(5)$	-0.18/0.08	0.04/0.02	0.19/0.08	81.6/ 7.9	0.04/ 6.3
$B(5)$	-0.20/0.04	0.05/0.04	0.20/0.04	83.5/ 4.6	0.02/ 2.7
$V(5)$	-0.22/0.03	0.05/0.02	0.23/0.03	84.1/ 2.4	0.02/ 2.9
$R(5)$	-0.18/0.03	0.06/0.03	0.19/0.03	80.4/ 5.0	0.02/ 3.1
$I(5)$	-0.17/0.06	0.06/0.04	0.18/0.05	79.7/ 8.4	0.04/ 7.4
08/87					
$U(28)$	-0.33/0.07	-0.04/0.04	0.33/0.07	93.7/ 3.6	0.03/ 2.9
$B(28)$	-0.33/0.04	0.00/0.04	0.33/0.04	90.0/ 3.1	0.02/ 1.6
$V(28)$	-0.30/0.04	0.01/0.04	0.30/0.04	89.2/ 3.5	0.02/ 2.4
$R(5)$	-0.28/0.03	0.05/0.02	0.29/0.03	85.0/ 2.2	0.02/ 1.6
$I(5)$	-0.24/0.06	0.04/0.07	0.25/0.05	84.9/ 9.6	0.04/ 4.2
07/88					
$U(4)$	-0.20/0.05	0.02/0.04	0.21/0.05	87.6/ 6.6	0.03/ 4.6
$B(4)$	-0.35/0.02	-0.04/0.04	0.36/0.01	93.2/ 2.9	0.02/ 1.3
$V(4)$	-0.31/0.04	0.01/0.02	0.31/0.04	89.0/ 1.8	0.02/ 1.8
$R(4)$	-0.30/0.03	-0.01/0.02	0.30/0.03	90.7/ 1.8	0.02/ 1.5
$I(4)$	-0.25/0.03	0.07/0.06	0.26/0.04	82.4/ 6.2	0.04/ 4.0
06/89					
$U(3)$	-0.43/0.07	-0.03/0.04	0.43/0.07	92.1/ 2.0	0.06/ 3.9
$B(3)$	-0.31/0.07	-0.07/0.04	0.32/0.06	96.9/ 5.1	0.03/ 2.4
$V(3)$	-0.37/0.04	-0.02/0.04	0.37/0.03	91.8/ 3.0	0.03/ 2.2
$R(3)$	-0.32/0.08*	0.03/0.01	0.33/0.08	87.7/ 0.6	0.02/ 2.0
$I(3)$	-0.22/0.03	0.02/0.06	0.22/0.03	88.5/ 7.8	0.05/ 6.5

Table 13. Summary of Indications of Night-to-Night Variability

Filter dpi(%)	(#"det") / (#sets) 0.02	0.03	0.04	0.05	0.06	>0.06
Polarized Standard Stars						
U	0/ 0	0/ 0	0/ 0	0/ 0	0/ 6	0/10
B	0/ 0	1/ 6	0/ 6	0/ 2	0/ 0	0/ 2
V	0/ 0	1/12	0/ 2	0/ 2	0/ 0	0/ 0
R	2/ 12	0/ 2	0/ 0	0/ 0	0/ 0	0/ 0
I	0/ 0	0/ 2	0/10	0/ 2	0/ 0	0/ 0
TOTAL	2/ 12	2/22	0/18	0/ 6	0/ 6	0/12
Program Stars						
U	4/ 12	1/ 8	0/16	0/ 8	0/12	0/ 8
B	7/ 34	1/22	0/ 6	0/ 2	0/ 0	0/ 0
V	4/ 26	3/24	0/10	0/ 4	0/ 0	0/ 0
R	13/ 46	0/14	0/ 4	0/ 0	0/ 0	0/ 0
I	2/ 8	1/ 4	0/26	0/10	0/ 6	0/10
TOTAL	30/126	6/72	0/62	0/24	0/18	0/18

In order to establish a basis for identifying variability of the program Be stars, we must first examine the observations of polarized standard stars in Tables 3 and 4. The values obtained here are in good agreement with those of Hsu & Breger (1982), which verifies that there are no gross systematic errors. Even though most of the samples are too small for rigorous statistical analysis, it appears by inspection that either the standard stars are variable or there are sources of error other than photon counting statistics and atmospheric scintillation. Bastien et al. (1988) have published evidence that many of the stars normally used as standards for polarimetric observations (including o Sco) may be slightly variable. However, the dearth of bright stars for which the polarization has been verified constant leaves no solution (short of an extensive project to establish a better system of standard stars) other than to accept the limitation of detecting only program star variability which exceeds that of the available standard stars.

Let us tentatively adopt the criterion that variability is indicated by a value of dq or du exceeding three times dpi, and compare the results for standard stars and program stars. Such a relaxed criterion is justified by the fact that a large proportion of the observations were made in the presence of varying conditions of clouds and moonlight. All resulting "detections" are marked with asterisks in Tables 3–12.

Table 13 is a comparison of number of "detections" with number of run-averaged data sets having a given value of dpi for each filter, done separately for the standard stars and the program stars. First, there are no "detections" for either the program stars or the standard stars unless the instrumental error averages 0.03% or smaller, which implies that night-to-night variability of the Be stars is detectable only at a level of instrumental precision on which the standard stars themselves may show variations. Secondly, relative to the total numbers of measurements evaluated, there is no marked tendency for variability to appear in any particular passband. Instead, there is only the indication that variability is most likely to be "detected" at the highest level of instrumental precision. This is obviously a dangerous interpretation without absolute verification based on observations of standard stars, since the same result would be found if the precision were being overestimated.

Even with the relaxed 3 σ criterion just described, the polarized standard star 2H Cam shows 4 marginal indications of variability out of 36 trials (see Table 3), although o Sco passes all trials as constant (see Table 4). We must therefore relax the requirements even further to devise a test consistent with constancy of the standard stars.

A very conservative scheme of analysis was finally adopted, as presented in Tables 14–16. The quantities in brackets are averages in each filter over the four annual data sets for each star. All values of $<dq>$ and $<du>$ which exceed three times $<dpi>$ are flagged with asterisks as evidence of variability, and comparison of $<dp>$ and $<d\theta>$ with $<dpi>$ and $<d\theta i>$ may be used to distinguish between amplitude and position angle effects. Although the standard stars are constant by this criterion, it should be considered only a weak indicator of night-to-night variability, since it will be found to lead to a problem with the interpretation of year-to-year variability in Section 4 to follow. (The other columns of Tables 14–16 also apply to year-to-year variability and will be explained in

Section 4.) This makes it necessary to form a set of grand averages over all filters, entered in the row labeled "GAV", after which the strict criterion for night-to-night variability is that the grand average of <*dq*> or <*du*> must exceed three times the grand average of <*dpi*>. No such variability is detected for either the standard stars or the program stars. It is possible that this test may fail to identify isolated cases of small, sporadic, short term variations in polarization, but such cases simply cannot be confidently verified by comparison with the observations of standard stars in the present investigation.

4. Analysis of Year-to-Year Variability

When we begin to assess the differences among the four annual sets of data to identify year-to-year variability for each star, we should not now be surprised that the most rigorous methods indicate that the standard stars are "variable." For instance, application of the one-way analysis of variance technique to the standard star data gives a probability of 95% or greater in several cases that the annual sets of q or u measurements are not all derived from the same population.

A less stringent test is to compute the mean and standard deviation of the four annual q and u averages in each separate filter from Tables 3 and 4, then compare the standard deviations (which now represent year-to-year scatter) with three times the corresponding average instrumental errors <*dpi*>. Table 14 shows the results, including data on p and θ. This approach still yields two instances of "variability" for 2H Cam (marked with asterisks) which is the problem mentioned in Section 3: year-to-year "variability" of a standard star appears when single-filter values of <*dpi*> are used to represent the level of observational error. Forming grand averages over all filters, however, finally brings us to a conservative but valid criterion for the detection of year-to-year variability: the grand average of *dq* or *du* must exceed three times the grand average of <*dpi*>. It may be seen from the rows labeled "GAV" in Table 14 that the standard stars are judged to have constant polarization according to this test. It is for consistency with this criterion that grand averages are also used in the strict test for night-to-night variability chosen in Section 3.

The results of applying the same procedures of analysis to the Be-star data are presented in Tables 15 and 16. Even though the criterion for year-to-year variability has now been substantially relaxed to a level at which the standard stars are constant, both ζ Tau and π Aquarii can still be confidently identified as variable on this time scale, as shown by asterisks in the rows labeled "GAV".

To investigate statistically the level of confidence in the 3 σ detection criterion, consider the example of searching for variability in a set of 4 annual measurements. The value of the reduced chi-square $\chi^2_\nu = s^2/\langle\sigma_i^2\rangle = (3\sigma)^2/\sigma^2 = 9$ with 3 degrees of freedom. Referring to a table of the χ^2 distribution, this value of χ^2_ν for $\nu = 3$ corresponds to a probability of less than 0.001 that the 3 σ dispersion occurred by random chance (Bevington 1969).

5. Discussion

In keeping with the conclusions of Sections 3 and 4, a discussion of polarization variability is warranted only for the long term changes in ζ Tau and π Aqr. These are the same two stars for which long term variability was detected in Paper I. Unfortunately, the exact times at which the changes occurred are unknown because of unavoidable gaps in the time base of this monitoring program, and it is possible that they were quite abrupt. Continued monitoring, as well as research into existing archival data, may reveal behavior which has so far escaped notice.

Poeckert et al. (1979) found a negligible interstellar polarization for ζ Tau, so it is reasonable to assume that the observed polarization is intrinsic. The same authors found a significant interstellar component for π Aqr (maximum 0.46% at 498 nm with position angle 116°), so a vectorial subtraction was applied to all observations of this star to produce Table 17, which gives the resulting intrinsic polarization data. Table 18 was then constructed to summarize the variability of the intrinsic polarization of π Aqr in the format of Tables 14–16.

It should be noted that the observed changes in polarization of both ζ Tau and π Aqr, although detected by analysis of q and u, seem to be associated primarily with the amplitude of the polarization rather than with the position angle. This is usually interpreted as evidence for axisymmetry of the CE, as in the case of ω Ori (Hayes & Guinan 1984), although there are documented observations of position angle variability for some Be stars (McLean & Clarke 1979).

As emphasized in Chapters 10–13 of the detailed summary by Underhill & Doazan (1982), there is as yet no complete model which comprehensively explains the wide range of existing observations of Be stars. Current outlines of the various competing hypotheses may be found in Slettebak & Snow (1987). It is widely agreed that any model must necessarily include a time dependence in order to show how the same star can at different times take on the characteristics of three different phases: Be, Be shell, and quasi-normal B. It is also clear that, since this variability typically occurs on a time scale of years to decades, a full characterization of the Be phenomenon will require the collection of data over the longest possible period of time. In addition, it has been found that interpretations based on isolated classes of observational data tend to be at odds; one such disparity is the apparent coexistence of a cool CE indicated by visible-wavelength emission lines with a superionized wind detected by ultraviolet spectroscopy.

For the above reasons, it is suggested that the polarimetry data presented here will best be used by theoreticians in combination with observations made by different techniques and in other spectral regions in order to build a consistent picture.

I would like to thank the administration of McDonald Observatory for making observing time available for this project. I am also grateful to the technical staff for continual support in maintaining the polarimeter. Helpful comments by the referee are respectfully acknowledged.

REFERENCES

Bastien, P., Drissen, L., Menard, F., Moffat, A.F.J., Robert, C., & St-Louis, N. 1988, AJ, 95, 900

Bevington, P.R. 1969, Data Reduction and Error Analysis for the Physical Sciences (New York: McGraw-Hill), 194

Breger, M. 1979, ApJ, 233, 97

Brown, J.C. & McLean, I.S. 1977, A&A, 57, 141

Brown, J.C., McLean, I.S., & Emslie, A.G. 1978, A&A, 68, 415

Clarke, D. & Stewart, B.G. 1986, Vistas Astron., 29, 27

Coyne, G.V. 1976, in IAU Symp. 70, Be and Shell Stars, ed. Slettebak, A. (Dordrecht: Reidel), 233

Coyne, G.V. & Gehrels, T. 1967, AJ, 72, 887

Coyne, G.V. & McLean, I.S. 1982, in IAU Symp. 98, Be Stars, ed. Jaschek, M. and Groth, H. (Dordrecht: Reidel), 77

Hayes, D.P. & Guinan, E.F. 1984, ApJ, 279, 721

Hoffleit, D. & Jaschek, C. 1982, The Bright Star Catalog, 4th Revised Edition (New Haven: Yale University Observatory)

Hsu, J.C. & Breger, M. 1982, ApJ, 262, 732

McDavid, D. 1986, PASP, 98, 572

McLean, I.S. 1979, MNRAS, 186, 265

McLean, I.S. & Brown, J.C 1978, A&A, 69, 291

McLean, I.S. & Clarke, D. 1979, MNRAS, 186, 245

Poeckert, R., Bastien, P., & Landstreet, J.D. 1979, AJ, 84, 812

Poeckert, R. & Marlborough, J.M. 1978, ApJ, 220, 940

Slettebak, A. 1982, ApJS, 50, 55

Slettebak, A. 1988, PASP, 100, 770

Slettebak, A. & Snow, T.P., ed. 1987, IAU Coll. 92, Physics of Be Stars (Cambridge: Cambridge University Press)

Underhill, A. & Doazan, V. 1982, B Stars With and Without Emission Lines (Washington: NASA)

Young, A.T. 1967, AJ, 72, 747

Table 14. Polarized Standard Star Summary

Star Filter	q/dq (%)	<dq> (%)	u/du (%)	<du> (%)	p/dp (%)	<dp> (%)	$\theta/d\theta$ (°)	<$d\theta$> (°)	<dpi> (%)	<$d\theta i$> (°)
2H Cam										
U	-1.93/0.12	0.09	-2.38/0.11	0.09	3.06/0.16	0.07	115.4/ 0.6	0.9	0.06	0.6
B	-2.02/0.10*	0.08	-2.60/0.02	0.05	3.29/0.06	0.05	116.1/ 0.7	0.8	0.03	0.2
V	-2.12/0.09	0.06	-2.76/0.06	0.05	3.48/0.06	0.05	116.3/ 0.8	0.5	0.03	0.2
R	-2.00/0.12*	0.05	-2.63/0.04	0.05	3.31/0.08	0.04	116.4/ 0.8	0.4	0.02	0.2
I	-1.76/0.07	0.05	-2.35/0.08	0.06	2.94/0.05	0.06	116.6/ 0.9	0.5	0.04	0.4
GAV	0.10	0.07	0.06	0.06	0.08	0.05	0.8	0.6	0.04	0.3
o Sco										
U	1.31/0.10	0.25	2.58/0.10	0.20	2.90/0.11	0.25	31.7/ 0.8	2.0	0.17	1.7
B	1.54/0.04	0.08	3.07/0.03	0.05	3.43/0.02	0.06	31.6/ 0.4	0.6	0.05	0.5
V	1.84/0.05	0.04	3.74/0.03	0.05	4.17/0.03	0.05	31.9/ 0.4	0.2	0.04	0.2
R	1.95/0.06	0.04	3.93/0.02	0.04	4.39/0.03	0.02	31.8/ 0.4	0.2	0.02	0.1
I	1.90/0.06	0.05	3.86/0.04	0.02	4.31/0.05	0.03	31.9/ 0.4	0.4	0.04	0.2
GAV	0.06	0.09	0.04	0.07	0.05	0.08	0.5	0.7	0.06	0.5

Table 15. Winter Be Star Summary

Star Filter	q/dq (%)	<dq> (%)	u/du (%)	<du> (%)	p/dp (%)	<dp> (%)	$\theta/d\theta$ (°)		<$d\theta$> (°)	<dpi> (%)	<$d\theta i$> (°)
γ Cas											
U	-0.50/0.08*	0.05	-0.29/0.05	0.07*	0.59/0.10	0.05	104.9/	0.5	3.4	0.02	0.8
B	-0.69/0.05	0.05	-0.43/0.05	0.04	0.82/0.06	0.06	105.9/	1.8	1.4	0.02	0.4
V	-0.64/0.05	0.06	-0.37/0.03	0.04	0.74/0.05	0.06	105.1/	0.3	1.6	0.02	0.5
R	-0.56/0.04	0.06	-0.23/0.03	0.06	0.61/0.05	0.06	101.2/	1.2	3.1	0.02	0.4
I	-0.49/0.03	0.07*	-0.20/0.03	0.05	0.53/0.02	0.07	101.1/	1.9	2.8	0.02	1.1
GAV	0.05	0.06	0.04	0.05	0.06	0.06		1.1	2.5	0.02	0.6
ϕ Per											
U	0.12/0.09	0.06	0.79/0.09	0.08	0.81/0.11	0.08	41.1/	2.8	2.2	0.04	1.4
B	0.48/0.06	0.07*	1.22/0.06	0.06	1.31/0.07	0.06	34.2/	0.7	1.3	0.02	0.5
V	0.38/0.04	0.08*	1.07/0.06	0.08*	1.14/0.06	0.08	35.0/	1.2	2.0	0.02	0.6
R	0.36/0.06	0.07*	1.04/0.05	0.05	1.11/0.06	0.05	35.3/	1.4	1.8	0.02	0.6
I	0.20/0.06	0.08	0.78/0.03	0.05	0.81/0.04	0.05	37.9/	2.2	2.8	0.04	1.6
GAV	0.06	0.07	0.06	0.07	0.07	0.07		1.7	2.0	0.03	0.9
48 Per											
U	0.73/0.08	0.05	-0.21/0.09	0.05	0.76/0.05	0.05	172.0/	4.1	2.1	0.04	1.6
B	0.82/0.04	0.03	-0.25/0.06	0.05	0.85/0.03	0.04	171.6/	2.2	1.4	0.02	0.8
V	0.91/0.03	0.03	-0.25/0.05	0.08	0.95/0.03	0.04	172.4/	1.3	2.4	0.03	0.8
R	0.94/0.04	0.04	-0.20/0.04	0.05	0.96/0.05	0.04	173.9/	0.8	1.7	0.02	0.6
I	0.87/0.06	0.08	-0.18/0.01	0.06	0.89/0.06	0.07	173.9/	0.3	2.2	0.05	1.7
GAV	0.05	0.05	0.05	0.06	0.05	0.04		1.7	2.0	0.03	1.1
ζ Tau											
U	0.44/0.06	0.05	1.00/0.07	0.09	1.10/0.07	0.09	33.1/	1.7	1.4	0.03	0.7
B	0.62/0.06	0.05	1.36/0.14*	0.09*	1.50/0.14	0.08	32.8/	1.0	1.1	0.02	0.3
V	0.57/0.04	0.06	1.25/0.12*	0.07*	1.37/0.13	0.08	32.8/	0.3	1.0	0.02	0.4
R	0.52/0.02	0.07*	1.21/0.13*	0.09*	1.32/0.12	0.09	33.2/	1.1	1.5	0.02	0.3
I	0.42/0.06	0.08	0.96/0.11*	0.06	1.05/0.12	0.06	33.1/	1.4	2.3	0.03	0.9
GAV	0.05	0.06	0.11*	0.08	0.11	0.08		1.1	1.4	0.03	0.5

Table 16. Summer Be Star Summary

Star Filter	q/dq (%)	<dq> (%)	u/du (%)	<du> (%)	p/dp (%)	<dp> (%)	$\theta/d\theta$ (°)		<$d\theta$> (°)	<dpi> (%)	<$d\theta i$> (°)
48 Lib											
U	-0.40/0.09	0.09	-0.48/0.13	0.13	0.64/0.09	0.09	114.8/	5.8	5.4	0.08	3.5
B	-0.42/0.03	0.05	-0.72/0.10	0.05	0.84/0.08	0.04	119.6/	2.4	1.9	0.04	1.3
V	-0.55/0.03	0.05	-0.67/0.08	0.08	0.88/0.04	0.05	115.0/	2.6	2.4	0.04	1.4
R	-0.53/0.03	0.06	-0.58/0.09	0.05	0.80/0.04	0.05	113.8/	3.2	1.7	0.03	1.2
I	-0.54/0.10	0.08	-0.58/0.08	0.06	0.79/0.09	0.09	113.7/	3.1	1.9	0.07	2.7
GAV	0.06	0.07	0.10	0.07	0.07	0.06		3.4	2.7	0.05	2.0
χ Oph											
U	-0.04/0.06	0.04	-0.38/0.06	0.06	0.39/0.06	0.06	131.9/	3.6	3.4	0.07	5.4
B	-0.06/0.03	0.04	-0.50/0.02	0.05	0.50/0.02	0.05	131.6/	1.8	2.4	0.03	1.9
V	-0.08/0.01	0.06	-0.51/0.02	0.03	0.52/0.02	0.04	130.5/	0.8	3.2	0.03	1.8
R	0.03/0.02	0.04	-0.39/0.02	0.05	0.39/0.01	0.04	137.0/	1.8	3.3	0.02	1.7
I	-0.03/0.05	0.07	-0.52/0.04	0.07	0.52/0.04	0.06	133.0/	2.8	4.5	0.04	2.3
GAV	0.03	0.05	0.03	0.05	0.03	0.05		2.2	3.4	0.04	2.7
π Aqr											
U	0.70/0.17*	0.07	-0.73/0.08	0.08	1.03/0.16	0.05	156.7/	2.9	2.5	0.05	1.6
B	1.00/0.27*	0.07	-0.99/0.14*	0.06	1.42/0.29	0.05	157.4/	1.9	1.5	0.03	0.7
V	0.84/0.27*	0.07	-0.91/0.13*	0.06	1.25/0.28	0.04	155.9/	3.0	1.6	0.04	0.9
R	0.80/0.23*	0.02	-0.80/0.11*	0.04	1.13/0.23	0.02	157.1/	2.6	0.9	0.03	0.8
I	0.60/0.16	0.09	-0.75/0.09	0.07	0.96/0.15	0.06	154.1/	3.1	2.8	0.06	1.9
GAV	0.22*	0.06	0.11	0.06	0.22	0.05		2.7	1.9	0.04	1.2
o And											
U	-0.28/0.12	0.07	-0.00/0.04	0.03	0.29/0.11	0.07	88.8/	5.4	5.0	0.04	4.4
B	-0.30/0.07*	0.04	-0.01/0.05	0.04	0.30/0.07	0.04	90.9/	5.7	3.9	0.02	2.0
V	-0.30/0.06	0.04	0.01/0.03	0.03	0.30/0.06	0.04	88.5/	3.2	2.7	0.02	2.3
R	-0.27/0.06	0.04	0.03/0.03	0.02	0.28/0.06	0.04	85.9/	4.4	2.4	0.02	2.0
I	-0.22/0.04	0.04	0.05/0.02	0.06	0.23/0.04	0.04	83.9/	3.7	8.0	0.04	5.5
GAV	0.07	0.05	0.03	0.04	0.07	0.05		4.5	4.4	0.03	3.3

Table 17. π Aqr Intrinsic Polarization

Date(Mo/Yr) Filter(n)	q/dq (%)	u/du (%)	p/dp (%)	$\theta/d\theta$ (°)	$dpi/d\theta i$ (%) (°)
06/86					
$U(5)$	1.17/0.03	-0.43/0.07	1.25/0.04	170.0/ 1.5	0.05/ 1.1
$B(5)$	1.49/0.09	-0.74/0.04	1.66/0.08	166.8/ 1.0	0.03/ 0.5
$V(5)$	1.37/0.08	-0.62/0.12	1.51/0.03	167.8/ 2.7	0.04/ 0.7
$R(5)$	1.27/0.02	-0.56/0.04	1.38/0.01	168.1/ 1.0	0.03/ 0.6
$I(5)$	0.94/0.06	-0.53/0.07	1.08/0.03	165.2/ 2.3	0.06/ 1.5
08/87					
$U(7)$	1.01/0.08	-0.52/0.11	1.14/0.08	166.4/ 2.8	0.05/ 1.2
$B(7)$	1.52/0.06	-0.77/0.09	1.70/0.07	166.6/ 1.4	0.03/ 0.5
$V(7)$	1.33/0.07	-0.70/0.06	1.51/0.06	166.1/ 1.3	0.03/ 0.6
$R(5)$	1.23/0.03	-0.55/0.07	1.35/0.02	167.9/ 1.5	0.03/ 0.6
$I(5)$	0.92/0.09	-0.54/0.08	1.07/0.06	164.8/ 2.8	0.05/ 1.4
07/88					
$U(4)$	0.88/0.04	-0.33/0.03	0.94/0.04	169.8/ 0.7	0.04/ 1.4
$B(20)$	0.98/0.05	-0.46/0.04	1.08/0.04	167.5/ 1.3	0.03/ 0.8
$V(4)$	0.95/0.06	-0.44/0.04	1.04/0.06	167.7/ 0.8	0.03/ 0.9
$R(4)$	0.96/0.01	-0.38/0.02	1.03/0.01	169.3/ 0.5	0.03/ 0.7
$I(4)$	0.81/0.07	-0.38/0.11	0.90/0.11	167.7/ 2.4	0.06/ 1.9
06/89					
$U(3)$	0.78/0.13	-0.38/0.11	0.88/0.09	166.9/ 4.5	0.08/ 2.5
$B(3)$	1.14/0.08	-0.58/0.06	1.28/0.06	166.4/ 1.7	0.04/ 0.9
$V(3)$	0.83/0.05	-0.44/0.02	0.94/0.05	165.9/ 0.8	0.05/ 1.4
$R(3)$	0.79/0.04	-0.36/0.04	0.87/0.05	167.6/ 0.9	0.04/ 1.2
$I(3)$	0.60/0.15	-0.40/0.03	0.73/0.12	162.9/ 4.2	0.08/ 3.2

Table 18. π Aqr Intrinsic Polarization Summary

Star Filter	q/dq (%)	<dq> (%)	u/du (%)	<du> (%)	p/dp (%)	<dp> (%)	$\theta/d\theta$ (°)	<$d\theta$> (°)	<dpi> (%)	<$d\theta i$> (°)
π Aqr										
U	0.96/0.17*	0.07	-0.41/0.08	0.08	1.05/0.17	0.06	168.3/ 1.9	2.4	0.05	1.6
B	1.28/0.27*	0.07	-0.64/0.14*	0.06	1.43/0.30	0.06	166.8/ 0.5	1.4	0.03	0.7
V	1.12/0.27*	0.07	-0.55/0.13*	0.06	1.25/0.30	0.05	166.9/ 1.0	1.4	0.04	0.9
R	1.06/0.23*	0.02	-0.46/0.11*	0.04	1.16/0.25	0.02	168.2/ 0.7	1.0	0.03	0.8
I	0.82/0.16	0.09	-0.46/0.08	0.07	0.95/0.17	0.08	165.1/ 2.0	2.9	0.06	2.0
GAV	0.22*	0.06	0.11	0.06	0.24	0.06	1.2	1.8	0.04	1.2

Chapter 4

Multicolor Polarimetry of Selected Be Stars: 1990–93

(originally published in 1994 PASP, 106, 949)

ABSTRACT

Optical polarization data in the *UBVRI* filter system for eight bright northern Be stars are presented here as the continuation of a long term monitoring project begun in 1984. There are no strong cases of night-to-night variability, and the only star showing unmistakable changes in polarization from year to year over the nine years covered by the program is Pi Aquarii. Even though the observed sample spans a wide range in spectral type, $v \sin i$, and degree of intrinsic polarization, the normalized wavelength dependence of the polarization is surprisingly similar for all of the stars. Analysis of the wavelength dependence of the variable polarization of π Aqr in terms of a simple equatorial disk model suggests that changes in the circumstellar electron number density alone may be sufficient to account for the observations, but it is not clear what real physical mechanism is involved.

1. Introduction

This paper is the third installment in a series reporting on the progress of a long term project to annually monitor the broad band optical linear polarization of several bright Be stars observable from northern latitudes. The purpose of the project is to accumulate a data base which can be analyzed together with multiwavelength spectroscopy and photometry by other observers to constrain and test hypotheses about the origin of the "Be phenomenon": sporadic mass loss by rapidly rotating B stars on unpredictable time scales ranging from days to decades, which gives rise to a circumstellar envelope producing emission lines, polarization, and ultraviolet and infrared excesses. The first installment of the series (McDavid 1986, hereafter Paper I) tied the observational system

to previous measurements from the literature, and the second installment (McDavid 1990, hereafter Paper II) reported data from the next four years, with a clear detection of year-to-year variability for Zeta Tauri and Pi Aquarii.

For the unfamiliar reader, an excellent general summary of the field of Be-star research is the review by Slettebak (1988). Many of the recent developments can be found in Balona, Henrichs, & Le Contel (1994), and several background references dealing specifically with polarimetry of Be stars are given in Papers I and II.

Capps, Coyne, & Dyck (1973) showed that the intrinsic polarization of Be stars could be explained by electron scattering in the circumstellar envelopes or extended atmospheres, with a wavelength dependence due to absorption and emission by partially ionized hydrogen. This model and later refinements (Brown & McLean 1977; Fox 1991), together with spectroscopic evidence for rapid rotation, still provide the strongest arguments that the envelopes must be equatorially flattened in order to give the observed intrinsic polarization, which can be as large as 2%.

In practice, polarization is a useful, but problematic, indicator of physical conditions in the envelopes or extended atmospheres of Be stars, because the models have too many free parameters to fit uniquely based on polarimetry alone. For example, Poeckert & Marlborough (1978) required the mutual constraints of continuum and Hα polarimetry, high-resolution Hα and Hβ line profiles, and visible, infrared, and radio continuum flux measurements to compute a detailed model for the envelope of Gamma Cassiopeiae. They concluded that their solution was lacking in part because the observations were not simultaneous, pointing out the complication that most of the observable quanitites are unpredictably variable with time and notoriously difficult to correlate.

While most recent work has been based on brief "snapshots" with relatively high spectral and time resolution, routine polarization monitoring with broad band filters is still useful to maintain the longest possible time base of continuous systematic observations for the study of long term variability, which is the most perplexing problem of the Be stars. Tables containing all of the annual observations reported in this paper, combined with the data from Papers I and II, will be included in Vol. 3 of the AAS CD-ROM Series.

Table 1. Program Be Stars

Name	HD	HR	V	Spectral Type	$v \sin i$ (km s^{-1})
γ Cas	5394	264	2.47	B0.5 IVe	230
ϕ Per	10516	496	4.07	B1.5 (V:)e-shell	400
48 Per	25940	1273	4.04	B4 Ve	200
ζ Tau	37202	1910	3.00	B1 IVe-shell	220
48 Lib	142983	5941	4.88	B3:IV:e-shell	400
χ Oph	148184	6118	4.42	B1.5 Ve	140
π Aqr	212571	8539	4.66	B1 III-IVe	300
o And	217675	8762	3.62	B6 III	260

Table 2. Filter System Parameters

Filter	Effective Wavelength (Å)	Bandpass (fwhm) (Å)
U	3650	700
B	4400	1000
V	5500	900
R	6400	1500
I	7900	1500

Table 3. 2H Cam (Standard Star)

Date(Mo/Yr) Filter(n)	q/dq (%)	u/du (%)	p/dp (%)	$\theta/d\theta$ (°)	$dpi/d\theta i$ (%) (°)
01/90					
$U(6)$	-1.86/0.10	-2.41/0.12	3.04/0.08	116.2/ 1.3	0.07/ 0.7
$B(6)$	-1.99/0.07	-2.56/0.05	3.24/0.06	116.0/ 0.5	0.03/ 0.3
$V(6)$	-2.09/0.05	-2.74/0.04	3.44/0.03	116.3/ 0.4	0.03/ 0.3
$R(6)$	-1.99/0.08	-2.66/0.06	3.32/0.07	116.6/ 0.5	0.03/ 0.3
$I(6)$	-1.75/0.06	-2.31/0.06	2.90/0.07	116.4/ 0.3	0.05/ 0.5
12/90					
$U(4)$	-1.86/0.13	-2.39/0.07	3.03/0.12	116.1/ 0.9	0.11/ 1.0
$B(4)$	-1.92/0.08	-2.70/0.09	3.32/0.06	117.3/ 1.0	0.05/ 0.4
$V(4)$	-2.07/0.11	-2.74/0.05	3.44/0.10	116.5/ 0.6	0.04/ 0.4
$R(4)$	-1.92/0.04	-2.62/0.05	3.25/0.03	116.9/ 0.5	0.04/ 0.3
$I(4)$	-1.78/0.08	-2.41/0.07	3.00/0.08	116.8/ 0.6	0.06/ 0.6
12/91					
$U(5)$	-1.75/0.22	-2.45/0.07	3.02/0.10	117.3/ 2.0	0.09/ 0.9
$B(5)$	-1.95/0.06	-2.50/0.06	3.17/0.07	116.0/ 0.4	0.04/ 0.4
$V(5)$	-2.14/0.05	-2.71/0.12	3.46/0.08	115.8/ 0.8	0.04/ 0.4
$R(5)$	-2.06/0.04	-2.64/0.07	3.34/0.04	116.0/ 0.6	0.03/ 0.3
$I(5)$	-1.66/0.17	-2.39/0.11	2.91/0.13	117.7/ 1.6	0.06/ 0.6
01/93					
$U(2)$	-1.83/0.01	-2.40/0.03	3.02/0.04	116.3/ 0.1	0.08/ 0.8
$B(2)$	-2.03/0.06	-2.63/0.08	3.32/0.03	116.1/ 0.9	0.04/ 0.3
$V(2)$	-1.99/0.07	-2.74/0.05	3.39/0.08	117.0/ 0.2	0.04/ 0.4
$R(2)$	-1.91/0.03	-2.74/0.06	3.34/0.07	117.6/ 0.1	0.03/ 0.2
$I(2)$	-1.81/0.05	-2.34/0.02	2.96/0.02	116.1/ 0.5	0.05/ 0.5

Note: Tables containing all of the annual observations reported in this paper, combined with the data from Papers I and II, will be included in Vol. 3 of the AAS CD-ROM Series.

Table 4. o Sco (Standard Star)

Date(Mo/Yr) Filter(n)	q/dq (%)	u/du (%)	p/dp (%)	$\theta/d\theta$ (°)	$dpi/d\theta i$ (%) (°)
05/90					
$U(10)$	1.26/0.22	2.68/0.28	2.96/0.30	32.4/ 1.7	0.18/ 1.8
$B(9)$	1.44/0.08	3.12/0.05	3.44/0.06	32.7/ 0.6	0.06/ 0.5
$V(11)$	1.84/0.07	3.76/0.05	4.18/0.07	32.0/ 0.4	0.06/ 0.4
$R(9)$	1.90/0.05	4.01/0.04	4.44/0.04	32.3/ 0.3	0.03/ 0.2
$I(9)$	1.75/0.07	3.90/0.08	4.27/0.09	32.9/ 0.4	0.05/ 0.3
08/91					
$U(2)$	1.66/0.22	2.45/0.17	2.96/0.27	28.0/ 0.9	0.19/ 1.9
$B(2)$	1.49/0.01	2.88/0.08	3.24/0.07	31.4/ 0.4	0.06/ 0.5
$V(2)$	1.84/0.01	3.74/0.01	4.17/0.01	31.9/ 0.1	0.04/ 0.3
$R(2)$	2.02/0.02	3.92/0.03	4.41/0.02	31.3/ 0.2	0.03/ 0.2
$I(2)$	1.79/0.02	3.81/0.05	4.21/0.04	32.4/ 0.3	0.04/ 0.3
07/92					
$U(4)$	1.27/0.11	2.44/0.27	2.75/0.26	31.2/ 1.3	0.19/ 2.0
$B(4)$	1.23/0.09	3.21/0.09	3.44/0.08	34.5/ 0.8	0.06/ 0.5
$V(4)$	1.47/0.09	3.88/0.07	4.15/0.08	34.6/ 0.5	0.04/ 0.3
$R(4)$	1.59/0.02	4.07/0.03	4.37/0.02	34.3/ 0.2	0.03/ 0.2
$I(4)$	1.51/0.09	3.96/0.03	4.24/0.05	34.6/ 0.6	0.05/ 0.3
06/93					
$U(7)$	1.22/0.24	2.45/0.28	2.74/0.28	31.8/ 2.7	0.24/ 2.6
$B(7)$	1.46/0.18	3.08/0.08	3.42/0.06	32.3/ 1.6	0.08/ 0.6
$V(7)$	2.08/0.30[a]	3.59/0.19	4.15/0.23	30.0/ 1.9	0.07/ 0.4
$R(7)$	2.12/0.18[a]	3.85/0.22[a]	4.40/0.10	30.5/ 1.8	0.05/ 0.3
$I(7)$	1.97/0.09	3.87/0.09	4.34/0.11	31.5/ 0.4	0.05/ 0.3

[a] dq or $du > 3dpi$: weak night-to-night variability (See Section 3.1.)

2. Observations

In keeping with the purpose of extending the long term data base, the program stars selected for this project have all been widely observed since the earliest days of Be-star polarimetry. They are listed in Table 1, with visual magnitudes taken from Hoffleit & Jaschek (1982) and spectral types and $v\,sin\,i$ values from Slettebak (1982).

The observations were made with the polarimeter described by Breger (1979), mounted on the 0.9 m telescope at the University of Texas McDonald Observatory. The *UBVRI* passbands, given in Table 2, were determined by a set of broad band filters, a neutral density filter of 10% transmission, and an EMI 9658AR S-20 photomultiplier tube cooled with dry ice. There has been no change in this instrumental system since the beginning of the project in 1984. The data reported here were acquired from 1990 through 1993 during one week in the winter and one week in the summer of each year.

The measurements were corrected for sky background polarization (significant because many were made with some moonlight) and also for instrumental polarization on the order of 0.10%, determined by repeated observations of unpolarized standard stars from the list of Serkowksi (1974). Position angles were calibrated by observations of polarized standard stars from the list of Hsu & Breger (1982). The polarized standard stars 2H Camelopardalis (HD 21291, HR 1035, $V = 4.21$, B9 Ia) and Omicron Scorpii (HD 147084, HR 6081, $V = 4.54$, A5 II) were also observed regularly during the winter and summer runs, repectively, as checks on the stability of the system.

3. Analysis of variability

The data are presented in Tables 3–12, with the same format as in Paper II. The columns give: first, approximate date (month/year) of the observing run, filter designation, and number (n) of repeated observations; second and third, mean and standard deviation of the normalized Stokes parameters q and u; fourth and fifth, mean and standard deviation of the polarization amplitude p and position angle θ, with no debiasing corrections (Clarke & Stewart 1986), and sixth, mean instrumental error dpi in polarization amplitude for each set of measurements according to photon statistics, unless photon statistics gives a value less than 0.02%, in which case the error is approximated as 0.02% due to atmospheric scintillation for the 200-second integration time (Young 1967), and the corresponding mean instrumental error in polarization position angle, based on the relation $d\theta i = 28\overset{\circ}{.}65(dpi/p)$.

Following the same method as in Paper II, Tables 13–15 were constructed to be used in addition to Tables 3–12 to determine what kinds of variability can be identified in the observations. These "Summary" tables give the mean and standard deviation of the normalized Stokes parameters for each star in each filter over the four annual data sets. The quantities in angled brackets are averages over the four annual data sets, and the quantities in rows labeled "GAV" for "grand average" are averages over all five filters.

As advised in Clarke & Stewart (1986), the main parameters used to assess variability are q and u, since p and θ are biased. However, the statistics of p and θ are also presented since they may help to distinguish between amplitude and position-angle variability. It should be kept in mind that the samples treated here are actually too small to be treated with rigorous statistical tests, but we can nevertheless hope to derive some useful information from a simple analysis.

3.1. Night-to-night variability

The repeated observations in Tables 3–12 were usually made on separate nights, so the scatter over a given run in these tables reflects variability on a night-to-night time scale. As the simplest possible test, any values of dq or du exceeding three times dpi are flagged by footnote marks "a" as evidence for 3 σ variability. This leads to the embarrassment that the polarized standard o Sco is variable (Table 4). Since this star shows more scatter than most of the program stars, it is reasonable to agree with Bastien et al. (1988) that it may indeed be variable in both amplitude and position angle. Program Be stars that may also be variable at this level are γ Cas, ϕ Per, ζ Tau, and o And, but the indications must be considered weak without more reliable standard star results.

The stronger requirement that <dq> or <du> exceed three times <dpi> for a single filter in Tables 13–15 seems to be a valid criterion, since it is consistent with the condition of no variability of either standard star. In contrast with the situation in Paper II, this second-level or single-filter approach is also valid for analyzing year-to-year variability, as will be seen in the next subsection. The only restriction involved is that short term variability which is continuous over time rather than episodic is more likely to be detected. The only program star variable at this level is ϕ Per, flagged by a footnote mark "b" in Table 14.

The strongest criterion for night-to-night variability, which was necessary in Paper II, is that the grand average of <dq> or <du> must exceed three times the grand average of <dpi> in Tables 13–15. This imposes the additional restriction that short-term variability not be confined to a narrow range of wavelengths. None of the stars observed is variable at this level.

3.2. Year-to-year variability

The most obvious approach to identifying year-to-year variability is to look in Tables 13–15 for values of dq and du greater than three times <dpi>. The standard stars are constant by this test (which they were not in Paper II), but there is evidence for variability of γ Cas, ϕ Per, ζ Tau, and π Aqr, as flagged by footnote marks "c". Thus the same program stars are found to be variable at this level as in Paper II, with the exception of o And.

Table 5. γ Cas

Date(Mo/Yr) Filter(n)	q/dq (%)	u/du (%)	p/dp (%)	$\theta/d\theta$ (°)	$dpi/d\theta i$ (%) (°)
01/90					
$U(5)$	-0.48/0.09[a]	-0.25/0.06	0.54/0.08	103.9/ 3.6	0.02/ 1.1
$B(5)$	-0.62/0.04	-0.43/0.03	0.75/0.04	107.4/ 0.6	0.02/ 0.8
$V(5)$	-0.60/0.07[a]	-0.38/0.04	0.71/0.05	106.3/ 2.6	0.02/ 0.8
$R(5)$	-0.51/0.03	-0.23/0.02	0.56/0.03	102.3/ 1.2	0.02/ 1.0
$I(5)$	-0.46/0.06	-0.24/0.06	0.52/0.08	103.4/ 1.2	0.02/ 1.3
12/90					
$U(4)$	-0.42/0.04	-0.23/0.02	0.48/0.03	104.3/ 2.1	0.04/ 2.4
$B(4)$	-0.64/0.04	-0.45/0.06	0.78/0.06	107.6/ 1.2	0.02/ 0.7
$V(4)$	-0.59/0.05	-0.38/0.06	0.70/0.05	106.6/ 2.3	0.03/ 1.2
$R(4)$	-0.52/0.06	-0.22/0.02	0.57/0.06	101.8/ 1.8	0.02/ 1.2
$I(4)$	-0.49/0.04	-0.30/0.06	0.58/0.06	105.4/ 2.5	0.04/ 2.1
12/91					
$U(5)$	-0.36/0.05	-0.31/0.06	0.48/0.04	110.6/ 4.0	0.02/ 1.2
$B(5)$	-0.66/0.03	-0.33/0.04	0.74/0.02	103.4/ 1.9	0.02/ 0.8
$V(5)$	-0.65/0.04	-0.30/0.03	0.72/0.04	102.4/ 1.5	0.02/ 0.8
$R(5)$	-0.55/0.03	-0.23/0.04	0.59/0.05	101.2/ 1.2	0.02/ 1.0
$I(5)$	-0.44/0.06	-0.27/0.05	0.52/0.04	105.8/ 3.8	0.03/ 1.5
01/93					
$U(3)$	-0.52/0.00	-0.29/0.08[a]	0.60/0.03	104.5/ 3.4	0.02/ 0.9
$B(3)$	-0.84/0.02	-0.50/0.09[a]	0.98/0.06	105.3/ 2.4	0.02/ 0.6
$V(3)$	-0.62/0.05	-0.34/0.03	0.71/0.03	104.7/ 2.0	0.02/ 0.8
$R(3)$	-0.52/0.05	-0.41/0.03	0.66/0.02	109.3/ 2.2	0.02/ 0.9
$I(3)$	-0.66/0.02	-0.21/0.07	0.69/0.03	98.6/ 2.5	0.03/ 1.4

[a] dq or $du > 3dpi$: weak night-to-night variability (See Section 3.1.)

Table 6. ϕ Per

Date(Mo/Yr) Filter(n)	q/dq (%)	u/du (%)	p/dp (%)	$\theta/d\theta$ (°)	$dpi/d\theta i$ (%) (°)
01/90					
$U(5)$	0.15/0.04	0.80/0.08	0.81/0.08	39.6/ 0.9	0.04/ 1.4
$B(5)$	0.52/0.04	1.22/0.03	1.32/0.04	33.5/ 0.9	0.02/ 0.5
$V(5)$	0.36/0.07	1.06/0.04	1.12/0.06	35.6/ 1.6	0.03/ 0.7
$R(5)$	0.33/0.07[a]	1.03/0.07[a]	1.08/0.07	36.2/ 1.7	0.02/ 0.6
$I(5)$	0.22/0.06	0.73/0.08	0.76/0.07	36.4/ 2.4	0.05/ 2.0
12/90					
$U(4)$	0.14/0.05	0.84/0.12	0.85/0.12	40.3/ 1.9	0.06/ 2.0
$B(4)$	0.40/0.07	1.08/0.04	1.16/0.05	34.8/ 1.4	0.03/ 0.7
$V(4)$	0.26/0.05	0.98/0.06	1.02/0.05	37.5/ 1.6	0.04/ 1.1
$R(4)$	0.26/0.04	1.02/0.07	1.05/0.06	37.8/ 1.4	0.03/ 0.8
$I(4)$	0.22/0.12	0.74/0.12	0.79/0.08	36.3/ 5.6	0.07/ 2.6
12/91					
$U(5)$	0.14/0.08	0.76/0.14	0.78/0.14	39.7/ 3.1	0.05/ 1.8
$B(5)$	0.44/0.03	1.29/0.13[a]	1.36/0.12	35.6/ 1.1	0.03/ 0.6
$V(5)$	0.34/0.09	1.05/0.08	1.11/0.08	36.1/ 2.2	0.04/ 0.9
$R(5)$	0.31/0.04	1.01/0.07	1.06/0.08	36.5/ 1.0	0.03/ 0.8
$I(5)$	0.21/0.08	0.65/0.07	0.68/0.07	36.2/ 3.1	0.06/ 2.7
01/93					
$U(2)$	0.05/0.12	0.68/0.34[a]	0.69/0.32	41.4/ 6.6	0.07/ 3.4
$B(2)$	0.28/0.06	1.18/0.17[a]	1.21/0.18	38.4/ 0.4	0.03/ 0.8
$V(2)$	0.31/0.07	1.04/0.26[a]	1.08/0.27	36.6/ 0.3	0.03/ 0.9
$R(2)$	0.29/0.02	0.84/0.09	0.89/0.07	35.4/ 1.6	0.03/ 0.9
$I(2)$	0.13/0.08	0.73/0.04	0.74/0.05	40.1/ 2.7	0.07/ 2.7

[a] dq or $du > 3dpi$: weak night-to-night variability (See Section 3.1.)

Table 7. 48 Per

Date(Mo/Yr) Filter(n)	q/dq (%)	u/du (%)	p/dp (%)	$\theta/d\theta$ (°)	$dpi/d\theta i$ (%) (°)
01/90					
$U(6)$	0.79/0.08	-0.20/0.06	0.82/0.07	172.9/ 2.4	0.05/ 1.6
$B(6)$	0.85/0.04	-0.27/0.04	0.90/0.04	171.1/ 1.3	0.02/ 0.8
$V(6)$	0.95/0.03	-0.28/0.05	0.99/0.03	171.8/ 1.5	0.03/ 0.8
$R(6)$	0.97/0.02	-0.24/0.04	1.00/0.02	173.0/ 1.1	0.02/ 0.7
$I(6)$	0.79/0.06	-0.26/0.07	0.84/0.04	170.9/ 2.9	0.05/ 1.8
12/90					
$U(4)$	0.71/0.13	-0.16/0.06	0.74/0.11	173.4/ 3.3	0.06/ 2.5
$B(4)$	0.90/0.04	-0.24/0.03	0.93/0.04	172.5/ 1.0	0.03/ 0.9
$V(4)$	1.00/0.04	-0.23/0.08	1.03/0.05	173.6/ 2.1	0.04/ 1.2
$R(4)$	0.92/0.06	-0.20/0.03	0.94/0.06	173.9/ 0.9	0.04/ 1.1
$I(4)$	0.88/0.12	-0.26/0.08	0.92/0.13	171.6/ 2.4	0.08/ 2.6
12/91					
$U(5)$	0.83/0.09	-0.30/0.08	0.88/0.10	169.9/ 1.8	0.06/ 2.1
$B(5)$	0.82/0.06	-0.24/0.01	0.85/0.06	172.0/ 0.5	0.04/ 1.3
$V(5)$	0.90/0.03	-0.25/0.12	0.94/0.05	172.5/ 3.4	0.04/ 1.2
$R(5)$	0.91/0.03	-0.24/0.03	0.94/0.03	172.5/ 0.9	0.03/ 0.9
$I(5)$	0.87/0.08	-0.24/0.08	0.90/0.06	172.0/ 3.0	0.07/ 2.2
01/93					
$U(2)$	0.74/0.00	-0.12/0.11	0.75/0.02	175.5/ 4.2	0.06/ 2.1
$B(2)$	0.72/0.09	-0.25/0.04	0.76/0.07	170.3/ 2.5	0.03/ 1.1
$V(2)$	0.96/0.01	-0.24/0.04	0.99/0.00	173.0/ 1.2	0.03/ 1.0
$R(2)$	0.96/0.09	-0.34/0.03	1.01/0.10	170.2/ 0.2	0.03/ 1.0
$I(2)$	0.73/0.02	0.00/0.02	0.73/0.02	0.0/ 0.9	0.09/ 3.4

Table 8. ζ Tau

Date(Mo/Yr) Filter(n)	q/dq (%)	u/du (%)	p/dp (%)	$\theta/d\theta$ (°)	$dpi/d\theta i$ (%) (°)
01/90					
$U(6)$	0.43/0.07[a]	0.95/0.05	1.05/0.07	32.8/ 1.4	0.02/ 0.7
$B(6)$	0.61/0.03	1.32/0.09[a]	1.45/0.09	32.6/ 0.7	0.02/ 0.4
$V(6)$	0.51/0.05	1.18/0.06	1.28/0.07	33.3/ 0.8	0.02/ 0.4
$R(6)$	0.52/0.03	1.11/0.05	1.22/0.06	32.4/ 0.7	0.02/ 0.5
$I(6)$	0.40/0.04	0.90/0.06	0.98/0.05	33.1/ 1.6	0.04/ 1.1
12/90					
$U(4)$	0.47/0.04	0.96/0.03	1.07/0.03	31.9/ 1.1	0.05/ 1.3
$B(4)$	0.68/0.07	1.31/0.03	1.48/0.02	31.3/ 1.4	0.03/ 0.6
$V(4)$	0.61/0.06	1.22/0.03	1.37/0.02	31.7/ 1.4	0.04/ 0.8
$R(4)$	0.55/0.04	1.16/0.06	1.29/0.07	32.3/ 0.5	0.03/ 0.6
$I(4)$	0.39/0.05	0.85/0.05	0.93/0.02	32.7/ 1.9	0.05/ 1.5
12/91					
$U(5)$	0.52/0.09	0.91/0.03	1.06/0.04	30.2/ 2.5	0.03/ 0.9
$B(5)$	0.50/0.08[a]	1.36/0.06	1.46/0.05	34.9/ 1.8	0.02/ 0.4
$V(5)$	0.46/0.06	1.25/0.07[a]	1.34/0.05	35.0/ 1.6	0.02/ 0.5
$R(5)$	0.46/0.09[a]	1.14/0.05	1.23/0.04	34.0/ 2.2	0.02/ 0.5
$I(5)$	0.48/0.03	0.90/0.04	1.02/0.03	30.9/ 0.9	0.05/ 1.3
01/93					
$U(3)$	0.40/0.03	1.14/0.08	1.21/0.09	35.2/ 0.4	0.03/ 0.8
$B(3)$	0.57/0.04	1.48/0.06	1.58/0.05	34.4/ 0.8	0.02/ 0.4
$V(3)$	0.61/0.09[a]	1.31/0.04	1.45/0.08	32.6/ 1.3	0.02/ 0.4
$R(3)$	0.60/0.01	1.08/0.03	1.23/0.03	30.4/ 0.0	0.02/ 0.5
$I(3)$	0.46/0.05	0.98/0.05	1.08/0.07	32.5/ 0.6	0.05/ 1.2

[a] dq or $du > 3dpi$: weak night-to-night variability (See Section 3.1.)

Table 9. 48 Lib

Date(Mo/Yr) Filter(n)	q/dq (%)	u/du (%)	p/dp (%)	$\theta/d\theta$ (°)	$dpi/d\theta i$ (%) (°)
05/90					
$U(6)$	-0.37/0.21	-0.34/0.10	0.53/0.18	112.1/ 8.3	0.09/ 5.1
$B(5)$	-0.44/0.04	-0.58/0.07	0.74/0.06	116.4/ 2.1	0.04/ 1.8
$V(5)$	-0.40/0.07	-0.69/0.07	0.80/0.07	119.8/ 2.5	0.05/ 1.9
$R(5)$	-0.52/0.07	-0.55/0.07	0.76/0.06	113.2/ 2.8	0.04/ 1.6
$I(5)$	-0.61/0.14	-0.59/0.07	0.86/0.09	112.2/ 4.2	0.09/ 3.0
08/91					
$U(3)$	-0.35/0.08	-0.52/0.02	0.63/0.03	118.2/ 3.6	0.10/ 4.6
$B(3)$	-0.41/0.02	-0.84/0.11	0.93/0.09	121.8/ 2.1	0.04/ 1.4
$V(3)$	-0.51/0.03	-0.78/0.11	0.94/0.08	118.2/ 2.6	0.05/ 1.6
$R(3)$	-0.48/0.07	-0.72/0.06	0.87/0.04	118.2/ 2.6	0.04/ 1.4
$I(3)$	-0.57/0.13	-0.61/0.24	0.84/0.21	112.7/ 6.3	0.10/ 3.4
07/92					
$U(4)$	-0.24/0.11	-0.56/0.12	0.62/0.11	123.5/ 5.5	0.09/ 4.4
$B(4)$	-0.43/0.05	-0.75/0.03	0.86/0.05	120.1/ 1.0	0.04/ 1.4
$V(4)$	-0.49/0.06	-0.80/0.02	0.94/0.04	119.3/ 1.4	0.05/ 1.6
$R(4)$	-0.43/0.08	-0.65/0.02	0.78/0.06	118.4/ 2.3	0.04/ 1.5
$I(4)$	-0.36/0.08	-0.65/0.16	0.75/0.16	120.0/ 3.0	0.10/ 3.9
06/93					
$U(7)$	-0.46/0.08	-0.57/0.11	0.74/0.12	115.7/ 1.8	0.11/ 4.4
$B(7)$	-0.41/0.09	-0.72/0.06	0.83/0.05	120.2/ 3.2	0.05/ 1.6
$V(7)$	-0.50/0.10	-0.62/0.05	0.80/0.08	115.8/ 2.8	0.06/ 2.1
$R(7)$	-0.49/0.05	-0.53/0.09	0.73/0.08	113.4/ 2.8	0.05/ 1.9
$I(7)$	-0.48/0.17	-0.46/0.16	0.69/0.13	112.0/ 7.8	0.12/ 5.0

Table 10. χ Oph

Date(Mo/Yr) Filter(n)	q/dq (%)	u/du (%)	p/dp (%)	$\theta/d\theta$ (°)	$dpi/d\theta i$ (%) (°)
05/90					
$U(5)$	0.03/0.14	-0.35/0.05	0.37/0.06	136.4/10.6	0.06/ 5.2
$B(5)$	-0.11/0.06	-0.43/0.05	0.45/0.06	128.0/ 3.8	0.03/ 2.2
$V(5)$	0.00/0.09	-0.49/0.05	0.50/0.04	134.9/ 5.6	0.04/ 2.0
$R(5)$	-0.02/0.05	-0.43/0.05	0.43/0.05	133.5/ 3.2	0.02/ 1.7
$I(5)$	-0.04/0.04	-0.50/0.07	0.50/0.07	132.7/ 1.9	0.05/ 2.8
08/91					
$U(2)$	-0.07/0.01	-0.38/0.04	0.38/0.04	129.9/ 0.3	0.07/ 5.5
$B(2)$	0.05/0.05	-0.52/0.01	0.52/0.01	137.5/ 2.7	0.04/ 2.1
$V(2)$	-0.05/0.03	-0.53/0.02	0.54/0.02	132.2/ 1.6	0.04/ 2.0
$R(2)$	0.08/0.04	-0.43/0.02	0.44/0.03	139.9/ 2.6	0.02/ 1.6
$I(2)$	-0.07/0.01	-0.37/0.01	0.38/0.01	129.4/ 0.3	0.05/ 3.6
07/92					
$U(4)$	0.07/0.08	-0.42/0.04	0.43/0.04	139.6/ 5.4	0.08/ 5.0
$B(4)$	-0.15/0.09	-0.52/0.05	0.54/0.04	127.0/ 5.1	0.04/ 2.1
$V(4)$	-0.02/0.08	-0.63/0.04	0.64/0.04	134.0/ 3.5	0.04/ 1.8
$R(4)$	0.03/0.07	-0.47/0.03	0.48/0.03	137.1/ 4.3	0.03/ 1.7
$I(4)$	0.03/0.02	-0.58/0.06	0.58/0.06	136.4/ 1.1	0.06/ 2.8
06/93					
$U(7)$	-0.07/0.10	-0.35/0.06	0.36/0.07	129.8/ 7.3	0.08/ 6.7
$B(7)$	-0.12/0.06	-0.48/0.05	0.50/0.04	127.9/ 4.0	0.05/ 2.7
$V(7)$	0.00/0.09	-0.56/0.06	0.57/0.06	135.5/ 4.3	0.06/ 3.1
$R(7)$	0.08/0.06	-0.41/0.07	0.42/0.06	140.4/ 4.9	0.03/ 2.3
$I(7)$	0.03/0.11	-0.45/0.09	0.47/0.08	137.5/ 8.0	0.06/ 3.7

Table 11. π Aqr

Date(Mo/Yr) Filter(n)	q/dq (%)	u/du (%)	p/dp (%)	$\theta/d\theta$ (°)	$dpi/d\theta i$ (%) (°)
05/90					
$U(4)$	0.32/0.14	-0.54/0.11	0.64/0.14	149.8/ 5.8	0.07/ 3.4
$B(4)$	0.30/0.06	-0.65/0.08	0.72/0.09	147.2/ 2.0	0.05/ 1.8
$V(4)$	0.24/0.08	-0.58/0.06	0.64/0.06	146.4/ 3.7	0.05/ 2.3
$R(4)$	0.31/0.08	-0.56/0.07	0.64/0.09	149.4/ 2.5	0.04/ 1.9
$I(4)$	0.18/0.04	-0.73/0.09	0.75/0.09	141.8/ 1.7	0.10/ 3.7
08/91					
$U(3)$	0.80/0.03	-0.85/0.06	1.17/0.07	156.6/ 0.5	0.07/ 1.7
$B(3)$	1.08/0.04	-1.03/0.10	1.50/0.04	158.3/ 1.9	0.04/ 0.8
$V(3)$	0.93/0.03	-0.92/0.04	1.31/0.04	157.6/ 0.6	0.04/ 0.9
$R(3)$	0.86/0.08	-0.84/0.09	1.20/0.09	157.7/ 1.8	0.03/ 0.8
$I(3)$	0.50/0.04	-0.70/0.08	0.86/0.05	152.9/ 2.5	0.08/ 2.5
07/92					
$U(4)$	0.14/0.10	-0.40/0.11	0.44/0.09	144.8/ 8.3	0.06/ 4.3
$B(4)$	-0.02/0.08	-0.43/0.03	0.43/0.03	133.7/ 5.3	0.04/ 2.5
$V(4)$	-0.01/0.07	-0.49/0.04	0.50/0.04	134.6/ 3.8	0.05/ 2.7
$R(4)$	0.03/0.09	-0.46/0.03	0.47/0.02	137.3/ 5.7	0.04/ 2.3
$I(4)$	0.04/0.05	-0.34/0.07	0.34/0.07	138.9/ 4.5	0.09/ 7.9
06/93					
$U(7)$	0.50/0.07	-0.67/0.15	0.84/0.09	153.6/ 5.1	0.07/ 2.6
$B(7)$	0.67/0.08	-0.80/0.07	1.04/0.08	154.9/ 1.8	0.04/ 1.1
$V(7)$	0.66/0.08	-0.83/0.07	1.06/0.08	154.2/ 1.9	0.05/ 1.4
$R(7)$	0.66/0.05	-0.76/0.07	1.00/0.06	155.4/ 1.5	0.04/ 1.2
$I(7)$	0.50/0.13	-0.65/0.10	0.83/0.13	153.6/ 3.6	0.10/ 3.4

Table 12. o And

Date(Mo/Yr) Filter(n)	q/dq (%)	u/du (%)	p/dp (%)	$\theta/d\theta$ (°)	$dpi/d\theta i$ (%) (°)
05/90					
$U(4)$	-0.20/0.06	0.03/0.08	0.21/0.06	84.2/12.1	0.05/ 6.6
$B(5)$	-0.38/0.06	0.00/0.04	0.38/0.06	89.3/ 2.7	0.02/ 1.7
$V(4)$	-0.27/0.01	-0.05/0.06	0.28/0.02	95.1/ 5.8	0.03/ 2.7
$R(4)$	-0.26/0.05	0.04/0.03	0.26/0.04	84.6/ 4.9	0.02/ 2.3
$I(4)$	-0.35/0.05	-0.06/0.10	0.36/0.04	95.0/ 8.2	0.05/ 3.8
08/91					
$U(3)$	-0.34/0.01	-0.02/0.03	0.34/0.01	91.6/ 2.8	0.04/ 3.7
$B(3)$	-0.39/0.08[a]	-0.05/0.01	0.40/0.07	93.5/ 1.5	0.02/ 1.6
$V(3)$	-0.34/0.02	-0.04/0.06	0.34/0.02	93.5/ 5.3	0.03/ 2.3
$R(3)$	-0.34/0.01	-0.03/0.03	0.35/0.01	92.2/ 2.4	0.02/ 1.7
$I(3)$	-0.34/0.04	0.14/0.09	0.37/0.06	79.6/ 5.6	0.05/ 3.7
07/92					
$U(4)$	-0.24/0.04	0.02/0.06	0.25/0.04	87.4/ 7.5	0.04/ 5.2
$B(4)$	-0.40/0.05	-0.03/0.06	0.40/0.05	91.6/ 4.6	0.02/ 1.6
$V(4)$	-0.39/0.03	-0.04/0.11[a]	0.41/0.02	92.6/ 8.0	0.03/ 1.9
$R(4)$	-0.33/0.04	-0.02/0.03	0.33/0.04	91.6/ 2.6	0.02/ 1.9
$I(4)$	-0.28/0.04	0.00/0.07	0.28/0.05	89.5/ 6.6	0.05/ 5.2
06/93					
$U(7)$	-0.35/0.12	0.02/0.04	0.36/0.12	87.6/ 5.5	0.06/ 5.8
$B(7)$	-0.43/0.05	-0.03/0.07	0.44/0.05	92.0/ 4.8	0.03/ 2.3
$V(7)$	-0.43/0.05	-0.02/0.08	0.44/0.05	91.4/ 5.2	0.03/ 2.1
$R(7)$	-0.36/0.05	-0.04/0.03	0.36/0.05	93.3/ 2.7	0.02/ 1.8
$I(7)$	-0.28/0.08	0.01/0.06	0.28/0.07	88.3/ 7.7	0.05/ 5.7

[a] dq or $du > 3dpi$: weak night-to-night variability (See Section 3.1.)

If we require the stronger condition that the grand average of dq or du exceed three times the grand average of <*dpi*> (requiring a significant scatter across the full range of filters), then only π Aqr is judged to be variable, as flagged by footnote marks "d" on the grand averages in Table 15. This is the criterion that had to be used in Paper II, since otherwise the standard stars did not appear constant. In that paper π Aqr was also found to be variable from year to year, but so was ζ Tau, which does not meet the test in the present data set.

3.3. Results for individual stars

Gamma Cas shows some weak indications of both short term and long term variability, but this may be seen to be the result of unusually small values of σ in the 3 σ criterion. Since the σ values are based on photon counting statistics and γ Cas is quite a bit brighter than the other stars observed, it is likely to be misjudged as variable. The actual scatter in the measurements is similar to that for other stars which were constant.

Phi Per also shows a few weak indications of variation on both time scales. As mentioned by Gies et al. (1993), it is possible that these could be related to the 127 day orbital period, but the correlation is unclear because the annual observations are widely spaced samples from many cycles, so that any orbital variations could be easily obscured by secular changes. The only valid way to solve this problem is to observe the star continuously for several orbital cycles.

Zeta Tau shows some evidence of variability, but the night-to-night and year-to-year scatter are both noticeably smaller in this study than in Paper II. Apparently the strong year-to-year variability seen in Paper II was a relatively isolated episode. This is another example of the situation just discussed for ϕ Per, in that ζ Tau is a spectroscopic binary with a 133 day orbital period, difficult to study polarimetrically without continuous monitoring.

Pi Aqr continues to exhibit some of the most remarkable and seemingly erratic long term variability ever observed for any Be star. Tables 16 and 17 were constructed by vectorially subtracting the interstellar polarization component (maximum 0.46% at 498 nm with position angle 116°) determined by Poeckert, Bastien, & Landstreet (1979), showing that the changes are entirely in the amplitude of the intrinsic polarization, with constant position angle. This star will be discussed in more detail in Section 4.3.

Omicron And shows only two weak indications of variability, both of them in the short term statistics. Harmanec et al. (1987) suspected a relation between the polarization and an 8.5 year cyclic variation in the amplitude of the 1.57 day light curve, so the data presented here and in Paper II may provide a further test.

3.4. Summary of long term variability

As an overview of the project results on variability to date, Figure 1 shows the B-band polarization and position angle for each of the eight program stars from 1984 through 1993, including the data from Papers I and II. Each data point is the mean for a run, with error bars showing the standard deviation.

There are some intriguing patterns in Figure 1, but for the most part, the graphs simply verify the statistics: the only clearly variable star is π Aqr.

The hint of long term oscillation in most of the plots brings to mind the variations in the V/R intensity ratios and shell line radial velocities of the Balmer emission lines of many Be stars (Dachs 1987). If series of recent high resolution spectra are available, correlations with the polarization could give some information about the internal layering of the envelopes (Delplace and Chambon 1976) and the proposed one-armed density structures in the disks (Okazaki 1991). Based on Scargle periodograms of q and u, however, none of the polarization patterns have statistically significant periodicities.

The apparently systematic change in the polarization position angle of o And between 1986 and 1990 looks very unusual, but the error bars are too large for the trend to be definitely established unless there is a correlation with other observations.

4. Discussion

4.1. Models and their limitations

For perspective, it is important to see that polarization and other circumstellar envelope phenomena are only symptoms of some unknown instability of rapidly rotating B stars which is the underlying cause of the Be phase. By studying the properties of the extended atmospheres, we hope to find clues to the stellar mass loss processes that produce them.

Most of the theoretical progress on polarization of Be stars has been limited to constraining the envelope parameters for the axisymmetric case when the polarization is constant in time. In the model of McLean (1979), for instance, the free parameters are the oblateness factor (which can be the same for more than one specific geometry), the electron number density and temperature (assumed constant throughout the envelope), the radius, and the inclination of the symmetry axis to the line of sight. As mentioned in Section 1, the polarization is produced by electron scattering, with a wavelength dependence due to absorption and emission by partially ionized hydrogen. It is usually possible to fit the observed *UBVRI* polarization of most Be stars in this simple way with an equatorial disk, and the additional complications of a nonuniform density distribution together with depolarization and occultation due to a finite stellar light source (Fox 1991) do not appear to strain the limits of reasonable parameters consistent with optical spectroscopy. However, it is difficult to coordinate the simultaneous spectro-

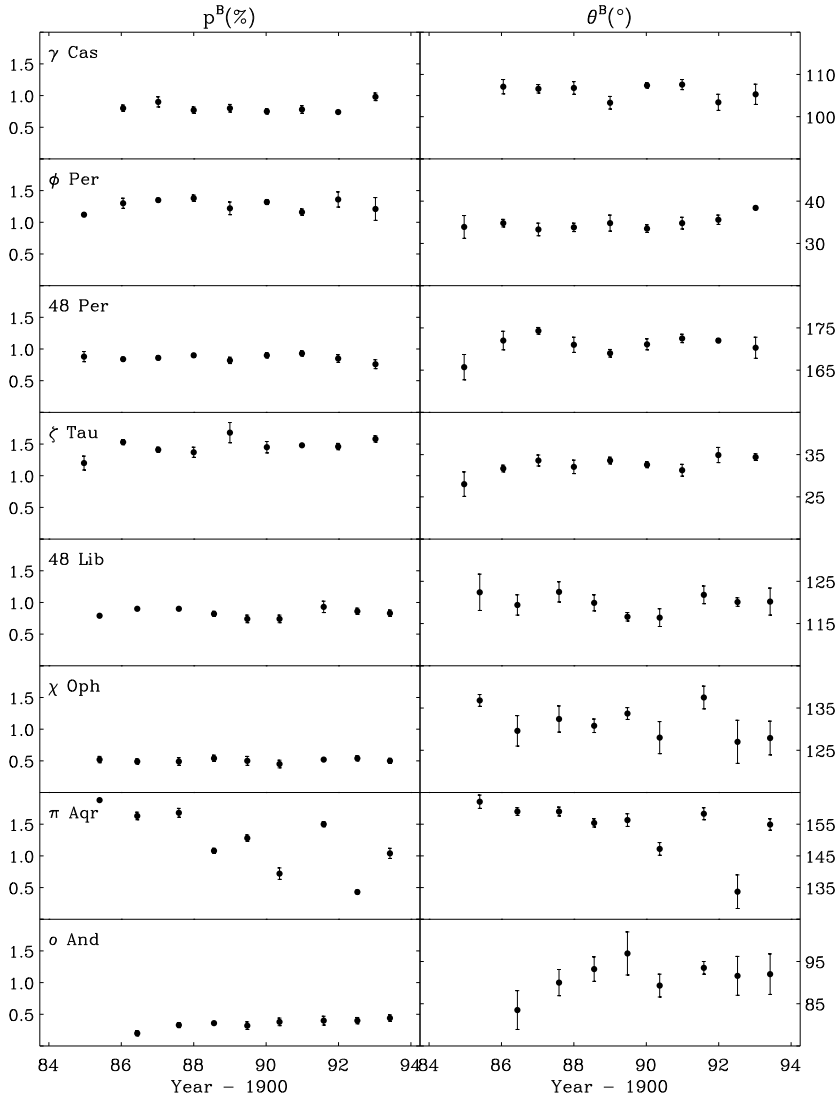

Fig. 1.— Long term behavior of the B-band polarization and position angle for the program stars, including the data from Papers I and II.

scopic and polarimetric observations that are needed to significantly refine the details of the models.

Ultraviolet, infrared, and X-ray studies have now led to the discovery of new phenomena which were not predicted by models based on optical data alone. The wind-compressed disk model (Bjorkman & Cassinelli 1993, Owocki, Cranmer, & Blondin 1994) is an interesting development for its explanation of how a cool circumstellar envelope, which fits the optical data, can coexist with the superionized wind required by ultraviolet spectroscopy. This is a steady-state model, though, and like most of the others it includes no explanation for the unpredictable variability of Be stars.

4.2. The program stars as a sample

Figure 2 shows the intrinsic polarization and position angle as a function of wavelength for the program stars after removal of the interstellar component according to Poeckert, Bastein, & Landstreet (1979) by vector subtraction from the averages given in Tables 14 and 15. (For π Aqr the 1991 data were chosen as typical.) This small group of eight stars is a good representative sample of Be stars in general, covering a considerable range in polarization, spectral type, and $v\,sin\,i$.

Although the sample is not large enough to give conclusive statistics, the fact that high polarizations appear only for the earlier spectral types is in accord with radiation-driven wind theories. The absence of high polarization for stars with low $v\,sin\,i$ is as expected for a flattened equatorial disk, since in this case the projection of the disk on the sky would be too symmetrical to cause a large net polarization (Poeckert & Marlborough 1976). For most of the stars, the intrinsic position angle of the broad band polarization appears to be constant with wavelength, which agrees with the mechanism of electron scattering in partially ionized hydrogen and also supports the estimated interstellar polarization values. The irregularities in position angle for o And and 48 Per are understandable, because the position angle is poorly determined when the polarization amplitude is small.

The wavelength dependence of the polarization is explored in Figure 3 in terms of ratios of the UBV filter values as suggested by McLean (1979). The ratio p^U/p^B is a measure of the polarization Balmer discontinuity due to bound-free absorption by neutral hydrogen, while the ratio p^V/p^B indicates the slope of the Paschen continuum polarization, which is theoretically determined by the λ^3 dependence of bound-free and free-free absorption together with dilution from the inverse emission processes. Since the broad band U filter is centered on the Balmer jump, p^U/p^B underestimates the strength of the discontinuity, but it is still a useful quantity when applied systematically to compare stars of similar spectral type. Normalization relative to p^B is convenient because the polarization usually has its maximum near that range of wavelengths.

The main point of Figure 3 is that the normalized wavelength dependence of p is very similar for all of the stars in the sample. Specifically, the scatter in both ratios is small,

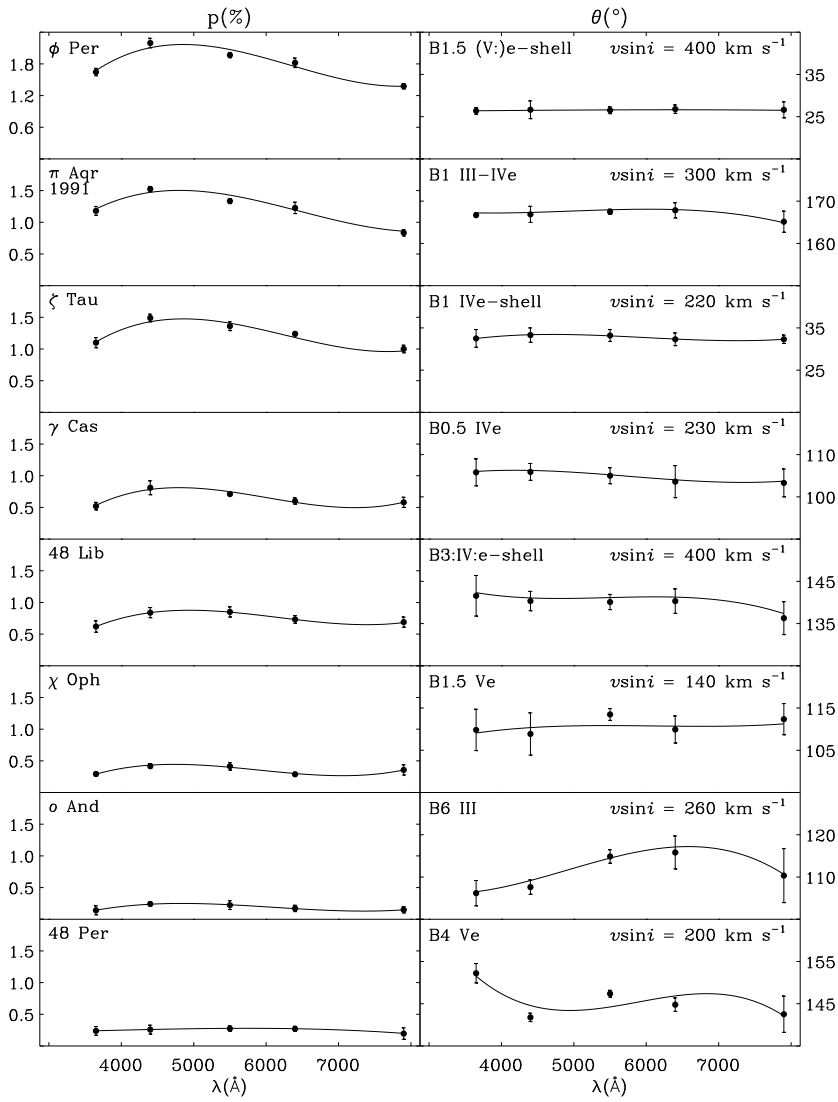

Fig. 2.— Intrinsic polarization and position angle as a function of wavelength for the program stars, arranged in order of decreasing polarization.

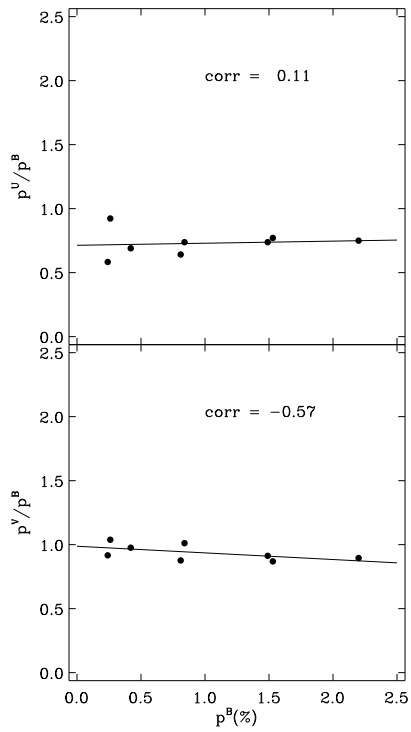

Fig. 3.— Tests for correlation of the ratios p^U/p^B and p^V/p^B with p^B for the intrinsic polarization of the program stars. The correlation coefficient shown has a critical value of 0.71 at the 5% level.

and neither ratio is correlated with p^B. (The correlation coefficient shown has a critical value of 0.71 at the 5% level.) If the wide range of polarization included in the sample were primarily a temperature sequence or a density sequence, McLean's analytical expression for $p(\lambda)$ would imply clearly observable differences in the normalized wavelength dependence. A sequence based purely on radial extent or disk thickness would not maintain the necessary scattering geometry, and inclination dependence is too weak an effect to account for the entire range of p. A reasonable conclusion is to agree with McLean that "In reality a combination of processes appears quite likely."

4.3. Variability of π Aqr

The variation of π Aqr over the past nine years presents a rare opportunity to follow an individual Be star over the entire range from the strongest to weakest envelope state normally seen in all Be stars taken as a group. Combined multiwavelength studies will appear elsewhere, but some tentative results can be derived from the *UBVRI* polarimetry alone.

Figure 4 is a plot of q and u including all the data from this paper together with Papers I and II, uncorrected for interstellar polarization. The data points fall along a straight line with very little scatter, which shows that the position angle of the intrinsic polarization has remained constant at about 167° (half the position angle of the line in the q, u plane). This is in good agreement with the values in Table 17, which confirms the interstellar polarization estimate used there. A constant polarization position angle implies that the envelope is symmetric about an axis that has a fixed orientation as projected on the plane of the sky. Figure 4 also illustrates that the position angle of the intrinsic polarization is independent of wavelength, since the data points for all bandpasses lie along the same straight line.

The wavelength dependence of the polarization of π Aqr is shown in Figure 5 for each year of the monitoring program. Figure 6 shows one possible analysis, using the same ratio approach described in Section 4.2 to study the normalized form. In contrast with the previous result, there appears to be a correlation between p^B and each of the two ratios, in the sense that the wavelength dependence is more pronounced for the larger values of p^B. (Here the correlation coefficient has a critical value of 0.67 at the 5% level.) This is also different from the finding of McLean (1979) for the variable polarization of π Aqr from 1967 through 1975, in which the ratios were constant while p^B changed. He concluded as quoted before that more than one physical quantity must have been changing.

However, in this case numerical calculations using McLean's equation for $p(\lambda)$, convolved with the filter system passbands, show that the changes in the polarization in Figures 4 and 5 can be matched by varying only the electron number density N_e, while holding the other parameters constant. In general, this is because the maximum polarization (due to electron scattering) is proportional to N_e, while the main term in the wavelength

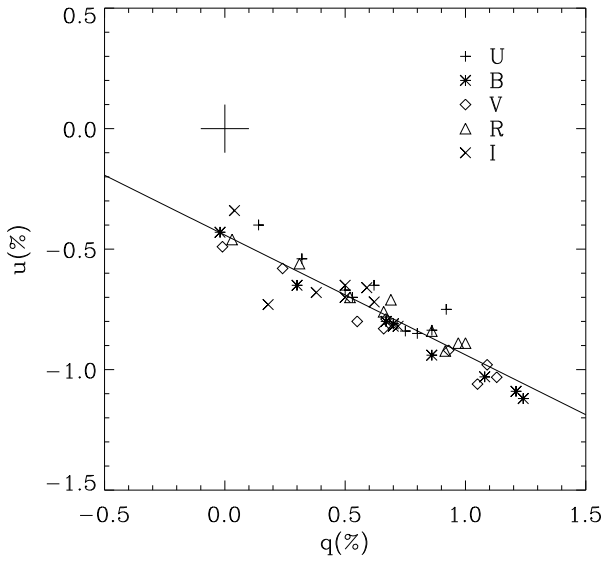

Fig. 4.— Stokes parameter plot of the observed *UBVRI* polarization of π Aqr from 1985 through 1993.

dependence (the optical depth due to hydrogen opacity) is proportional to N_e^2, so that increasing the maximum polarization by increasing N_e makes the normalized wavelength dependence stronger. The exact values of the parameters are insignificant given the assumptions of the model, and they may not be unique, but the basic result is appealing because it is simple.

The adjustment of model parameters to fit observations is only valuable to the extent that the changes can be understood to reflect real physical processes. For Be stars, changes in the model envelope conditions that reproduce the observed variations in polarization must be traced to some physical origin, which is likely to be unstable mass loss by the underlying star. For example, in the case of π Aqr just described, we should ask if there is a plausible mechanism of variable mass loss that would change only the electron density of the envelope. In a radiation-driven wind theory this would require analysis of how the luminosity of the star is related to the ionization and thermal equilibrium conditions in the wind, including the effects of elemental abundances (Drew 1989). In a pulsation theory there would be changes in the pulsation amplitude or mode, and this might be distinguishable from the a wind theory if the predicted changes in effective temperature of the underlying star are different. A theory based on starspots or active regions might also be a possibility. In any case we would ultimately need a more fundamental explanation for the instability in the luminosity, pulsation, or surface activity of the star in terms of the theory of stellar structure and evolution.

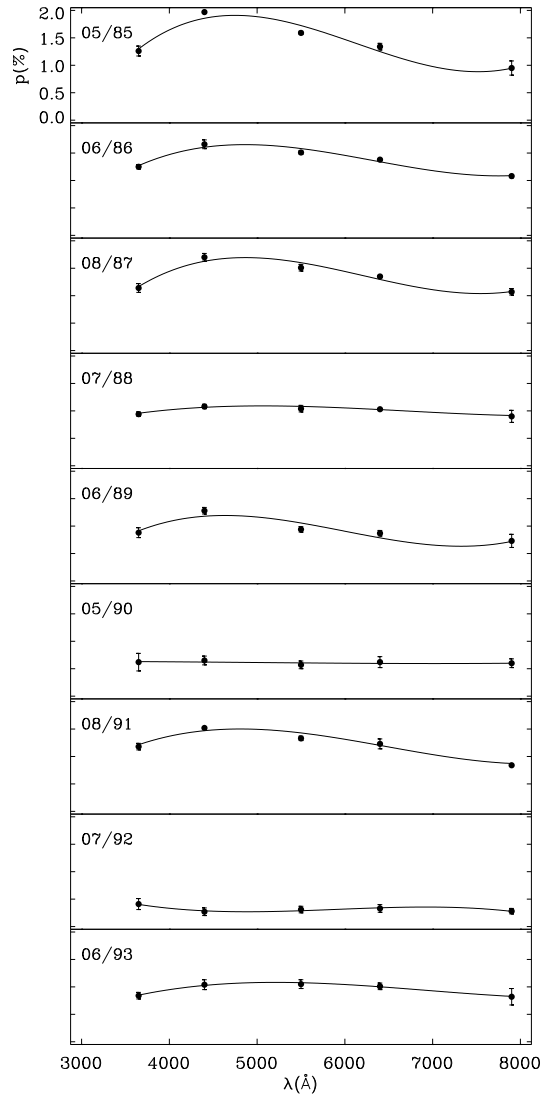

Fig. 5.— The variable intrinsic polarization of π Aqr as a function of wavelength from 1985 through 1993.

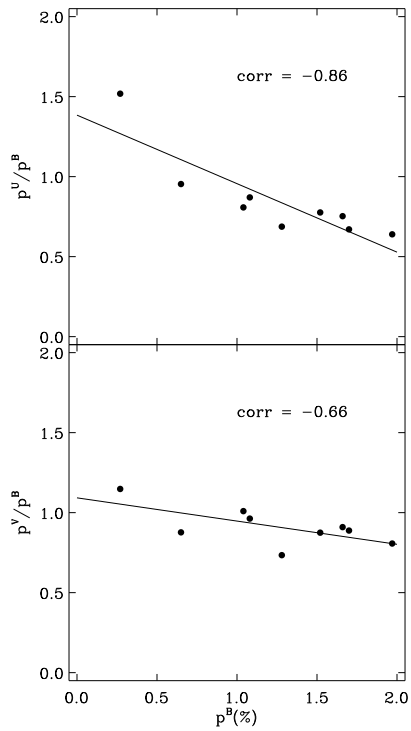

Fig. 6.— Tests for correlation of the ratios p^U/p^B and p^V/p^B with p^B for the variable intrinsic polarization of π Aqr from 1985 through 1993. The correlation coefficient shown has a critical value of 0.67 at the 5% level.

I am grateful to the administration of McDonald Observatory for continuing to support this long term project and to the technical staff for maintaining the polarimeter in good working condition. I also thank the referee, Laurent Drissen, for his substantial contribution to the content of this paper.

REFERENCES

Balona, L., Henrichs, H., & Le Contel, J.M. 1994, ed., IAU Symp. 162, Pulsation, Rotation & Mass Loss in Early-Type Stars (Dordrecht: Kluwer)

Bastien, P., Drissen, L., Ménard, F., Moffat, A.F.J., Robert, C., & St-Louis, N. 1988, AJ, 95, 900

Bjorkman, J.E. & Cassinelli, J.P. 1993, ApJ, 409, 429

Breger, M. 1979, ApJ, 233, 97

Brown, J.C. & Henrichs, H.F. 1987, A&A, 182, 107

Brown, J.C. & McLean, I.S. 1977, A&A, 57, 141

Capps, R.W., Coyne, G.V., & Dyck, H.M. 1973, ApJ, 184, 173

Clarke, D. & Stewart, B.G. 1986, Vistas Astr., 29, 27

Dachs, J. 1987 in IAU Coll. 92, Physics of Be Stars, ed. Slettebak, A., & Snow, T.P. (Cambridge: Cambridge University Press), 149

Delplace, A.M. & Chambon, M.Th. 1976, in IAU Symp. 70, Be and Shell Stars, ed. Slettebak, A. (Dordrecht: Reidel), 79

Drew, J.E. 1989, ApJS, 71, 267

Fox G.K. 1991, ApJ, 379, 663

Gies, D.R., Willis, C.Y., Penny, L.R., & McDavid, D. 1993, PASP, 105, 281

Harmanec, P., et al. 1987, in IAU Coll. 92, Physics of Be Stars, ed. Slettebak, A. & Snow, T.P. (Cambridge: Cambridge University Press), 456

Hoffleit, D. & Jaschek, C. 1982, The Bright Star Catalog, 4th Revised Edition (New Haven: Yale University Observatory)

Hsu, J.C. & Breger, M. 1982, ApJ, 262, 732

McDavid, D. 1986, PASP, 98, 572

McDavid, D. 1990, PASP, 102, 773

McLean, I.S. 1979, MNRAS, 186, 265

Okazaki, A.T. 1991, PASJ, 43, 75

Owocki, S.P., Cranmer, S.R., & Blondin, J.M. 1994, ApJ, 424, 887

Poeckert, R., Bastien, P., & Landstreet, J.D. 1979, AJ, 84, 812

Poeckert, R. & Marlborough, J.M. 1976, ApJ, 206, 182

Poeckert, R. & Marlborough, J.M. 1978, ApJ, 220, 940

Serkowski, K. 1974, in Planets, Stars and Nebulae Studied with Photopolarimetry, ed. Gehrels, T. (Tucson: University of Arizona), 135

Slettebak, A. 1982, ApJS, 50, 55

Slettebak, A. 1988, PASP, 100, 770

Young, A.T. 1967, AJ, 72, 747

Table 13. Polarized Standard Star Summary

Star Filter	q/dq (%)	<dq> (%)	u/du (%)	<du> (%)	p/dp (%)	<dp> (%)	$\theta/d\theta$ (°)	<$d\theta$> (°)	<dpi> (%)	<$d\theta i$> (°)
2H Cam										
U	-1.83/0.05	0.11	-2.41/0.03	0.07	3.03/0.01	0.08	116.5/ 0.6	1.1	0.09	0.8
B	-1.97/0.05	0.07	-2.60/0.09	0.07	3.26/0.07	0.05	116.3/ 0.6	0.7	0.04	0.4
V	-2.07/0.06	0.07	-2.73/0.01	0.07	3.43/0.03	0.07	116.4/ 0.5	0.5	0.04	0.4
R	-1.97/0.07	0.05	-2.66/0.05	0.06	3.31/0.04	0.05	116.8/ 0.7	0.4	0.03	0.3
I	-1.75/0.06	0.09	-2.36/0.05	0.06	2.94/0.05	0.08	116.8/ 0.7	0.8	0.05	0.6
GAV	0.06	0.08	0.05	0.07	0.04	0.07	0.6	0.7	0.05	0.5
o Sco										
U	1.35/0.21	0.20	2.51/0.12	0.25	2.85/0.12	0.28	30.9/ 2.0	1.6	0.20	2.1
B	1.40/0.12	0.09	3.07/0.14	0.08	3.39/0.10	0.07	32.7/ 1.3	0.9	0.06	0.5
V	1.81/0.25	0.12	3.74/0.12	0.08	4.16/0.01	0.10	32.1/ 1.9	0.7	0.05	0.3
R	1.91/0.23	0.07	3.96/0.10	0.08	4.41/0.03	0.05	32.1/ 1.6	0.6	0.04	0.2
I	1.76/0.19	0.07	3.88/0.06	0.06	4.26/0.06	0.07	32.8/ 1.3	0.4	0.05	0.3
GAV	0.20	0.11	0.11	0.11	0.06	0.11	1.6	0.9	0.08	0.7

Table 14. Winter Be Star Summary

Star Filter	q/dq (%)	<dq> (%)	u/du (%)	<du> (%)	p/dp (%)	<dp> (%)	$\theta/d\theta$ (°)	<$d\theta$> (°)	<dpi> (%)	<$d\theta i$> (°)
γ Cas										
U	-0.44/0.07[c]	0.04	-0.27/0.04	0.05	0.52/0.06	0.05	105.8/ 3.2	3.3	0.02	1.4
B	-0.69/0.10[c]	0.03	-0.43/0.07[c]	0.05	0.81/0.11	0.04	105.9/ 2.0	1.5	0.02	0.7
V	-0.62/0.03	0.05	-0.35/0.04	0.04	0.71/0.01	0.04	105.0/ 1.9	2.1	0.02	0.9
R	-0.52/0.02	0.04	-0.27/0.09[c]	0.03	0.60/0.05	0.04	103.6/ 3.8	1.6	0.02	1.0
I	-0.51/0.10[c]	0.04	-0.26/0.04	0.06	0.58/0.08	0.05	103.3/ 3.3	2.5	0.03	1.6
GAV	0.06	0.04	0.06	0.05	0.06	0.05	2.8	2.2	0.02	1.1
ϕ Per										
U	0.12/0.05	0.07	0.77/0.07	0.17[b]	0.78/0.07	0.16	40.2/ 0.8	3.1	0.05	2.2
B	0.41/0.10[c]	0.05	1.19/0.09	0.09	1.26/0.09	0.10	35.6/ 2.1	1.0	0.03	0.7
V	0.32/0.04	0.07	1.03/0.04	0.11	1.08/0.05	0.12	36.4/ 0.8	1.4	0.04	0.9
R	0.30/0.03	0.04	0.97/0.09	0.08	1.02/0.09	0.07	36.5/ 1.0	1.4	0.03	0.8
I	0.19/0.04	0.08	0.71/0.04	0.08	0.74/0.05	0.07	37.2/ 1.9	3.5	0.06	2.5
GAV	0.05	0.06	0.06	0.10	0.07	0.10	1.3	2.1	0.04	1.4
48 Per										
U	0.77/0.05	0.08	-0.20/0.08	0.08	0.80/0.07	0.08	172.9/ 2.3	2.9	0.06	2.1
B	0.82/0.08	0.06	-0.25/0.01	0.03	0.86/0.07	0.05	171.5/ 1.0	1.3	0.03	1.0
V	0.95/0.04	0.03	-0.25/0.02	0.07	0.99/0.04	0.03	172.7/ 0.8	2.0	0.04	1.0
R	0.94/0.03	0.05	-0.25/0.06	0.03	0.97/0.04	0.05	172.4/ 1.6	0.8	0.03	0.9
I	0.82/0.07	0.07	-0.19/0.13	0.06	0.85/0.09	0.06	173.6/ 4.3	2.3	0.07	2.5
GAV	0.05	0.06	0.06	0.05	0.06	0.05	2.0	1.9	0.04	1.5
ζ Tau										
U	0.45/0.05	0.06	0.99/0.10[c]	0.05	1.10/0.08	0.06	32.5/ 2.1	1.4	0.03	0.9
B	0.59/0.08[c]	0.05	1.37/0.08[c]	0.06	1.49/0.06	0.05	33.3/ 1.7	1.2	0.02	0.4
V	0.55/0.08[c]	0.06	1.24/0.05	0.05	1.36/0.07	0.05	33.2/ 1.4	1.3	0.02	0.5
R	0.53/0.06	0.04	1.12/0.03	0.05	1.24/0.03	0.05	32.3/ 1.5	0.9	0.02	0.5
I	0.43/0.04	0.04	0.91/0.05	0.05	1.00/0.06	0.04	32.3/ 1.0	1.2	0.05	1.3
GAV	0.06	0.05	0.06	0.05	0.06	0.05	1.5	1.2	0.03	0.7

[b] <dq> or <du> > 3<dpi>: moderate night-to-night variability (See Section 3.1.)

[c] dq or du > 3<dpi>: moderate year-to-year variability (See Section 3.2.)

Table 15. Summer Be Star Summary

Star Filter	q/dq (%)	<dq> (%)	u/du (%)	<du> (%)	p/dp (%)	<dp> (%)	$\theta/d\theta$ (°)	<$d\theta$> (°)	<dpi> (%)	<$d\theta i$> (°)
48 Lib										
U	-0.36/0.09	0.12	-0.50/0.11	0.09	0.63/0.09	0.11	117.4/	4.8	4.8	0.10	4.6
B	-0.42/0.02	0.05	-0.72/0.11	0.07	0.84/0.08	0.06	119.6/	2.3	2.1	0.04	1.5
V	-0.47/0.05	0.06	-0.72/0.08	0.06	0.87/0.08	0.07	118.3/	1.8	2.3	0.05	1.8
R	-0.48/0.04	0.07	-0.61/0.09	0.06	0.78/0.06	0.06	115.8/	2.9	2.6	0.04	1.6
I	-0.50/0.11	0.13	-0.58/0.08	0.16	0.79/0.08	0.15	114.2/	3.9	5.3	0.10	3.8
GAV	0.06	0.09	0.09	0.09	0.08	0.09		3.1	3.4	0.07	2.7
χ Oph										
U	-0.01/0.07	0.08	-0.38/0.03	0.05	0.39/0.03	0.05	133.9/	4.9	5.9	0.07	5.6
B	-0.08/0.09	0.06	-0.49/0.04	0.04	0.50/0.04	0.04	130.1/	5.0	3.9	0.04	2.3
V	-0.02/0.02	0.07	-0.55/0.06	0.04	0.56/0.06	0.04	134.1/	1.4	3.8	0.04	2.2
R	0.04/0.05	0.05	-0.44/0.03	0.04	0.44/0.03	0.04	137.7/	3.2	3.8	0.03	1.8
I	-0.01/0.05	0.04	-0.48/0.09	0.06	0.48/0.08	0.05	134.0/	3.7	2.8	0.05	3.2
GAV	0.06	0.06	0.05	0.05	0.05	0.05		3.6	4.0	0.05	3.0
π Aqr										
U	0.44/0.28[c]	0.09	-0.62/0.19	0.11	0.77/0.31	0.10	151.2/	5.1	4.9	0.07	3.0
B	0.51/0.47[c]	0.06	-0.73/0.25[c]	0.07	0.92/0.46	0.06	148.5/	10.9	2.8	0.04	1.5
V	0.45/0.42[c]	0.06	-0.70/0.20[c]	0.05	0.88/0.37	0.05	148.2/	10.2	2.5	0.05	1.8
R	0.47/0.37[c]	0.08	-0.65/0.18[c]	0.06	0.83/0.33	0.06	149.9/	9.1	2.9	0.04	1.5
I	0.31/0.23	0.06	-0.61/0.18	0.09	0.69/0.24	0.09	146.8/	7.5	3.1	0.09	4.4
GAV	0.36[d]	0.07	0.20[d]	0.08	0.34	0.07		8.6	3.2	0.06	2.5
o And										
U	-0.28/0.07	0.06	0.01/0.02	0.05	0.29/0.07	0.06	87.7/	3.0	7.0	0.05	5.3
B	-0.40/0.02	0.06	-0.03/0.02	0.05	0.40/0.03	0.06	91.6/	1.7	3.4	0.02	1.8
V	-0.36/0.07	0.03	-0.04/0.01	0.08	0.37/0.07	0.03	93.2/	1.6	6.1	0.03	2.2
R	-0.32/0.04	0.04	-0.01/0.04	0.03	0.33/0.05	0.04	90.4/	3.9	3.1	0.02	1.9
I	-0.31/0.04	0.05	0.02/0.08	0.08	0.32/0.05	0.05	88.1/	6.4	7.0	0.05	4.6
GAV	0.05	0.05	0.04	0.06	0.05	0.05		3.3	5.3	0.03	3.2

[c] dq or du > 3<dpi>: moderate year-to-year variability (See Section 3.2.)

[d] dq(GAV) or du(GAV)> 3<dpi> (GAV): strong year-to-year variability (See Section 3.2.)

Table 16. π Aqr Intrinsic Polarization

Date(Mo/Yr) Filter(n)	q/dq (%)	u/du (%)	p/dp (%)	$\theta/d\theta$ (°)	$dpi/d\theta i$ (%) (°)
05/90					
$U(4)$	0.58/0.14	-0.22/0.11	0.62/0.16	169.9/ 3.6	0.07/ 3.6
$B(4)$	0.58/0.06	-0.30/0.08	0.65/0.08	166.5/ 3.0	0.05/ 2.0
$V(4)$	0.52/0.08	-0.22/0.06	0.57/0.07	168.4/ 3.1	0.05/ 2.6
$R(4)$	0.58/0.08	-0.22/0.07	0.62/0.10	169.8/ 1.9	0.04/ 2.0
$I(4)$	0.40/0.04	-0.45/0.09	0.60/0.08	156.1/ 3.2	0.10/ 4.6
08/91					
$U(3)$	1.06/0.03	-0.53/0.06	1.18/0.06	166.7/ 1.0	0.07/ 1.7
$B(3)$	1.36/0.04	-0.67/0.10	1.52/0.02	166.8/ 2.0	0.04/ 0.8
$V(3)$	1.21/0.03	-0.56/0.04	1.33/0.04	167.5/ 0.7	0.04/ 0.9
$R(3)$	1.12/0.08	-0.51/0.09	1.23/0.09	167.8/ 1.9	0.03/ 0.8
$I(3)$	0.72/0.04	-0.41/0.08	0.84/0.02	165.1/ 3.0	0.08/ 2.6
07/92					
$U(4)$	0.39/0.10	-0.08/0.11	0.41/0.10	173.5/ 8.4	0.06/ 4.7
$B(4)$	0.26/0.08	-0.07/0.03	0.27/0.07	171.5/ 5.0	0.04/ 4.2
$V(4)$	0.27/0.07	-0.14/0.04	0.31/0.06	166.4/ 5.2	0.05/ 4.4
$R(4)$	0.30/0.09	-0.13/0.03	0.33/0.07	167.4/ 5.6	0.04/ 3.4
$I(4)$	0.26/0.05	-0.06/0.07	0.28/0.05	173.8/ 7.7	0.09/ 9.7
06/93					
$U(7)$	0.75/0.07	-0.35/0.15	0.84/0.06	167.6/ 5.4	0.07/ 2.6
$B(7)$	0.94/0.08	-0.44/0.07	1.04/0.09	167.4/ 1.7	0.04/ 1.1
$V(7)$	0.94/0.08	-0.47/0.07	1.05/0.08	166.6/ 1.9	0.05/ 1.4
$R(7)$	0.92/0.05	-0.42/0.07	1.01/0.06	167.7/ 1.7	0.04/ 1.2
$I(7)$	0.72/0.13	-0.37/0.10	0.82/0.15	166.5/ 2.7	0.10/ 3.4

Table 17. π Aquarii Intrinsic Polarization Summary

Star Filter	q/dq (%)	<dq> (%)	u/du (%)	<du> (%)	p/dp (%)	<dp> (%)	$\theta/d\theta$ (°)	<$d\theta$> (°)	<dpi> (%)	<$d\theta i$> (°)
π Aqr										
U	0.69/0.28[c]	0.09	-0.29/0.19	0.11	0.76/0.33	0.09	169.4/ 3.0	4.6	0.07	3.2
B	0.79/0.47[c]	0.06	-0.37/0.25[c]	0.07	0.87/0.54	0.06	168.0/ 2.3	2.9	0.04	2.0
V	0.74/0.42[c]	0.06	-0.35/0.20[c]	0.05	0.81/0.46	0.06	167.2/ 0.9	2.7	0.05	2.3
R	0.73/0.36[c]	0.08	-0.32/0.18[c]	0.06	0.80/0.40	0.08	168.2/ 1.1	2.8	0.04	1.8
I	0.52/0.23	0.06	-0.32/0.18	0.09	0.63/0.26	0.08	165.4/ 7.3	4.2	0.09	5.1
GAV	0.35[d]	0.07	0.20[d]	0.08	0.40	0.08	2.9	3.4	0.06	2.9

[c] dq or du > 3<dpi>: moderate year-to-year variability (See Section 3.2.)

[d] dq(GAV) or du(GAV)> 3<dpi>(GAV): strong year-to-year variability (See Section 3.2.)

Chapter 5

Multicolor Polarimetry of Selected Be Stars: 1995–1998

(originally published in 1999 PASP, 111, 494)

ABSTRACT

A new polarimeter called AnyPol has been used at Limber Observatory for four years to annually monitor the broadband linear polarization of a sample of bright northern Be stars. This is the fourth report on a program started in 1985 at McDonald Observatory and the first one to come entirely from the new installation. Although no variability was detected at the 3 σ level during the current reporting period, analysis of the full 13 year data set is beginning to reveal hints of long term variability that may provide clues for understanding the Be phenomenon.

1. Introduction

Be stars are non-supergiant B-type stars whose spectra have, or had at some time, one or more Balmer lines in emission. The mystery of the Be phenomenon is that the emission, which is well understood to originate from a flattened circumstellar envelope or disk, can come and go episodically on time scales of days to decades. This has yet to be explained as a predictable consequence of stellar evolution theory, although many contributing factors have been discussed, including rapid rotation, radiation-driven stellar winds, nonradial pulsation, flarelike magnetic activity, and binary interaction. For the unfamiliar reader, the review of Be stars by Slettebak (1988) will provide an excellent introduction.

Recent optical interferometry combined with spectropolarimetry has directly confirmed that the circumstellar envelopes surrounding Be stars are equatorially flattened (Quirrenbach et al. 1997). Given the small observed polarization of only about 1%, Monte Carlo computer simulations of polarization by electron scattering of the starlight in the

circumstellar envelope (Wood, Bjorkman, & Bjorkman 1997) constrain it to be an extremely thin disk, with opening angle (half width in latitude) on the order of 3°. This example shows that polarimetry is a very useful observational technique for studying physical properties of the envelopes, with the ultimate purpose of understanding their origin. Toward this end it is of great interest to measure polarization variations and the time scales on which they occur, in order to characterize the physical processes involved.

This paper is the fourth status report on an ongoing program of annual polarimetric monitoring of a sample of bright northern Be stars begun in 1985 (McDavid 1994 and references therein). The program stars are listed in Table 1, with visual magnitudes taken from Hoffleit & Jaschek (1982) and spectral types and $v \sin i$ values from Slettebak (1982). A broad band filter system (Table 2) was chosen to extend the time base of continuous systematic observations for the study of long term variability, taking advantage of earlier work which dates back to the 1950s. After 10 years on the 0.9 m telescope at McDonald Observatory the project was relocated to a new polarimeter on the 0.4 m telescope at Limber Observatory, where more flexible scheduling allows the study of variability on a greater variety of time scales. Advancements in commercially available instrumentation have made it possible to do so without compromising the quality of the data.

2. AnyPol: A generic linear polarimeter

AnyPol got its name from the fact that it is completely generic and incorporates no new principles of design or construction. In most respects, including the color system as specified by prescription, it is a simplified and miniaturized version of the McDonald Observatory polarimeter (Breger 1979): a rapidly rotating Glan-Taylor prism as an analyzer, followed by a Lyot depolarizer, Johnson/Cousins *UBVRI*glass filters, a Fabry lens, and an uncooled S-20 photomultiplier tube. It is very compact, with stepper motors and belt drives for separate analyzer and filter wheel modules which fit into a single main head unit. A simple postviewer using a right-angle prism at one position

Table 1. Program Be Stars

Name	HD	HR	V	Spectral Type	$v \sin i$ (km s^{-1})
γ Cas	5394	264	2.47	B0.5 IVe	230
ϕ Per	10516	496	4.07	B1.5 (V:)e-shell	400
48 Per	25940	1273	4.04	B4 Ve	200
ζ Tau	37202	1910	3.00	B1 IVe-shell	220
48 Lib	142983	5941	4.88	B3:IV:e-shell	400
χ Oph	148184	6118	4.42	B1.5 Ve	140
π Aqr	212571	8539	4.66	B1 III-IVe	300
o And	217675	8762	3.62	B6 III	260

of the filter wheel is adequate for finding and centering, and three aperture sizes are available in a slide mechanism with a pair of LEDs for backlighting.

The control system for AnyPol is based on a 66 MHz 486 PC with plugin multichannel analyzer and stepper motor controller cards, interfaced to the polarimeter head through an electronics chassis unit containing the power supplies and microstepping drivers. A point-and-click display serves to control all selectable functions and parameters and also shows 10 s updates of the measurement in progress, including a graph of the data buffer. The mathematical details of the data processing were adapted from the control program for the Minipol polarimeter of the University of Arizona (Frecker & Serkowski 1976).

On the 0.4 m telescope at Limber Observatory the photon count rates are comparable to those obtained with the 0.9 m telescope at McDonald Observatory with a neutral density filter of 10% transmission which was necessary for the bright stars (V = 2–5) in the Be star monitoring program. Observational error estimates are derived from the repeatability of multiple independent measurements, and they are in general agreement with checks based on the residuals in the fit to the modulated signal and the uncertainty derived from photon counting statistics. Typical errors are on the order of 0.05% in the degree of polarization and 2° in position angle. One of the main sources of error is a slight variation in the speed of the motor driving the analyzer, which becomes significant at the level of a few hundredths of a percent. All observations are corrected for an instrumental polarization on the order of 0.10%, tracked by repeated observations of unpolarized standard stars from the list of Serkowski (1974). The position angle is calibrated by observing polarized standard stars from the list of Hsu & Breger (1982).

3. Observations

The targets for the annual monitoring program were selected to include Be stars with a variety of different characteristics and with the longest possible history of continuous observation. They fall into summer and winter groups, so the basic observing strategy is to make the polarization measurements during about one week in summer and one week in winter. The only interruption in the project has been the loss of 1994 while the new polarimeter was under construction.

Table 2. Filter System Parameters

Filter	Effective Wavelength (Å)	Bandpass (fwhm) (Å)
U	3650	700
B	4400	1000
V	5500	900
R	6400	1500
I	7900	1500

One individual measurement consists of 3 cycles through all 5 filters with a 200 s integration time on each filter. If there is a bright Moon, a sky cycle is taken to correct for the background polarization. The result for each single filter is taken to be the mean and standard deviation of the 3 integrations in that filter. (The standard deviation is a more conservative error estimate than the standard deviation of the mean, but it may be more realistic because 3 measurements is a very small sample.) During a typical observing run for this project, about 3 to 5 observations of each program star are collected on different nights during the same week.

4. Analysis of variability

The first goal in analyzing the data is to identify clear cases of variable polarization over the time scales covered by this installment of the project. The data are presented in Tables 3–12, which begin with the month and year of the observing run and the number of measurements in each filter. The q and u normalized Stokes parameters, the degree of polarization p, and the polarization position angle θ are all given as the mean and standard deviation for each run. The last column shows the average error in p and θ for a single measurement. In addition to the program Be stars, two polarized standard stars were also observed as checks on the stability of the system: 2H Cam (HD 21291, HR 1035, $V = 4.21$, B9 Ia) in winter and o Sco (HD 147084, HR 6081, $V = 4.54$, A5 II) in summer.

As in previous papers in this series, summary tables (Tables 13–15) were constructed giving the means and standard deviations of the measurements for each star in each filter over the four annual data sets. The quantities in angled brackets are also four-year averages, and the quantities in rows labeled "GAV" for "grand average" are averages over all five filters.

Since p and θ carry a statistical bias, q and u are more appropriate quantities for evaluating variability (Clarke & Stewart 1986). Nevertheless, it may provide more physical insight to study p and θ to see if the variability is mainly in polarization degree or position angle. In fact, with the limited number of measurements at hand, statistical tests must be applied with caution regardless of which set of parameters is used.

We can apply various simple 3 σ criteria to conservatively identify variability, as in previous papers in this series. Looking for night-to-night variability, we see that Tables 3–12 show only two cases in which dq or du is greater than $3dpi$: du^B of γ Cas in 01/96 and du^B of o And in 06/95. Both cases are negligible, since they occur in only one filter and during only one observing run. For year-to-year variability, Tables 13–15 show not a single case in which dq or du is greater than $3\langle dpi\rangle$. The conclusion is that we can demonstrate no statistically significant variability in the polarization of any of the program stars over the latest 4 year time period.

Since variable polarization was detected in the two previous reports on this project, it seems advisable to search for an explanation by comparing the Limber Observatory

Table 3. 2H Cam (Standard Star)

Date(Mo/Yr) Filter(n)	q/dq (%)	u/du (%)	p/dp (%)	$\theta/d\theta$ (°)	$dpi/d\theta i$ (%) (°)
12/94					
$U(4)$	-1.82/0.07	-2.33/0.06	2.96/0.02	116.0/ 0.8	0.09/ 1.3
$B(4)$	-2.06/0.03	-2.58/0.09	3.30/0.08	115.7/ 0.5	0.05/ 0.8
$V(4)$	-2.07/0.08	-2.69/0.11	3.40/0.10	116.2/ 0.8	0.05/ 0.8
$R(4)$	-2.00/0.07	-2.61/0.11	3.29/0.07	116.3/ 1.0	0.04/ 0.7
$I(4)$	-1.82/0.09	-2.24/0.02	2.88/0.06	115.5/ 0.7	0.08/ 0.7
01/96					
$U(3)$	-1.94/0.01	-2.43/0.08	3.11/0.05	115.7/ 0.6	0.10/ 1.0
$B(3)$	-1.97/0.11	-2.67/0.04	3.32/0.10	116.8/ 0.6	0.08/ 0.7
$V(3)$	-2.06/0.09	-2.75/0.05	3.44/0.09	116.6/ 0.4	0.04/ 0.5
$R(3)$	-1.98/0.06	-2.70/0.08	3.35/0.10	116.9/ 0.3	0.06/ 0.3
$I(3)$	-1.79/0.10	-2.43/0.04	3.02/0.09	116.8/ 0.6	0.11/ 0.9
12/96					
$U(3)$	-1.73/0.02	-2.44/0.02	3.00/0.02	117.4/ 0.2	0.06/ 0.9
$B(3)$	-1.86/0.10	-2.72/0.03	3.29/0.05	117.8/ 0.8	0.07/ 0.3
$V(3)$	-2.03/0.06	-2.78/0.05	3.45/0.01	117.0/ 0.6	0.04/ 0.5
$R(3)$	-1.98/0.05	-2.66/0.03	3.32/0.01	116.7/ 0.5	0.05/ 0.4
$I(3)$	-1.80/0.01	-2.41/0.08	3.01/0.07	116.6/ 0.5	0.10/ 0.7
12/97					
$U(5)$	-1.81/0.06	-2.46/0.02	3.06/0.04	116.8/ 0.5	0.12/ 1.4
$B(5)$	-1.93/0.04	-2.62/0.03	3.26/0.03	116.8/ 0.4	0.06/ 0.6
$V(5)$	-2.02/0.02	-2.78/0.05	3.44/0.04	117.0/ 0.4	0.10/ 0.5
$R(5)$	-1.95/0.04	-2.67/0.04	3.31/0.04	116.9/ 0.4	0.05/ 0.7
$I(5)$	-1.74/0.08	-2.38/0.10	2.95/0.09	116.9/ 1.0	0.08/ 0.8

Table 4. o Sco (Standard Star)

Date(Mo/Yr) Filter(n)	q/dq (%)	u/du (%)	p/dp (%)	$\theta/d\theta$ (°)	$dpi/d\theta i$ (%) (°)
06/95					
$U(4)$	1.25/0.28	2.40/0.17	2.73/0.18	31.2/ 2.8	0.17/ 3.2
$B(4)$	1.58/0.13	3.03/0.06	3.42/0.11	31.3/ 0.8	0.09/ 1.1
$V(4)$	1.96/0.08	3.72/0.10	4.21/0.11	31.2/ 0.4	0.11/ 1.0
$R(4)$	2.05/0.05	3.94/0.06	4.44/0.08	31.3/ 0.2	0.11/ 0.7
$I(4)$	1.93/0.03	3.85/0.08	4.31/0.07	31.7/ 0.3	0.19/ 1.2
06/96					
$U(4)$	0.93/0.12	2.36/0.38	2.54/0.39	34.3/ 0.8	0.19/ 2.1
$B(4)$	1.37/0.05	3.14/0.08	3.43/0.10	33.2/ 0.3	0.06/ 0.8
$V(4)$	1.68/0.10	3.81/0.05	4.17/0.01	33.1/ 0.8	0.10/ 0.9
$R(4)$	1.76/0.08	4.07/0.07	4.44/0.07	33.3/ 0.5	0.09/ 0.8
$I(4)$	1.70/0.08	3.98/0.03	4.33/0.04	33.4/ 0.5	0.06/ 0.8
07/97					
$U(5)$	1.05/0.16	2.34/0.20	2.58/0.23	33.0/ 1.5	0.24/ 2.5
$B(5)$	1.34/0.05	3.14/0.04	3.41/0.05	33.5/ 0.4	0.06/ 0.5
$V(5)$	1.57/0.12	3.80/0.10	4.11/0.12	33.8/ 0.7	0.09/ 0.7
$R(5)$	1.68/0.10	4.03/0.08	4.36/0.07	33.7/ 0.7	0.05/ 0.5
$I(5)$	1.56/0.13	4.06/0.05	4.35/0.07	34.5/ 0.8	0.15/ 0.9
07/98					
$U(4)$	1.00/0.15	2.29/0.17	2.51/0.18	33.3/ 1.7	0.15/ 3.1
$B(4)$	1.37/0.07	3.06/0.05	3.35/0.06	33.0/ 0.5	0.09/ 0.6
$V(4)$	1.72/0.02	3.73/0.08	4.11/0.08	32.6/ 0.2	0.09/ 0.6
$R(4)$	1.82/0.07	3.97/0.07	4.37/0.08	32.7/ 0.4	0.11/ 0.6
$I(4)$	1.75/0.06	3.85/0.03	4.23/0.03	32.8/ 0.4	0.15/ 1.0

Table 5. γ Cas

Date(Mo/Yr) Filter(n)	q/dq (%)	u/du (%)	p/dp (%)	$\theta/d\theta$ (°)	$dpi/d\theta i$ (%) (°)
12/94					
$U(4)$	-0.43/0.08	-0.24/0.08	0.50/0.10	103.9/ 3.1	0.07/ 2.5
$B(4)$	-0.66/0.05	-0.42/0.02	0.79/0.04	106.1/ 1.4	0.05/ 1.7
$V(4)$	-0.58/0.04	-0.35/0.03	0.69/0.02	105.7/ 2.1	0.05/ 1.8
$R(4)$	-0.62/0.06	-0.32/0.03	0.70/0.05	103.8/ 2.2	0.05/ 1.5
$I(4)$	-0.54/0.05	-0.22/0.04	0.59/0.05	100.8/ 1.4	0.06/ 3.6
01/96					
$U(3)$	-0.56/0.08	-0.28/0.04	0.63/0.08	103.5/ 1.8	0.08/ 2.1
$B(3)$	-0.70/0.05	-0.50/0.12	0.87/0.06	107.7/ 3.9	0.03/ 2.5
$V(3)$	-0.59/0.03	-0.40/0.05	0.72/0.01	107.0/ 2.2	0.05/ 1.5
$R(3)$	-0.60/0.08	-0.31/0.09	0.68/0.08	103.7/ 3.8	0.06/ 2.1
$I(3)$	-0.41/0.04	-0.25/0.03	0.49/0.05	106.4/ 1.4	0.09/ 3.5
12/96					
$U(5)$	-0.38/0.05	-0.30/0.08	0.49/0.07	109.3/ 3.1	0.07/ 3.7
$B(5)$	-0.61/0.06	-0.42/0.08	0.74/0.06	107.3/ 3.1	0.07/ 2.9
$V(5)$	-0.56/0.08	-0.33/0.09	0.66/0.09	105.3/ 3.1	0.06/ 2.6
$R(5)$	-0.55/0.08	-0.28/0.08	0.62/0.07	103.2/ 3.8	0.10/ 3.2
$I(5)$	-0.46/0.06	-0.24/0.06	0.52/0.07	103.2/ 3.0	0.09/ 3.2
12/97					
$U(6)$	-0.50/0.08	-0.31/0.03	0.60/0.08	106.2/ 1.6	0.08/ 4.9
$B(6)$	-0.64/0.04	-0.39/0.09	0.76/0.08	105.6/ 2.5	0.11/ 2.9
$V(6)$	-0.58/0.06	-0.40/0.06	0.70/0.08	107.2/ 1.2	0.08/ 2.3
$R(6)$	-0.58/0.06	-0.27/0.08	0.65/0.04	102.4/ 4.0	0.11/ 3.4
$I(6)$	-0.45/0.05	-0.20/0.05	0.50/0.05	102.2/ 2.6	0.06/ 6.8

Table 6. ϕ Per

Date(Mo/Yr) Filter(n)	q/dq (%)	u/du (%)	p/dp (%)	$\theta/d\theta$ (°)	$dpi/d\theta i$ (%) (°)
12/94					
$U(4)$	0.25/0.06	0.85/0.10	0.89/0.10	36.9/ 2.2	0.08/ 2.0
$B(4)$	0.46/0.11	1.09/0.08	1.19/0.08	33.6/ 2.5	0.04/ 1.7
$V(4)$	0.34/0.08	0.99/0.08	1.05/0.09	35.5/ 1.8	0.05/ 1.5
$R(4)$	0.24/0.07	0.90/0.08	0.94/0.07	37.5/ 2.2	0.06/ 2.6
$I(4)$	0.10/0.08	0.72/0.03	0.73/0.03	41.0/ 3.0	0.10/ 2.4
01/96					
$U(3)$	0.04/0.08	0.85/0.11	0.86/0.11	43.7/ 2.5	0.07/ 3.8
$B(3)$	0.41/0.06	1.23/0.06	1.30/0.07	35.8/ 1.2	0.06/ 1.2
$V(3)$	0.37/0.07	1.10/0.08	1.16/0.09	35.8/ 1.4	0.07/ 1.1
$R(3)$	0.25/0.03	0.94/0.09	0.97/0.08	37.5/ 1.2	0.06/ 1.4
$I(3)$	0.22/0.03	0.69/0.08	0.73/0.09	36.5/ 0.4	0.11/ 2.6
12/96					
$U(5)$	0.18/0.05	0.81/0.12	0.83/0.12	38.5/ 1.6	0.10/ 2.1
$B(5)$	0.50/0.04	1.28/0.10	1.37/0.08	34.3/ 1.5	0.05/ 1.4
$V(5)$	0.39/0.06	1.12/0.10	1.19/0.10	35.4/ 1.3	0.07/ 1.6
$R(5)$	0.25/0.05	1.01/0.10	1.05/0.10	37.8/ 1.5	0.05/ 2.6
$I(5)$	0.19/0.07	0.81/0.17	0.84/0.17	38.1/ 2.3	0.06/ 3.2
12/97					
$U(6)$	0.15/0.07	0.83/0.08	0.85/0.08	39.7/ 2.1	0.07/ 3.8
$B(6)$	0.52/0.01	1.34/0.06	1.44/0.06	34.4/ 0.4	0.05/ 1.3
$V(6)$	0.44/0.04	1.21/0.04	1.29/0.05	35.0/ 0.8	0.07/ 2.3
$R(6)$	0.33/0.02	1.09/0.08	1.14/0.07	36.6/ 0.7	0.05/ 1.8
$I(6)$	0.29/0.05	0.95/0.08	1.00/0.08	36.5/ 1.7	0.09/ 3.2

Table 7. 48 Per

Date(Mo/Yr) Filter(n)	q/dq (%)	u/du (%)	p/dp (%)	$\theta/d\theta$ (°)	$dpi/d\theta i$ (%) (°)
12/94					
$U(4)$	0.77/0.05	-0.21/0.06	0.81/0.04	172.3/ 2.7	0.11/ 2.2
$B(4)$	0.76/0.06	-0.28/0.05	0.81/0.04	169.7/ 2.3	0.05/ 1.8
$V(4)$	0.91/0.07	-0.34/0.07	0.97/0.05	169.9/ 2.4	0.09/ 1.8
$R(4)$	0.85/0.05	-0.29/0.03	0.90/0.05	170.6/ 1.2	0.07/ 1.3
$I(4)$	0.72/0.05	-0.23/0.06	0.76/0.05	171.2/ 2.2	0.06/ 2.8
01/96					
$U(3)$	0.61/0.06	-0.14/0.04	0.63/0.07	173.3/ 2.1	0.09/ 3.3
$B(3)$	0.82/0.03	-0.20/0.06	0.85/0.03	173.2/ 1.8	0.03/ 1.8
$V(3)$	0.89/0.05	-0.20/0.06	0.91/0.04	173.6/ 2.1	0.05/ 3.0
$R(3)$	0.92/0.05	-0.24/0.04	0.96/0.05	172.6/ 1.4	0.07/ 0.8
$I(3)$	0.81/0.04	-0.17/0.05	0.83/0.04	174.1/ 1.8	0.08/ 1.3
12/96					
$U(4)$	0.83/0.07	-0.24/0.08	0.87/0.05	171.6/ 3.3	0.08/ 2.0
$B(4)$	0.90/0.02	-0.25/0.04	0.94/0.02	172.1/ 1.2	0.07/ 1.4
$V(4)$	0.96/0.07	-0.24/0.06	0.99/0.08	172.9/ 1.7	0.06/ 2.4
$R(4)$	0.97/0.04	-0.21/0.09	1.00/0.02	173.9/ 2.7	0.07/ 2.0
$I(4)$	0.85/0.09	-0.25/0.08	0.90/0.08	171.5/ 2.9	0.11/ 4.4
12/97					
$U(6)$	0.71/0.06	-0.23/0.07	0.75/0.07	170.9/ 2.0	0.08/ 2.9
$B(6)$	0.83/0.04	-0.22/0.05	0.86/0.04	172.5/ 1.3	0.06/ 2.2
$V(6)$	0.97/0.08	-0.23/0.03	1.00/0.08	173.3/ 0.8	0.08/ 2.0
$R(6)$	0.90/0.03	-0.21/0.06	0.93/0.03	173.5/ 2.0	0.08/ 2.3
$I(6)$	0.88/0.12	-0.17/0.07	0.90/0.12	174.4/ 2.6	0.10/ 2.7

Table 8. ζ Tau

Date(Mo/Yr) Filter(n)	q/dq (%)	u/du (%)	p/dp (%)	$\theta/d\theta$ (°)	$dpi/d\theta i$ (%) (°)
12/94					
$U(4)$	0.51/0.06	1.12/0.06	1.24/0.06	32.8/ 1.3	0.07/ 1.2
$B(4)$	0.57/0.08	1.31/0.08	1.43/0.10	33.3/ 1.0	0.04/ 0.9
$V(4)$	0.63/0.06	1.24/0.05	1.39/0.04	31.5/ 1.6	0.03/ 0.7
$R(4)$	0.49/0.01	1.15/0.02	1.26/0.02	33.4/ 0.3	0.06/ 1.3
$I(4)$	0.31/0.06	1.05/0.10	1.10/0.10	36.7/ 1.6	0.07/ 1.4
01/96					
$U(3)$	0.44/0.04	1.01/0.08	1.10/0.06	33.2/ 1.5	0.04/ 1.2
$B(3)$	0.65/0.01	1.26/0.10	1.42/0.08	31.3/ 1.0	0.05/ 1.3
$V(3)$	0.59/0.05	1.25/0.08	1.38/0.08	32.4/ 0.3	0.05/ 1.7
$R(3)$	0.51/0.02	1.20/0.02	1.30/0.02	33.5/ 0.4	0.10/ 1.5
$I(3)$	0.52/0.03	1.06/0.10	1.18/0.10	31.9/ 0.5	0.06/ 1.6
12/96					
$U(4)$	0.59/0.02	1.04/0.04	1.21/0.03	30.2/ 0.6	0.08/ 2.9
$B(4)$	0.64/0.04	1.42/0.05	1.57/0.04	32.8/ 0.8	0.05/ 2.8
$V(4)$	0.59/0.03	1.30/0.05	1.44/0.03	32.8/ 0.9	0.06/ 2.3
$R(4)$	0.52/0.04	1.26/0.05	1.36/0.04	33.8/ 1.1	0.11/ 1.5
$I(4)$	0.44/0.06	1.01/0.10	1.11/0.11	33.3/ 0.9	0.11/ 2.5
12/97					
$U(6)$	0.50/0.08	1.08/0.08	1.20/0.06	32.6/ 2.3	0.09/ 2.5
$B(6)$	0.74/0.07	1.45/0.11	1.63/0.09	31.5/ 1.4	0.08/ 2.0
$V(6)$	0.71/0.05	1.37/0.12	1.55/0.10	31.3/ 1.5	0.10/ 1.8
$R(6)$	0.55/0.07	1.30/0.11	1.42/0.10	33.5/ 1.7	0.07/ 2.0
$I(6)$	0.57/0.02	1.12/0.12	1.26/0.11	31.4/ 1.1	0.07/ 2.5

Table 9. 48 Lib

Date(Mo/Yr) Filter(n)	q/dq (%)	u/du (%)	p/dp (%)	$\theta/d\theta$ (°)	$dpi/d\theta i$ (%) (°)
06/95					
$U(4)$	-0.40/0.12	-0.61/0.07	0.74/0.10	118.3/ 4.4	0.13/ 5.9
$B(4)$	-0.36/0.06	-0.83/0.06	0.91/0.05	123.3/ 2.2	0.03/ 2.9
$V(4)$	-0.46/0.03	-0.71/0.04	0.85/0.04	118.7/ 1.4	0.06/ 2.2
$R(4)$	-0.43/0.05	-0.60/0.04	0.74/0.02	117.1/ 2.3	0.07/ 2.1
$I(4)$	-0.51/0.06	-0.54/0.13	0.76/0.10	112.6/ 4.1	0.10/ 4.9
06/96					
$U(4)$	-0.43/0.04	-0.69/0.09	0.82/0.06	118.9/ 2.8	0.12/ 3.0
$B(4)$	-0.40/0.03	-0.87/0.06	0.96/0.07	122.6/ 0.7	0.07/ 2.6
$V(4)$	-0.52/0.05	-0.73/0.08	0.90/0.09	117.2/ 1.0	0.06/ 1.9
$R(4)$	-0.55/0.07	-0.64/0.06	0.86/0.07	114.7/ 2.1	0.06/ 2.6
$I(4)$	-0.52/0.02	-0.51/0.11	0.74/0.08	112.2/ 3.1	0.12/ 5.4
07/97					
$U(4)$	-0.35/0.10	-0.41/0.06	0.56/0.06	114.8/ 5.0	0.12/ 6.0
$B(4)$	-0.46/0.05	-0.72/0.08	0.86/0.08	118.5/ 1.5	0.09/ 1.6
$V(4)$	-0.60/0.04	-0.65/0.05	0.88/0.06	113.8/ 1.2	0.11/ 1.9
$R(4)$	-0.57/0.09	-0.63/0.05	0.85/0.09	114.0/ 1.4	0.09/ 2.6
$I(4)$	-0.67/0.11	-0.60/0.09	0.91/0.12	111.4/ 2.1	0.11/ 5.3
07/98					
$U(5)$	-0.35/0.08	-0.53/0.08	0.65/0.10	118.5/ 2.3	0.09/ 5.4
$B(5)$	-0.42/0.06	-0.78/0.08	0.89/0.06	120.7/ 2.6	0.04/ 3.9
$V(5)$	-0.51/0.04	-0.71/0.08	0.88/0.08	117.1/ 1.0	0.07/ 3.0
$R(5)$	-0.53/0.02	-0.63/0.06	0.83/0.04	114.8/ 1.8	0.09/ 2.3
$I(5)$	-0.42/0.03	-0.58/0.09	0.74/0.06	117.2/ 3.0	0.14/ 6.6

Table 10. χ Oph

Date(Mo/Yr) Filter(n)	q/dq (%)	u/du (%)	p/dp (%)	$\theta/d\theta$ (°)	$dpi/d\theta i$ (%) (°)
06/95					
$U(4)$	0.03/0.06	-0.39/0.05	0.41/0.06	137.6/ 4.9	0.11/ 8.5
$B(4)$	-0.06/0.06	-0.52/0.08	0.54/0.08	132.1/ 2.9	0.06/ 5.0
$V(4)$	0.00/0.05	-0.52/0.06	0.53/0.06	134.8/ 2.9	0.10/ 5.4
$R(4)$	-0.04/0.07	-0.46/0.07	0.47/0.07	132.7/ 4.4	0.05/ 4.8
$I(4)$	-0.02/0.04	-0.43/0.06	0.45/0.04	136.0/ 3.5	0.15/12.1
06/96					
$U(4)$	-0.03/0.20	-0.28/0.03	0.38/0.05	134.9/18.7	0.12/15.7
$B(4)$	0.00/0.08	-0.42/0.08	0.44/0.07	135.5/ 8.3	0.09/ 9.2
$V(4)$	0.01/0.08	-0.45/0.07	0.46/0.07	135.8/ 4.9	0.13/ 3.9
$R(4)$	-0.05/0.07	-0.47/0.06	0.48/0.06	131.8/ 3.7	0.14/ 6.0
$I(4)$	-0.16/0.06	-0.41/0.05	0.47/0.05	126.0/ 5.7	0.10/12.4
07/97					
$U(4)$	0.12/0.11	-0.28/0.05	0.36/0.05	144.7/ 9.8	0.08/18.9
$B(4)$	-0.01/0.12	-0.45/0.05	0.47/0.05	135.0/ 7.4	0.08/ 4.6
$V(4)$	0.00/0.19	-0.44/0.07	0.48/0.07	136.2/11.5	0.08/ 5.5
$R(4)$	0.05/0.13	-0.48/0.07	0.50/0.06	138.7/ 7.7	0.07/ 7.6
$I(4)$	-0.04/0.11	-0.38/0.11	0.41/0.10	134.5/10.6	0.13/ 6.1
07/98					
$U(5)$	0.03/0.13	-0.37/0.08	0.40/0.10	134.7/ 7.6	0.13/10.7
$B(5)$	0.01/0.07	-0.47/0.05	0.48/0.05	135.6/ 4.6	0.12/ 4.8
$V(5)$	-0.03/0.04	-0.47/0.06	0.49/0.06	133.4/ 2.7	0.10/ 7.9
$R(5)$	0.01/0.07	-0.47/0.03	0.48/0.03	135.6/ 3.6	0.08/ 7.1
$I(5)$	0.01/0.14	-0.46/0.08	0.50/0.07	135.5/ 8.4	0.12/ 8.6

Table 11. π Aqr

Date(Mo/Yr) Filter(n)	q/dq (%)	u/du (%)	p/dp (%)	$\theta/d\theta$ (°)	$dpi/d\theta i$ (%) (°)
06/95					
$U(3)$	-0.01/0.11	-0.44/0.15	0.47/0.14	131.6/ 7.0	0.13/12.1
$B(3)$	-0.08/0.07	-0.50/0.04	0.51/0.04	130.0/ 3.8	0.10/ 5.1
$V(3)$	-0.06/0.05	-0.48/0.00	0.49/0.01	130.9/ 3.0	0.09/ 4.7
$R(3)$	-0.05/0.04	-0.45/0.04	0.46/0.03	132.0/ 2.5	0.09/ 4.0
$I(3)$	0.04/0.03	-0.40/0.01	0.42/0.02	137.8/ 2.4	0.08/ 9.4
06/96					
$U(4)$	-0.34/0.03	-0.32/0.05	0.48/0.04	112.2/ 2.3	0.10/ 5.2
$B(4)$	-0.38/0.04	-0.31/0.02	0.50/0.02	109.6/ 2.3	0.07/ 5.4
$V(4)$	-0.41/0.11	-0.30/0.07	0.52/0.06	108.9/ 6.0	0.08/ 3.6
$R(4)$	-0.37/0.08	-0.29/0.03	0.48/0.06	109.5/ 3.8	0.09/ 4.6
$I(4)$	-0.29/0.14	-0.31/0.04	0.46/0.08	114.2/ 9.5	0.14/10.4
07/97					
$U(4)$	-0.26/0.02	-0.29/0.05	0.40/0.05	113.0/ 2.8	0.10/ 7.8
$B(4)$	-0.36/0.02	-0.34/0.07	0.50/0.06	111.8/ 2.5	0.08/ 3.1
$V(4)$	-0.40/0.04	-0.31/0.03	0.51/0.03	108.8/ 2.4	0.04/ 2.8
$R(4)$	-0.37/0.06	-0.31/0.03	0.49/0.03	110.1/ 3.2	0.08/ 3.4
$I(4)$	-0.31/0.08	-0.26/0.08	0.43/0.07	110.4/ 7.0	0.07/ 9.6
07/98					
$U(5)$	-0.37/0.10	-0.27/0.09	0.48/0.11	107.6/ 4.9	0.10/ 6.4
$B(5)$	-0.36/0.06	-0.32/0.03	0.49/0.05	110.8/ 2.5	0.05/ 2.4
$V(5)$	-0.40/0.04	-0.30/0.05	0.51/0.02	108.6/ 3.5	0.08/ 4.5
$R(5)$	-0.41/0.06	-0.27/0.07	0.50/0.08	106.7/ 2.4	0.07/ 4.5
$I(5)$	-0.33/0.11	-0.25/0.08	0.44/0.10	110.8/ 5.6	0.09/ 9.5

Table 12. o And

Date(Mo/Yr) Filter(n)	q/dq (%)	u/du (%)	p/dp (%)	$\theta/d\theta$ (°)	$dpi/d\theta i$ (%) (°)
06/95					
$U(3)$	-0.48/0.02	-0.11/0.03	0.50/0.01	96.5/ 1.8	0.07/ 5.0
$B(3)$	-0.56/0.07	-0.16/0.11	0.59/0.09	97.8/ 4.4	0.03/ 3.2
$V(3)$	-0.53/0.01	-0.05/0.01	0.54/0.02	92.6/ 0.7	0.06/ 1.0
$R(3)$	-0.48/0.03	-0.03/0.02	0.49/0.03	91.8/ 1.0	0.04/ 2.9
$I(3)$	-0.46/0.09	-0.06/0.07	0.48/0.10	93.6/ 3.4	0.05/ 7.6
06/96					
$U(4)$	-0.40/0.07	-0.06/0.07	0.41/0.07	93.8/ 4.7	0.09/ 6.6
$B(4)$	-0.37/0.04	-0.05/0.06	0.38/0.04	93.6/ 3.6	0.08/ 3.6
$V(4)$	-0.32/0.06	-0.07/0.07	0.35/0.05	96.7/ 5.7	0.05/ 9.2
$R(4)$	-0.29/0.07	-0.06/0.04	0.31/0.06	95.6/ 4.0	0.07/ 9.8
$I(4)$	-0.30/0.10	-0.04/0.08	0.32/0.11	94.3/ 6.0	0.11/ 8.9
07/97					
$U(4)$	-0.27/0.03	0.00/0.06	0.28/0.03	89.7/ 6.4	0.10/ 7.5
$B(4)$	-0.36/0.02	-0.05/0.05	0.37/0.02	94.1/ 4.6	0.06/ 4.4
$V(4)$	-0.36/0.05	-0.02/0.01	0.37/0.05	91.0/ 1.1	0.06/ 7.4
$R(4)$	-0.35/0.04	-0.04/0.02	0.36/0.04	93.1/ 1.7	0.04/ 5.3
$I(4)$	-0.30/0.08	0.04/0.08	0.32/0.08	88.0/ 7.8	0.05/ 9.5
07/98					
$U(5)$	-0.43/0.06	-0.26/0.05	0.51/0.06	105.4/ 2.9	0.08/ 3.6
$B(5)$	-0.57/0.04	-0.27/0.04	0.64/0.04	102.9/ 1.9	0.07/ 4.2
$V(5)$	-0.60/0.06	-0.19/0.08	0.64/0.07	98.8/ 3.0	0.07/ 4.2
$R(5)$	-0.59/0.05	-0.19/0.07	0.62/0.06	98.9/ 2.8	0.07/ 3.3
$I(5)$	-0.56/0.07	-0.18/0.06	0.60/0.07	99.2/ 3.1	0.13/ 4.9

system with the system used at McDonald Observatory. For this purpose Table 13 of McDavid (1994) is reproduced here as Table 16 for direct comparison with the present Table 15. These observations of polarized standard stars show very clearly that the two systems match extremely well. The only outstanding difference is the typical precision of a single observation, which is higher in the McDonald system. This is readily understood since the McDonald estimates were based on theoretical photon counting statistics, while the Limber estimates are based on experimental scatter in repeated measurements. With a larger value for the error in a single observation, the Limber system is sometimes a less sensitive detector of variability, but it may also give more realistic results.

Work is underway to make a complete data set available at the Strasbourg Astronomical Data Center (CDS), including all of the annual observations from both McDonald Observatory and Limber Observatory published to date in this series of papers. The times will be given in decimal years for better precision than the current specification of month and year.

5. Discussion

The 3 σ criterion used here and in the previous papers of this series is very conservative, practically guaranteeing the validity of any detections of variability. This project has shown that such unquestionable detections are by no means common. However, as the data base has now grown to cover more than a decade in time, some patterns of long-term variability are beginning to appear, even though they may not have been previously recognizable at the 3 σ level. What follows is a commentary on the behavior of each individual program star, illustrated with q, u plots and graphs of intrinsic polarization as a function of time in all 5 filters over the entire duration of the monitoring program.

In each q, u plot the data points are filled circles, the mean is a cross drawn to the size of the average error of a single measurement, the standard deviation is represented by a dotted ellipse centered on the mean, and three times the average error of a single measurement is represented by a solid ellipse centered on the mean. For each star there is one additional q, u plot showing the mean value for each filter. Note that for all the program stars except 48 Lib it is possible to fit the 5 single filter data points with a straight line which passes close to the origin. This implies that either the interstellar component of the polarization is small or its position angle is nearly the same as that of the intrinsic component. In either case, the straight line fit gives a good approximation to the position angle of the intrinsic polarization. Any elongation of the distribution of data points along that general direction in the single filter q, u plots is good evidence for intrinsic polarization that is variable in degree but constant in position angle, as is commonly expected for polarization caused by electron scaterring in an equatorially flattened axisymmetric disk. This technique makes it possible to identify variable intrinsic polarization even when it is too small to meet the 3 σ test.

The graphs of polarization degree and position angle as a function of time for each filter

Table 13. Winter Be Star Summary

Star Filter	q/dq (%)	<dq> (%)	u/du (%)	<du> (%)	p/dp (%)	<dp> (%)	$\theta/d\theta$ (°)	<$d\theta$> (°)	<dpi> (%)	<$d\theta i$> (°)
γ Cas										
U	-0.47/0.08	0.07	-0.28/0.03	0.06	0.56/0.07	0.08	105.7/ 2.7	2.4	0.08	3.3
B	-0.65/0.04	0.05	-0.43/0.05	0.08	0.79/0.06	0.06	106.7/ 1.0	2.7	0.06	2.5
V	-0.58/0.01	0.05	-0.37/0.04	0.06	0.69/0.02	0.05	106.3/ 0.9	2.2	0.06	2.0
R	-0.59/0.03	0.07	-0.29/0.02	0.07	0.66/0.03	0.06	103.3/ 0.6	3.5	0.08	2.6
I	-0.47/0.05	0.05	-0.23/0.02	0.04	0.52/0.05	0.05	103.2/ 2.4	2.1	0.08	4.3
GAV	0.04	0.06	0.03	0.06	0.05	0.06	1.5	2.6	0.07	2.9
ϕ Per										
U	0.16/0.09	0.06	0.83/0.02	0.10	0.86/0.02	0.10	39.7/ 2.9	2.1	0.08	2.9
B	0.47/0.05	0.06	1.24/0.11	0.08	1.33/0.11	0.07	34.5/ 0.9	1.4	0.05	1.4
V	0.38/0.04	0.06	1.11/0.09	0.07	1.17/0.10	0.08	35.4/ 0.3	1.3	0.06	1.6
R	0.27/0.04	0.04	0.99/0.08	0.09	1.02/0.09	0.08	37.3/ 0.5	1.4	0.05	2.1
I	0.20/0.08	0.06	0.79/0.12	0.09	0.82/0.13	0.09	38.0/ 2.1	1.8	0.09	2.8
GAV	0.06	0.06	0.08	0.09	0.09	0.09	1.4	1.6	0.07	2.2
48 Per										
U	0.73/0.09	0.06	-0.20/0.05	0.06	0.76/0.10	0.06	172.0/ 1.0	2.5	0.09	2.6
B	0.83/0.06	0.04	-0.24/0.04	0.05	0.87/0.05	0.03	171.9/ 1.5	1.7	0.05	1.8
V	0.93/0.04	0.07	-0.25/0.06	0.05	0.97/0.04	0.06	172.4/ 1.7	1.8	0.07	2.3
R	0.91/0.05	0.04	-0.24/0.04	0.05	0.95/0.04	0.04	172.6/ 1.5	1.8	0.07	1.6
I	0.82/0.07	0.08	-0.20/0.04	0.06	0.85/0.07	0.07	172.8/ 1.7	2.4	0.09	2.8
GAV	0.06	0.06	0.04	0.06	0.06	0.05	1.5	2.0	0.07	2.2
ζ Tau										
U	0.51/0.06	0.05	1.06/0.05	0.06	1.19/0.06	0.05	32.2/ 1.4	1.4	0.07	2.0
B	0.65/0.07	0.05	1.36/0.09	0.09	1.51/0.10	0.08	32.2/ 1.0	1.0	0.05	1.8
V	0.63/0.06	0.05	1.29/0.06	0.07	1.44/0.08	0.06	32.0/ 0.7	1.1	0.06	1.6
R	0.52/0.03	0.04	1.23/0.07	0.05	1.34/0.07	0.05	33.5/ 0.2	0.9	0.08	1.6
I	0.46/0.11	0.04	1.06/0.05	0.11	1.16/0.07	0.11	33.3/ 2.4	1.0	0.08	2.0
GAV	0.07	0.04	0.06	0.08	0.08	0.07	1.1	1.1	0.07	1.8

Table 14. Summer Be Star Summary

Star Filter	q/dq (%)	<dq> (%)	u/du (%)	<du> (%)	p/dp (%)	<dp> (%)	$\theta/d\theta$ (°)	<$d\theta$> (°)	<dpi> (%)	<$d\theta i$> (°)
48 Lib										
U	-0.38/0.04	0.08	-0.56/0.12	0.08	0.69/0.11	0.08	117.6/ 1.9	3.6	0.12	5.1
B	-0.41/0.04	0.05	-0.80/0.06	0.07	0.90/0.04	0.06	121.3/ 2.2	1.8	0.06	2.8
V	-0.52/0.06	0.04	-0.70/0.03	0.06	0.88/0.02	0.07	116.7/ 2.1	1.2	0.07	2.2
R	-0.52/0.06	0.06	-0.62/0.02	0.05	0.82/0.05	0.05	115.1/ 1.3	1.9	0.08	2.4
I	-0.53/0.10	0.05	-0.56/0.04	0.10	0.79/0.08	0.09	113.3/ 2.6	3.1	0.12	5.6
GAV	0.06	0.06	0.06	0.07	0.06	0.07	2.0	2.3	0.09	3.6
χ Oph										
U	0.04/0.06	0.12	-0.33/0.06	0.05	0.39/0.02	0.06	138.0/ 4.7	10.2	0.11	13.4
B	-0.02/0.03	0.08	-0.46/0.04	0.06	0.48/0.04	0.06	134.6/ 1.7	5.8	0.09	5.9
V	-0.00/0.02	0.09	-0.47/0.04	0.06	0.49/0.03	0.06	135.0/ 1.2	5.5	0.10	5.7
R	-0.01/0.05	0.08	-0.47/0.01	0.06	0.48/0.01	0.05	134.7/ 3.1	4.8	0.08	6.4
I	-0.05/0.07	0.09	-0.42/0.03	0.08	0.46/0.04	0.06	133.0/ 4.7	7.0	0.12	9.8
GAV	0.05	0.09	0.04	0.06	0.03	0.06	3.1	6.7	0.10	8.2
π Aqr										
U	-0.25/0.16	0.06	-0.33/0.08	0.09	0.46/0.04	0.09	116.1/10.6	4.2	0.11	7.9
B	-0.30/0.14	0.05	-0.37/0.09	0.04	0.50/0.01	0.04	115.6/ 9.7	2.8	0.08	4.0
V	-0.32/0.17	0.06	-0.35/0.09	0.04	0.51/0.01	0.03	114.3/11.1	3.7	0.07	3.9
R	-0.30/0.17	0.06	-0.33/0.08	0.04	0.48/0.02	0.05	114.6/11.7	3.0	0.08	4.1
I	-0.22/0.18	0.09	-0.31/0.07	0.05	0.44/0.02	0.07	118.3/13.1	6.1	0.09	9.7
GAV	0.16	0.06	0.08	0.05	0.02	0.05	11.2	4.0	0.09	5.9
o And										
U	-0.39/0.09	0.05	-0.11/0.11	0.05	0.42/0.11	0.04	96.3/ 6.6	3.9	0.08	5.7
B	-0.46/0.12	0.04	-0.13/0.11	0.06	0.49/0.14	0.05	97.1/ 4.3	3.6	0.06	3.9
V	-0.45/0.13	0.05	-0.08/0.07	0.04	0.47/0.14	0.05	94.8/ 3.6	2.6	0.06	5.4
R	-0.43/0.13	0.05	-0.08/0.07	0.04	0.45/0.14	0.05	94.8/ 3.1	2.4	0.05	5.3
I	-0.40/0.13	0.08	-0.06/0.09	0.07	0.43/0.14	0.09	93.8/ 4.6	5.1	0.08	7.7
GAV	0.12	0.05	0.09	0.05	0.13	0.05	4.5	3.5	0.07	5.6

Table 15. Polarized Standard Star Summary (Limber)

Star Filter	q/dq (%)	<dq> (%)	u/du (%)	<du> (%)	p/dp (%)	<dp> (%)	$\theta/d\theta$ (°)	<$d\theta$> (°)	<dpi> (%)	<$d\theta i$> (°)
2H Cam										
U	-1.83/0.09	0.04	-2.41/0.06	0.04	3.03/0.07	0.03	116.5/ 0.8	0.5	0.09	1.1
B	-1.95/0.08	0.07	-2.65/0.06	0.05	3.29/0.02	0.06	116.8/ 0.9	0.6	0.06	0.6
V	-2.05/0.02	0.06	-2.75/0.04	0.06	3.43/0.02	0.06	116.7/ 0.4	0.6	0.06	0.6
R	-1.98/0.02	0.05	-2.66/0.04	0.06	3.32/0.02	0.05	116.7/ 0.3	0.6	0.05	0.5
I	-1.79/0.03	0.07	-2.37/0.09	0.06	2.96/0.06	0.08	116.4/ 0.6	0.7	0.09	0.8
GAV	0.05	0.06	0.06	0.06	0.04	0.06	0.6	0.6	0.07	0.7
o Sco										
U	1.06/0.14	0.18	2.35/0.05	0.23	2.59/0.10	0.25	33.0/ 1.3	1.7	0.19	2.7
B	1.41/0.11	0.07	3.09/0.06	0.06	3.40/0.04	0.08	32.8/ 1.0	0.5	0.08	0.8
V	1.73/0.16	0.08	3.76/0.05	0.08	4.15/0.05	0.08	32.7/ 1.1	0.5	0.10	0.8
R	1.83/0.16	0.07	4.00/0.06	0.07	4.40/0.04	0.08	32.8/ 1.1	0.4	0.09	0.6
I	1.74/0.15	0.07	3.93/0.10	0.05	4.30/0.05	0.05	33.1/ 1.2	0.5	0.14	1.0
GAV	0.14	0.10	0.06	0.10	0.06	0.11	1.1	0.7	0.12	1.2

Table 16. Polarized Standard Star Summary (McDonald)

Star Filter	q/dq (%)	<dq> (%)	u/du (%)	<du> (%)	p/dp (%)	<dp> (%)	$\theta/d\theta$ (°)	<$d\theta$> (°)	<dpi> (%)	<$d\theta i$> (°)
2H Cam										
U	-1.83/0.05	0.11	-2.41/0.03	0.07	3.03/0.01	0.08	116.5/ 0.6	1.1	0.09	0.8
B	-1.97/0.05	0.07	-2.60/0.09	0.07	3.26/0.07	0.05	116.3/ 0.6	0.7	0.04	0.4
V	-2.07/0.06	0.07	-2.73/0.01	0.07	3.43/0.03	0.07	116.4/ 0.5	0.5	0.04	0.4
R	-1.97/0.07	0.05	-2.66/0.05	0.06	3.31/0.04	0.05	116.8/ 0.7	0.4	0.03	0.3
I	-1.75/0.06	0.09	-2.36/0.05	0.06	2.94/0.05	0.08	116.8/ 0.7	0.8	0.05	0.6
GAV	0.06	0.08	0.05	0.07	0.04	0.07	0.6	0.7	0.05	0.5
o Sco										
U	1.35/0.21	0.20	2.51/0.12	0.25	2.85/0.12	0.28	30.9/ 2.0	1.6	0.20	2.1
B	1.40/0.12	0.09	3.07/0.14	0.08	3.39/0.10	0.07	32.7/ 1.3	0.9	0.06	0.5
V	1.81/0.25	0.12	3.74/0.12	0.08	4.16/0.01	0.10	32.1/ 1.9	0.7	0.05	0.3
R	1.91/0.23	0.07	3.96/0.10	0.08	4.41/0.03	0.05	32.1/ 1.6	0.6	0.04	0.2
I	1.76/0.19	0.07	3.88/0.06	0.06	4.26/0.06	0.07	32.8/ 1.3	0.4	0.05	0.3
GAV	0.20	0.11	0.11	0.11	0.06	0.11	1.6	0.9	0.08	0.7

show the intrinsic polarization, calculated by vectorially subtracting the interstellar component determined by Poeckert, Bastien, & Landstreet (1979) or by McLean & Brown (1978), using a Serkowski law of the form $p_{ISi} = p_{max} \exp[-1.15 \ln^2(\lambda_{max}/\lambda_i)]$ with parameters as summarized in Table 17.

5.1. γ Cas

Gamma Cas provides a good example of how the mean values of the polarization in 5 filters can sometimes be nearly collinear in the q, u plane, so that a straight line fit can give a good approximation to the position angle of the intrinsic polarization (see Figure 1, lower right panel). The individual filter plots all show some evidence for elongation of the data point patterns along this direction (especially in U and R), which is good evidence that there is some real low level variability. Figure 2, however, shows only slight changes from year to year. The polarization of γ Cas, and therefore the state of its circumstellar envelope, appears to have been mostly stable since this monitoring program began.

5.2. ϕ Per

The polarization of ϕ Per has been almost certainly variable from year to year, as may be seen in Figure 3, where the data patterns are clearly elongated along the direction indicated by a straight line fit to the filter means. Some sinusoidal tendencies can be seen in Figure 4, especially in the R bandpass. Periodogram analysis suggests a period on the order of 11 to 12 years. If the circumstellar disk is tilted with respect to the binary orbital plane, as advanced by Clarke & Bjorkman (1998), it might be expected to precess with a similar period. However, the almost perfectly constant position angle of the polarization argues against this explanation for the periodic polarization.

Table 17. Interstellar Polarization Parameters

Star	p_{max} (%)	λ_{max} (Å)	θ_{IS} (°)	Reference
γ Cas	0.26	5900	95	MB
ϕ Per	1.06	4460	106	PBL
48 Per	0.85	5990	0	PBL
ζ Tau	0.00	...	...	PBL
48 Lib	0.64	5670	85	PBL
χ Oph	0.37	5740	158	PBL
π Aqr	0.46	4980	116	PBL
o And	0.26	5970	75	PBL

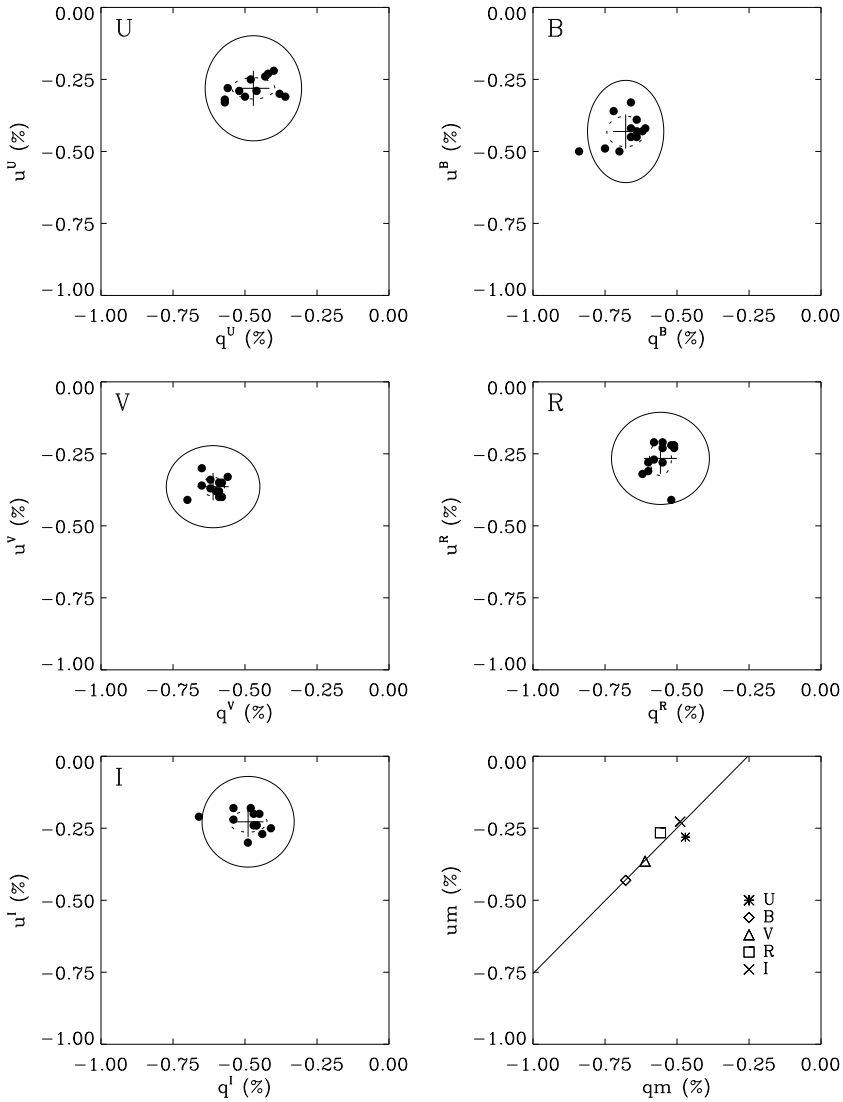

Fig. 1.— Normalized Stokes parameter plots of the polarization of γ Cas (see text for explanation of the symbols).

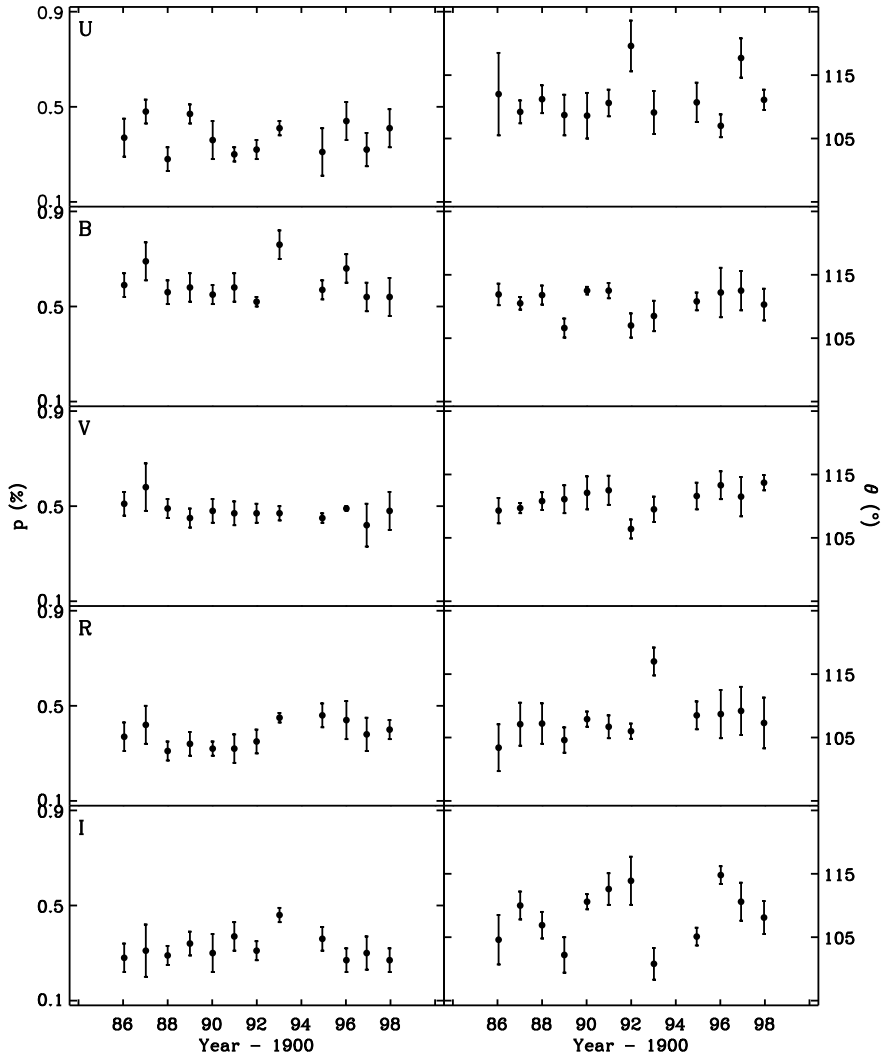

Fig. 2.— Degree and position angle of the intrinsic polarization of γ Cas.

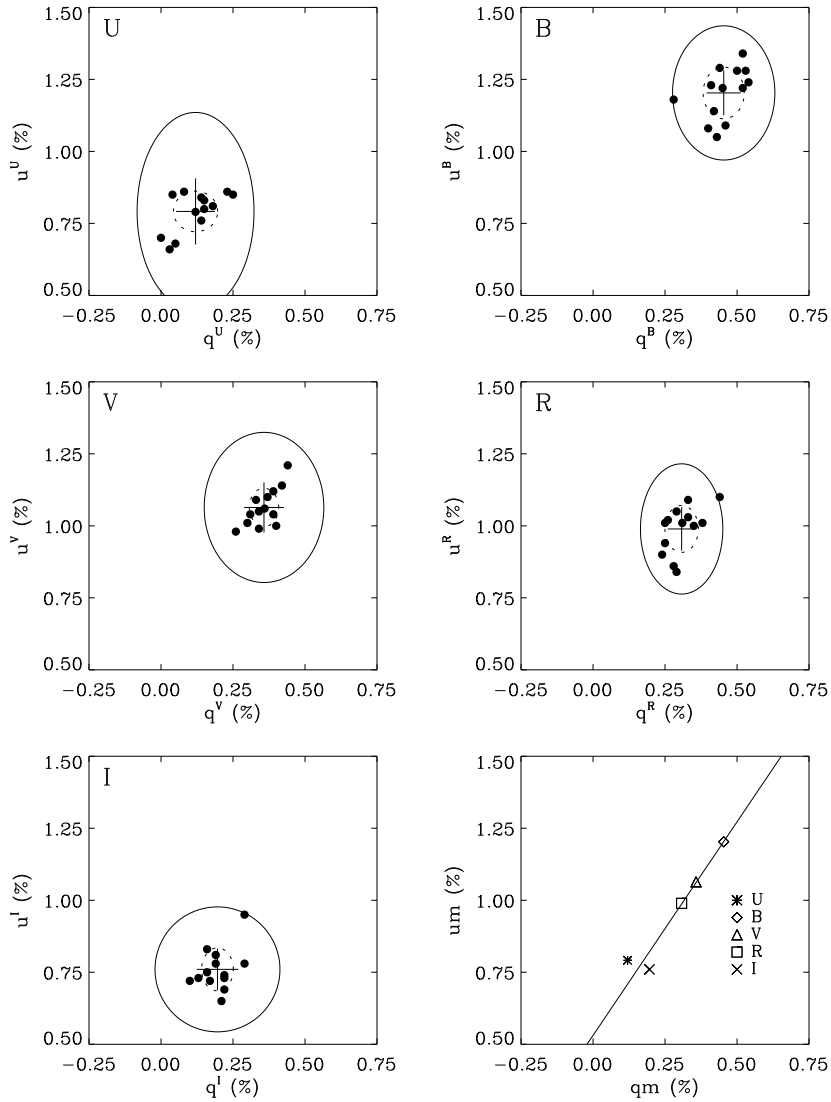

Fig. 3.— Normalized Stokes parameter plots of the polarization of ϕ Per (see text for explanation of the symbols).

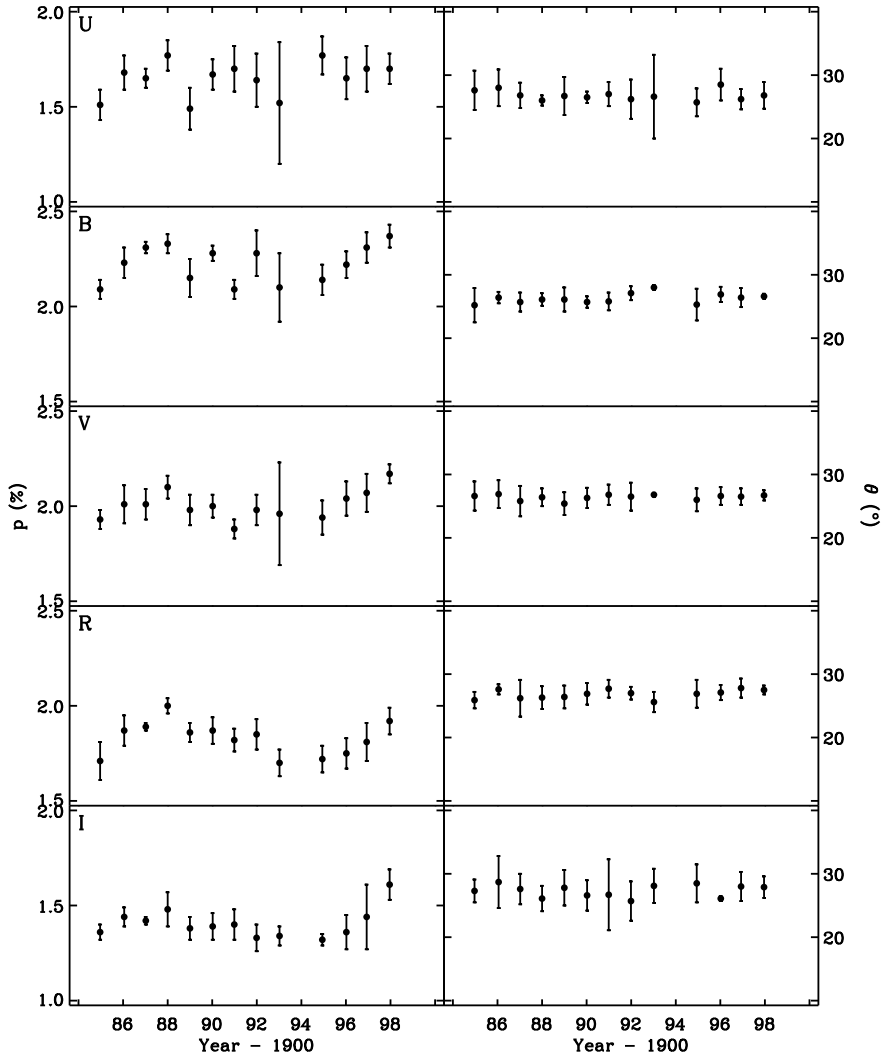

Fig. 4.— Degree and position angle of the intrinsic polarization of ϕ Per.

5.3. 48 Per

With $v\,sin\,i = 200$ km $\mathtt{s}^{-1}$, 48 Per is probably viewed at a relatively low inclination of its rotation axis to the line of sight. This is consistent with its relatively small polarization, even though it is a strong Hα emitter. It is interesting to see from Figure 6 that the position angle shows stronger variability than the degree of polarization, including a hint of a 4–5 year cycle in the B filter. A precessing bar-shaped nonuniformity embedded in the disk would be expected to generate this kind of variability. The absence of a preferred direction in the q, u plots (Figure 5) lends further strength to this interpretation.

5.4. ζ Tau

Zeta Tau is one of the most highly polarized and strongly variable of all the program stars. A look at Figure 8 shows a slow and steady rise in the degree of polarization with occasional mild outbursts or local maxima, while the position angle remains constant. The filter averages in Figure 7 are very nearly collinear, and the individual filter plots clearly show alignment in that direction.

Work is in progress on a possible correlation between continuum polarization and V/R variations of the Hα emission line profile of ζ Tau as a test of the theory of "one-armed" density perturbations of the circumstellar disk (Okazaki 1997) and their effects on the polarization. Hopefully the results will place some constraints on the nature of Be disks and the processes leading to their formation.

5.5. 48 Lib

In Figure 9 the intrinsic position angle of the polarization of 48 Lib is poorly determined because the interstellar component is large and has a very different position angle than the intrinsic component. In Figure 10 the interstellar polarization has been removed, resulting in a better straight line fit that passes acceptably close to the origin to approximate the intrinsic position angle. This angle is indeed favored by the elongations of the q, u data sets in the individual filters.

Figure 11 shows that the degree of intrinsic polarization is nearly cyclic with a period on the order of 4–5 years, although somewhat noisy due to short term variations. As in the case of ζ Tau there is a correlation between the polarization period and that of V/R in the Hα emission line, and it is currently being pursued in the same context.

5.6. χ Oph

Chi Oph has the lowest $v\,sin\,i$ of all the program stars: 140 km s^{-1}. It also has one of the least degrees of intrinsic polarization, as would be expected if its rotation axis is

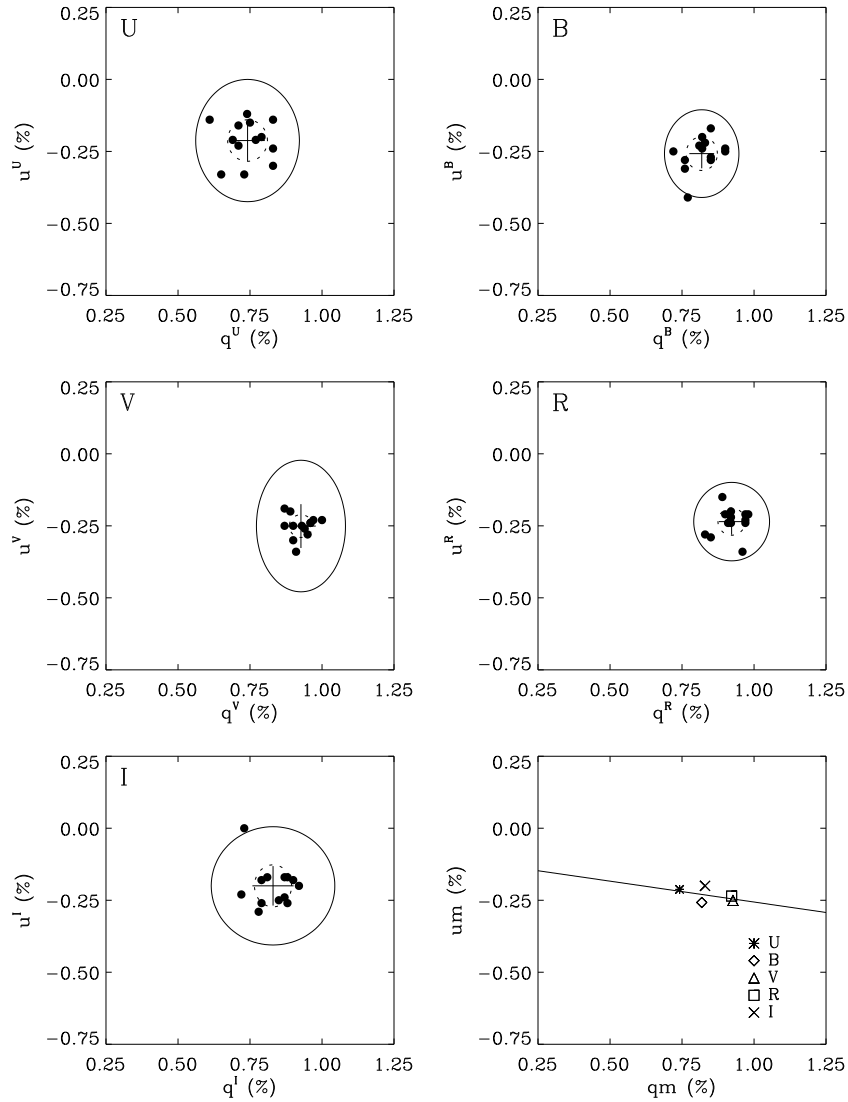

Fig. 5.— Normalized Stokes parameter plots of the polarization of 48 Per (see text for explanation of the symbols).

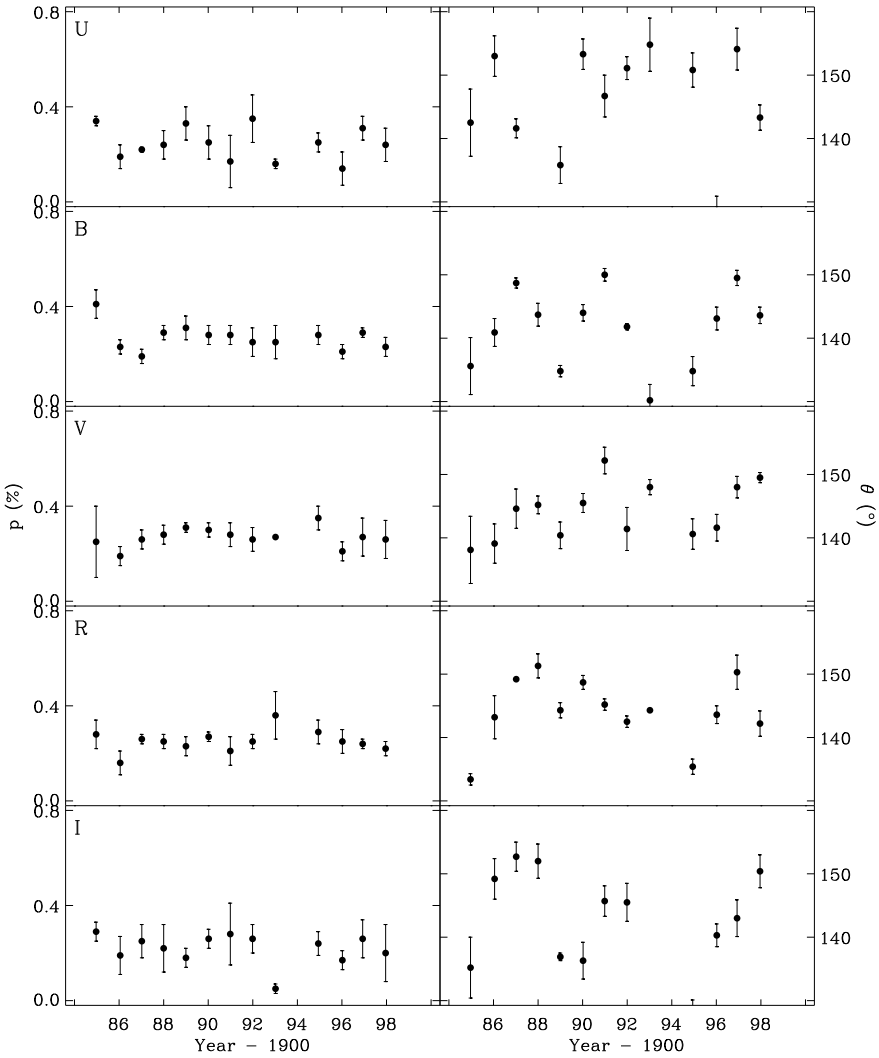

Fig. 6.— Degree and position angle of the intrinsic polarization of 48 Per.

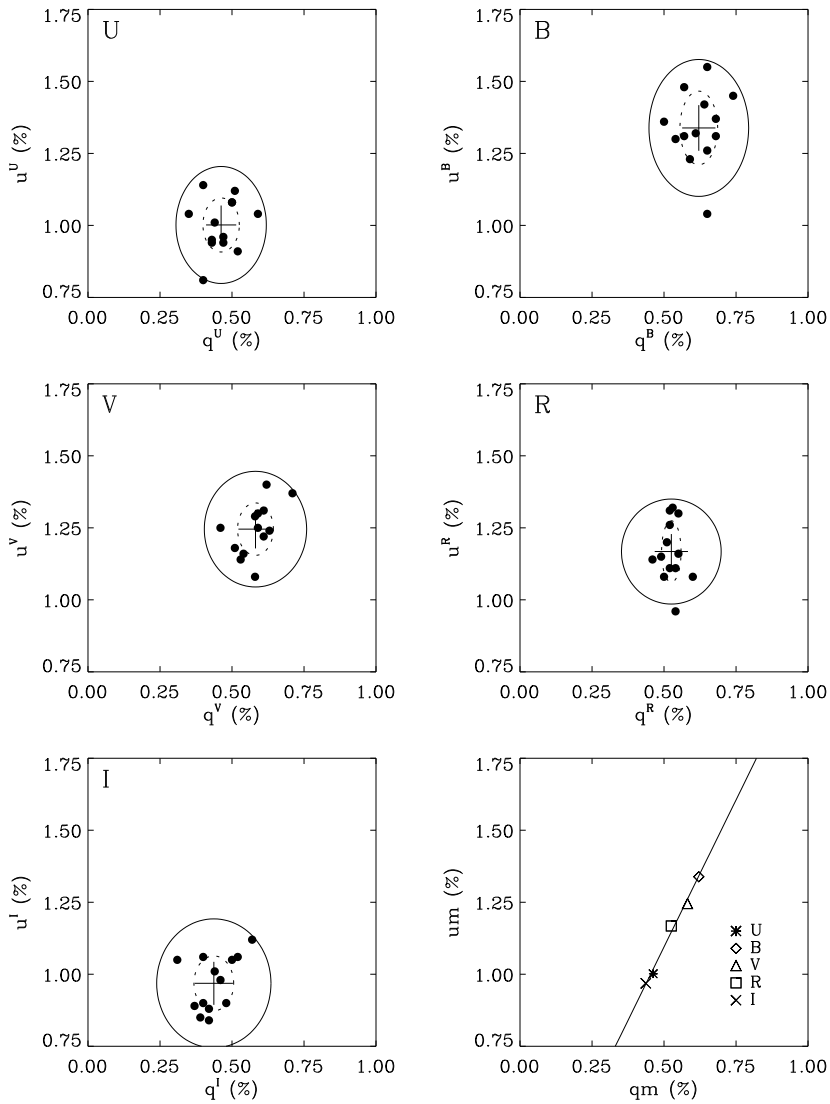

Fig. 7.— Normalized Stokes parameter plots of the polarization of ζ Tau (see text for explanation of the symbols).

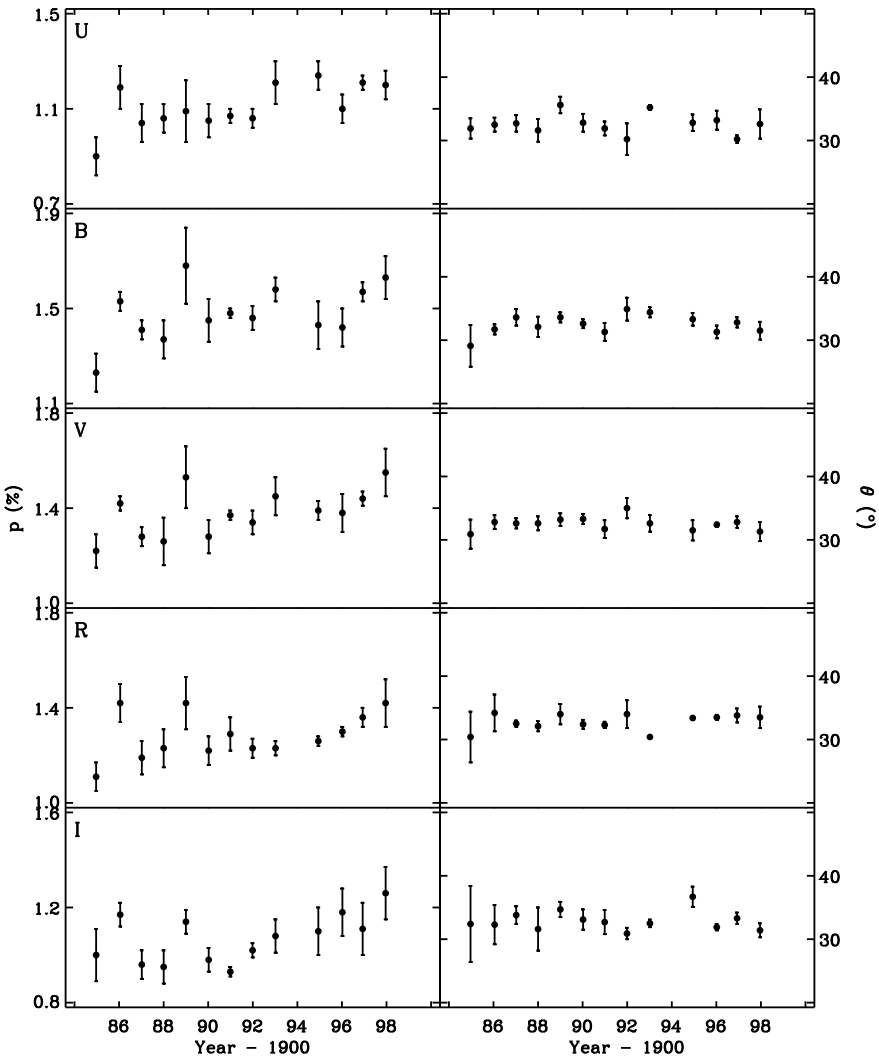

Fig. 8.— Degree and position angle of the intrinsic polarization of ζ Tau.

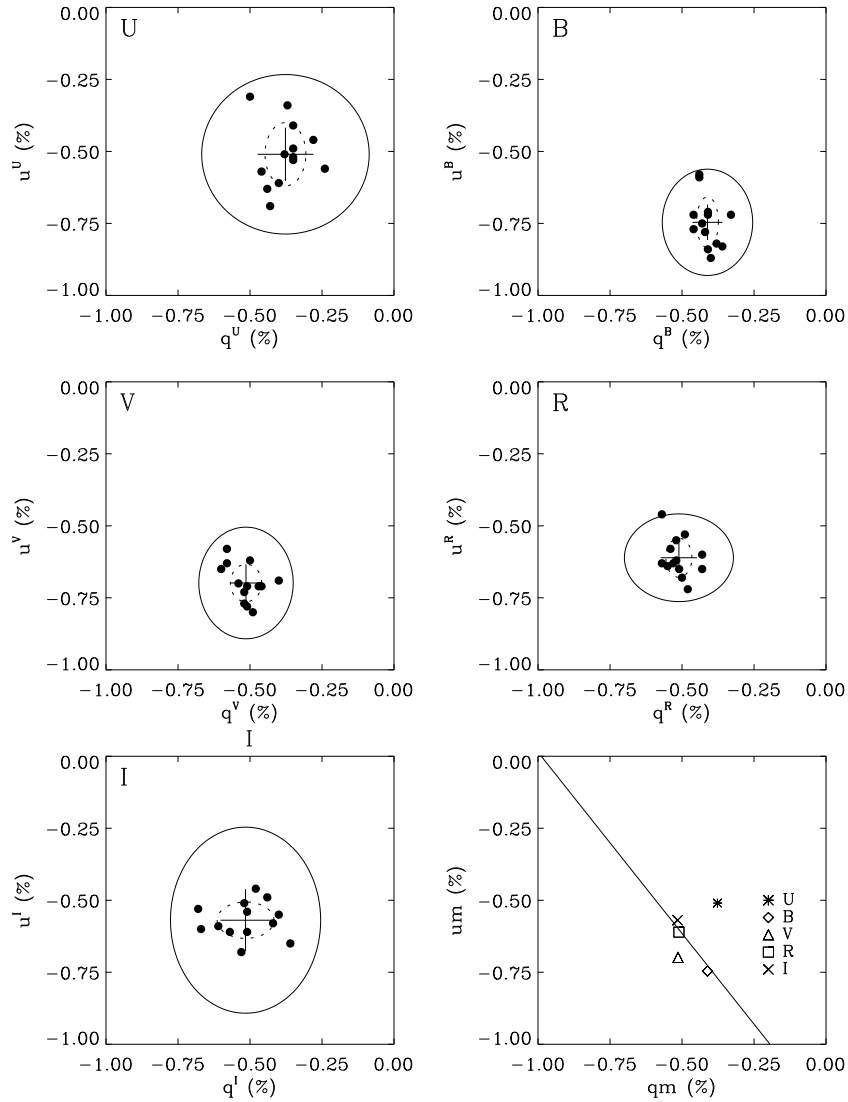

Fig. 9.— Normalized Stokes parameter plots of the polarization of 48 Lib (see text for explanation of the symbols).

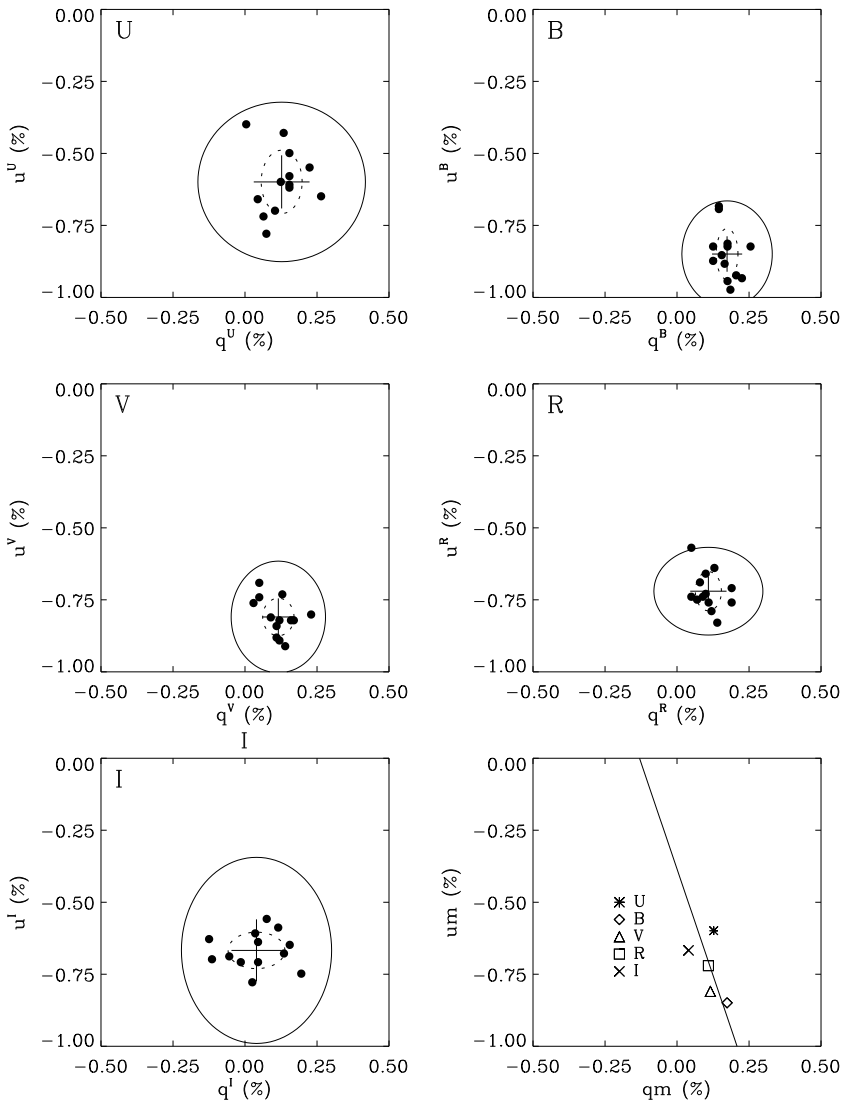

Fig. 10.— Normalized Stokes parameter plots of the intrinsic polarization of 48 Lib (see §5.5 for comment).

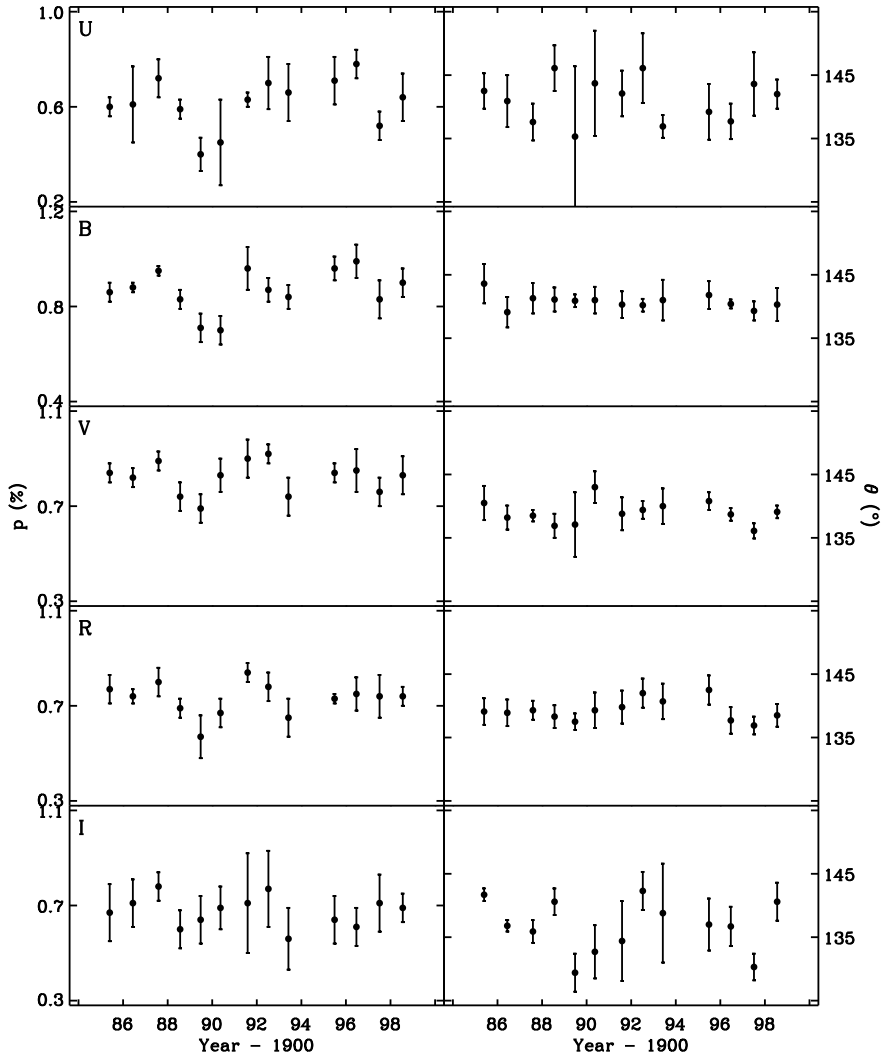

Fig. 11.— Degree and position angle of the intrinsic polarization of 48 Lib.

only slightly inclined to the line of sight. In Figure 12 the fit of the intrinsic position angle line is somewhat weak, and the individual filter plots have only a slight tendency for alignment.

The graphs of Figure 13 show how small the intrinsic polarization is and how poorly determined the position angle is as a result. Apart from an interesting ripple in the degree of polarization, there is little evidence for any significant variability.

5.7. π Aqr

Figure 14 shows what $> 3\sigma$ variable polarization of a Be star should look like in the q, u plane. The degree of intrinsic polarization of π Aqr has changed more by far than that of any other star on the program list. The strong alignment evident in the q, u plots indicates that the position angle is very stable. This is also demonstrated by the position angle graphs of Figure 15.

When monitoring began in 1985, π Aqr had nearly the largest (if not the largest) polarization of any Be star in the sky. Now, 13 years later, that polarization has almost completely disappeared. If we could explain exactly what happened, we would be close to understanding the Be phenomenon itself. Did a dynamic disk lose a source of continuous replenishment? If there were such a source, what might have turned it off? Was the disk a static structure? If so, what prompted it to dissipate? Were there any changes in the underlying star? There are still far more questions than answers.

5.8. o And

Since 1986 the polarization of o And has been increasing almost uniformly except for two or three minor outbursts and dropouts. The relatively small degree of polarization makes the position angle difficult to determine (see Figure 16), but Figure 17 shows good definition of the intrinsic position angle based on fitting to the filter means. The polarization is well-behaved in the single filter q, u plots, which show that there is real variability by their strong alignment to the intrinsic position angle. This gives a good record of the gradual buildup of a polarizing Be envelope or disk.

I am very grateful to Michel Breger and Santiago Tapia for introducing me to the basics of astronomical polarimetry. I also thank Paul Krueger for his skillful machine work in transforming AnyPol from line drawings on paper into the reality of metal. Jon Bjorkman's constructive suggestions as referee helped to clarify this presentation in many ways.

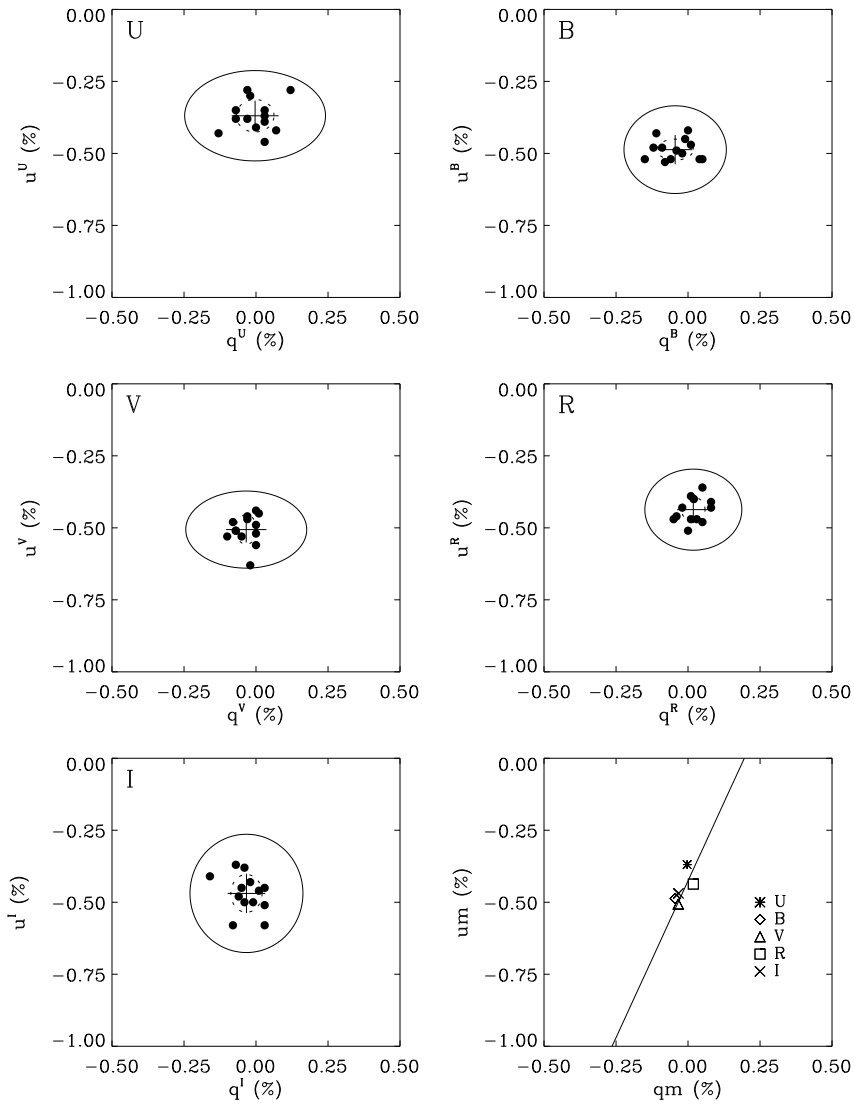

Fig. 12.— Normalized Stokes parameter plots of the polarization of χ Oph (see text for explanation of the symbols).

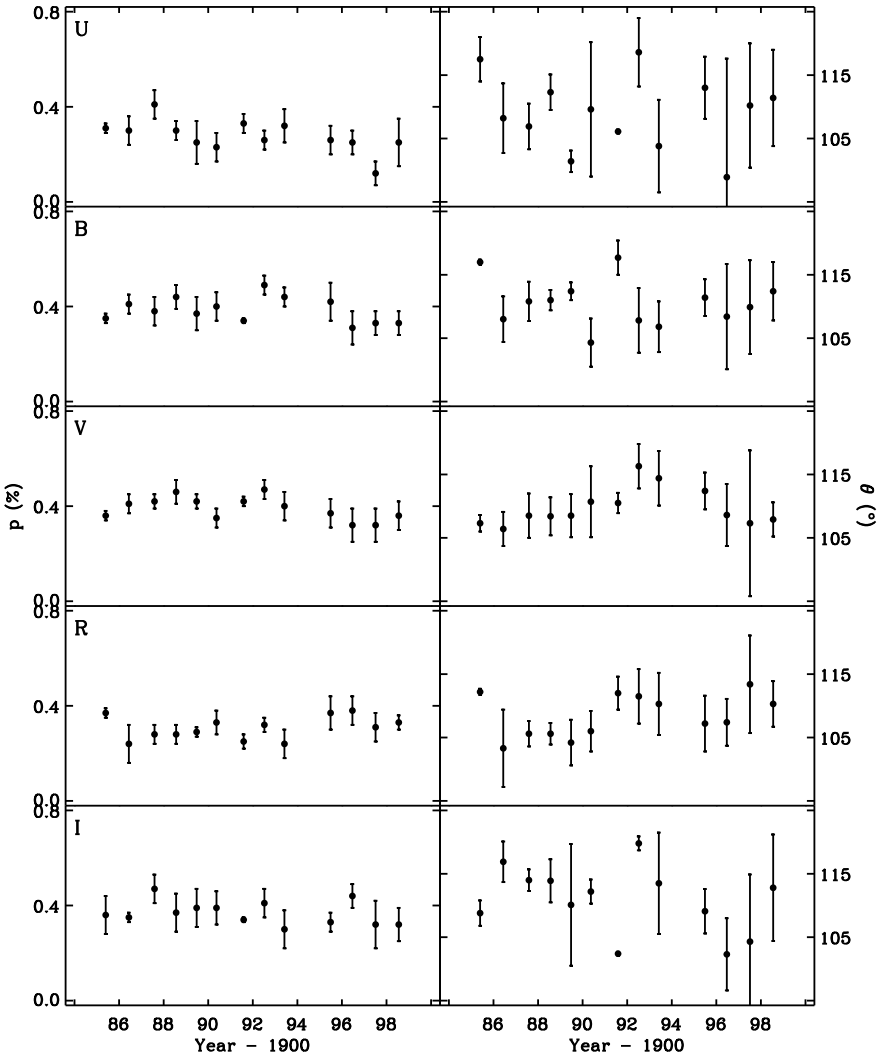

Fig. 13.— Degree and position angle of the intrinsic polarization of χ Oph.

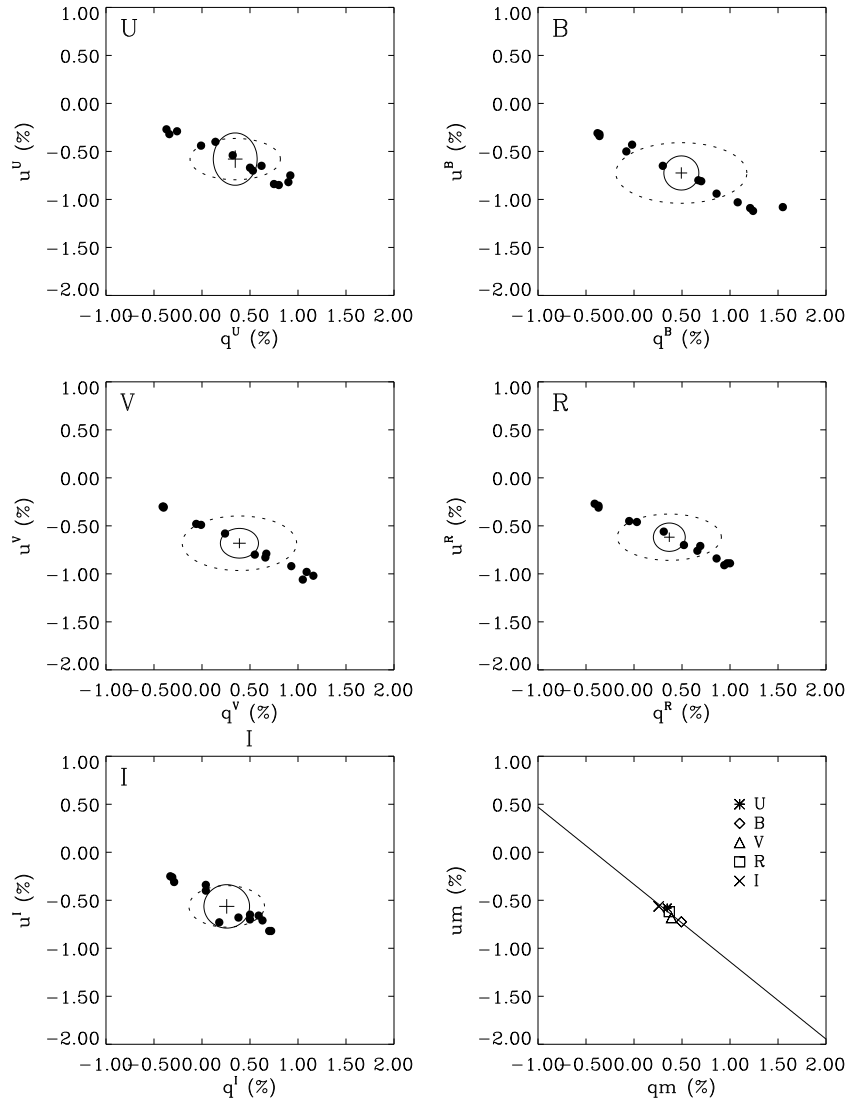

Fig. 14.— Normalized Stokes parameter plots of the polarization of π Aqr (see text for explanation of the symbols).

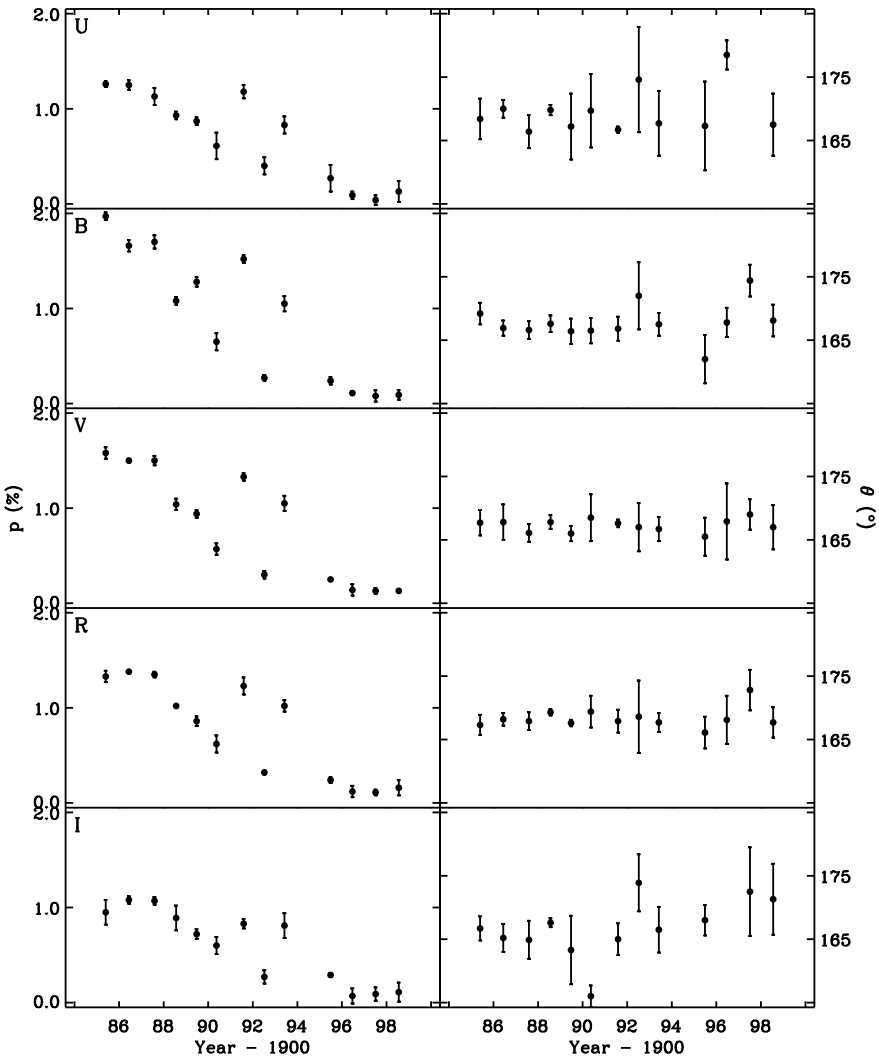

Fig. 15.— Degree and position angle of the intrinsic polarization of π Aqr.

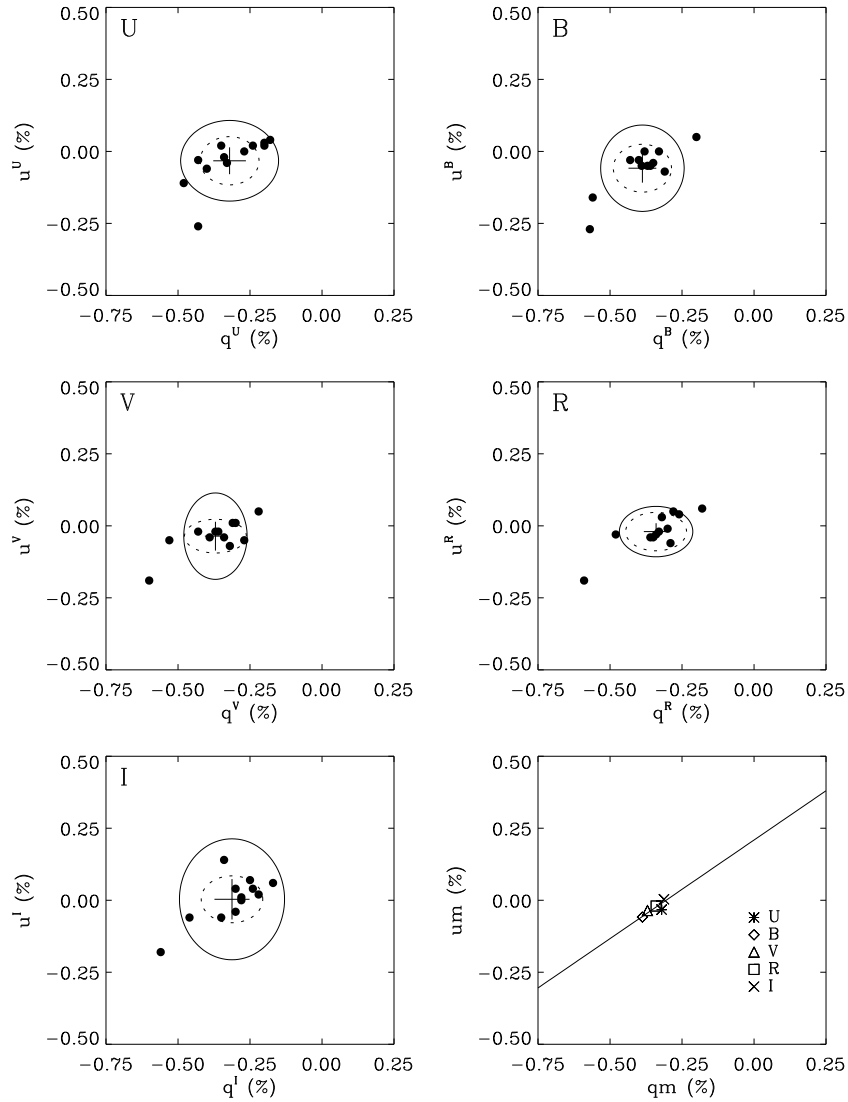

Fig. 16.— Normalized Stokes parameter plots of the polarization of o And (see text for explanation of the symbols).

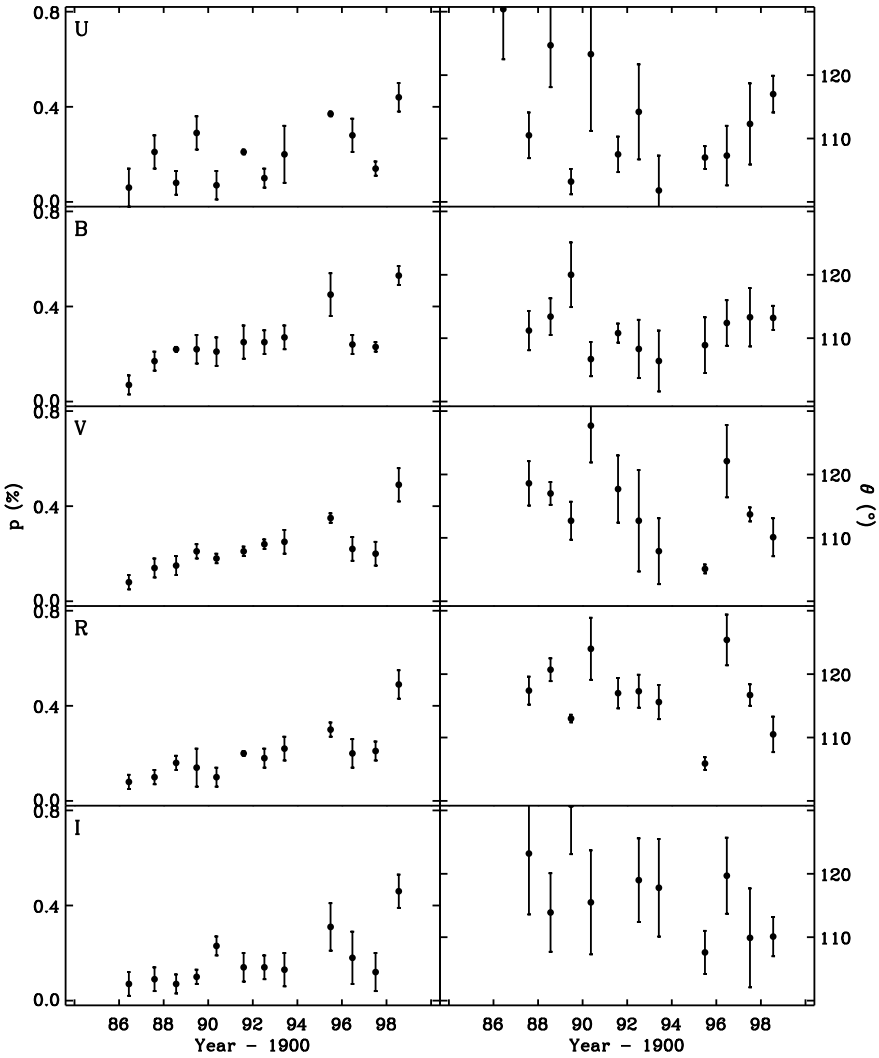

Fig. 17.— Degree and position angle of the intrinsic polarization of o And.

REFERENCES

Breger, M. 1979, ApJ, 233, 97

Clarke, D. & Bjorkman, K.S. 1998, A&A, 331, 1059

Clarke, D. & Stewart, B.G. 1986, Vistas Astron., 29, 27

Frecker J.E. & Serkowski K. 1976, Appl. Optics 15, 605

Hoffleit, D. & Jaschek, C. 1982, The Bright Star Catalog, 4th Revised Edition (New Haven: Yale University Observatory)

Hsu, J.C. & Breger, M. 1982, ApJ, 262, 732

McDavid, D. 1994, PASP, 106, 949

McLean, I.S., & Brown, J.D. 1978, A&A, 69, 291

Okazaki, A.T. 1997, A&A, 318, 548

Poeckert, R., Bastien, P., & Landstreet, J.D. 1979, AJ, 84, 812

Quirrenbach, A., Bjorkman, K.S., Bjorkman, J.E., Hummel, C.A., Buscher, D.F., Armstrong, J.T., Mozurkewich, D., Elias, N.M., II, & Babler, B.L. 1997, ApJ, 479, 477

Serkowski, K. 1974, in Planets, Stars, and Nebulae Studied with Photopolarimetry, ed. Gehrels, T. (Tucson: University of Arizona), 135

Slettebak, A. 1982, ApJS, 50, 55

Slettebak, A. 1988, PASP, 100, 770

Wood, K., Bjorkman, K.S., & Bjorkman, J.E. 1997, ApJ, 477, 926

Chapter 6

A Connection Between V/R and Polarization in Be Stars

with
K.S. Bjorkman, J.E. Bjorkman (University of Toledo),
& A.T. Okazaki (Hokkai-Gakuen University)

(originally published in 2000, IAU Coll. 175, The Be Phenomenon in Early-Type Stars, ed. Smith, M.A., Henrichs, H.F., & Fabregat, J. (San Francisco: ASP), 460)

ABSTRACT

It has been suggested that the quasi-cyclic V/R variability observed in the emission line profiles of many Be stars is caused by a precessing one-armed density wave in the circumstellar disk. It seems likely that the changing aspect of such a non-axisymmetric density pattern might also lead to a related variation of the continuum polarization. We have searched for such an effect in two well-studied Be shell stars, ζ Tau and 48 Lib, based on data compiled from several groups of observers from 1984 to 1998. Using a Monte Carlo radiation transfer code to calculate the polarization due to electron scattering in Be disks in the presence of one-armed density perturbations, we have been able to find specific modes that are consistent with the observed V/R line profile variations together with the suspected polarization cycles. Although the notorious long and short term deviations from strict periodicity present in Be stars make it impossible to rigorously demonstrate this connection, we can nevertheless say that theoretical calculations based on the one-armed density wave hypothesis are not directly at odds with the polarization observations.

1. Introduction

Be stars are rapidly rotating non-supergiant B-type stars whose spectra have, or had at some time, one or more Balmer lines in emission. In the overall context of stellar structure and evolution, the subject of Be stars is important for its close association with rapid rotation, whose effects are poorly understood. One of the mysteries of the Be phenomenon is that the emission, which originates from an equatorially flattened circumstellar envelope or disk (Quirrenbach et al. 1997), can come and go episodically on time scales of days to decades. This has yet to be explained as a predictable consequence of stellar evolution theory, although many contributing factors have been discussed, including disk formation conditions, rapid rotation, radiation-driven winds, nonradial pulsation, flarelike magnetic activity, and binary interaction. Slettebak (1988) has written a comprehensive review which is highly recommended for the unfamiliar reader.

The Balmer line emission produced by the rotating circumstellar disks of Be stars is double-peaked when viewed at high inclinations (close to edge-on). Interestingly, the ratio of violet to red peak intensity V/R of many Be stars sometimes shows nearly cyclic variations on time scales of several years (Dachs 1987). A promising explanation for this variability is a slowly precessing one-armed ($m = 1$) density wave in a Keplerian equatorial disk, orbiting around the star (Okazaki 1991; Papaloizou, Savonije, & Henrichs 1992). The Keplerian orbital motion of the gas in the disk carries gas elements through this more slowly moving density structure. The overdense region produces excess emission in the double-peaked Balmer line profiles at a wavelength corresponding to its projected line-of-sight velocity, while the underdense region (on the opposite side of the disk) produces an emission deficit on the opposite side of line center. As the density wave precesses around the star, the emission excess and deficit oscillate about line center, producing cyclic V/R variations at the precession frequency of the density wave.

In addition to line emission, Be stars also show intrinsic linear polarization. This polarization arises from electron scattering of starlight in the disk. Although electron scattering is wavelength independent, the polarization develops a wavelength dependence due to attenuation by neutral hydrogen (Coyne & Kruszewski 1969). If a uniform disk is seen along its polar axis, it looks circular and there is no net polarization, because the polarization from every region is exactly cancelled by that from another region 90° away in azimuth. As the inclination of the polar axis to the line of sight increases, the disk isophotes become elliptical. This decreases the cancellation, leading to a net polarization with a position angle parallel to the projection of the rotation axis onto the plane of the sky.

The density wave proposed to cause the (rather large) spectroscopic V/R variations described above breaks the axisymmetry of the disk. In the single scattering limit, the polarization P is linear in the density ρ (Brown & McLean 1977), so one naively expects large polarization variations $\delta P/P \sim \delta\rho/\rho$ with corresponding position angle variations that are correlated with V/R. However, the polarization change δP is given by a volume

integral of the density perturbation $\delta\rho$. For a one-armed mode, $\delta\rho/\rho \propto \exp(im\phi)$ with $m = 1$. This produces a high density arm, but on the opposite side there is a corresponding low density region — the density perturbation is antisymmetric under reflection through the plane perpendicular to the arm. Consequently the polarization volume integral vanishes because the integration kernel is symmetric under reflection (see Eq. 31 of Brown, Carlaw, & Cassinelli 1989). This implies that in the single scattering limit there is no net change in the polarization in the presence of one-armed density waves. Nonetheless there are second order effects that occur because Be star disks are optically thick to electron scattering (see Wood, Bjorkman, & Bjorkman 1997). In particular, multiple scattering and attenuation effects produce small changes in the polarization as the density wave precesses around the star.

We chose ζ Tau (B3 IVe-shell, $v \sin i = 220$ km s^{-1}) and 48 Lib (B3:IV:e-shell, $v \sin i = 400$ km s^{-1}) as test objects because they have been continuously monitored by spectroscopy and polarimetry for many years and have shown hints of roughly periodic variations in polarization on time scales similar to those of the V/R variations (Okazaki 1997). We combined our polarization measurements of these two stars covering the past 14 years (Bjorkman et al. 1998; McDavid 1999) and also assembled corresponding V/R measurements of the Hα emission line from the literature. Private communications from colleagues helped to fill gaps in the record.

2. ζ Tau

The upper panel of Figure 1 shows the observed B-band polarization, averaged over quarter-year intervals. According to Poeckert, Bastien, & Landstreet (1979) the interstellar polarization is negligible, so no correction was applied. The position angle of the polarization was constant. The values of V/R plotted logarithmically in the lower panel are quarterly averages of data gathered from Slettebak, Collins, & Truax (1992), Guo et al. (1995), Hanuschik et al. (1996), and Kaye & Gies (1997).

Based on the work of Guo et al. (1995) and Hanuschik et al. (1996), the most recent episode of cyclic V/R variations began about 1990 and was preceded by a time of little or no activity. This is illustrated by the horizontal line at $\log(V/R) = 0$ from 1984 through 1990 in the lower panel of Figure 1. It appears that the polarization was rising linearly during that period of time, as shown by the sloping straight line through the open circles in the upper panel. This initial slope was removed to give the flattened polarization data (filled circles).

Both the flattened polarization and V/R were searched for periodicity using the periodogram method of Scargle (1982). The confidence level (probability that a periodogram peak with power signal-to-noise ratio z at one given frequency out of N independent frequencies being searched is real) is $p_0 = [1 - \exp(-z)]^N$. No periodicity in the polarization was detected at the 99% confidence level, but the most prominent signal (34% confidence) occurs at a period of T = 2.3 yr. The strongest peak in the V/R

periodogram (61% confidence) was found at T = 7.2 yr.

Using these periods as starting points for nonlinear least squares fitting to sine waves, we obtained a polarization period of 2.2 yr and a V/R period of 5.3 yr, which are overplotted in Figure 1. A simplistic interpretation is that the polarization follows a double wave, making two cycles for every one cycle of V/R. To estimate the quantities necessary to generate a model we assumed a polarization period of 2.2 yr and a V/R period of 4.4 yr, with a phase relationship such that extrema of V/R correspond to polarization minima.

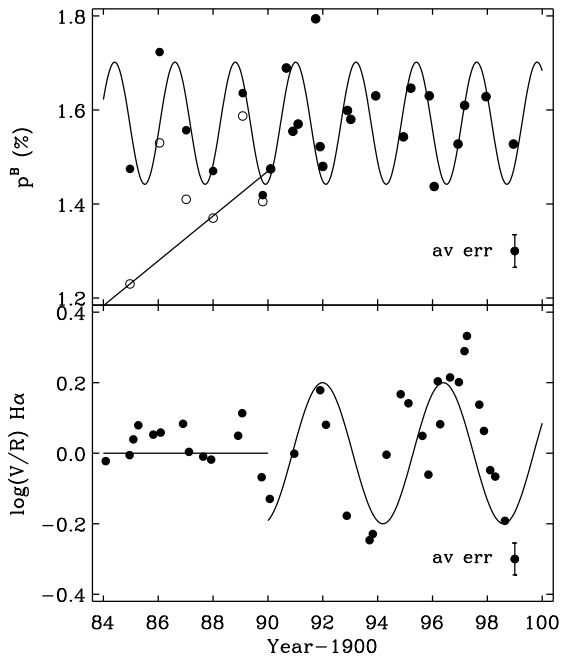

Fig. 1.— The observed B-band polarization and V/R of ζ Tau.

The simplest one-armed density perturbation of a Be disk is the kidney-shaped mode shown in Figure 2, where the grayscale image shows the density perturbation pattern within 10 stellar radii. The unperturbed disk is assumed to be inviscid and the eigenfunctions of the density perturbation were calculated according to the model of Okazaki (1977). Both the sense of rotation of the disk and the sense of precession of the density perturbation are clockwise in this illustration (prograde precession). Sample Hα line profiles are shown for various azimuthal viewing angles ϕ (phase angles of the observed moving pattern), labeled around the perimeter of the disk. The line profiles, normalized to the peak intensity of the unperturbed profile, are computed for i = 82° and $(\rho_1/\rho_0)_{\max} = 0.95$, where i is the inclination angle and $(\rho_1/\rho_0)_{\max}$ is the maximum value of the local density perturbation.

The upper panel of Figure 3 shows the Monte Carlo calculation of the polarization that would be observed as a function of ϕ, for a sample of disk inclinations near the value $i = 82°$ adopted by Wood, Bjorkman, & Bjorkman (1997) for ζ Tau. The behavior of V/R according to the model line profiles is shown in the lower panel. These results are in good qualitative agreement with the observations in Figure 1.

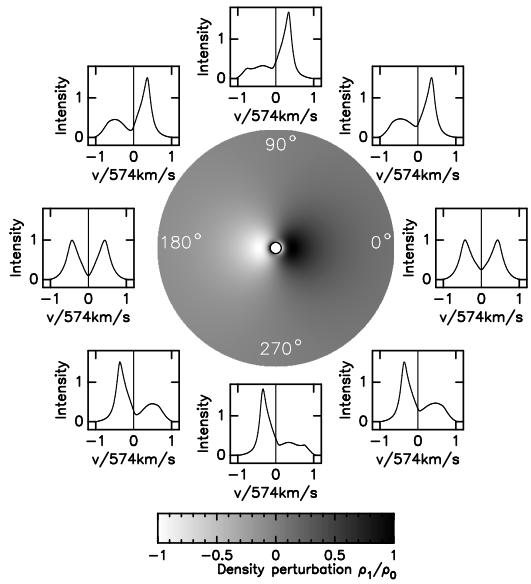

Fig. 2.— The kidney-shaped density perturbation and the variability of the Hα emission line profile of ζ Tau.

According the the upper panel of Figure 3, for our chosen inclination of $i = 82°$, there are polarization maxima at $\phi = 0°$ and $\phi = 180°$, when the perturbed region is parallel to the line of sight. Physically, the electron scattering polarization saturates (no longer rising linearly with density) in the overdense region, so its contribution to increasing the polarization is less than the contribution of the underdense region to decreasing the polarization. Thus the polarization perturbation is negative (i.e., parallel to the location of the arm). This produces a polarization variation with two minima at phases $\phi = 90°$ & $\phi = 270°$ and maxima at phases $\phi = 0°$ & $\phi = 180°$. However, at large inclination when one is looking through the disk, attenuation by the overdense region becomes important and removes the maximum at $\phi = 0°$. Thus the polarization curve for $i = 89°$ has only a single maximum at $\phi = 180°$.

3. 48 Lib

Quarterly averages of the B-band polarization after removing the interstellar component found by Poeckert, Bastien, & Landstreet (1979) are presented in the upper panel of Figure 4. The intrinsic position angle was constant. The quarterly V/R data plotted in

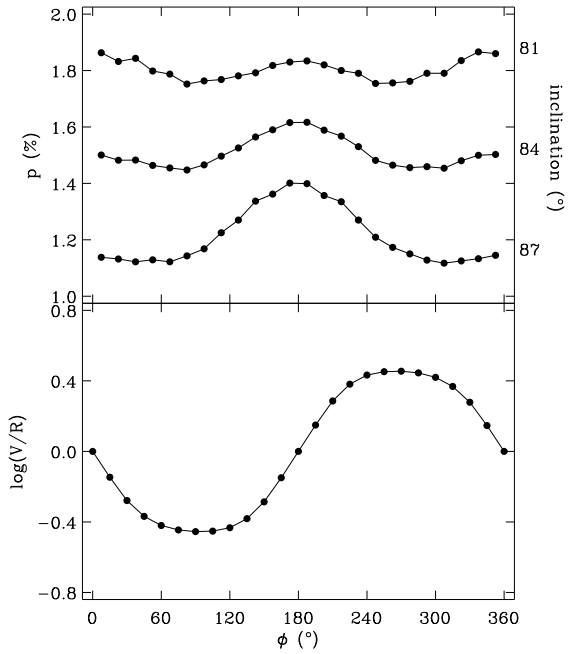

Fig. 3.— The model polarization and V/R for ζ Tau.

the lower panel are from Hanuschik et al. (1995) and the archives of Ritter Observatory.

Scargle periodogram analysis yielded no periodicity in the polarization at the 99% confidence level, but the highest peak (42% confidence) in the power spectrum occurs at T = 4.4 yr. A periodicity in V/R appears with 99% confidence at T = 13.5 yr.

With these periods as initial input, nonlinear least squares fitting to sine waves gave a polarization period of 4.2 yr and a V/R period of 11.0 yr, shown overplotted in Figure 4. As in the case of ζ Tau, there appears to be evidence for a double wave. For the purpose of constructing a model we adopted a polarization period of 4.2 yr and a V/R period of 8.4 yr (c.f. Hanuschik et al. 1995), but for 48 Lib the phasing is such that extrema of V/R correspond to polarization maxima rather than minima.

To produce the phase shift of the V/R maxima relative to the polarization maxima observed for the disk of 48 Lib, we employed the leading, one-armed spiral density wave shown in Figure 5, where the grayscale image represents the density perturbation pattern within 10 stellar radii. To produce a spiral density wave, we assumed that the unperturbed disk is a viscous decretion disk with Shakura-Sunyaev (1973) viscosity parameter $\alpha = 0.1$. In this figure both the sense of rotation of the disk and the sense of precession of the density perturbation are clockwise (prograde precession of a leading spiral). The phased line profiles, normalized to the peak intensity of the un-

perturbed profile, are computed for i = 87° (consistent with $v\,sin\,i = 400$ km s^{-1}) and $(\rho_1/\rho_0)_{\rm max} = 0.50$.

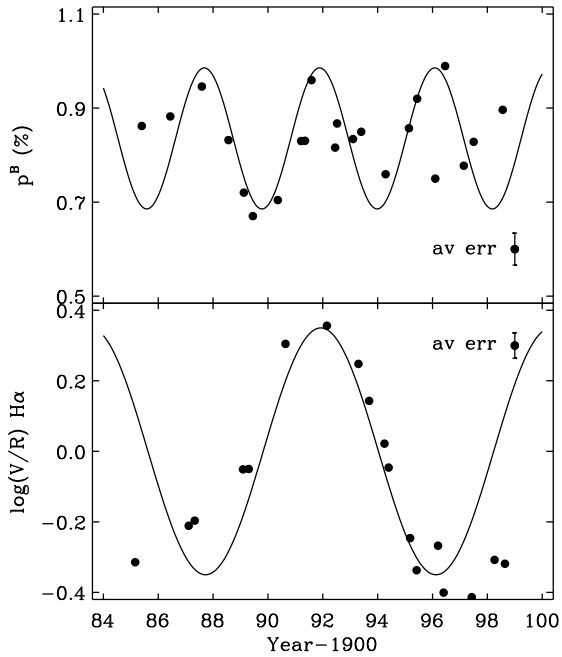

Fig. 4.— The observed B-band polarization and V/R of 48 Lib.

The Monte Carlo results for polarization due to the spiral mode are presented in the upper panel of Figure 6. The variation of V/R based on the model line profiles is shown in the lower panel. These results are an acceptable match to the observations in Figure 4.

Physically, it is simpler in this case to account for the polarization minima rather than for the maxima. The dip at $\phi = 150°$ may be understood as dilution of the polarized light from electron scattering in the disk by direct unpolarized light from the star shining through the underdense side of the perturbation. The other dip, at $\phi = 330°$, might be expected because of the extinction of polarized light in the overdense side, so that unpolarized light from the parts of the star not so heavily occulted by the disk would alter the balance toward lower net polarization.

4. Conclusion

We do not claim to have formally detected periodicities in the polarization of the program stars, but given the well known fact that Be stars are only quasi-periodic, this is

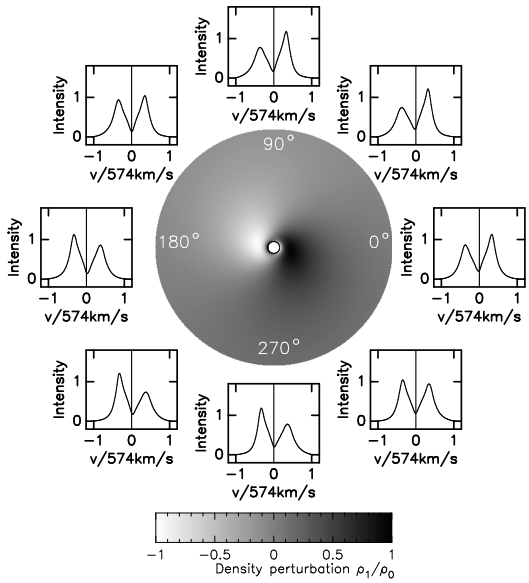

Fig. 5.— The spiral-shaped density perturbation and the variability of the Hα emission line profile of 48 Lib.

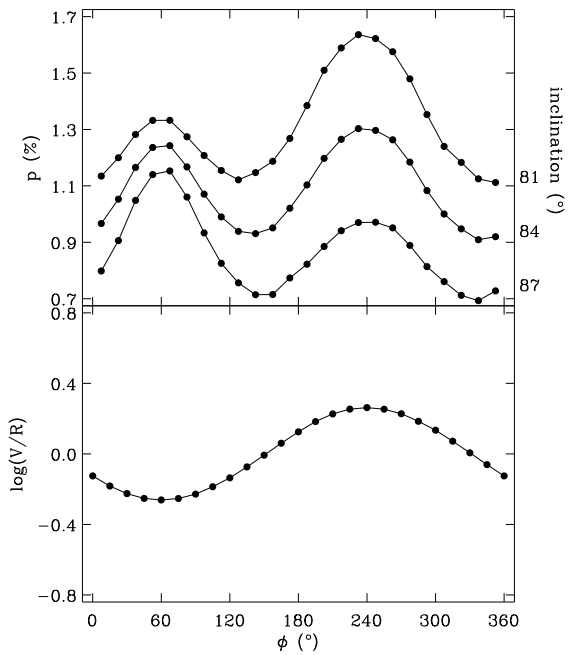

Fig. 6.— The model polarization and V/R for 48 Lib.

not at all surprising. We can conclude, at very least, that the polarization observations are not at odds with theoretical models based on the one-armed density wave hypothesis, and therefore that the hypothesis has passed the observational test for two specific stars. Our results are consistent with those of Ignace (2000), who showed analytically that polarization variations on the order of 15% of the mean value may be produced by density patterns similar to those considered here.

We greatly appreciate contributions of unpublished spectroscopic line profile data by Dietrich Baade, Lex Kaper, Geraldine Peters, Thomas Rivinius, and Stan Stefl, as well as the contribution of polarimetry data by Ryuko Hirata. Thanks are also due to Don Winget and Travis Metcalfe for providing access to the Metacomputer facility of the Astronomy Department of the University of Texas at Austin for initial computing experiments. This work was partially supported by National Computational Science Alliance under Grant Number AST980007N and utilized the University of Wisconsin Condor flock of workstations. Polarization observation at PBO were supported by NASA contract NAS5-26777 with the University of Wisconsin. KSB acknowledges support from NASA grant NAG5-8054, and JEB from NASA grant NAG5-3248.

REFERENCES

Bjorkman, K.S., Meade M.R., & Babler, B.L. 1997, BAAS, 29, 1275

Brown, J.C., Carlaw, V.A., & Cassinelli, J.P. 1989, ApJ, 344, 341

Brown, J.C. & McLean, I.S. 1977, A&A, 57, 141

Coyne, G.V. & Kruszewski, A. 1969, AJ, 74, 528

Dachs, J. 1987 in IAU Coll. 92, Physics of Be Stars, ed. Slettebak, A. & Snow, T.P. (Cambridge: Cambridge University Press), 149

Guo, Y., Huang, L., Hao, J., Cao, H., Guo, Z., & Guo, X. 1995, A&AS, 112, 201

Hanuschik, R.W., Hummel, W., Dietle, O., & Sutorius, E. 1995, A&A, 300, 163

Hanuschik, E.W., Hummel, W., Sutorius, E., Dietle, O., & Thimm, G. 1996, A&AS, 116, 309

Ignace, R. 2000, in IAU Coll. 175, The Be Phenomenon in Early-Type Stars, ed. Smith, M.A., Henrichs, H.F., & Fabregat, J. (San Francisco: ASP), 452

Kaye, A.B. & Gies, D.R. 1997, ApJ, 482, 1028

McDavid, D. 1999, PASP, 111, 494

Okazaki, A.T. 1991, PASJ, 43, 75

Okazaki, A.T. 1997, A&A, 318, 548

Papaloizou, J.C., Savonije, G.J., & Henrichs, H.F. 1992, A&A, 265, 45

Poeckert, R., Bastien, P., & Landstreet, J.D. 1979, AJ, 84, 812

Quirrenbach, A., Bjorkman, K.S., Bjorkman, J.E., Hummel, C.A., Buscher, D.F., Armstrong, J.T., Mozurkewich, D., Elias II, N.M., & Babler, B.L. 1997, ApJ, 479, 477

Scargle, J.D. 1982, ApJ, 263, 835

Shakura, N.I. & Sunyaev, R.A. 1973, A&A, 24, 337

Slettebak, A. 1988, PASP, 100, 770

Slettebak, A., Collins, G.W.II, & Truax, R. 1992, ApJS, 81, 335

Wood, K., Bjorkman, J.E., Whitney, B.A., & Code, A.D. 1996, ApJ, 461, 828

Wood, K., Bjorkman, K.S., & Bjorkman, J.E. 1997, ApJ, 477, 926

Chapter 7

A Useful Approximation for Computing the Continuum Polarization of Be Stars

(accepted by ApJ, January 26, 2001)

ABSTRACT

This paper describes a practical model for the polarization of Be stars which can be used to estimate roughly the physical parameters for optically thin circumstellar envelopes from broad band *UBVRI* photopolarimetry data. Analysis of long term variability in terms of these parameters is a promising approach toward understanding the Be phenomenon. An interesting result from fitting the model to observations of eight Be stars is that all of them may have geometrically thin disks, with opening half-angles on the order of ten degrees or less. This contributes to the growing evidence that most Be disks are geometrically thin.

1. Motivation

The idea that the Hα emission lines of Be stars originate from an equatorially flattened circumstellar envelope or disk has now been directly verified by interferometric imaging (Quirrenbach et al. 1997). The related explanation of the linear polarization of Be stars as due to scattering of the starlight by free electrons in the disk was also confirmed, because the observed position angle of the polarization was found to be perpendicular to the direction of elongation of the disk as projected onto the plane of the sky. It is this apparent asymmetry of the scattering region that results in a net polarization, by defeating the cancellation which would take place if there were identical scattering subregions in adjacent quadrants of the projected disk (see Fig. 1).

A thorough historical review of both observation and theory of polarization in Be stars was given by Coyne & McLean (1982). Since that time the major observational developments in the field have been increased spectral resolution by spectropolarimetry and

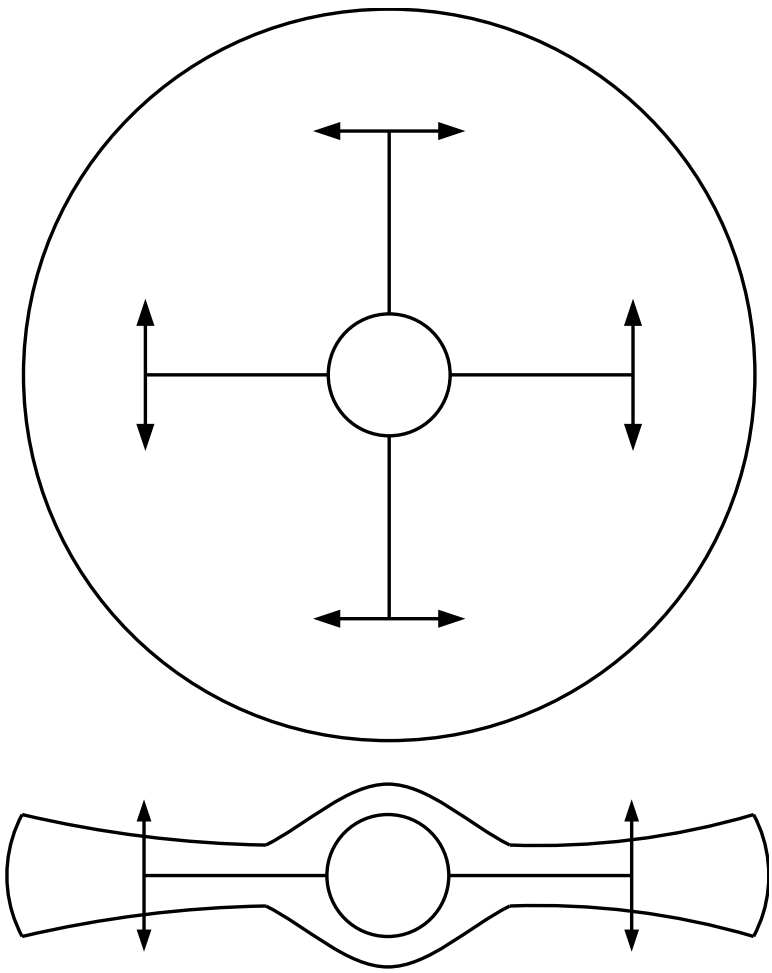

Fig. 1.— Scattering geometry in the disk of a Be star, illustrating by extremes how the net polarization depends on the orientation of the disk on the sky. In the upper sketch the disk is viewed pole-on, with angle of inclination to the line of sight $i = 0°$, while in the lower sketch the disk is viewed equator-on, with $i = 90°$. Double arrows show the direction of vibration of the electric field of starlight scattered in the disk. For the pole-on case cancellation occurs between adjacent quadrants of the disk, and the net polarization is zero because the electric fields of the scattered light are perpendicular. When the disk is viewed equator-on there is no cancellation, so the observed polarization is a maximum.

extension of the wavelength coverage into the ultraviolet by space-based observations (Bjorkman 2000). Theoretical analysis and modeling of the continuum polarization has progressed through increasingly generalized treatments, including the depolarizing effect of the finite size of the star and the effect of occultation of the scattering disk by the star (Brown & Fox 1989; Fox & Brown 1991; Fox 1991; Fox 1994; see also Cassinelli, Norsieck, & Murison 1987, hereafter CNM; and Brown, Carlaw, & Cassinelli 1989). Bjorkman & Bjorkman (1994) extended the single scattering calculations to include attenuation and emission within the envelope. Hillier (1994) developed a numerical method to solve the polarized radiation transfer equation, while Wood, Bjorkman, Whitney, & Code (1996) applied a Monte Carlo computational scheme to simulate the polarization by tracing stellar photons in their interactive paths through the circumstellar envelope.

One may wonder, then, if there is anything new to be learned about Be stars from continued broadband polarimetry. An excellent example is the recent work of Yudin (2001), who studied a sample of 627 Be stars to explore the statistical correlations among polarization, rotational velocity, and near IR excesses. And even though we now have firmer knowledge of the disk characteristics, including temperature, density, and geometry, broadband polarization monitoring is still a primary source of information on the variability of these quantities over time scales of years to decades, which are typical of the most fundamental aspect of the Be phenomenon: the unpredictable transition from the normal B phase to the Be phase and back again, associated with the formation and dissipation of the circumstellar envelope.

This paper attempts to establish a simple and approximate, but nevertheless serviceable approach to the modeling and analysis of *UBVRI* polarimetry data to derive the basic envelope parameters. Tracing the observed variability in terms of these parameters still promises to give valuable hints about the nature of the unknown processes involved in the Be phenomenon.

2. A Spherical Sector Envelope Model

Figure 2 shows the geometry of the circumstellar envelope model adopted for this study. Introduced by Kruszewski, Gehrels, & Serkowski (1968) to investigate the polarization of red variables, it was later used by Brown & McLean (1977) to illustrate their theoretical formulation of the polarization by electron scattering in a Be disk. Its shape may be described as an axially symmetrical sector of a sphere, with a wedge-shaped cross section opening outward at half-angle α.

For small opening angles the spherical sector is a good representation of an equatorial disk, with the advantage of being mathematically suited for spherical coordinates. A basic starting point is to assume the disk is pure hydrogen with uniform electron temperature T_e, extending to infinite distance ($R_e \rightarrow \infty$ in Fig. 2) from a central star of

radius R_*, with electron number density N_e given by a radial power law with exponent η:

$$N_e(r) = N_{0e}\left(\frac{R_*}{r}\right)^{\eta} . \tag{7.1}$$

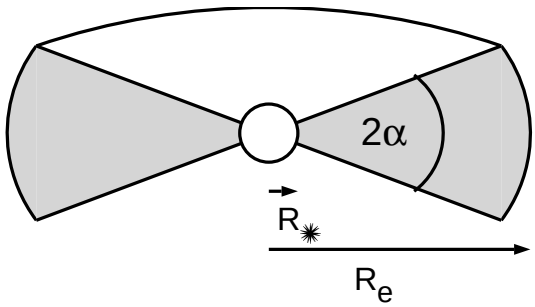

Fig. 2.— Cutaway view of the spherical sector model adopted for the circumstellar envelope.

Waters, Coté, & Lamers (1987) derived values of $2.0 < \eta < 3.5$ for some of the stars also studied in this paper using the slope of the infrared continuum from *IRAS* observations, but the spherical sector model with $R_e \to \infty$ has the peculiarity that the disk mass is infinite unless $\eta > 3.0$. In what follows, the symbol η will be retained for generality, but $\eta = 3.1$ is used as a representative mean value in all the numerical computations.

3. An Approximation for the Gray Polarization

According to Fox (1991) except for a sign error in the first argument of the beta function B, the net polarization of light from a central star due to scattering of photons by free electrons (Thomson scattering) in a surrounding envelope may be roughly approximated for the specific case of the infinite spherical sector geometry as

$$p_0 = \frac{3(\eta-1)}{16} B\left(\frac{\eta-1}{2}, \frac{3}{2}\right) \tau_e \sin\alpha \cos^2\alpha \sin^2 i\,, \tag{7.2}$$

where i is the angle of inclination of the rotation axis of the star to the line of sight and

$$\begin{aligned} \tau_e &= \int_{R_*}^{\infty} N_{0e}\left(\frac{R_*}{r}\right)^{\eta} \sigma_e dr \\ &= \frac{N_{0e}\sigma_e R_*}{\eta-1} \text{ (finite only for } \eta > 1.0) \end{aligned} \tag{7.3}$$

is the total radial optical depth for electron scattering in the equatorial plane of the spherical sector in terms of the Thomson scattering cross section

$$\sigma_e = \frac{8\pi}{3}\left(\frac{e^2}{mc^2}\right)^2 . \tag{7.4}$$

Equation (7.2) is only a single scattering approximation, based on the assumption that the disk is optically thin and neglecting multiple scattering. It includes the finite source correction, but not the correction for occultation. For $\eta = 3.1$, Figure 11 of Fox (1991) shows that the finite source correction reduces the polarization by a factor of about 0.66 with no dependence on α or i, while Figures 18 and 21 show that occultation further reduces the polarization by another factor which varies from about 0.80 to 1.00 over the full range of α and i. This means that in the worst possible case the model presented here may overestimate the polarization by some 25%.

4. Including the Wavelength Dependence

So far the calculated polarization has no dependence on wavelength, since it comes from pure electron scattering. However, neutral hydrogen in the envelope absorbs some light both before and after scattering, and the envelope emission (which is treated here as unpolarized and is not considered to scatter) dilutes the polarization. It is therefore necessary to include these wavelength-dependent effects, since they combine to produce the slope of the continuum polarization and the well known abrupt changes in the polarization at the H I ionization series limits, as first demonstrated by Capps, Coyne, & Dyck (1973) and later refined by McLean (1979).

Assuming LTE ionization fractions and level populations, equation (7.5) gives the total wavelength-dependent opacity $\kappa(\lambda)$ per gram of neutral hydrogen in the ground state (Aller 1963). C_0 is a fixed numerical factor, $X(n)$ is the ionization energy from level n in units of kT_e, and C_{se} is the correction factor for stimulated emission. The three individual terms in the equation are a summation over the ionization edges of the first seven discrete energy levels, an integrated term for the combination of all the remaining levels, and a free-free absorption term (with Gaunt factors taken to be unity). See Appendix A for a discussion of NLTE corrections.

$$\kappa(\lambda) = C_0 e^{-X(1)} \lambda^3 \left(\sum_{\lambda<\lambda_n}^{X(n)} \frac{e^{X(n)}}{n^3} + \frac{(e^{X(8)}-1)}{2X(1)} + \frac{1}{2X(1)} \right) C_{se} , \tag{7.5}$$

where

$$C_0 = \frac{32\pi^2 e^6 R}{3\sqrt{3} m_H h^3 c^3} , \tag{7.6}$$

$$X(n) = \frac{2\pi^2 m_e e^4}{n^2 h^2 k T_e}\,, \tag{7.7}$$

and

$$C_{se} = \left(1 - e^{-hc/\lambda k T_e}\right)\,. \tag{7.8}$$

If the free electron number density $N_e(r)$ and the electron temperature T_e are known, then the number density $N_1(r)$ of neutral hydrogen atoms in the ground state can be found from the Saha equation:

$$\begin{aligned} N_1(r) &= \frac{h^3}{(2\pi m_e k T_e)^{3/2}} N_e^2(r) e^{X(1)} \\ &= N_{01}\left(\frac{R_*}{r}\right)^{2\eta}\,, \end{aligned} \tag{7.9}$$

where

$$N_{01} = \frac{h^3}{(2\pi m_e k T_e)^{3/2}} N_{0e}^2 e^{X(1)}\,. \tag{7.10}$$

The total radial optical depth for neutral hydrogen absorption in the equatorial plane of the spherical sector is therefore

$$\begin{aligned} \tau_a(\lambda) &= \int_{R_*}^{\infty} \kappa(\lambda) m_H N_{01}\left(\frac{R_*}{r}\right)^{2\eta} dr \\ &= \frac{N_{01} m_H \kappa(\lambda) R_*}{2\eta - 1} \text{ (finite only for } \eta > 0.5)\,, \end{aligned} \tag{7.11}$$

which acts as a wavelength-dependent attenuation factor to reduce the gray polarization.

The volume emission coefficient of the envelope is

$$j(\lambda, r) = m_H \kappa(\lambda) N_{01}\left(\frac{R_*}{r}\right)^{2\eta} B(\lambda)\,, \tag{7.12}$$

where

$$B(\lambda) = \frac{2hc^2}{\lambda^5 (e^{hc/\lambda k T_e} - 1)} \tag{7.13}$$

is the Planck function (not to be confused with the beta function in §3). The total luminosity of the envelope is then

$$\begin{aligned} L(\lambda) &= 4\pi \int_0^{2\pi} \int_{\frac{\pi}{2}-\alpha}^{\frac{\pi}{2}+\alpha} \int_{R_*}^{\infty} j(\lambda, r) r^2 \sin\theta dr d\theta d\phi \\ &= \frac{16\pi^2}{2\eta - 3} N_{01} m_H \kappa(\lambda) B(\lambda) R_*^3 \sin\alpha \text{ (finite only for } \eta > 1.5)\,, \end{aligned} \tag{7.14}$$

which together with the stellar flux $F_*(\lambda)$ produces a further wavelength dependence of the polarization. Theoretical values of the stellar flux $F_*(\lambda)$ are taken from tabulated model atmospheres by Kurucz (1994).

With the wavelength dependence included, our polarization estimate may now be written as

$$p(\lambda) = \frac{p_0 e^{-\tau_a(\lambda)}}{1 + L(\lambda)/(4\pi R_*^2 F_*(\lambda))}\,. \tag{7.15}$$

It should be emphasized that this equation is only an approximation (even if the disk is optically thin), since it includes neither the contribution of scattering of the disk emission to the polarization nor attenuation of the direct starlight by the disk. Also the neutral hydrogen opacity is treated in a very crude way, using only the maximum radial optical depth in the equatorial plane.

It may be of interest to calculate the total mass of the disk, which can be done approximately by simply counting pairs of electrons and protons under the assumption that it consists purely of fully ionized hydrogen:

$$\begin{aligned} M &= \int_0^{2\pi} \int_{\frac{\pi}{2}-\alpha}^{\frac{\pi}{2}+\alpha} \int_{R_*}^{\infty} m_H N_{0e} \left(\frac{R_*}{r}\right)^{\eta} r^2 \sin\theta dr d\theta d\phi \\ &= \frac{4\pi}{\eta - 3} N_{0e} m_H R_*^3 \sin\alpha \text{ (finite only for } \eta > 3.0)\,. \end{aligned} \tag{7.16}$$

5. Synthesizing Broadband Data

Adjustment of the envelope parameters in the theoretical model to give results consistent with observations might be expected to yield valuable information about the nature of Be disks. To compare with observations on the Johnson-Cousins *UBVRI* system, it is first necessary to convolve the theoretically estimated polarization p(λ) from equation (7.15) with the bandpass characteristics of the optical system.

As a first approximation, let us assume Gaussian filter transmission curves based on the

standard *UBVRI* wavelengths and $fwhm$ (Bessell 1979), which are closely matched by the system actually used for the observations (see Table 1).

Given the central wavelength λ_c, the standard deviation σ can be calculated from the $fwhm$ Γ since $\Gamma = 2.354\,\sigma$ for a Gaussian distribution, so that the transmission function may be written as

$$T(\lambda) = \exp\left[-\frac{1}{2}\left(\frac{\lambda - \lambda_c}{\Gamma/2.354}\right)^2\right]. \tag{7.17}$$

The theoretical total flux $F(\lambda)$ is due to the stellar component $F_*(\lambda)$ plus the envelope component:

$$F(\lambda) = F_*(\lambda) + L(\lambda)/(4\pi R_*^2)\,. \tag{7.18}$$

Convolving the polarization in terms of flux with the transmission function, where λ_{min} and λ_{max} are, to a realistic approximation, the 10% response points, we find a theoretical expression for the expected polarization over the given bandpass:

$$P(BP) = \frac{\sum_{\lambda=\lambda_{min}}^{\lambda_{max}} p(\lambda)F(\lambda)T(\lambda)\Delta\lambda}{\sum_{\lambda=\lambda_{min}}^{\lambda_{max}} F(\lambda)T(\lambda)\Delta\lambda}\,. \tag{7.19}$$

6. Adjustable Parameters & Model Fits

With the model in hand, an interactive graphical computer interface was designed to allow adjusting the input parameters by trial and error to fit *UBVRI* polarization measurements (McDavid 1999) of eight Be stars. Solutions obtained this way should be viewed with some caution since they may not be unique: different geometrical distri-

Table 1. Filter System Parameters

Filter	Effective Wavelength (Å)	Bandpass ($fwhm$) (Å)
U	3650	700
B	4400	1000
V	5500	900
R	6400	1500
I	7900	1500

butions of scatterers can produce the same net polarization. Moreover, given the gross approximations involved, only order-of-magnitude results should be expected.

The model disk has three adjustable parameters: the maximum electron number density N_{0e}, the angle of inclination i of the rotation axis to the line of sight, and the opening half-angle α. Additionally required fixed parameters for each individual star are the radius R_*, the effective temperature T_*, and the surface gravity log g, which were estimated from Table 1 of Collins, Truax, & Cranmer (1991) based on spectral types from Slettebak (1982). The electron temperature of the disk was then fixed at $T_e = 0.75\ T_*$ and the appropriate Kurucz flux table chosen to match T_* and log g.

The fixed disk temperature T_e affects the wavelength dependence of the polarization through its influence on the neutral hydrogen opacity by setting the degree of ionization and the populations of the excited states (eq. [7.5]). It influences not only the hydrogen absorption optical depth (eq. [7.11]), but also the disk luminosity (eq. [7.14]), which is another contributor to the wavelength dependence of the polarization. As a result, T_e is important in determining the polarization Balmer jump and the slope of the polarization over the Paschen continuum, both of which generally increase at lower temperatures. Appendix A explains the NLTE corrections to the level populations which are necessary to fit these features for some of the program stars.

It is instructive to summarize individually the effects of the three adjustable parameters on the behavior of $p(\lambda)$ according to equation (7.15).

(1) The overall degree of gray polarization is directly proportional to N_{e0} through the factor τ_e in equation (7.2). However, simply increasing N_{e0} does not always result in an overall polarization increase, because it also increases the attenuation and adds to the wavelength dependence of the polarization through $\tau_a(\lambda)$ (eq. [7.11]) and $L(\lambda)$ (eq. [7.14]).

(2) The earliest basic electron scattering models (e.g. Brown & McLean 1977) gave a $\sin^2 i$ dependence of the polarization on i, and further refinements have not qualitatively changed the simple picture of Figure 1 in which a face-on disk shows no net polarization because of symmetrical cancellation, while the maximum asymmetry of an edge-on disk results in the maximum polarization. It may seem likely that i is poorly determined in this model since the same polarization might be obtained, for example, by decreasing i while increasing α, keeping N_{e0} constant. Experiments do not bear this out, though, because a thicker disk has a higher luminosity, which changes the wavelength dependence of the polarization enough to ruin the fit (eq. [7.15]). Another helpful constraint on i is the presence or absence of shell lines, which are thought to be absorption features in the spectral line profiles due to circumstellar material in the line of sight for nearly edge-on equatorial disks. Since Be stars are generally rapid rotators, spectroscopic measurement of the projected rotational velocity $v \sin i$ can also suggest roughly the value of i.

(3) Figure 3 shows how the model polarization p^B in the B passband varies as α increases from 0° to 90° using a typical set of parameters. The polarization first rises as the widening disk presents an increasing number of scatterers, then begins to decline due

to the buildup of enough density at high latitudes to cancel the polarization from the equatorial regions. The model of Waters & Marlborough (1992) also shows this behavior, which becomes of practical concern because the hump-shaped graph allows for both a "thick disk" and a "thin disk" solution, producing identical polarization at α values on opposite sides of the peak. For equal densities, however, the thick disk will have a higher luminosity than the thin disk, giving the polarization a recognizably different wavelength dependence.

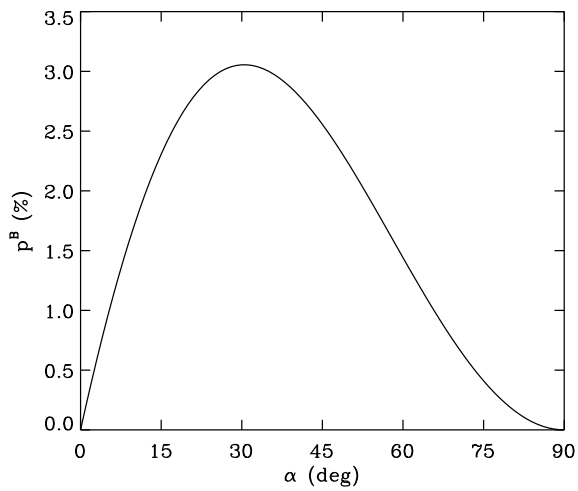

Fig. 3.— The dependence of the model blue polarization p^B on the opening half-angle α of the disk using a typical set of parameters.

Figures 4–11 present possible (but not necessarily unique) model fits for the eight program Be stars, with the parameters summarized in Table 2. The observational data points, plotted as open squares with vertical error bars, are intrinsic polarization, corrected for the interstellar component by Stokes vector subtraction (McDavid 1999). The corresponding model result is plotted as a solid line, using open circles for the broadband values with horizontal line segments to show the filter passbands. Several additional quantities derived from the model are also included in Table 2 for each fit: the maximum polarization $pmax$ and its wavelength $\lambda(pmax)$, the maximum of the H I absorption optical depth $\tau_a max$ and its wavelength $\lambda(\tau_a max)$, the electron scattering optical depth τ_e, the total envelope mass M, and the NLTE departure coefficients b_2 and b_3 for the populations of the first two excited states of the neutral hydrogen in the disk. Refer to Appendix A for a discussion of NLTE considerations.

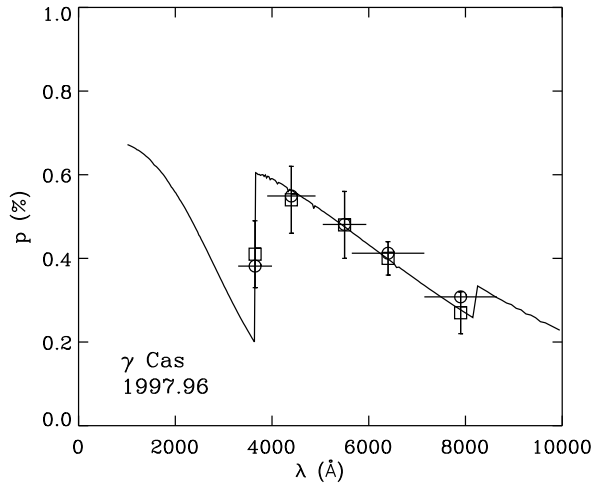

Fig. 4.— Fit of a spherical sector disk to the *UBVRI* polarization of γ Cas.

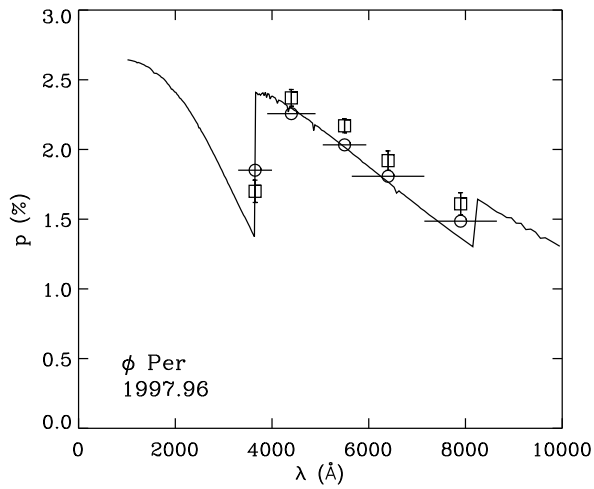

Fig. 5.— Fit of a spherical sector disk to the *UBVRI* polarization of ϕ Per.

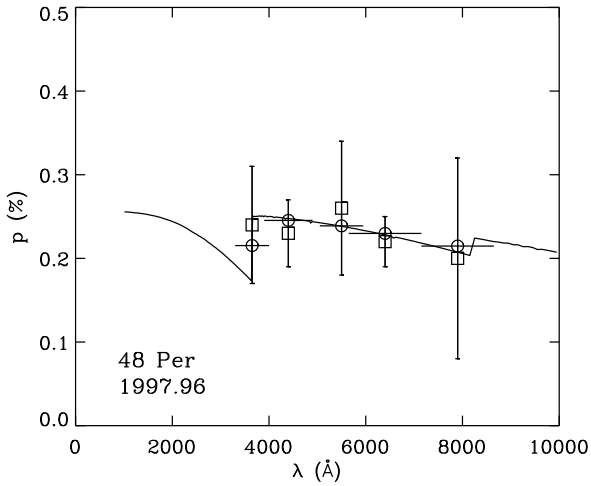

Fig. 6.— Fit of a spherical sector disk to the *UBVRI* polarization of 48 Per.

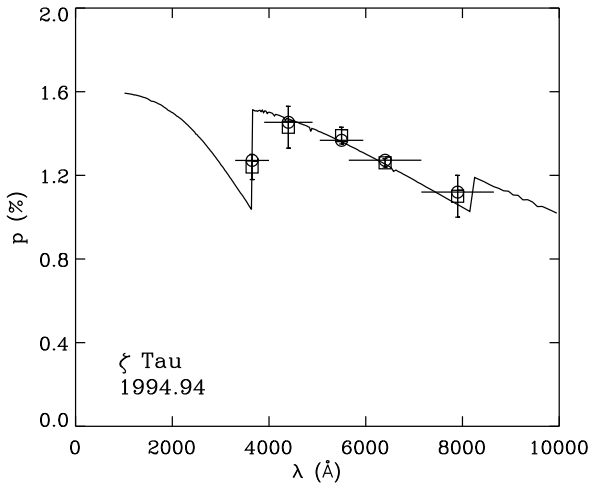

Fig. 7.— Fit of a spherical sector disk to the *UBVRI* polarization of ζ Tau.

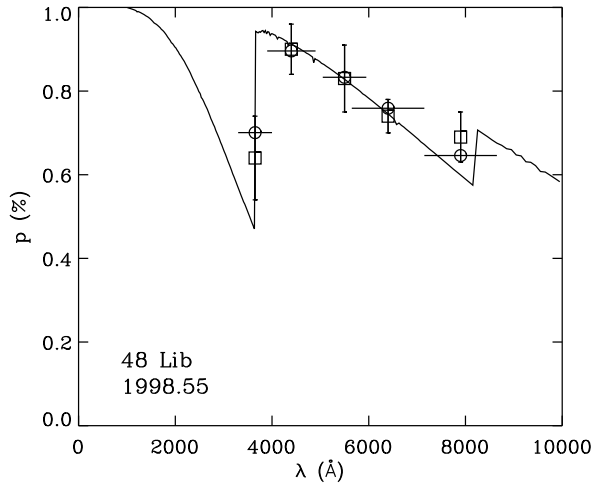

Fig. 8.— Fit of a spherical sector disk to the *UBVRI* polarization of 48 Lib.

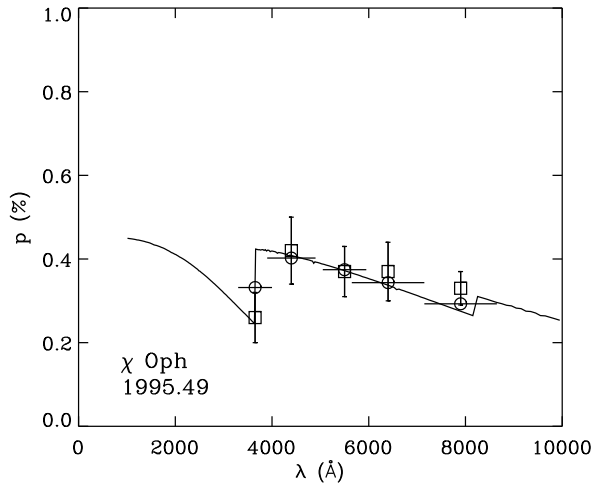

Fig. 9.— Fit of a spherical sector disk to the *UBVRI* polarization of χ Oph.

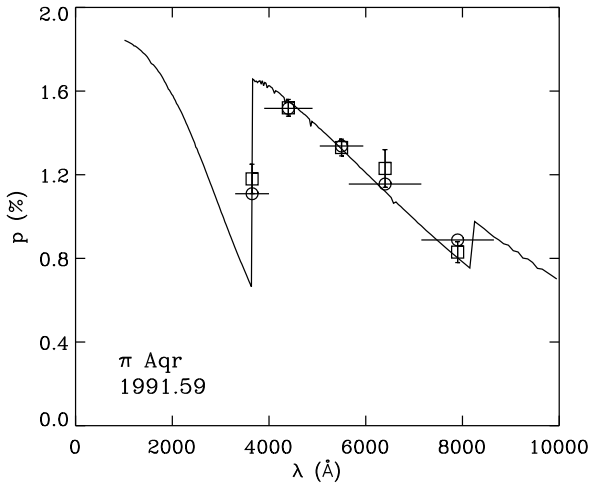

Fig. 10.— Fit of a spherical sector disk to the *UBVRI* polarization of π Aqr.

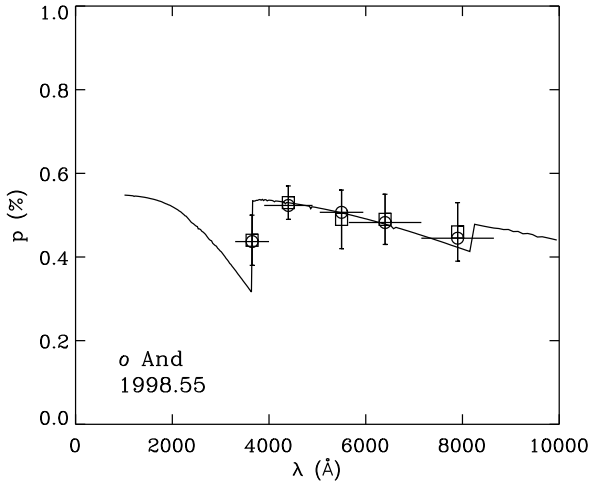

Fig. 11.— Fit of a spherical sector disk to the *UBVRI* polarization of o And.

Table 2. Parameters of the fits

	γ Cas	ϕ Per	48 Per	ζ Tau	48 Lib	χ Oph	π Aqr	o And
Spectral Type	B0.5 IVe	B1.5 (V:)e-shell	B4 Ve	B1 IVe-shell	B3:IV:e-shell	B1.5 Ve	B1 III-IVe	B6 III
Date of Obs.	1997.96	1997.96	1997.96	1994.94	1998.55	1995.49	1991.59	1998.55
$R_*(R_\odot)$	6.5	6.0	4.5	7.0	6.0	6.0	9.0	5.5
T_* (K)	25,000	25,000	17,000	25,000	20,000	25,000	25,000	14,000
$\log g$	4.0	4.0	4.0	4.0	3.5	4.0	3.5	3.5
$N_{0e}(10^{12}\mathrm{cm}^{-3})$	9.00	5.00	3.00	4.20	4.60	6.20	6.50	2.00
T_e (K)	18,750	18,750	12,750	18,750	15,000	18,750	18,750	10,500
α(deg)	2.0	10.0	3.0	6.0	4.0	3.0	3.5	5.5
i(deg)	52.0	80.0	55.0	80.0	80.0	41.0	80.0	80.0
$pmax(\%)$	0.60	2.41	0.25	1.51	0.94	0.42	1.66	0.54
$\lambda(pmax)$ (Å)	3661	3862	3862	3661	3812	3661	3661	3862
$\tau_a max$	0.94	0.27	0.23	0.22	0.44	0.41	0.68	0.22
$\lambda(\tau_a max)$ (Å)	3636	3636	3636	3636	3636	3636	3636	3636
τ_e	1.29	0.66	0.30	0.65	0.61	0.82	1.29	0.24
$M(10^{-9}M_\odot)$	3.07	6.69	0.51	5.37	2.47	2.50	10.3	1.14
b_2	1.69	1.69	1.05	1.69	1.35	1.69	1.69	0.70
b_3	0.29	0.29	0.23	0.29	0.26	0.29	0.29	0.19

7. Test of Accuracy

Since the model presented here is such a crude approximation, it is important to compare its results with those from a more sophisticated model to investigate, at least qualitatively, the accuracy we can expect. The Monte Carlo code of Wood, Bjorkman, & Bjorkman (1997, hereafter WBB) is one such standard, and it is based on the same set of input parameters except that the density input is the electron scattering optical depth rather than the electron number density, which requires only a minor conversion. Ideally we would like to determine WBB fits to the program star observations, and then quantitatively evaluate the simplified model by direct comparison of the fit parameters. Unfortunately, because of the slow convergence of the Monte Carlo method, deriving a WBB fit is a complex process requiring substantial amounts of cpu time even on a fast computer. Otherwise there would be no reason for interest in the kind of quick approximation that is the subject of this paper.

For the time being, though, we can at least make use of the existing WBB fit to ζ Tau. Figure 12 shows examples of $p(\lambda)$ for the quick approximation (solid line with broad band filter points marked by open circles) compared to the full optically thick multiple scattering WBB simulation (dashed line connecting filled circles). Errors in the WBB data points are on the order of 0.03%, limited by computing time. The observed *UBVRI* data are plotted as open squares with error bars. Using the parameters $R_* = 5.5\ R_\odot$, $T_* = 19,000$ K, $T_e = 15,000$ K, $\alpha = 2\overset{\circ}{.}5$, and $i = 82\overset{\circ}{.}0$ from the WBB solution as input to both models, the six plots show what happens as τ_e is increased by steps from 0.10 to 3.00 (the best fit value according to WBB).

This test shows that the optically thin approximation agrees quite well with the WBB calculation up to and including an optical depth of 1.00. It is also encouraging that for ζ Tau the best fit of the approximate method as shown in Figure 7 and Table 2 has $N_{e0} = 4.20 \times 10^{12}$ cm^{-3}, which is well within the range of $2.38 \times 10^{12} \leq N_{0e} \leq 7.54 \times 10^{12}$ cm^{-3} found by Waters, Coté, & Lamers (1987) in their infrared study.

However, it must be noted that there is a possibly serious disagreement between the WBB model and the simplified model presented here with regard to the best fit values of τ_e and α for ζ Tau. While the WBB disk ($\tau_e = 3.00$ and $\alpha = 2\overset{\circ}{.}5$) is optically thick but geometrically thin, the simplified model disk ($\tau_e = 0.65$ and $\alpha = 6\overset{\circ}{.}0$) is optically thin and geometrically thicker (although it still qualifies as "geometrically thin").

In Figure 12 the approximate model fails to produce a polarization large enough to fit the observations of ζ Tau by increasing τ_e at constant α because it becomes dominated by H I opacity. As shown in Table 2, this problem is seemingly avoided by increasing α instead of τ_e, but the resulting optically thin solution could possibly be ruled out on other grounds, such as the associated infrared emission as discussed by WBB. This is only one cautionary example emphasizing the importance of independent observational consistency checks in the interpretation of Be-star polarimetry data.

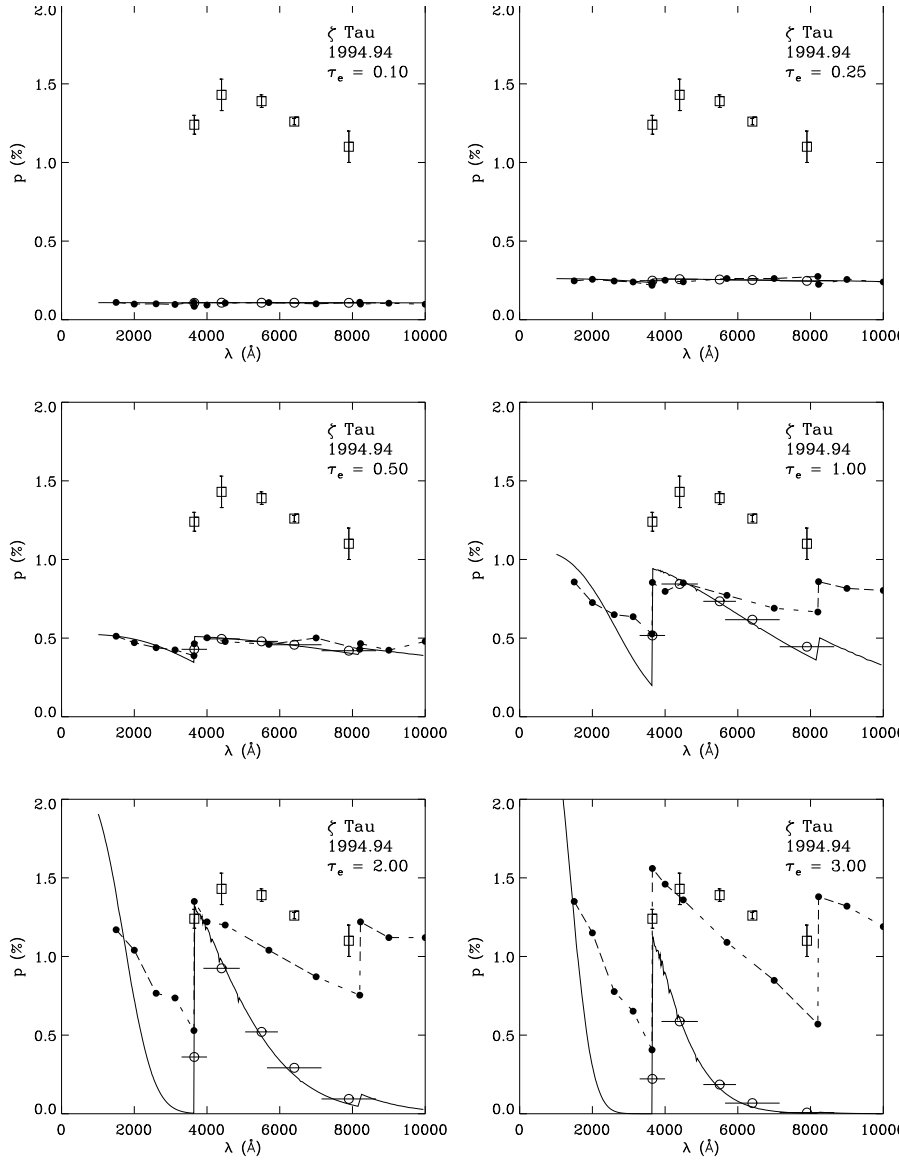

Fig. 12.— A comparison of the simple approximation (solid line with open circles) against the WBB solution (dashed line with filled circles) for a range of electron scattering optical depths τ_e. The observational data points for ζ Tau are shown as open squares.

8. Conclusion

In summary, the model presented here appears to give reasonable results for optically thin cases, but we should only trust it for order-of-magnitude accuracy because it is based on so many simplifying assumptions. Even so, it may be useful for estimating trial values of the parameters as starting points for rigorous fitting with more elaborate models.

An interesting result from applying the model to observations of the eight program stars is that all of them may be fit with geometrically thin disks, with opening half-angles of ten degrees or less. This adds tentative support to the statistics in favor of thin disks as presented by Bjorkman & Cassinelli (1990) and later discussed at length by WBB. If most Be disks prove to be similarly flat, it will surely have important implications concerning their formation process.

It may seem discouraging that this model will never find optically thick solutions even if they physically exist. And with three adjustable parameters, there might be any number of apparently valid optically thin fits to a set of *UBVRI* data points, rendering the entire exercise inconclusive. Nevertheless, there are good reasons for a more optimistic point of view. Due to the efforts of many investigators, as documented, for example, in the references in §1 of this paper, the range of physically allowable parameters has been narrowed significantly. And within even the most liberal of these constraints, experience with a quick, interactive trial-and-error system based on even the elementary physics presented here will show that it is surprisingly difficult to find multiple solutions with qualitatively different sets of parameters. I will be glad to share my IDL modeling program with interested users on request.

Thanks to Joe Cassinelli for critical reading and commentary on early drafts of this paper, and especially for suggesting a method to estimate the NLTE departure coefficients for the neutral hydrogen in a Be disk. Kenny Wood and Barbara Whitney also provided very helpful discussions, and Jon Bjorkman kindly gave me a version of the Monte Carlo polarization code. I especially thank the anonymous referee for pointing out many serious errors in the original manuscript and for patiently explaining the necessary corrections.

A. APPENDIX
Estimating the NLTE Departure Coefficients

Fits to the polarization Balmer jump were difficult and in some cases impossible without NLTE corrections to the level populations of the first two excited states of H I. According to the combined Saha and Boltzmann equations, the maximum population of the first excited state normally occurs at a temperature of about 10,000 K and declines rapidly toward higher temperatures with increasing excitation and ionization. At temperatures

closer to 20,000 K appropriate for Be disks, the LTE value of the absorption coefficient at the U-band is sometimes too small to match the large polarization Balmer jumps which are commonly observed. NLTE correction is applied only to the first two excited states because they dominate the opacity at optical wavelengths for the conditions of density and temperature of interest.

Since only averages over a line of sight are required for this very approximate polarization model, departure coefficients were simply estimated from the calculations of CNM. Their Figure 3 shows mean population parameters $\overline{q}_n$ for $n = 2$ and $n = 3$ defined by

$$\begin{aligned} \overline{q}_{nNLTE} &\equiv \frac{\int_{R_*}^{\infty} q_n(r, T_*) N_e^2 dr}{\int_{R_*}^{\infty} N_e^2 dr} \\ &= \frac{\int_{R_*}^{\infty} N_n dr}{\int_{R_*}^{\infty} N_e^2 dr}, \end{aligned} \tag{A1}$$

based on the detailed NLTE analysis of a stellar wind immersed in the radiation field of a central star, with statistical balance between photoionization and radiative recombination. The departure coefficient for level n is then the ratio of the NLTE and LTE values of $\overline{q}_n$.

The calculation of $\overline{q}_{nLTE}$ is done as follows:

$$\begin{aligned} \int_{R_*}^{\infty} N_n(r) dr &= n^2 N_{01} e^{X(n)-X(1)} \int_{R_*}^{\infty} \left(\frac{R_*}{r}\right)^{2\eta} dr \\ &= \frac{n^2 N_{01} R_*}{2\eta - 1} e^{X(n)-X(1)} \end{aligned} \tag{A2}$$

and

$$\begin{aligned} \int_{R_*}^{\infty} N_e^2 dr &= N_{0e}^2 \int_{R_*}^{\infty} \left(\frac{R_*}{r}\right)^{2\eta} dr \\ &= \frac{N_{0e}^2 R_*}{2\eta - 1}, \end{aligned} \tag{A3}$$

so that

$$\begin{aligned} \overline{q}_{nLTE} &= \frac{\int_{R_*}^{\infty} N_n dr}{\int_{R_*}^{\infty} N_e^2 dr} \\ &= \frac{N_{01}}{N_{0e}^2} n^2 e^{X(n)-X(1)} \\ &= (2\pi m_e k T_e)^{-1.5} h^3 n^2 e^{X(n)}. \end{aligned} \tag{A4}$$

The population parameters $\overline{q}_{2NLTE}$ and $\overline{q}_{3NLTE}$ may be estimated by extrapolation of power law fits to the disk temperatures (10,000–20,000 K) and mass-loss rates ($\sim 10^{-8}\ M_\odot\ yr^{-1}$) characteristic of Be stars, based on Figure 3 of CNM:

$$\overline{q}_{2NLTE} = 1.11 \times 10^{-8}\, T_e^{-2.83}\,, \tag{A5}$$

$$\overline{q}_{3NLTE} = 4.59 \times 10^{-13}\, T_e^{-2.02}\,. \tag{A6}$$

The approximate departure coefficients are then $b_2 = \overline{q}_{2NLTE}/\overline{q}_{2LTE}$ and $b_3 = \overline{q}_{3NLTE}/\overline{q}_{3LTE}$, so that the corrected level populations are roughly $N_{2NLTE} = b2 \times N_{2LTE}$ and $N_{3NLTE} = b3 \times N_{3LTE}$. These correction factors are applied to the appropriate terms in the summation inside the parentheses in equation (7.5). The corrected form of $\kappa(\lambda)$ is used only in calculating the absorption optical depth and not in calculating the emission coefficient, since recombination and free-free emission are LTE processes.

REFERENCES

Aller, L.H. 1963, The Atmospheres of the Sun and Stars (New York: Ronald Press)

Bessell, M.S. 1979, PASP, 91, 589

Bjorkman, J.E. & Bjorkman, K.S. 1994, ApJ, 436, 818

Bjorkman, J.E. & Cassinelli, J.P. 1990, in Angular Momentum and Mass Loss from Hot Stars, ed. Willson, L.A. & Stalio, R. (Dordrecht: Kluwer), 185

Bjorkman, K.S. 2000, in IAU Coll. 175: The Be Phenomenon in Early-Type Stars, ed. Smith, M., Henrichs, H., & Fabregat, J. (San Francisco: ASP), 384

Brown, J.C., Carlaw, V.A., & Cassinelli, J.P. 1989, ApJ, 344, 341

Brown, J.C. & Fox, G.K. 1989, ApJ, 347, 468

Brown, J.C. & McLean, I. 1977, A&A, 57, 141

Capps, R.W., Coyne, G.V., & Dyck, H.M. 1973, ApJ, 184, 173

Cassinelli, J.P., Nordsieck, K.H., & Murison, M.A. 1987, ApJ, 317, 290

Collins, G.W., II, Truax, R.Y., & Cranmer, S.R. 1991, ApJS, 77, 541

Coyne, G.V. & McLean, I.S. 1982, in IAU Symp. 98, Be Stars, ed. Jaschek, M. & Groth, H. (Dordrecht: Reidel), 77

Fox, G.K. 1991, ApJ, 379, 663

Fox, G.K. 1994, ApJ, 435, 372

Fox, G.K. & Brown, J.C. 1991, ApJ, 375, 300

Hillier, D.J. 1994, A&A, 289, 492

Kruszewski, A., Gehrels, T., & Serkowski, K. 1968, AJ, 73, 677

Kurucz, R.L. 1994, Solar Model Abundance Model Atmospheres, Smithsonian Astrophysical Observatory, CD-ROM No. 19

McDavid, D. 1999, PASP, 111, 494

McLean, I.S. 1979, MNRAS, 186, 265

Millar, C.E. & Marlborough, J.M. 1998, ApJ, 494, 715

Poeckert, R. & Marlborough, J.M. 1978a, ApJ, 220, 940

Poeckert, R. & Marlborough, J.M. 1978b, ApJS, 38, 229

Quirrenbach, A., Bjorkman, K.S., Bjorkman, J.E., Hummel, C.A., Buscher, D.F., Armstrong, J.T., Mozurkewich, D., Elias, N.M., II, & Babler, B.L. 1997, ApJ, 479, 477

Slettebak, A. 1982, ApJS, 50, 55

Waters, L.B.F.M., Coté, J., & Lamers, H.J.G.L.M. 1987, A&A, 185, 206

Waters, L.B.F.M. & Marlborough, J.M. 1992, A&A, 256, 195

Wood, K., Bjorkman, K.S., & Bjorkman, J.E. 1997, ApJ, 477, 926

Wood, K., Bjorkman, J.E., Whitney, B.A., & Code, A.D. 1996, ApJ, 461, 828

Yudin, R.V. 2001, A&A, 368, 912

Chapter 8

International Multiwavelength Campaigns on Short Term Variability of OB Stars: Optical Polarimetry

(originally published in 1993 IAU Symp. 162, Pulsation, Rotation and Mass Loss in Early-Type Stars, ed. Balona, L.A., Henrichs, H.F., & Le Contel, J.M. (Dordrecht: Kluwer))

From 1986 through 1992, wide band optical (B or V filter) linear polarization measurements of eight Be stars and seven O stars were obtained simultaneously with ultraviolet observations from *IUE* and worldwide ground-based optical spectroscopy and photometry in a series of campaigns designed to study the short term variability of these objects. Each campaign consisted of intensive monitoring of a few carefully chosen stars over a period of several days and nights, with the greatest possible continuity subject to the limitations of instrument scheduling, weather, and the longitudes of the observing sites.

With a typical instrumental uncertainty of about 0.03% for a single observation, no polarization variability was detected at the 3 σ level for any of the program stars. Normalized Stokes parameter plots are shown in Figure 1, where the data points are filled circles, the mean is a cross drawn to the size of the average instrumental uncertainty of a single observation, the standard deviation is represented by a dotted ellipse centered on the mean, and three times the average instrumental uncertainty of a single observation is represented by a solid ellipse centered on the mean.

Since most of the stars showed definite signs of activity in their winds and photospheres during the time intervals covered, it appears that associated changes in polarization are uncommon, or at least too small to measure by current techniques. In some cases, weak periodicities may be present in the polarization at frequencies which match those found in the simultaneous photometric and spectroscopic data sets from the campaigns, but their significance has not yet been thoroughly evaluated.

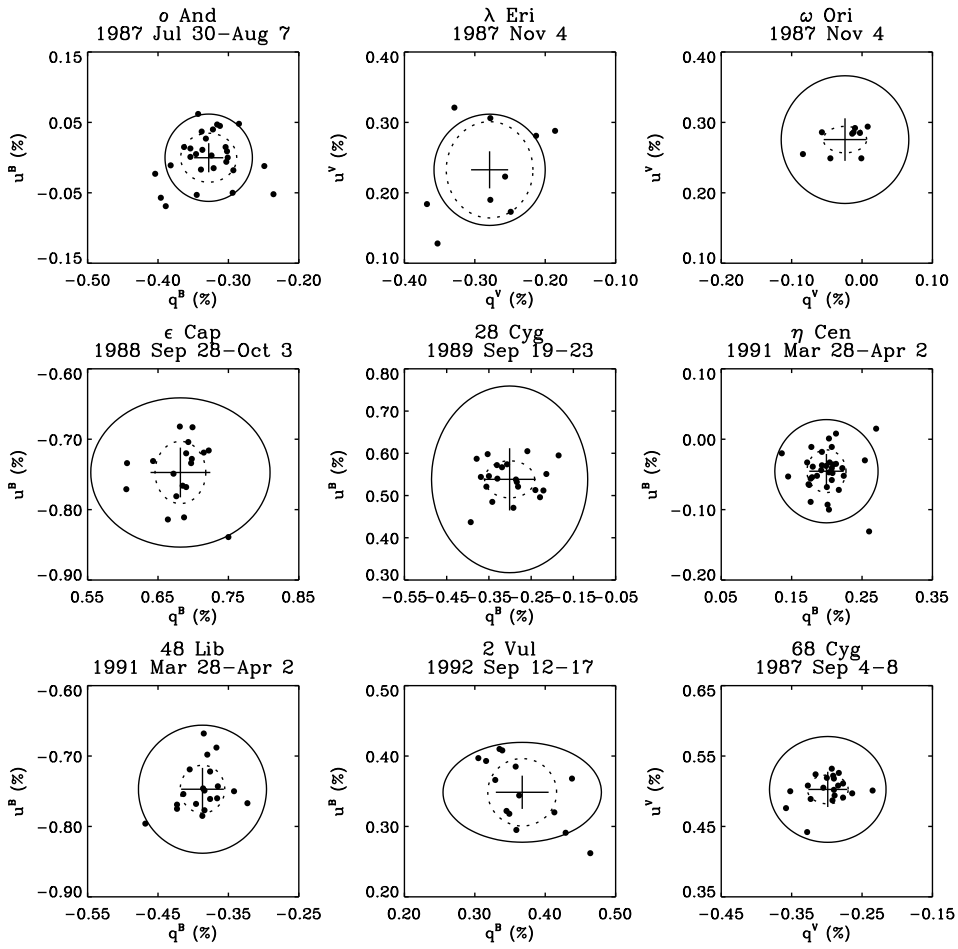

Fig. 1.— Normalized Stokes parameter plots for program stars. (The symbols are explained in the text.)

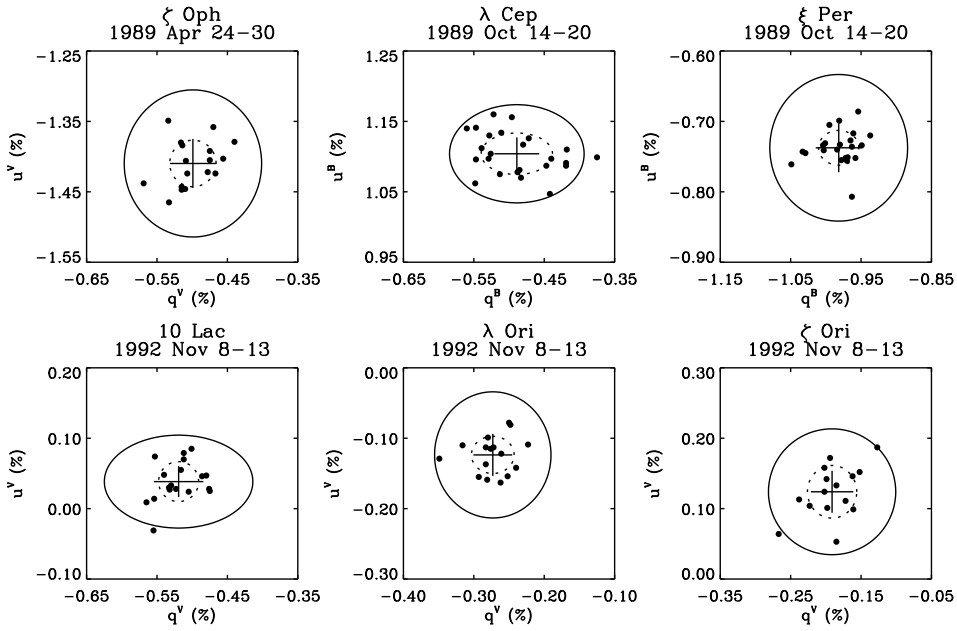

Fig. 2.— Normalized Stokes parameter plots for program stars. (The symbols are explained in the text.)

Chapter 9

A Search for Intrinsic Polarization in O Stars with Variable Winds

(originally published in 2000, AJ, 119, 352)

ABSTRACT

New observations of nine of the brightest northern O stars have been made with the Breger polarimeter on the 0.9 m telescope at McDonald Observatory and the AnyPol polarimeter on the 0.4 m telescope at Limber Observatory, using the Johnson-Cousins *UBVRI* broadband filter system. Comparison with earlier measurements shows no clearly defined long term polarization variability. For all nine stars the wavelength dependence of the degree of polarization in the optical range can be fit by a normal interstellar polarization law. The polarization position angles are practically constant with wavelength and are consistent with those of neighboring stars. Thus the simplest conclusion is that the polarization of all the program stars is primarily interstellar. The O stars chosen for this study are generally known from ultraviolet and optical spectroscopy to have substantial mass loss rates and variable winds, as well as occasional circumstellar emission. Their lack of intrinsic polarization in comparison with the similar Be stars may be explained by the dominance of radiation as a wind driving force due to higher luminosity, which results in lower density and less rotational flattening in the electron scattering inner envelopes where the polarization is produced. However, time series of polarization measurements taken simultaneously with Hα and UV spectroscopy during several coordinated multiwavelength campaigns suggest two cases of possible small-amplitude, periodic short term polarization variability, and therefore intrinsic polarization, which may be correlated with the more widely recognized spectroscopic variations.

1. Introduction

While it is well understood that the luminosities of O stars are high enough to cause mass loss in the form of radiation-driven winds, it is not so easily understood that the outflows are observed to be both episodically and also periodically or quasi-periodically variable (Kaper & Fullerton 1998). By analogy with the slightly cooler Be stars, it might be expected that the winds of the most rapidly rotating O stars would be equatorially concentrated, even if the lower densities and higher velocities were to prevent the formation of equatorial disks. It is then plausible that the scattering of light from the central star by free electrons in the envelope or in the wind might lead to a measurable polarization if the degree of rotational flattening were sufficient and the orientation favorable. Polarimetric observations are therefore a valuable asset in the study of O-star winds, particularly as an indicator of the geometrical distribution of the outflowing material.

The discovery that most O stars exhibit deep-seated spectroscopic variability (Fullerton, Gies, & Bolton 1996) opened up the tantalizing possibility that photospheric activity may modulate the stellar wind by acting at its base. At nearly the same time, exploratory observations of O stars with *IUE* revealed spectral features (discrete absorption components, or DACs) accelerating blueward across the profiles of UV resonance lines, as if tracing the outflow of density perturbations in the wind (Prinja & Howarth 1986). Thus began a series of international multiwavelength observing campaigns extending over several years (McDavid 1994), using *IUE* together with simultaneous high resolution optical spectroscopy, photometry, and polarimetry at various ground-based observatories, in a search for "the photospheric connection": observational evidence that wind variations are directly linked to stellar surface activity. As a sensitive technique for monitoring conditions in the inner wind regions, polarimetry had a natural role to play in these observing campaigns, and the purpose of this paper is to presents the results. Some later followup observations are also included.

2. Collected Data

The program stars and relevant data are listed in Table 1. Tables 2–10 contain the results of a literature search for observations of each star, followed by new observations which have not been previously published. The reference codes given in parentheses immediately after the dates of observation are as follows: (1) Mathewson et al. 1978, (2a) Coyne & Gehrels 1966, (2b) Serkowski, Gehrels, & Wisniewski 1969, (2c) Gehrels 1974, (3a) Hayes 1975, (3b) Hayes 1978, (3c) Hayes 1984, (4) Poeckert, Bastien, & Landstreet 1979, (5) Lupie & Nordsieck 1987, (6) McDavid (McDonald Observatory, previously unpublished), (7) McDavid (Limber Observatory, previously unpublished). The McDonald observations (6) were made with the Breger polarimeter (Breger 1979) on the 0.9 m telescope, and the Limber observations (7) were made with AnyPol (McDavid 1999) on the 0.4 m telescope.

Where multiple measurements were available, the normalized Stokes parameters q and u, the degree p of polarization, and the equatorial position angle θ are the means of the given number n of individual measurements, and dq, du, dp, and $d\theta$ are the associated standard deviations. Results are presented for p and θ to help distinguish between variability in the degree of polarization and variability of the position angle, even though these parameters are not normally distributed (Clarke & Stewart 1986). For single measurements (1, 2c) and some cases of only two measurements (2a, 2b), dq, du, dp, and $d\theta$ are simply representative error estimates, usually based on repeatability of frequent observations of standard stars. In many references q and u were not given, so they were calculated as $q = p\cos 2\theta$, $u = p\sin 2\theta$, and $dq = du = dp$ for the sake of statistical completeness. In cases where $d\theta$ was missing, it was estimated as $28\overset{\circ}{.}65(dp/p)$. The quantities dpi and $d\theta i$ are estimates of the uncertainty in a single measurement, which are sometimes equivalent to the "representative error estimates" mentioned above (1,2), sometimes derived from the residuals of the fits used in the data reduction procedure (4,5), and sometimes calculated from photon counting statistics (3, 6). For the Limber Observatory data (7) a single measurement and its error are the mean and standard deviation of three repetitions.

3. Long Term Analysis: The Interstellar Component

Simple inspection of Tables 2–10 is all that is necessary to see that there is no compelling evidence for long term variable polarization at the 3 σ level for any of the program stars. The complete data set is far too heterogeneous and the sample sizes far too small to expect any meaningful result from application of a rigorous analysis of variance with F-test probabilities. Relaxing the requirements, but still in search of a more quantitative conclusion, Table 11 was constructed as a statistical summary of the data on all of the program stars. This was done by calculating the mean and standard deviation of q, u, p, and θ over the subsets of observations for each of the stars (columns [2], [4], [6], and [8]), averaging the standard deviations from each subset (bracketed quantities in columns [3], [5], [7], and [9]), and averaging the error estimates for a single observation (bracketed quantities in columns [10] and [11]).

It is then quite clear that the overall scatter dq, du, dp, and $d\theta$ from combining individual data subsets is never substantially greater than would be expected on average as seen in <dq>, <du>, <dp>, and <$d\theta$> or, alternatively, as seen in <dpi> and <$d\theta i$>. The Grand Averages over all 5 passbands (in rows beginning with "GAV"), based on the expectation that any variations should appear more or less in all filters, further demonstrate the absence of any detectable variability.

Can we use Table 11 to make a quantitative statement about the amplitude of genuine variability that would escape detection in this study, as well as an amplitude of variability that would surely be detected? A conservative criterion for the break point would be the average of the Grand Averages of dp over all the stars in Table 11, which is 0.07%. Smaller variations might be completely hidden, and the threshold for 3 σ detection

would be 0.21%. Compared to state-of-the-art precision on the order of 0.02% this may seem to be a weak result, but considering that it was obtained from the combination of at least seven different instrumental systems over a span of 40 years, it is a perfectly realistic conclusion that none of the program stars has varied substantially. This absence of variability constitutes strong evidence that the polarization is predominantly interstellar.

To continue the test for an interstellar origin of the polarization, a Serkowski law of the modified form $p(\lambda) = p_{max} \exp[-1.7\lambda_{max} \ln^2(\lambda_{max}/\lambda)]$ found by Whittet et al. (1992) was fitted to the *UBVRI* data on each star by weighted nonlinear least squares. The latest Limber Observatory observations were used because they comprise the most uniform data set. The top panels of Figures 1–9 show the results, including the fit parameters. Since the best fit values of λ_{max} generally fall within the normal range of 0.45 μm to 0.8 μm (Serkowski, Methewson, & Ford 1975), this experiment can be taken to support the interpretation of the polarization as interstellar.

The middle panels of Figures 1–9 show the polarization of the program star and neighboring stars taken from the agglomeration catalog of Heiles (2000), superimposed on the *IRAS* 100 μm survey image, which traces the interstellar dust. In most cases the position angle of the program star is similar to those of its neighbors, as would be expected if all the stars are polarized by selective extinction due to a locally uniform alignment of the interstellar dust grains (Aannestad & Greenberg 1983).

The bottom panels of Figures 1–9 show the *UBVRI* polarization of the program star plotted as 1σ confidence ellipses in the q, u plane. A solid line is drawn through the origin at the average of the *UBVRI* position angles. For comparison, a dashed line is drawn showing the best straight line fit to the *UBVRI* data points. These two lines will coincide if the position angle of the polarization is independent of wavelength, which is expected if it is purely interstellar. The shaded region is centered on the mean polarization position angle of the neighboring stars, extended by one standard deviation on either side, and defines the region of agreement between the position angle of the program star and those of the neighboring stars. The figures clearly show that the solid and dashed lines generally match well, with the greatest differences occurring when the degree of polarization is small and the position angle therefore poorly defined. In all cases except 19 Cep, which has only a negligible mismatch, the solid and dashed lines fall within the shaded regions.

Table 1. Program Stars

HD	Name	V[a] (mag)	Spectral Type[b]	R[c] ($R_\odot$)	T_{eff}[c] (K)	$\log L$[c] ($L_\odot$)	Dist[d] (pc)	$v \sin i$[e] (km s^{-1})
24912	ξ Per	4.04	O7.5 III(n)((f))	11	36 000	5.3	457	213
30614	α Cam	4.29	O9.5 Ia	22	29 900	5.5	1088	129
36861	λ Ori	3.66	O8 III((f))	12	35 000	5.3	372	74
37742	ζ Ori	1.75	O9.7 Ib	29	30 000	5.8	332	124
149757	ζ Oph	2.56	O9.5 V	8	34 000	4.9	163	372
203064	68 Cyg	5.00	O7.5 III:n((f))	14	36 000	5.5	660	305
209975	19 Cep	5.11	O9.5 Ib	18	30 200	5.4	1090	95
210839	λ Cep	5.04	O6 I(n)fp	17	42 000	5.9	550	219
214680	10 Lac	4.88	O9 V	9	38 000	5.1	704	35

References. — (a) Hoffleit & Jaschek 1982; (b) Walborn 1972, 1973; (c) Howarth & Prinja 1989; (d) Heiles 2000; (e) Howarth et al. 1997

Table 2. ξ Per

Year(Source) Filter(n)	q/dq (%)	u/du (%)	p/dp (%)	$\theta/d\theta$ (deg)	dpi (%)	$d\theta i$ (deg)
1949–1958(1)						
B(1)	-1.12/0.20	-0.65/0.20	1.29/0.20	105.0/ 4.4	0.20	4.4
1966(2b)						
U(2)	-0.96/0.10	-0.66/0.10	1.16/0.10	107.2/ 2.0	0.10	2.0
B(2)	-1.09/0.10	-0.82/0.10	1.37/0.10	108.5/ 2.0	0.10	2.0
V(2)	-1.15/0.10	-0.89/0.10	1.46/0.10	108.9/ 2.0	0.10	2.0
R(2)	-1.19/0.10	-0.87/0.10	1.47/0.10	108.1/ 2.0	0.10	2.0
I(2)	-1.00/0.10	-0.75/0.10	1.25/0.10	108.5/ 2.0	0.10	2.0
1989.79(6)						
U(6)	-0.86/0.05	-0.60/0.06	1.05/0.03	107.4/ 1.9	0.04	1.1
B(22)	-0.98/0.03	-0.74/0.02	1.23/0.03	108.4/ 0.5	0.03	0.9
V(6)	-1.11/0.02	-0.83/0.06	1.39/0.03	108.4/ 1.1	0.03	1.3
R(6)	-1.12/0.03	-0.82/0.02	1.39/0.02	108.2/ 0.5	0.02	0.5
I(6)	-0.99/0.06	-0.74/0.08	1.24/0.05	108.4/ 2.0	0.05	1.1
1991.82(6)						
V(15)	-1.13/0.03	-0.85/0.02	1.41/0.02	108.5/ 0.6	0.02	0.5
1996.13(7)						
U(1)	-0.79/0.14	-0.59/0.14	0.99/0.20	108.2/ 1.0	0.20	1.0
B(1)	-0.96/0.01	-0.79/0.11	1.24/0.06	109.7/ 2.1	0.06	2.1
V(1)	-0.99/0.12	-0.79/0.06	1.28/0.06	109.4/ 2.7	0.06	2.7
R(1)	-1.14/0.12	-0.90/0.03	1.46/0.09	109.2/ 1.9	0.09	1.9
I(1)	-1.07/0.09	-0.76/0.14	1.32/0.01	107.8/ 3.6	0.01	3.6
1997.04(7)						
U(4)	-0.90/0.02	-0.56/0.08	1.06/0.04	106.1/ 1.8	0.10	1.9
B(4)	-0.95/0.05	-0.65/0.06	1.16/0.07	107.2/ 0.8	0.06	1.7
V(4)	-1.07/0.05	-0.74/0.10	1.30/0.09	107.2/ 1.4	0.05	1.1
R(4)	-1.06/0.05	-0.68/0.06	1.27/0.07	106.4/ 0.6	0.11	3.4
I(4)	-1.06/0.07	-0.65/0.07	1.24/0.05	105.7/ 2.1	0.11	2.0

Table 3. α Cam

Year(Source) Filter(n)	q/dq (%)	u/du (%)	p/dp (%)	$\theta/d\theta$ (deg)	dpi (%)	$d\theta i$ (deg)
1949–1958(1)						
B(1)	0.35/0.20	-1.62/0.20	1.66/0.20	141.0/ 3.4	0.20	3.4
1963–1965(2a)						
U(2)	0.20/0.08	-1.67/0.08	1.68/0.08	138.4/ 2.7	0.08	0.9
B(2)	0.25/0.08	-1.74/0.08	1.76/0.08	139.1/ 0.9	0.08	0.9
V(2)	0.22/0.08	-1.82/0.08	1.83/0.08	138.4/ 0.9	0.08	0.9
R(2)	0.10/0.08	-1.44/0.08	1.44/0.08	136.9/ 0.9	0.08	0.9
I(2)	0.04/0.08	-1.13/0.08	1.13/0.08	136.0/ 0.9	0.08	0.9
1978.8(3c)						
B(41)	0.16/0.08	-1.54/0.08	1.55/0.08	138.0/ 1.0	0.02	0.4
1979–1982(5)						
V(8)	0.01/0.07	-1.46/0.07	1.46/0.07	135.2/ 1.8	0.02	0.4
R(8)	0.02/0.15	-1.59/0.15	1.59/0.13	135.3/ 1.7	0.04	1.0
I(8)	0.04/0.05	-1.41/0.05	1.41/0.05	135.9/ 2.6	0.04	1.2
1997.10(7)						
U(4)	0.16/0.12	-1.37/0.16	1.39/0.15	138.4/ 2.7	0.14	2.7
B(4)	0.15/0.08	-1.51/0.10	1.52/0.09	137.9/ 1.6	0.06	1.4
V(4)	0.15/0.08	-1.47/0.09	1.48/0.09	137.9/ 1.7	0.07	1.3
R(4)	0.14/0.10	-1.39/0.16	1.40/0.16	137.9/ 2.0	0.06	1.7
I(4)	0.09/0.12	-1.16/0.12	1.18/0.12	137.4/ 2.7	0.06	4.0

Table 4. λ Ori

Year(Source) Filter(n)	q/dq (%)	u/du (%)	p/dp (%)	$\theta/d\theta$ (deg)	dpi (%)	$d\theta i$ (deg)
1949–1958(1)						
B(1)	-0.16/0.20	-0.20/0.20	0.26/0.20	116.0/22.0	0.20	22.0
1974.54(3a)						
B(12)	-0.23/0.02	-0.11/0.02	0.26/0.02	102.7/ 2.2	0.02	2.2
1992.86(6)						
U(3)	-0.22/0.02	-0.10/0.06	0.25/0.04	101.8/ 5.0	0.03	3.2
B(3)	-0.25/0.03	-0.14/0.03	0.29/0.02	105.0/ 3.0	0.02	1.8
V(16)	-0.27/0.04	-0.12/0.04	0.30/0.04	102.2/ 3.7	0.03	2.8
R(3)	-0.23/0.07	-0.10/0.02	0.25/0.07	102.2/ 1.9	0.02	2.3
I(3)	-0.23/0.02	-0.05/0.04	0.24/0.02	96.6/ 5.6	0.02	2.2
1997.10(7)						
U(4)	-0.25/0.03	-0.17/0.09	0.31/0.07	106.2/ 7.0	0.04	7.6
B(4)	-0.29/0.02	-0.22/0.08	0.38/0.06	108.9/ 5.5	0.04	9.1
V(4)	-0.24/0.04	-0.16/0.06	0.31/0.04	106.7/ 5.7	0.03	10.7
R(4)	-0.27/0.03	-0.13/0.09	0.32/0.05	102.0/ 8.0	0.04	8.4
I(4)	-0.27/0.07	-0.07/0.12	0.32/0.07	97.5/10.2	0.07	12.0

Table 5. ζ Ori

Year(Source) Filter(n)	q/dq (%)	u/du (%)	p/dp (%)	$\theta/d\theta$ (deg)	dpi (%)	$d\theta i$ (deg)
1949–1958(1)						
B(1)	-0.23/0.12	0.06/0.12	0.24/0.12	83.0/14.3	0.12	14.3
1979–1982(5)						
V(3)	-0.38/0.02	0.11/0.02	0.40/0.02	81.9/ 0.5	0.02	1.4
1992.86(6)						
U(3)	-0.15/0.02	0.10/0.01	0.18/0.02	72.8/ 2.3	0.01	2.1
B(3)	-0.12/0.04	0.14/0.02	0.19/0.01	65.7/ 6.7	0.01	1.4
V(15)	-0.19/0.04	0.12/0.04	0.23/0.03	73.5/ 5.5	0.03	3.6
R(3)	-0.21/0.04	0.08/0.01	0.22/0.04	79.6/ 1.6	0.01	1.2
I(3)	-0.11/0.03	0.19/0.03	0.22/0.04	59.8/ 3.1	0.02	2.9
1997.10(7)						
U(4)	-0.23/0.10	0.03/0.11	0.28/0.08	81.8/13.6	0.10	11.2
B(4)	-0.21/0.17	0.00/0.05	0.27/0.12	89.0/16.8	0.09	25.1
V(4)	-0.19/0.14	0.07/0.09	0.25/0.12	84.0/15.7	0.07	25.7
R(4)	-0.20/0.09	0.09/0.12	0.25/0.11	81.2/12.9	0.10	12.6
I(4)	-0.23/0.15	0.03/0.08	0.28/0.13	86.9/13.3	0.05	17.5

Table 6. ζ Oph

Year(Source) Filter(n)	q/dq (%)	u/du (%)	p/dp (%)	$\theta/d\theta$ (deg)	dpi (%)	$d\theta i$ (deg)
1949–1958(1)						
B(1)	-0.34/0.12	-1.37/0.12	1.41/0.12	128.0/ 2.4	0.12	2.4
1964–1966(2c)						
U(1)	-0.28/0.01	-1.08/0.01	1.12/0.01	127.8/ 0.3	0.01	0.3
B(1)	-0.32/0.02	-1.28/0.02	1.32/0.02	127.9/ 0.5	0.02	0.5
V(1)	-0.39/0.01	-1.43/0.01	1.48/0.01	127.4/ 0.1	0.01	0.1
R(1)	-0.40/0.01	-1.44/0.01	1.49/0.01	127.2/ 0.4	0.01	0.4
I(1)	-0.34/0.01	-1.24/0.01	1.29/0.01	127.3/ 0.2	0.01	0.2
1974.54(3a)						
B(12)	-0.33/0.02	-1.25/0.02	1.29/0.02	127.5/ 0.4	0.02	0.4
1976.4(4)						
U(2)	-0.24/0.12	-0.97/0.12	1.00/0.12	128.2/ 0.7	0.02	0.6
B(2)	-0.37/0.04	-1.13/0.04	1.17/0.04	127.4/ 0.2	0.02	0.5
I(1)	-0.38/0.01	-1.17/0.01	1.23/0.01	126.1/ 0.2	0.01	0.2
1981–1982(5)						
V(6)	-0.56/0.04	-1.31/0.04	1.43/0.04	123.4/ 1.1	0.03	0.6
R(6)	-0.60/0.04	-1.34/0.04	1.47/0.04	123.0/ 0.5	0.04	1.0
I(6)	-0.55/0.04	-1.29/0.05	1.40/0.04	123.4/ 1.4	0.04	1.1
1989.32(6)						
B(5)	-0.41/0.03	-1.28/0.05	1.35/0.06	126.2/ 0.2	0.03	0.6
V(17)	-0.50/0.03	-1.41/0.03	1.50/0.04	125.3/ 0.6	0.04	0.6

Table 6—Continued

Year(Source) Filter(n)	q/dq (%)	u/du (%)	p/dp (%)	$\theta/d\theta$ (deg)	dpi (%)	$d\theta i$ (deg)
1992.71(6)						
$U(1)$	-0.26/0.04	-1.01/0.04	1.05/0.04	127.8/ 1.0	0.04	1.0
$B(1)$	-0.28/0.02	-1.34/0.02	1.37/0.02	129.0/ 0.4	0.02	0.4
$V(1)$	-0.56/0.02	-1.37/0.02	1.48/0.02	124.0/ 0.4	0.02	0.4
$R(1)$	-0.50/0.02	-1.40/0.02	1.49/0.02	125.1/ 0.3	0.02	0.3
$I(1)$	-0.56/0.04	-1.52/0.04	1.62/0.04	124.8/ 0.7	0.04	0.7
1996.35(7)						
$U(3)$	-0.28/0.02	-1.16/0.05	1.19/0.06	128.3/ 0.1	0.10	1.7
$B(3)$	-0.36/0.05	-1.26/0.03	1.31/0.02	127.1/ 1.2	0.04	1.1
$V(3)$	-0.41/0.02	-1.44/0.01	1.50/0.01	127.1/ 0.3	0.05	1.4
$R(3)$	-0.45/0.08	-1.32/0.05	1.40/0.07	125.7/ 1.4	0.06	1.0
$I(3)$	-0.41/0.07	-1.29/0.06	1.36/0.04	126.0/ 1.7	0.08	2.6
1997.51(7)						
$U(3)$	-0.16/0.04	-1.04/0.07	1.05/0.07	130.7/ 1.3	0.06	2.0
$B(3)$	-0.31/0.05	-1.25/0.02	1.29/0.03	128.0/ 0.9	0.05	1.0
$V(3)$	-0.33/0.07	-1.39/0.04	1.44/0.02	128.2/ 1.5	0.06	1.2
$R(3)$	-0.31/0.04	-1.43/0.08	1.46/0.09	128.9/ 0.4	0.05	0.8
$I(3)$	-0.43/0.03	-1.24/0.09	1.31/0.09	125.5/ 0.8	0.08	1.5

Table 7. 68 Cyg

Year(Source) Filter(n)	q/dq (%)	u/du (%)	p/dp (%)	$\theta/d\theta$ (deg)	dpi (%)	$d\theta i$ (deg)
1949–1958(1)						
B(1)	-0.13/0.20	0.35/0.20	0.37/0.20	55.0/15.5	0.20	15.5
1986.65(6)						
B(3)	-0.28/0.02	0.49/0.02	0.57/0.02	60.0/ 0.8	0.01	0.4
V(10)	-0.27/0.02	0.54/0.02	0.61/0.02	58.4/ 1.3	0.01	0.6
1987.68(6)						
V(20)	-0.30/0.03	0.50/0.02	0.59/0.02	60.3/ 1.5	0.03	1.2
1991.82(6)						
U(3)	-0.32/0.02	0.40/0.04	0.51/0.04	64.1/ 1.0	0.01	0.6
B(3)	-0.38/0.05	0.44/0.08	0.59/0.04	65.3/ 4.5	0.01	0.5
V(17)	-0.40/0.02	0.50/0.03	0.64/0.02	64.3/ 1.4	0.03	1.7
R(3)	-0.40/0.04	0.44/0.04	0.60/0.05	66.1/ 1.3	0.01	0.6
I(3)	-0.42/0.07	0.40/0.02	0.58/0.06	68.0/ 2.2	0.04	2.0
1996.54(7)						
U(4)	-0.28/0.02	0.52/0.05	0.61/0.03	59.3/ 1.8	0.14	7.5
B(4)	-0.34/0.03	0.48/0.03	0.60/0.04	62.6/ 1.0	0.08	2.8
V(4)	-0.36/0.04	0.52/0.06	0.64/0.05	62.4/ 2.4	0.10	1.2
R(4)	-0.37/0.05	0.54/0.01	0.66/0.03	62.0/ 2.2	0.07	3.1
I(4)	-0.31/0.06	0.46/0.11	0.57/0.12	61.9/ 1.6	0.11	9.1
1997.53(7)						
U(3)	-0.23/0.09	0.50/0.08	0.56/0.07	57.5/ 4.9	0.13	5.6
B(3)	-0.32/0.02	0.45/0.03	0.56/0.02	62.7/ 1.8	0.07	3.1
V(3)	-0.39/0.05	0.51/0.06	0.65/0.03	64.1/ 3.2	0.06	3.5
R(3)	-0.34/0.04	0.47/0.07	0.58/0.05	62.9/ 2.8	0.05	2.2
I(3)	-0.34/0.06	0.49/0.08	0.60/0.07	62.0/ 2.9	0.13	3.6
1997.66(7)						
V(32)	-0.31/0.06	0.50/0.06	0.59/0.06	60.9/ 2.3	0.05	2.8

Table 8. 19 Cep

Year(Source) Filter(n)	q/dq (%)	u/du (%)	p/dp (%)	$\theta/d\theta$ (deg)	dpi (%)	$d\theta i$ (deg)
1949–1958(1)						
$B(1)$	-0.79/0.20	0.66/0.20	1.03/0.20	70.0/ 5.6	0.20	5.6
1986.65(6)						
$B(2)$	-0.96/0.02	0.78/0.03	1.23/0.00	70.5/ 0.9	0.01	0.2
$V(6)$	-0.88/0.04	0.78/0.07	1.18/0.02	69.2/ 1.9	0.01	0.3
1996.59(7)						
$U(4)$	-0.88/0.12	0.67/0.10	1.12/0.15	71.4/ 0.2	0.12	2.5
$B(4)$	-1.01/0.09	0.60/0.06	1.18/0.10	74.7/ 1.1	0.06	2.0
$V(4)$	-0.90/0.08	0.57/0.08	1.07/0.09	73.9/ 2.1	0.10	1.4
$R(4)$	-0.83/0.04	0.55/0.06	1.01/0.04	73.4/ 1.7	0.04	4.2
$I(4)$	-0.73/0.10	0.45/0.04	0.86/0.10	74.2/ 1.9	0.15	3.8

Table 9. λ Cep

Year(Source) Filter(n)	q/dq (%)	u/du (%)	p/dp (%)	$\theta/d\theta$ (deg)	dpi (%)	$d\theta i$ (deg)
1949–1958(1)						
B(1)	-0.55/0.20	1.03/0.20	1.17/0.20	59.0/ 4.9	0.20	4.9
1974–1976(3b)						
B(74)	-0.48/0.06	1.13/0.06	1.23/0.06	56.4/ 0.9	0.02	0.5
1979–1982(5)						
V(8)	-0.52/0.04	1.10/0.04	1.22/0.04	57.7/ 1.4	0.03	0.6
R(8)	-0.63/0.05	1.17/0.05	1.33/0.05	59.1/ 1.4	0.06	1.5
I(8)	-0.48/0.07	1.06/0.07	1.16/0.07	57.2/ 2.3	0.05	1.6
1986.65(6)						
B(2)	-0.47/0.01	1.11/0.01	1.20/0.01	56.5/ 0.2	0.01	0.2
V(5)	-0.41/0.02	1.14/0.05	1.21/0.05	55.0/ 0.7	0.02	0.4
1987.68(6)						
V(7)	-0.48/0.01	1.09/0.03	1.19/0.02	57.0/ 0.4	0.02	0.6
1989.79(6)						
U(6)	-0.58/0.09	1.02/0.09	1.17/0.06	59.9/ 2.6	0.08	1.9
B(24)	-0.49/0.05	1.10/0.03	1.21/0.04	56.9/ 1.0	0.03	0.7
V(6)	-0.51/0.03	1.01/0.19	1.14/0.18	58.7/ 2.0	0.05	1.2
R(6)	-0.44/0.04	1.07/0.03	1.16/0.02	56.2/ 1.1	0.03	0.8
I(6)	-0.33/0.12	0.88/0.10	0.95/0.10	55.2/ 3.7	0.07	2.2
1991.82(6)						
V(16)	-0.46/0.07	1.09/0.04	1.18/0.04	56.3/ 1.7	0.04	1.1
1996.54(7)						
U(4)	-0.44/0.10	0.99/0.10	1.09/0.12	56.9/ 2.1	0.12	2.7
B(4)	-0.54/0.08	1.07/0.07	1.20/0.08	58.4/ 1.9	0.06	1.5
V(4)	-0.53/0.09	1.09/0.05	1.21/0.08	58.1/ 1.5	0.06	2.3
R(4)	-0.51/0.08	1.05/0.03	1.17/0.03	57.9/ 2.0	0.07	1.5
I(4)	-0.42/0.09	0.90/0.09	1.00/0.11	57.2/ 2.0	0.14	3.6

Table 10. 10 Lac

Year(Source) Filter(n)	q/dq (%)	u/du (%)	p/dp (%)	$\theta/d\theta$ (deg)	dpi (%)	$d\theta i$ (deg)
1949–1958(1)						
B(1)	-0.49/0.12	0.00/0.12	0.49/0.12	90.0/ 7.0	0.12	7.0
1992.86(6)						
U(3)	-0.45/0.08	0.08/0.03	0.46/0.08	84.8/ 2.0	0.05	3.2
B(3)	-0.50/0.04	0.10/0.06	0.52/0.02	84.1/ 3.7	0.04	1.9
V(18)	-0.52/0.03	0.04/0.03	0.52/0.03	87.9/ 1.6	0.04	1.2
R(3)	-0.52/0.06	0.01/0.02	0.52/0.06	89.6/ 1.3	0.04	2.0
I(3)	-0.47/0.05	0.03/0.04	0.47/0.05	88.3/ 2.1	0.04	2.4
1996.59(7)						
U(4)	-0.39/0.03	-0.01/0.10	0.41/0.03	90.4/ 7.5	0.07	6.7
B(4)	-0.52/0.07	-0.10/0.07	0.54/0.06	95.6/ 4.0	0.06	4.6
V(4)	-0.53/0.05	-0.07/0.05	0.54/0.05	93.7/ 2.7	0.05	5.2
R(4)	-0.50/0.07	-0.06/0.03	0.52/0.08	93.3/ 1.2	0.06	5.9
I(4)	-0.48/0.08	-0.10/0.06	0.52/0.05	95.9/ 4.0	0.14	9.4

Table 11. Statistical Summary

Star Filter [1]	q/dq (%) [2]	<dq> (%) [3]	u/du (%) [4]	<du> (%) [5]	p/dp (%) [6]	<dp> (%) [7]	$\theta/d\theta$ (deg) [8]	<$d\theta$> (deg) [9]	<dpi> (%) [10]	<$d\theta i$> (deg) [11]
ξ Per										
U	-0.88/0.07	0.08	-0.60/0.04	0.09	1.07/0.07	0.09	107.2/ 0.9	1.7	0.11	1.5
B	-1.02/0.08	0.08	-0.73/0.08	0.10	1.26/0.08	0.09	107.8/ 1.8	2.0	0.09	2.2
V	-1.09/0.06	0.06	-0.82/0.06	0.07	1.37/0.08	0.06	108.5/ 0.8	1.6	0.05	1.5
R	-1.13/0.05	0.08	-0.82/0.10	0.05	1.40/0.09	0.07	108.0/ 1.2	1.2	0.08	2.0
I	-1.03/0.04	0.08	-0.73/0.05	0.10	1.26/0.04	0.05	107.6/ 1.3	2.4	0.07	2.2
GAV	··· /0.06	0.07	··· /0.07	0.08	··· /0.07	0.07	··· / 1.2	1.8	0.08	1.9
α Cam										
U	0.18/0.03	0.10	-1.52/0.21	0.12	1.53/0.21	0.12	138.4/ 0.0	2.7	0.11	1.8
B	0.23/0.09	0.11	-1.60/0.10	0.12	1.62/0.11	0.11	139.0/ 1.4	1.7	0.09	1.5
V	0.13/0.11	0.08	-1.58/0.21	0.08	1.59/0.21	0.08	137.2/ 1.7	1.5	0.06	0.9
R	0.09/0.06	0.11	-1.47/0.10	0.13	1.48/0.10	0.12	136.7/ 1.3	1.5	0.06	1.2
I	0.06/0.03	0.08	-1.23/0.15	0.08	1.24/0.15	0.08	136.4/ 0.8	2.1	0.06	2.0
GAV	··· /0.06	0.10	··· /0.16	0.11	··· /0.15	0.10	··· / 1.1	1.9	0.08	1.5
λ Ori										
U	-0.23/0.02	0.02	-0.14/0.05	0.08	0.28/0.04	0.05	104.0/ 3.1	6.0	0.04	5.4
B	-0.23/0.05	0.07	-0.17/0.05	0.08	0.30/0.06	0.07	108.2/ 5.8	8.2	0.07	8.8
V	-0.25/0.02	0.04	-0.14/0.03	0.05	0.31/0.01	0.04	104.4/ 3.2	4.7	0.03	6.8
R	-0.25/0.03	0.05	-0.11/0.02	0.05	0.28/0.05	0.06	102.1/ 0.1	4.9	0.03	5.3
I	-0.25/0.03	0.05	-0.06/0.01	0.08	0.28/0.06	0.05	97.1/ 0.6	7.9	0.05	7.1
GAV	··· /0.03	0.05	··· /0.03	0.07	··· /0.04	0.05	··· / 2.6	6.3	0.04	6.7
ζ Ori										
U	-0.19/0.06	0.06	0.06/0.05	0.06	0.23/0.07	0.05	77.3/ 6.4	8.0	0.05	6.6
B	-0.19/0.06	0.11	0.07/0.07	0.06	0.23/0.04	0.08	79.2/12.1	12.6	0.07	13.6
V	-0.25/0.11	0.07	0.10/0.03	0.05	0.29/0.09	0.06	79.8/ 5.6	7.2	0.04	10.2
R	-0.20/0.01	0.06	0.09/0.01	0.06	0.23/0.02	0.08	80.4/ 1.1	7.2	0.05	6.9
I	-0.17/0.08	0.09	0.11/0.11	0.05	0.25/0.04	0.08	73.3/19.2	8.2	0.04	10.2
GAV	··· /0.06	0.08	··· /0.05	0.06	··· /0.05	0.07	··· / 8.9	8.6	0.05	9.5
ζ Oph										
U	-0.24/0.05	0.05	-1.05/0.07	0.06	1.08/0.07	0.06	128.6/ 1.2	0.7	0.05	1.1
B	-0.34/0.04	0.04	-1.27/0.07	0.04	1.31/0.07	0.04	127.6/ 0.8	0.8	0.04	0.9
V	-0.46/0.10	0.03	-1.39/0.05	0.02	1.47/0.03	0.02	125.9/ 2.0	0.7	0.04	0.7
R	-0.45/0.11	0.04	-1.39/0.05	0.04	1.46/0.04	0.05	126.0/ 2.2	0.6	0.04	0.7
I	-0.45/0.09	0.03	-1.29/0.12	0.04	1.37/0.14	0.04	125.5/ 1.3	0.8	0.04	1.1
GAV	··· /0.08	0.04	··· /0.07	0.04	··· /0.07	0.04	··· / 1.5	0.7	0.04	0.9

Table 11—Continued

Star Filter [1]	q/dq (%) [2]	<dq> (%) [3]	u/du (%) [4]	<du> (%) [5]	p/dp (%) [6]	<dp> (%) [7]	$\theta/d\theta$ (deg) [8]	<$d\theta$> (deg) [9]	<dpi> (%) [10]	<$d\theta i$> (deg) [11]
68 Cyg										
U	-0.28/0.05	0.04	0.47/0.06	0.06	0.56/0.05	0.05	60.3/ 3.4	2.6	0.09	4.6
B	-0.29/0.10	0.06	0.44/0.06	0.07	0.54/0.10	0.06	61.1/ 3.9	4.7	0.07	4.5
V	-0.34/0.05	0.04	0.51/0.02	0.04	0.62/0.03	0.03	61.7/ 2.3	2.0	0.05	1.8
R	-0.37/0.03	0.04	0.48/0.05	0.04	0.61/0.04	0.04	63.7/ 2.2	2.1	0.04	2.0
I	-0.36/0.06	0.06	0.45/0.05	0.07	0.58/0.02	0.08	64.0/ 3.5	2.2	0.09	4.9
GAV	··· /0.06	0.05	··· /0.05	0.06	··· /0.05	0.05	··· / 3.1	2.7	0.07	3.5
19 Cep										
U	-0.88/0.00	0.12	0.67/0.00	0.10	1.12/0.00	0.15	71.4/ 0.0	0.2	0.12	2.5
B	-0.92/0.12	0.10	0.68/0.09	0.10	1.15/0.10	0.10	71.7/ 2.6	2.5	0.09	2.6
V	-0.89/0.01	0.06	0.67/0.15	0.08	1.12/0.08	0.05	71.6/ 3.3	2.0	0.05	0.9
R	-0.83/0.00	0.04	0.55/0.00	0.06	1.01/0.00	0.04	73.4/ 0.0	1.7	0.04	4.2
I	-0.73/0.00	0.10	0.45/0.00	0.04	0.86/0.00	0.10	74.2/ 0.0	1.9	0.15	3.8
GAV	··· /0.03	0.08	··· /0.05	0.07	··· /0.04	0.09	··· / 1.2	1.7	0.09	2.8
λ Cep										
U	-0.51/0.10	0.09	1.00/0.02	0.09	1.13/0.06	0.09	58.4/ 2.1	2.3	0.10	2.3
B	-0.51/0.04	0.08	1.09/0.04	0.07	1.20/0.02	0.08	57.4/ 1.2	1.8	0.06	1.6
V	-0.48/0.05	0.04	1.09/0.04	0.07	1.19/0.03	0.07	57.1/ 1.3	1.3	0.04	1.0
R	-0.53/0.10	0.06	1.10/0.06	0.04	1.22/0.10	0.03	57.7/ 1.5	1.5	0.05	1.3
I	-0.41/0.08	0.09	0.95/0.10	0.09	1.04/0.11	0.09	56.5/ 1.2	2.7	0.09	2.5
GAV	··· /0.07	0.07	··· /0.05	0.07	··· /0.06	0.07	··· / 1.5	1.9	0.07	1.7
10 Lac										
U	-0.42/0.04	0.05	-0.04/0.05	0.06	0.44/0.04	0.05	87.6/ 4.0	4.8	0.06	4.9
B	-0.50/0.02	0.08	-0.07/0.06	0.08	0.52/0.03	0.07	89.9/ 5.8	4.9	0.07	4.5
V	-0.52/0.01	0.04	-0.05/0.02	0.04	0.53/0.01	0.04	90.8/ 4.1	2.2	0.05	3.2
R	-0.51/0.01	0.06	-0.04/0.04	0.02	0.52/0.00	0.07	91.4/ 2.6	1.2	0.05	4.0
I	-0.47/0.01	0.06	-0.06/0.05	0.05	0.50/0.04	0.05	92.1/ 5.4	3.0	0.09	5.9
GAV	··· /0.02	0.06	··· /0.04	0.05	··· /0.02	0.06	··· / 4.4	3.2	0.06	4.5

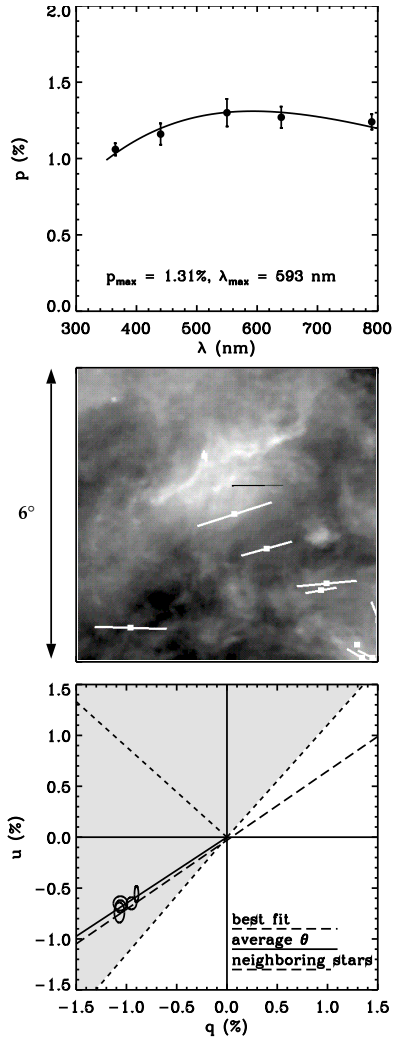

Fig. 1.— (top panel): Revised Serkowski law fit to the *UBVRI* polarization of ξ Per, showing values of the parameters p_{max} and λ_{max}. (middle panel): *IRAS* 100 μm image, centered on the program star, showing polarization of neighboring stars. North is up and East is left. (bottom panel): q, u plot with analysis of the *UBVRI* polarization position angles. See §3 for further explanation.

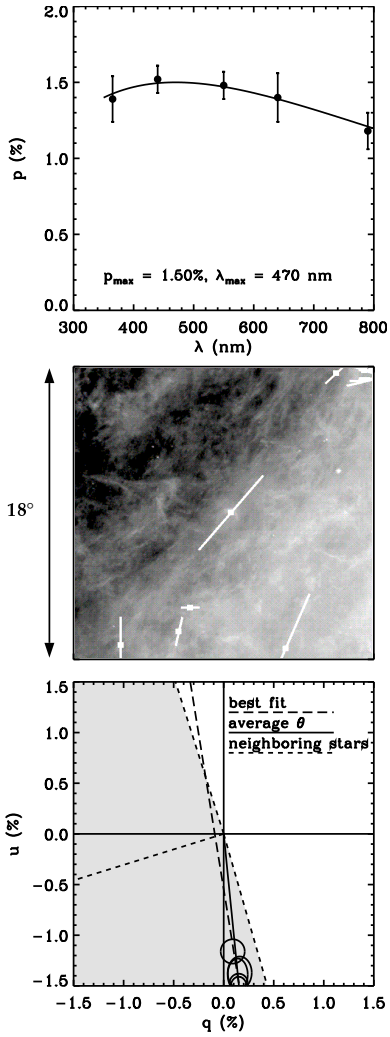

Fig. 2.— Same as Fig. 1, only for α Cam.

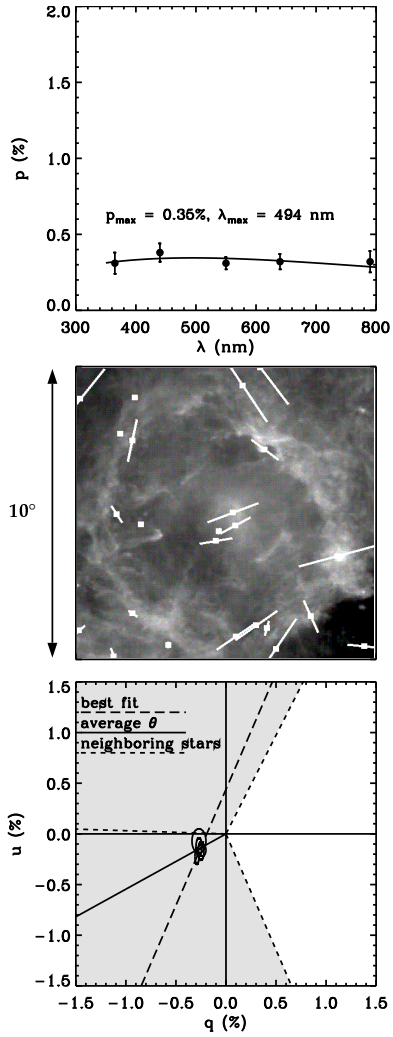

Fig. 3.— Same as Fig. 1, only for λ Ori.

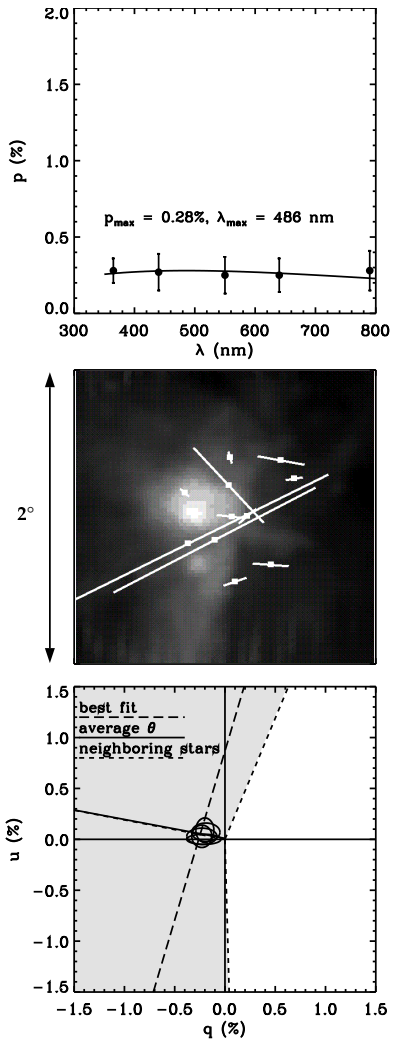

Fig. 4.— Same as Fig. 1, only for ζ Ori.

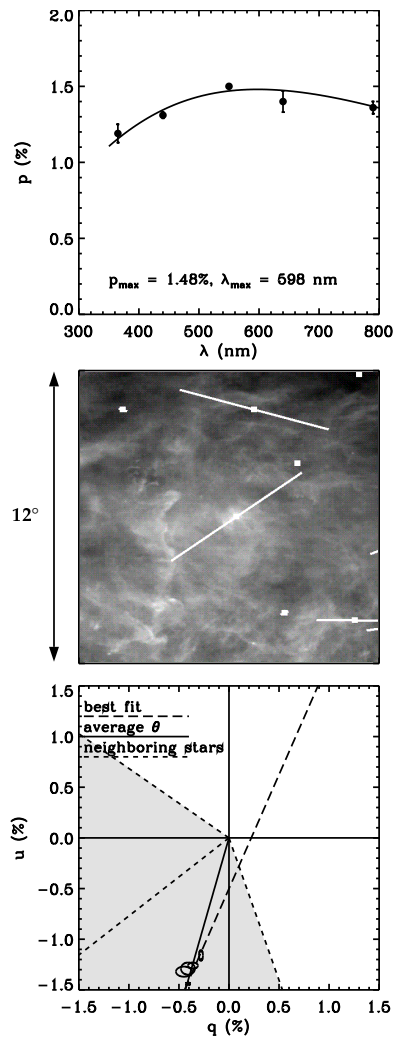

Fig. 5.— Same as Fig. 1, only for ζ Oph.

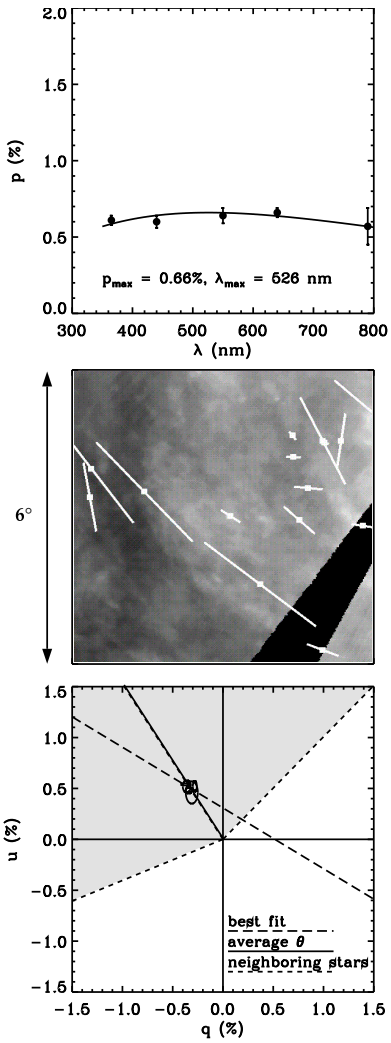

Fig. 6.— Same as Fig. 1, only for 68 Cyg.

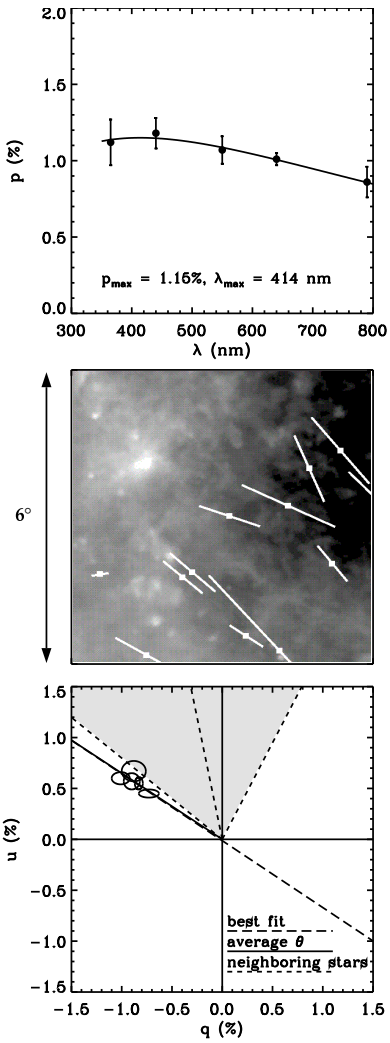

Fig. 7.— Same as Fig. 1, only for 19 Cep.

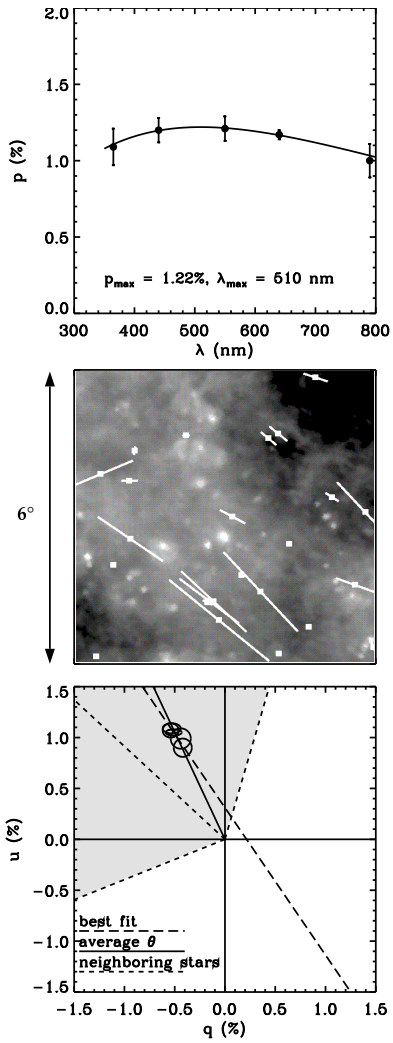

Fig. 8.— Same as Fig. 1, only for λ Cep.

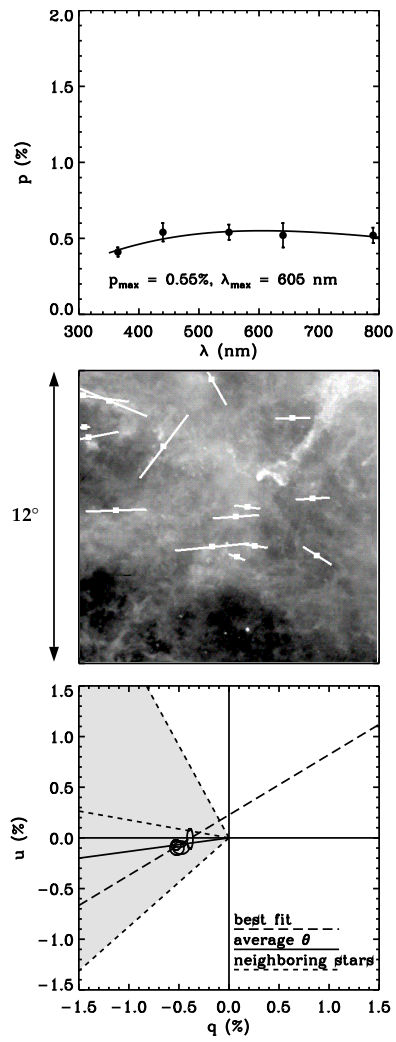

Fig. 9.— Same as Fig. 1, only for 10 Lac.

To summarize, four arguments imply that the polarization of all 9 program stars is interstellar: (1) No long-term variability has ever been detected. (2) The wavelength dependence of the polarization follows a Serkowski law typical of interstellar polarization. (3) The position angle of the polarization is independent of wavelength. (4) The position angle is consistent with those of neighboring stars.

In spite of this evidence against intrinsic polarization, it should be mentioned that there have also been some investigations resulting in its favor. Hayes (1975) made rigorous statistical analyses on his polarization measurements of several O stars with dense monitoring coverage over periods of months and concluded that λ Cep (Hayes 1978) and α Cam (Hayes 1984) were variable at the 3 σ level. He gave convincing proof of instrumental stability to the photon counting limit of $\sim 0.02\%$, which justified his detection of variability at levels of 0.06% to 0.08%. In a later study Lupie & Nordsieck (1987) found evidence for spectropolarimetric variability of the same two stars with only a slightly lower level of signal to noise.

As another example of the evidence for intrinsic polarization in emission-line O stars, Harries & Howarth (1996) discovered a spectropolarimetric change across the Hα emission line of ζ Pup, which implies a polarizing wind asymmetry. Also, Ebbets (1981) summarized the Hα emission episodes of ζ Oph, which seem to have escaped polarimetric observation but might well have included polarization effects (Reid et al. 1993). The x-ray outburst of ζ Ori (Berghöfer & Schmitt 1994), which was attributed to a propagating wind shock, also escaped polarimetric observation.

4. Short Term Analysis: Hints of Cyclic Variability

Most of the program stars were monitored at McDonald Observatory in conjunction with simultaneous ultraviolet and optical spectroscopy during several roughly week-long campaigns from 1986 through 1992. These time series are identifiable in Tables 2–10 by entries with large numbers of individual measurements, where only the averages are given. With a typical instrumental uncertainty of about 0.03% for a single observation, no polarization variability was detected at the 3 σ level for any of the series (McDavid 1998). However, during the campaign of October 1991, both 68 Cyg and ξ Per showed small-amplitude periodicities in polarization which are a priori significant because they match those found by Kaper et al. (1997) in the simultaneous optical and ultraviolet spectra. These variations constitute evidence for intrinsic polarization of a form that could have very easily escaped detection in the long term monitoring discussed earlier in this paper, but their reality should be regarded as tentative.

A CLEANed Fourier periodogram (Roberts, Lehar, & Dreher 1987) of the polarization of 68 Cyg using 15 iterations at a gain of 0.9 shows maximum power at 0.75 ± 0.03 d^{-1} (period 1.33 d), equal to the frequency of both the Hα and Si IV equivalent widths. The amplitude of this variation is about 0.045% (see Figure 10). Interestingly, the polarization is in antiphase with the Hα EW, exactly as expected in the corotating

interaction region (CIR) model applied to O-star winds (Cranmer & Owocki 1996). The notes in Figure 11 give a qualitative plausibility argument for how this might come about. For a thorough theoretical treatment see Harries (2000, in preparation). Assuming a radius of 14 $R_\odot$ and an inclination of 90°, the rotation period of 68 Cyg is 2.59 d. This gives two cycles per rotation, also in agreement with the CIR model with two diametrically opposite equatorial bright areas.

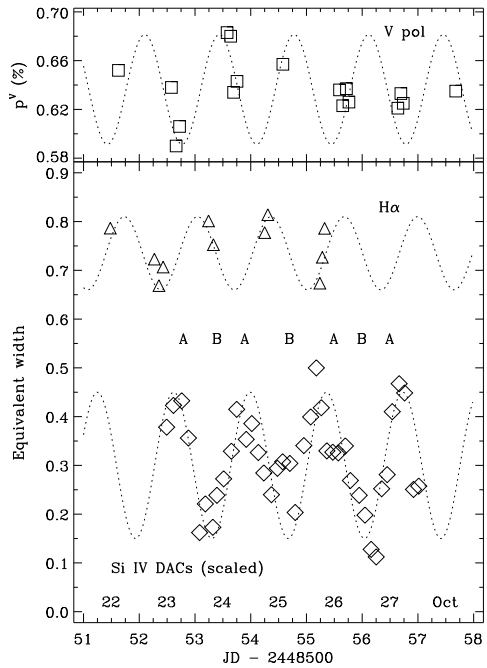

Fig. 10.— Correlations among cycles in the equivalent widths of Si IV and Hα and the polarization of 68 Cyg during the campaign of October 1991, adapted from Kaper et al. (1997).

The case of ξ Per is more complicated. Kaper et al. (1997) found the Hα and Si IV EWs to vary with a frequency of 0.50 ± 0.10 d^{-1} (period 2.0 d) and also noted the presence of another Hα frequency at 1.12 ± 0.03 d^{-1} (period 0.89 d), which they interpreted as a harmonic. As shown in Figure 12, the simultaneous polarimetry shows exactly this frequency, with an amplitude of about 0.025%. Assuming a radius of $11R_\odot$, the rotation period of ξ Per is less than about 2.78 d, depending on the inclination. It is possible, then, that the 2.0 d period is the rotation period, in which case ξ Per had only one photospheric bright area and associated CIR structure at the time of the observations. This would result in one EW cycle per rotation, but two polarization cycles, as observed.

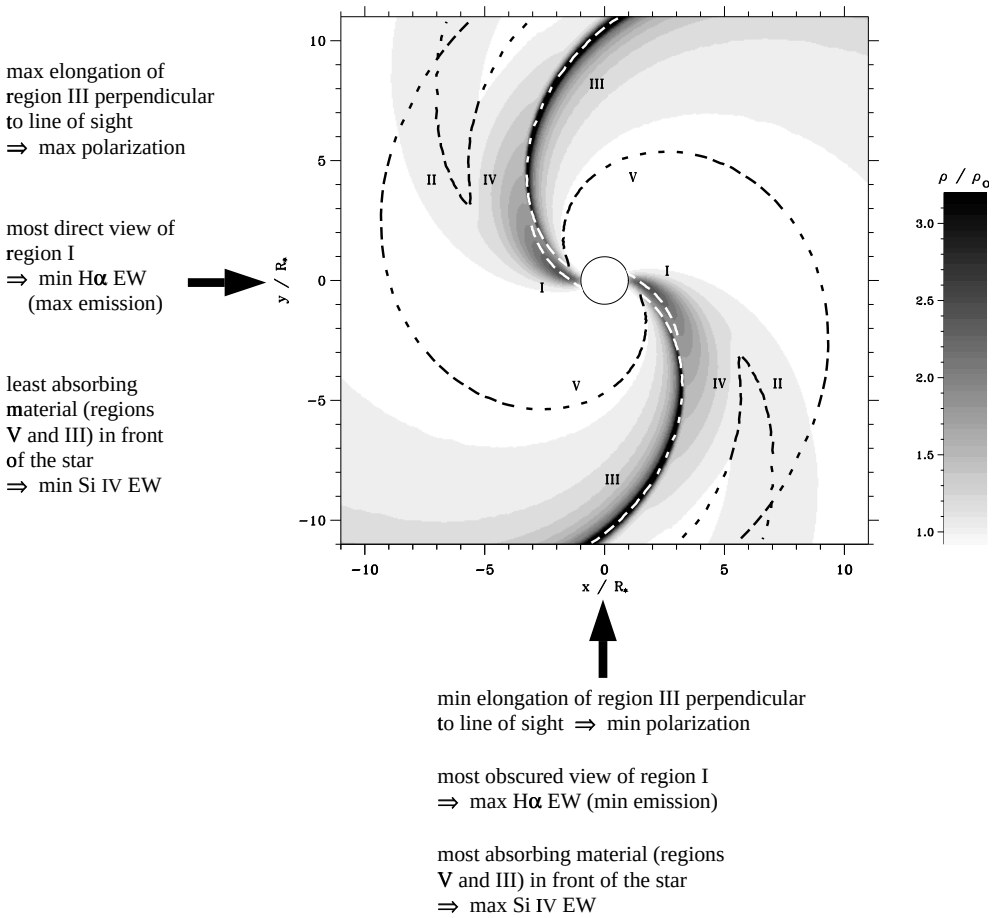

Fig. 11.— Illustration of the CIR model for a hot-star wind, with annotations explaining qualitatively the expected relations among Si IV and Hα equivalent widths and the polarization when viewed from different directions, adapted from Cranmer & Owocki (1996).

5. Conclusions

This study has illustrated that intrinsic polarization in O stars is clearly a rare phenomenon in spite of the similarity between emission line O stars and the cooler and less luminous Be stars, which have well known intrinsic polarization. Both classes of stars have significant mass loss in the form of variable winds, but the origin of the variability is still poorly understood. It seems a likely conclusion that the long-lived flattened envelopes or disks characteristic of Be stars almost never form around even the most rapidly rotating O stars because the circumstellar regions of O stars are more completely swept out by their stronger, luminosity-driven winds. The only indications of variable polarization found in the O stars are weak suggestions of rapid cycles on the time scale of the stellar rotation period (a few days at most) which appear to involve wind density patterns that change aspect with rotation.

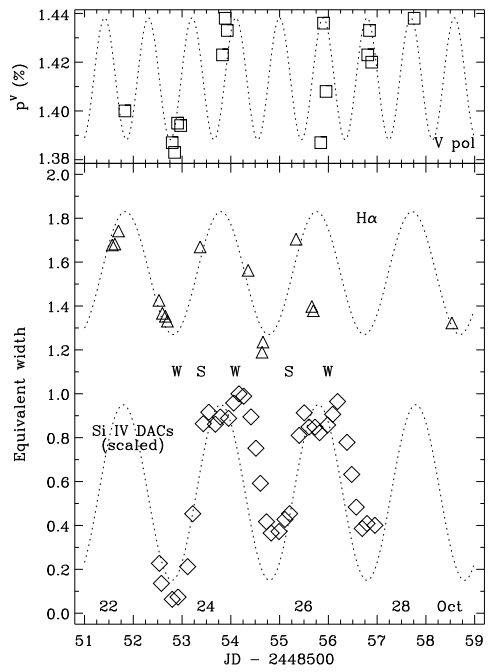

Fig. 12.— Correlations among cycles in the equivalent widths of Si IV and Hα and the polarization of ξ Per during the campaign of October 1991, adapted from Kaper et al. (1997).

The O stars presented here deserve continued long term polarization monitoring for the type of outburst behavior seen in ζ Oph and ζ Ori. Further pursuit of the suspected rapid cyclic variations, however, is likely to require dense time series polarimetry of unprecedented precision, with random errors not to exceed 0.01%.

I would like to take this opportunity to thank my friends and coworkers on the "O-Team": Tom Bolton, Doug Gies, Alex Fullerton, and Huib Henrichs, for their enthusiasm and encouragement. We were all inspired by the work of Andy Reid and Lex Kaper, who dispelled some of our skepticism and showed us the value of our observations. I also appreciate the advice of Dietrich Baade and Ian Howarth, who both took the time to read and comment on early versions of this paper.

I am grateful to the administration of McDonald Observatory for generous allotments of observing time, as well as to Ed Dutchover and the rest of the technical staff for maintaining the Breger polarimeter in stable working order for year after year.

This research has made use of the SIMBAD database, operated at CDS, Strasbourg, France. I acknowledge the use of NASA's *SkyView* facility (http://skyview.gsfc.nasa.gov) located at NASA Goddard Space Flight Center.

REFERENCES

Aannestad, P.A. & Greenberg, J.M. 1983, ApJ, 272, 551

Berghöfer, T.W. & Schmitt, J.H.M.M. 1994, Science, 265, 1689

Breger, M. 1979, ApJ, 233, 97

Clarke, D. & Stewart, B.G. 1986, Vistas Astron., 29, 27

Coyne, G.V. & Gehrels, T. 1966, AJ, 71, 355 (2a)

Cranmer, S.R. & Owocki, S.P. 1996, ApJ, 462, 469

Ebbets, D. 1981, PASP, 93, 119

Fullerton, A.W., Gies, D.R., & Bolton, C.T. 1996, ApJS, 103, 475

Gehrels, T. 1974, AJ, 79, 590 (2c)

Harries, T.J. & Howarth, I.D. 1996, A&A, 310, 533

Hayes, D.P. 1975, ApJ, 197, L55 (3a)

Hayes, D.P. 1978, ApJ, 219, 952 (3b)

Hayes, D.P. 1984, AJ, 89, 1219 (3c)

Heiles, C. 2000, AJ, 119, 923

Hoffleit, D., & Jaschek, C. 1982, The Bright Star Catalog, 4th Revised Edition (New Haven: Yale University Observatory)

Howarth, I.D. & Prinja, R. 1989, ApJ, 69, 527

Howarth, I.D., Siebert, K.W., Hussain, G.A.J., & Prinja, R.K. 1997, MNRAS, 284, 265

Kaper, L. & Fullerton, A.W., ed. 1998, Cyclic Variability in Stellar Winds, Proceedings of the ESO Workshop (Berlin: Springer-Verlag)

Kaper, L., Henrichs, H.F., Fullerton, A.W., Ando, H., Bjorkman, K.S., Gies, D.R., Hirata, R., Kambe, E., McDavid, D., & Nichols, J.S. 1997, A&A, 327, 281

Lupie, O.L. & Nordsieck, K.H. 1987, AJ, 92, 214 (5)

Mathewson, D.S., Ford, V.I., Klare, G., Neckel, Th., & Krautter, J. 1978, BICDS, 14, 115

McDavid, D. 1994, in Pulsation, Rotation and Mass Loss in Early-Type Stars, IAU Symp. 162, ed. Balona, L.A., Henrichs, H.F., & Le Contel, J.M. (Dordrecht: Kluwer), 530

McDavid, D. 1998, in Cyclic Variability in Stellar Winds, Proceedings of the ESO Workshop, ed. Kaper, L. & Fullerton, A.W. (Berlin: Springer-Verlag), 108

McDavid, D. 1999, PASP, 111, 494

Poeckert, R., Bastien, P., & Landstreet, J.D. 1979, AJ, 84, 812 (4)

Prinja, R.K. & Howarth, I.D. 1986, ApJS, 61, 357

Reid, A.H.N., Bolton, C.T., Crowe, R.A., Fieldus, M.S., Fullerton, A.W., Gies, D.R., Howarth, I.D., McDavid, D., Prinja, R.K., & Smith, K.C. 1993, ApJ, 417, 320

Roberts, D.H., Lehar, J., & Dreher, J.W. 1987, AJ, 93, 968

Serkowski, K., Gehrels, T., & Wisniewski, W. 1969, AJ, 74, 85 (2b)

Serkowski, K., Mathewson, D.S., & Ford, V.L. 1975, ApJ, 196, 261

Walborn, N.R. 1972, AJ, 77, 312

Walborn, N.R. 1973, AJ, 78, 1067

Whittet, D.C.B., Martin, P.G., Hough, J.H., Rouse, M.F., Bailey, J.A., & Axon, D.J. 1992, ApJ, 386, 562

Chapter 10

Samenvatting

1. Introductie

Een Be ster is een B-type ster die niet tot de superreuzen behoort, en waarvan één of meer Balmerlijnen in het spectrum tenminste eenmaal in emissie zijn aangetroffen. (Deze geaccepteerde definitie is van Collins, 1987). Bij superreuzen zijn Balmerlijnen gewoonlijk altijd in emissie, want het signaleert de aanwezigheid van een uitgebreide atmosfeer, terwijl bij gewone B sterren een dergelijke atmosfeer niet verwacht wordt. Uit de essentiële clausule "tenminste eenmaal" in bovenstaande definitie volgt al dat de emissiespectra bij Be sterren variabel kunnen zijn. De overgang van een standaard B-type absorptiespectrum in de waterstoflijnen naar een Be-type emissiespectrum en vice versa kan plaats vinden op een tijdschaal van enige jaren tot enige decennia, en wordt het Be fenomeen genoemd. Het wordt toegeschreven aan een episode van massaverlies in de vorm van een circumstellair omhulsel, waarin de emissielijnen ontstaan. Sinds Struve (1931) werd algemeen aangenomen dat de snelle rotatie van de ster verantwoordelijk is voor het massaverlies, maar thans is het nu overduidelijk geworden dat alleen rotatie het verschijnsel niet kan verklaren. Het omhulsel verdwijnt (dissipeert) dus in de loop van enige tijd, maar het hoe en waarom van het ontstaan en van de dissipatie is na 135 jaar onderzoek (sinds Secchi in 1866 de emissielijnen in de Be ster γ Cas visueel waarnam) nog altijd een raadsel, en vormt de drijfveer van deze studie.

De ontwikkeling van het onderzoek aan Be sterren staat het best beschreven in de Proceedings van de vijf IAU conferenties die aan dit onderwerp gewijd zijn (Slettebak 1976; Jaschek & Groth 1982; Slettebak & Snow 1987; Balona, Henrichs, & LeContel 1994; Smith, Henrichs, & Fabregat 2000). De twee algemene overzichtsartikelen van Slettebak (1979, 1988) en de uitgebreide introductie van Underhill & Doazan (1982) worden tevens aanbevolen.

Figuur 1 (Peters 1986) illustreert het verschil in de Balmer Hα lijn gedurende een B- en een Be-fase van de bekende Be ster μ Centauri. Karakteristiek is de dubbelgepiekte emissie. Vaak verandert de verhouding van de sterkte van de violette (V) piek ten opzichte van de rode (R) piek op quasi-periodieke wijze. Deze V/R veranderingen zijn geïllustreerd in figuur 2 (Guo 1994).

Ongeveer 10% van alle B niet-superreuzen zijn geklassificeerd als Be sterren. Rond spectraaltype B2 is wel 20% Be ster (Jascheck & Jascheck 1983). Deze fractie neemt sterk af naar de nog hetere sterren, maar toch zijn enkele Oe sterren als verlengstuk van het Be fenomeen te zien (Frost & Conti 1978). De vraag of iedere B ster door een Be fase gaat, of dat er aan bepaalde (vooralsnog niet goed bekende) voorwaarden voldaan moet zijn, is niet opgelost. Veel van de voorgestelde verklaringen hebben te maken met de opvallend hoge rotatiesnelheden van de Be sterren, waarvan de snelstdraaiende ook bij spectraaltype B2 voorkomen. De hoogste gevonden rotatiesnelheden zijn echter niet hoger dan 85% van de maximumdraaisnelheid waarbij de centrifugale versnelling het wint van de zwaartekracht (Slettebak 1987). Vandaar dat er minstens één extra mechanisme blijkbaar aan het werk moet zijn. Voorgestelde oorzaken zijn o.a. de aanwezigheid van niet-radiële pulsaties in het equatorvlak, stralingsgedreven sterrenwind in combinatie met de snelle rotatie, magnetische activiteit, en interactie met een begeleider als lid van een dubbelstersysteem. Geen van deze verklaringen blijkt te werken voor alle Be sterren, maar eveneens kan er geen worden uitgesloten. Een opmerkelijke vondst is dat in twee sterren de uitbarstingen plaatsvinden op het moment dat twee niet-radiële pulsatiemodes constructief interfereren (Rivinius et al. 1998; Tubbesing et al. 2000).

Dit proefschrift houdt zich bezig met de lineaire polarisatie eigenschappen op lange termijn van een representatieve groep Be sterren. De polarisatie kan namelijk informatie geven over de geometrie en de dichtheidsverdeling van het gasomhulsel gedurende de Be fase. Deze informatie geeft samen met andere observationele eigenschappen sterke randvoorwaarden aan modellen voor de ster plus omhulsel ter verklaring van het Be fenomeen. We besteden daarom bijzondere aandacht in deze introductie aan de ontwikkeling van het Be sterren onderzoek door middel van polarisatietechnieken.

De intrinsieke polarisatie van Be sterren werd ontdekt zodra de sterrenkundige polarimetrie was uitgegroeid tot een volwaardige en betrouwbare techniek door de toepassing van polarisatie analysators gekoppeld aan de eerste fotoelectrische fotometers. (Zie Shurcliff 1962, Gehrels 1974, Serkowski 1974, Tinbergen 1996 en Leroy 2000 voor goede

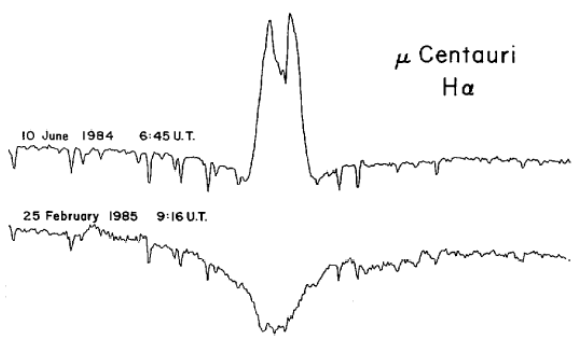

Fig. 1.— Hα lijnprofielen van de ster μ Centauri (B2IV-Ve) in een Be fase (emissie) en een B fase (absorptie). De overgang vond plaats in een half jaar (Peters 1986).

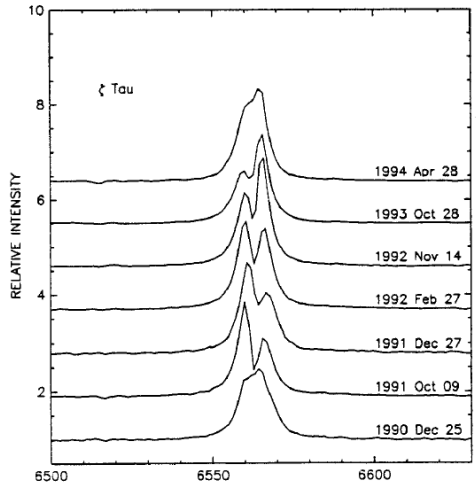

Fig. 2.— Hα lijnprofielen van de Be ster ζ Tauri (B1 IVe-shell) waar de verandering in de verhouding van de sterkte van de emissiepiek aan de violette (V) kant en van die aan de rode (R) kant, de zogeheten V/R variatie, duidelijk te zien is (Guo 1994).

discussies over polarisatie en de historische ontwikkeling van de instrumentatie en de toepassingen ervan in de sterrenkunde.) Alhoewel Be sterren werden meegenomen in de eerste overzichtsstudies die leidden tot de ontdekking van de galactische interstellaire polarisatie (Hiltner 1949; Hall 1949), de eerste aanwijzing dat Be sterren intrinsiek gepolariseerd zijn bleek uit de variabiliteit die waargenomen was door Behr (1959) en Coyne & Gehrels (1967). Serkowski (1968) vestigde de aandacht op de ongewoon grote verhouding tussen de polarisatie van het blauwe ten opzichte van het ultraviolette deel van het spectrum, die ver uitsteeg boven de normaal bekende interstellaire golflengte afhankelijkheid, zoals volgde uit eerdere *UBVRI* metingen, waaruit tevens de intrinsieke polarisatie van Be sterren volgde. Het werk van Poeckert, Bastien, & Landstreet (1979) is een goede introductie tot methodes waarmee onderscheid gemaakt kan worden tussen interstellaire en intrinsieke polarisatie van Be sterren. Zij geven bovendien het resultaat voor zo'n 70 sterren.

Het licht van Be sterren kan wel tot 2% gepolariseerd zijn, hetgeen wijst op een sterke asymmetrie. Het werk van Coyne & Kruszewski (1969), Capps, Coyne, & Dyck (1973), Gehrz, Hackwell, & Jones (1974) heeft tot het beeld bijgedragen dat men te maken heeft met een door draaiing afgeplat equatoriaal omhulsel, of schijf. Een dergelijke geometrie kan de karakteristieke emissielijnen verklaren. De polarisatie ontstaat door verstrooiing van het licht van de centrale ster aan de vrije electronen in de axisymmetrisch veronderstelde schijf. De waargenomen golflengte-afhankelijkheid wordt verklaard door de absorptie van de neutrale waterstof. Het moge duidelijk zijn dat als het vlak van de schijf niet loodrecht op het hemelvlak staat, de asymmetrie van de dichtheidsverdeling zal leiden tot een netto-polarisatie met een positiehoek evenwijdig aan de geprojecteerde rotatieas van de ster. Deze hoek zal loodrecht staan op de projectie van de schijf op

het hemelvlak. Op deze wijze worden waarnemingen van de polarisatie eigenschappen en de golflengte afhankelijkheid ervan zeer goed gebruikt om de dichtheid, temperatuur en geometrie van omhulsels van Be sterren te bestuderen. Dit model van een afgeplatte schijf werd op spectaculaire wijze bevestigd door de interferometrisch waarneming van de circumstellaire schijf van ζ Tauri door Quirrenbach et al. (1994), zie figuur 3.

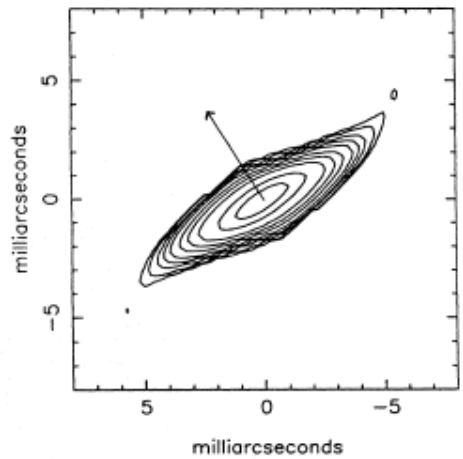

Fig. 3.— Reconstructie van het gebied aan de hemel van Hα emissie rond de Be ster ζ Tauri, verkregen met behulp van de maximum entropie methode, afgeleid uit interferometrische waarnemingen (Quirrenbach et al. 1994). De pijl geeft de positiehoek weer van de lineaire polarisatie.

Het standaard schijfmodel werd analytisch quantitatief ontwikkeld in een aantal theoretische artikelen door Brown & McLean (1977), Brown, McLean, & Emslie (1978), McLean & Brown (1979), en McLean (1979). Poeckert & Marlborough (1978) construeerden een gedetailleerd model voor het circumstellaire omhulsel van de heldere B0.5 IVe ster γ Cassiopeia, waarbij gebruikt gemaakt werd van een numerieke benadering om waarnemingen te beschrijven van zowel de emissielijnprofielen alsook tegelijkertijd van de breedband continuum polarisatie. In een andere reeks van theoretische artikelen (Brown & Fox 1989; Fox & Brown 1991; Fox 1991; Fox 1994) worden de depolariserende effecten beschreven vanwege het feit dat de ster een uitgebreide lichtbron is (zie ook Cassinelli, Nordsieck, & Murison 1987, en Brown, Carlaw, & Cassinelli 1989), alsmede vanwege het feit dat de schijf waarin de verstrooiing plaatsvindt gedeeltelijk de ster bedekt. In een interessante theoretische discussie van Fox & Henrichs (1994) werd de mogelijkheid onderzocht om verdichtingen of condensaties in de uitstromende winden van vroeg-type sterren polarimetrisch waar te nemen. Zulke verdichtingen zijn te verwachten in samenhang met de zogenoemde discrete absorptie componenten in ultraviolet spectraallijnen van dit soort sterren, maar tot nu toe is dit niet gevonden.

Het was Coyne (1975) die voor het eerste de polarisatie van verscheidene Be sterren over langere perioden, van wel 5 tot 8 jaar, waarnam. Hij vond variabiliteit op een

tijdschaal van door de band genomen 100 dagen, gesuperponeerd op veranderingen op een tijdschaal van enige dagen. Hij vond echter geen correlatie van de polarisatie met bekende radiële snelheidsvariaties of met helderheidsvariaties die optreden vanwege het dubbelsterkarakter. Huang, Hsu, & Guo (1989) volgden zeer nauwkeurig 14 Be sterren gedurende 6 maanden, met vergelijkbare resultaten, behalve een mogelijke periodiciteit gerelateerd aan de baanperiode in de Be dubbelster CX Draconis. Spectaculaire korte termijn veranderingen werden gevonden in de polarisatie eigenschappen tijdens een uitbarsting van de Be ster ω Orionis (Hayes & Guinan 1984; Brown & Henrichs 1987; Sonneborn et al. 1988), waarbij het begin en de afname van een episode met aanzienlijke massaverlies van deze ster over zo'n 100 dagen voortdurend werd gevolgd.

Sinds Clarke & McLean (1974), die een scheef gezet smalbandig interferentiefilter gebruikten om de polarisatie te meten over de breedte van de Hβ lijn van verscheidene Be sterren, is polarimetrie van Be sterren met een toenemend spectraal oplossend vermogen uitgevoerd, om zo steeds meer informatie over het omhulsel te verkrijgen (Poeckert & Marlborough 1977). McLean et al. (1979) verbeterde de techniek van het meten over een emissielijn met een hoge-resolutie spectropolarimeter door een Digicon detector te gebruiken, hetgeen geleid heeft tot een gedetailleerd overzicht van de snelheidsverdeling in schijven rond Be sterren, welke overeenstemde met een gecompliceerde combinatie van rotatie en expansie. Een lage-resolutie optische spectropolarimeter (Nordsieck et al. 1992) is in gebruik vanaf 1989 om de polarisatie in Be sterren te volgen, welke tevens als ondersteuning dient voor een vergelijkbaar instrument maar dan vanuit de ruimte in het ultraviolette deel van het spectrum. Gecombineerde gegevens va n deze instrumenten resulteerde in de ontdekking van een onverwachte afname in de polarisatie in Be sterren in het nabije ultraviolet, hetgeen toegeschreven is aan een sterk circumstellair blanketing effect door ijzerlijnen (Bjorkman et al. 1991).

De analyse van moderne spectropolarimetrische waarnemingen vereisen een hoogstaande theoretische behandeling van polarisatie door electronenverstrooiing samen met de opaciteit van neutrale waterstof. Hillier (194) ontwikkelde een numerieke methode om de transportvergelijking waarin polarisatie in rekening wordt gebracht op te lossen, terwijl Wood, Bjorkman, Whitney, & Code (1996) een Monte Carlo methode gebruikten om de polarisatie te simuleren door individuele fotonen te volgen langs hun weg door het circumstellaire omhulsel. Wood, Bjorkman, & Bjorkman (1997) konden hun Monte Carlo methode met succes toepassen op de spectropolarimetrie van ζ Tauri. De conclusie was dat de schijf optisch dik was, maar geometrisch dun. Tevens ontdekten zij dat polarisatie dankzij meervoudige verstrooiing hoger is dan de benaderde berekening aangaf in het geval van enkelvoudige verstrooiing.

2. Overzicht van de inhoud

Dit proefschrift is gericht op de waarnemingen van lineaire polarimetrie in het continuum. Gegevens zijn verzameld om de lange-termijn veranderingen van een representatief geachte groep van Be sterren te karakteriseren, welke kunnen worden gebruikt samen

met andere waarneemgegevens om de fysische veranderingen in de parameters van de ster met omhulsel vast te leggen die het Be fenomeen bepalen.

We vatten de resultaten samen van jaarlijkse lineaire polarimetrische waarnemingen over een periode van 15 jaar. Een nauwkeurige analyse van het verzamelde materiaal, waarbij het accent gelegd is op een zo goed mogelijke behoud van consistentie van de lange reeks waarnemingen, laat zien dat significante variabiliteit in de polarisatie op allerlei tijdschalen eigenlijk veel minder algemeen voorkomt dan men oorspronkelijk dacht toen dit onderzoek begonnen werd. Verder zijn enige bijzondere gevallen van wel duidelijke variabele polarisatie naar voren gekomen, en zijn bovendien theoretische methodes ontwikkeld en toegepast voor de interpretatie ervan. Het is bijvoorbeeld duidelijk geworden dat uit de waargenomen correlatie tussen de veranderingen in polarisatie en de bovengenoemde V/R verhouding volgt dat de materie in de circumstellaire schijf roteert volgens de wet van Kepler, iets wat a priori zeker niet evident is. Bovendien volgt uit modelaanpassingen aan waargenomen polarisatiemetingen in de *UBVRI* fotometriebanden dat Be schijven geometrisch dun moeten zijn. Deze resultaten geven hopelijk aanwijzingen hoe deze schijven kunnen ontstaan.

Nu volgen de beschrijvingen van de individuele hoofdstukken, welke bijna alle in druk zijn verschenen in tijdschriften.

Hoofdstuk 2 beschrijft het begin van het waarneemprogramma aan het McDonald Observatory van de University of Texas. Dit programma was erop gericht om lange termijn veranderingen in polarisatie te meten van een representatief gekozen groep heldere en goedbekende Be sterren, en wel in het bijzondere gedurende de groei en dissipatie van het circumstellaire omhulsel tijdens de overgangen van de B- naar de Be-fase en weer terug naar de B-fase. Het *UBVRI* fotometrische systeem werd gekozen om vergelijking mogelijk te maken met bestaande gegevens, welke in de meeste gevallen ook breedbandige metingen zijn. Een vergelijking van de nieuw verkregen metingen met die van de 20 jaar ervoor lieten significante veranderingen op lange termijn in de Be sterren ζ Tauri en π Aquarii zien.

Hoofdstuk 3 vat de resultaten samen van de daarop volgende 4 jaar. Het hoofdstuk is primair gewijd aan een statistisch onderbouwde methode waarmee variabiliteit van nacht tot nacht, en van jaar tot jaar te vinden zijn uit kleine hoeveelheden gegevens, die jaarlijks gemiddeld gedurende een week per jaar verkregen zijn, zowel voor de zomer als voor de winterobjecten. Wederom vertoonde ζ Tauri en π Aquarii veranderlijke polarisatie over de jaren, maar geen enkele van de programmasterren liet significante veranderingen van nacht tot nacht zien.

Hoofdstuk 4 geeft de resultaten van het monitorprogramma van de volgende 4 jaar en geeft conclusies over het hele project vanaf het begin. De enige ster waarvan de polarisatie overtuigend veranderd was π Aquarii, die in 8 jaar tijd van de hoogste polarisatiegraad van alle Be sterren langzaam terugkeerde naar een praktisch geheel ongepolariseerde fase. Ook was de golflengte afhankelijkheid van de polarisatie langzaam afgenomen zoals verwacht, omdat de neutrale waterstofabsorptie evenredig is aan het

kwadraat van de electronendichtheid N_e^2, terwijl de electronen verstrooiing evenredig is met N_e.

Hoofdstuk 5 beschrijft de overgang van het jaarlijkse monitorprogramma op het McDonald Observatory, waar de 90 cm telescoop buiten gebruik gesteld werd, naar de 40 cm telescoop van het Limber Observatory, waar een nieuwe polarimeter speciaal voor dit doel gebouwd werd. Een nauwkeurige vergelijking van metingen van standaardsterren bevestigde dat de twee instrumenten goed overeenstemden. Er werd geen significante veranderlijkheid gevonden in de programmasterren over een 4 jaar periode, alhoewel de verdeling van de gegevens in een diagram van cumulatieve Stokes parameters sterk suggereert dat er wel degelijk kleine maar significante verschillen kunnen optreden voor een aantal sterren. Alle individuele sterren worden hier besproken.

Hoofdstuk 6 stelt een belangrijke polarimetrische test aan de orde, waar het gaat om de hypothese dat de veelvuldig waargenomen bovengenoemde cyclische V/R variaties, met periodes van meerder jaren, verklaard kunnen worden door de aanwezigheid van een eenarmige dichtheidsverstoring in de schijf. Een dergelijke dichtheidsverstoring precedeert zeer langzaam, als gevolg van de niet-sferische gravitatiepotentiaal vanwege de snelle rotatie van de ster. We gebruiken hier een numerieke aanpak, waarbij we een model nemen waarin de verstoring gegenereerd is, en die de emissielijnprofielen kan verklaren. Een Monte Carlo methode wordt dan gebruikt om de electronenverstrooiing te simuleren om aldus het gedrag van de polarisatie te voorspellen. De gevonden resultaten komen overeen met de waarnemingen van de representatieve Be sterren ζ Tauri en 48 Librae. Een zeer belangrijke conclusie is de implicatie dat de circumstellaire schijf in Be sterren een Keplerschijf is, iets wat op geen andere methode aangetoond is.

Hoofdstuk 7 is gewijd aan een theoretisch model voor om de polarisatie in Be sterren te berekenen in een redelijke benadering. We gebruiken een sferisch model waarin sectoren de circumstellaire schijf representeren. Bij de bespreking van de methode komen aan de orde de electronenverstrooiing, de correctie voor de niet te verwaarlozen afmeting van centrale ster, de golflengteafhankelijkheid van de polarisatie vanwege de absorptie van neutrale waterstof in de schijf, en tenslotte de convolutie van het berekende signaal met het instrumentele profiel. De fundamentele aanname wordt gemaakt dat de schijf optisch dun is. Toepassing van dit model op waarnemingen van acht Be sterren geven goede overeenstemming, hetgeen impliceert dat de schijven rond Be sterren geometrisch dun moeten zijn.

Hoofdstuk 8 geeft de resultaten van uitgebreide polarimetrische metingen gedurende een aantal gecoördineerde multiwavelength campaigns die georganiseerd waren met als doel de korte tijdsveranderingen (uren, dagen) te onderzoeken in O en B sterren, met name in de emissielijnen die wijzen op de variabele uitstroming van sterrenwind. Een van de motivaties van deze campaigns was om observationeel onderscheid te kunnen maken tussen twee voorgestelde modellen voor de waargenomen variabiliteit: de aanwezigheid van niet-radiële pulsaties, en/of de aanwezigheid van aktieve gebieden in de fotosfeer. Tijdens deze campaigns heerste de in de literatuur gestaafde mening dat al dit soort sterren wel kortetijdsvariaties in de polarisatie te zien gaven, zodat het voor de hand lag

te zoeken naar correlaties met spectroscopische veranderingen. Verrassenderwijs konden er geen onafhankelijke aanwijzingen gevonden worden van variabiliteit in de polarisatie in de onderzochte sterren, bestaande uit acht Be sterren, en zev en O sterren. In enkele gevallen lijkt een zwakke correlatie aanwezig tussen veranderingen in polarimetrie en spectroscopie (zie ook hoofdstuk 9), zodat de conclusie is dat waarschijnlijk de verwachte polarisatie variabiliteit eenvoudig te klein is om met de gebruikte instrumentatie met zekerheid waar te nemen.

Hoofdstuk 9 houdt zich bezig met de polarimetrie van een aantal heldere O sterren met emissielijnen, welke in een aantal opzichten de vergelijkbaar zijn met de Be sterren, maar dan met een hogere lichtkracht. De meeste van de programmasterren werden intensief polarimetrisch waargenomen simultaan met ultraviolette en optische spectroscopische waarnemingen gedurende een reeks campagnes om de oorsprong van de korte-termijn veranderingen in de winden en het massaverlies van hete sterren te onderzoeken (Zie proefschriften van Kaper (1993) en de Jong (2000)). De twee O7.5 III sterren 68 Cygni en ξ Persei lieten slechts een marginale correlatie zien tussen de polarisatie en de Hα emissie, hetgeen in overeenstemming is met het zogenoemde Corotating Interacting Regions model. Het merendeel van de polarisatie blijkt interstellair te zijn. Blijkbaar laten de sterke stralingsgedreven winden van O sterren niet de formatie toe van een equatoriale schijf zoals in de Be sterren, zelfs niet voor de snelstdraaiende sterren.

Appendix A geeft een gedetailleerde beschrijving van AnyPol, een gewone Glan prisma fotopolarimeter, die is gebouwd om de afgebroken reeks waarnemingen op de 0.9 m McDonald telescoop (toen deze uit dienst genomen werd) voor te zetten op de 0.4 m telescoop van het Limber Observatory. Het ontwerp en de constructie van de polarimeter worden deel voor deel uitgelegd, zoals de fysieke en mechanische gegevens, het optische systeem, de electronica, en de controle apparatuur voor het daadwerkelijk verzamelen van de gegevens per computer.

Appendix B is een complete lijst van publikaties van de auteur in gerefereerde tijdschriften.

REFERENCES

Balona, L., Henrichs, H., & Le Contel, J.M. 1994, ed., IAU Symp. 162, Pulsation, Rotation and Mass Loss in Early-Type Stars (Dordrecht: Kluwer)

Behr, A. 1959, Nach. Akad. Wiss. Göttingen, 2, Math-Phys. Kl., No. 7, 185 (Veröff. Göttingen, No. 126)

Bjorkman, K.S., Nordsieck, K.H., Code, A.D., Anderson, C.M., Babler, B.L., Clayton, G.C., Magalhaes, A.M., Meade, M.R., Nook, M.A., Schulte-Ladbeck, R.E., Taylor, M., & Whitney, B.A. 1991, ApJ, 383, 67

Brown, J.C., Carlaw, V.A., & Cassinelli, J.P. 1989, ApJ, 344, 341

Brown, J.C. & Fox, G.K. 1989, ApJ, 347, 468

Brown, J.C. & Henrichs, H.F. 1987, A&A, 182, 107

Brown, J.C. & McLean, I. 1977, A&A, 57, 141

Brown, J.C., McLean, I.S., & Emslie, A.G. 1978, A&A, 68, 415

Capps, R.W., Coyne, G.V., & Dyck, H.M. 1973, ApJ, 184, 173

Cassinelli, J.P., Nordsieck, K.H., & Murison, M.A. 1987, ApJ, 317, 290

Clarke, D. & McLean, I.S. 1974, MNRAS, 167, 27

Collins, G.W., II 1987, in IAU Coll. 92, Physics of Be Stars, ed. Slettebak, A. & Snow, T.P. (Cambridge: Cambridge University Press), 5

Coyne, G.V. 1975, Specola Vatic. Ric. Astron., 8, 533

Coyne, G. V. & Gehrels, T. 1967, AJ, 72, 887

Coyne, G.V. & Kruszewski, A. 1969, AJ, 74, 1969

de Jong, J.A. 2000, Thesis, University of Amsterdam

Fox, G.K. 1991, ApJ, 379, 663

Fox, G.K. 1994, ApJ, 435, 372

Fox, G.K. & Brown, J.C. 1991, ApJ, 375, 300

Fox, G.K. & Henrichs, H.F. 1994, MNRAS, 266, 945

Frost, S.A. & Conti, P.S. 1978, in IAU Coll. 70, Be and Shell Stars, ed. Slettebak, A. (Dordrecht: Reidel), 139

Gehrels, T. 1974, ed., Planets, Stars and Nebulae Studied With Photopolarimetry (Tucson: Arizona University Press)

Gehrz, R.D., Hackwell, J.A., & Jones, T.W. 1974, ApJ, 191, 675

Guo, Y. 1994, IBVS 4112

Hall, J.S. 1949, Science, 109, 166

Hayes, D.P. & Guinan, E.F. 1984, ApJ, 279, 721

Hillier, D.J. 1994, A&A, 289, 492

Hiltner, W.A. 1949, Science, 109, 165

Huang, L., Hsu, J.C., & Guo, Z.H. 1989, A&AS, 78, 431

Jaschek, M., & Groth, H. 1982, ed., IAU Symp. 98, Be Stars (Dordrecht: Reidel)

Jaschek, C. & Jaschek, M. 1983, A&A, 117, 357

Kaper, L. 1993, Thesis, University of Amsterdam

Leroy, J. 2000, Polarization of Light and Astronomical Observation (London: Gordon and Breach)

McLean, I.S. 1979, MNRAS, 186, 265

McLean, I.S. & Brown, J.C. 1978, 69, 291

McLean, I.S., Coyne, G.V., Frecker, J.E., & Serkowski, K. 1979, ApJ, 228, 802

Nordsieck, K.H., Babler, B., Bjorkman, K.S., Meade, M.B., Schulte-Ladbeck, B.F., & Taylor, M.J. 1992, in Nonisotropic and Variable Outflows from Stars, ASP Conference Series, Vol. 22, ed. Drissen, L., Leitherer, C., & Nota, A. (San Francisco: ASP), 114

Peters, G.J. 1986, ApJ, 301, 61

Poeckert, R., Bastien, P., & Landstreet, J.D. 1979, AJ, 84, 812

Poeckert, R. & Marlborough, J.M. 1977, ApJ, 218, 220

Poeckert, R. & Marlborough, J.M. 1978, ApJ, 220, 940

Quirrenbach, A., Buscher, D.F., Mozurkewich, D., Hummel, C.A., & Armstrong, J.T. 1994, A&A, 283, 13

Rivinius, Th., Baade, D., Stefl, S., Stahl, O., Wolf, B., & Kaufer, A. 1998, A&A, 336, 177

Secchi, A. 1866, Astron. Nachr., 68, 63

Serkowski, K. 1968, ApJ, 154, 115

Serkowski, K. 1974, in Methods of Experimental Physics, Volume 12: Astrophysics (Part A) (New York: Academic Press), 361

Shurcliff, W.A. 1962, Polarized Light: Production and Use (Cambridge: Harvard University Press)

Slettebak, A. 1976, ed., IAU Symp. 70, Be and Shell Stars (Dordrecht: Reidel)

Slettebak, A. 1979, Space. Sci. Rev., 23, 541

Slettebak, A. 1987, in IAU Coll. 92, Physics of Be Stars, ed. Slettebak, A. & Snow, T.P. (Cambridge: Cambridge University Press), 24

Slettebak, A. 1988, PASP, 100, 770

Slettebak, A. & Snow, T.P. 1987, ed., IAU Coll. 92, Physics of Be Stars (Cambridge: Cambridge University Press)

Smith, M.A., Henrichs, H.F., & Fabregat, J. 2000, ed., IAU Coll. 175, The Be Phenomenon in Early-Type Stars (San Francisco: ASP), 384

Sonneborn, G., Grady, C.A., Wu, Chi-Chao, Hayes, D.P., Guinan, E.F., Barker, P.K., & Henrichs, H.F. 1988, ApJ, 325, 784

Struve, O. 1931, ApJ, 73, 94

Tinbergen, J. 1996, Astronomical Polarimetry (Cambridge: Cambridge University Press)

Tubbesing, S., Rivinius, Th., Wolf. B., & Kaufer, A. 2000, in IAU Coll. 175, The Be Phenomenon in Early-Type Stars, ed. Smith, M.A., Henrichs, H.F., & Fabregat, J. (San Francisco: ASP), 232

Underhill, A. & Doazan, V. 1982, Be Stars With and Without Emission Lines (Washington: NASA)

Wood, K., Bjorkman, K.S., & Bjorkman, J.E. 1997, ApJ, 477, 926

Wood, K., Bjorkman, J.E., Whitney, B.A., & Code, A.D. 1996, ApJ, 461, 828

Wood, K., Bjorkman, J.E., Whitney, B.A., & Code, A.D. 1996, ApJ, 461, 847

Appendix A

AnyPol: A Generic Linear Polarimeter

ABSTRACT

AnyPol is a high quality broadband optical linear polarimeter for astronomy, assembled from components that have become commercially available as a result of recent advancements in technology. Its design and construction are described in detail, and observations of standard stars are presented to verify its proper operation. It is currently being used on the 0.4 m telescope at Limber Observatory to monitor the variable polarization of bright Be stars.

1. Motivation

AnyPol was built in 1993–94 to study the linear polarization of bright Be stars with the 0.4 m telescope at Limber Observatory, a private observatory in the Texas Hill Country near San Antonio. The purpose was to relocate and continue the ongoing project of annual polarization monitoring of Be stars begun in 1985 (McDavid 1999) using the Breger polarimeter (Breger 1979) on the 0.9 m telescope at the University of Texas McDonald Observatory. The change was necessary because of the decommissioning of the McDonald telescope, and it was made possible by the rapidly growing commercial availability of research grade scientific instrumentation.

A comprehensive review on Be stars has been given by Slettebak (1988). Their intrinsic polarization comes from Thomson scattering of the starlight by free electrons in a rotationally flattened circumstellar envelope, with a wavelength dependence due to absorption by neutral hydrogen. The envelope is also the source of the erratically variable emission lines which are the distinguishing characteristic of the Be stars. By studying the polarization we can hope to learn more about the geometry and the physical conditions of the envelope, and variability of the polarization may give clues to the basic processes which lead to envelope formation and dissipation.

2. Design and Construction by Subsystem

The Limber Observatory polarimeter is called AnyPol because of its common generic simplicity. It is basically a miniaturized and technologically upgraded copy of the Breger polarimeter mentioned earlier.

The polarimeter system consists of a main head unit which is mounted on the telescope tailpiece, an electronics interface unit, two power supplies, and a control computer. The Physical/Mechanical, Optical, Electronic, and Control/Data Acquisition subsystems are described in detail in the following subsections.

2.1. Physical/Mechanical

The polarimeter head is constructed of 0.25 in aluminum plates which interlock by a tongue-and-groove system to make a light-tight box. The top plate is 0.375 in thick and is drilled for 0.375 in bolts to serve as a flange for mounting on the telescope tailpiece. The compactness of the polarimeter head unit was achieved by offsetting the optical axis by 2.125 in from the center toward the front plate (Figure 1). See Figure 2 for an exploded diagram of the head.

The head (Figure 3) contains two removable modules: the polarization analyzer assembly (Figure 4) and the filter wheel assembly (Figure 5). The analyzer assembly consists of a cylindrical cell for the optical components, mounted in ball bearings and rotated by a stepper motor through a belt drive. The filter wheel assembly uses an identical stepper motor and a similar belt drive to rotate a custom-made filter wheel with 8 positions on a circle, mounted in ball bearings with a 0.25 in shaft. Both drive motors are double-shafted to carry encoders and are mounted in slots to allow for tensioning of the belts.

There is an aperture slide before the analyzer and a dark slide after the filter wheel, both operated from the front plate by knobs controlling rack-and-pinion mechanisms with detent grooves engaged by adjustable ball plungers. A 1.25 in helical focuser for the viewer eyepiece is also mounted on the front plate.

Light passes through a Fabry lens into an enclosed lower chamber of the head which contains the uncooled end window photomultiplier tube and associated wiring, with a cap over the protruding part of the tube. A signal conditioning unit is mounted on the side of the head with aluminum brackets.

The electronics interface is a separate box constructed of 0.125 in aluminum plates with a 0.25 in base plate. It contains an AC power bus, the power supplies and microstepping drivers for the stepper motors, and a push-pull pair of cooling fans.

The high voltage power supply for the photomultiplier tube and the power supply for the signal conditioning electronics are both standalone units. A dedicated PC is used for the interactive control, data acquisition, data processing, and display functions.

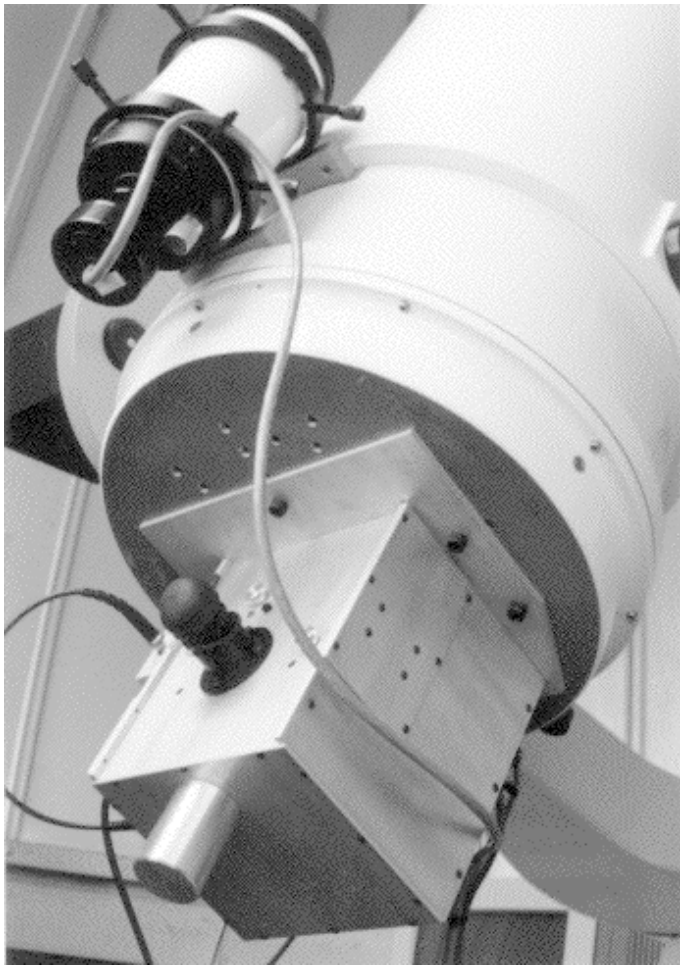

Fig. 1.— AnyPol attached to the 0.4 m telescope at Limber Observatory.

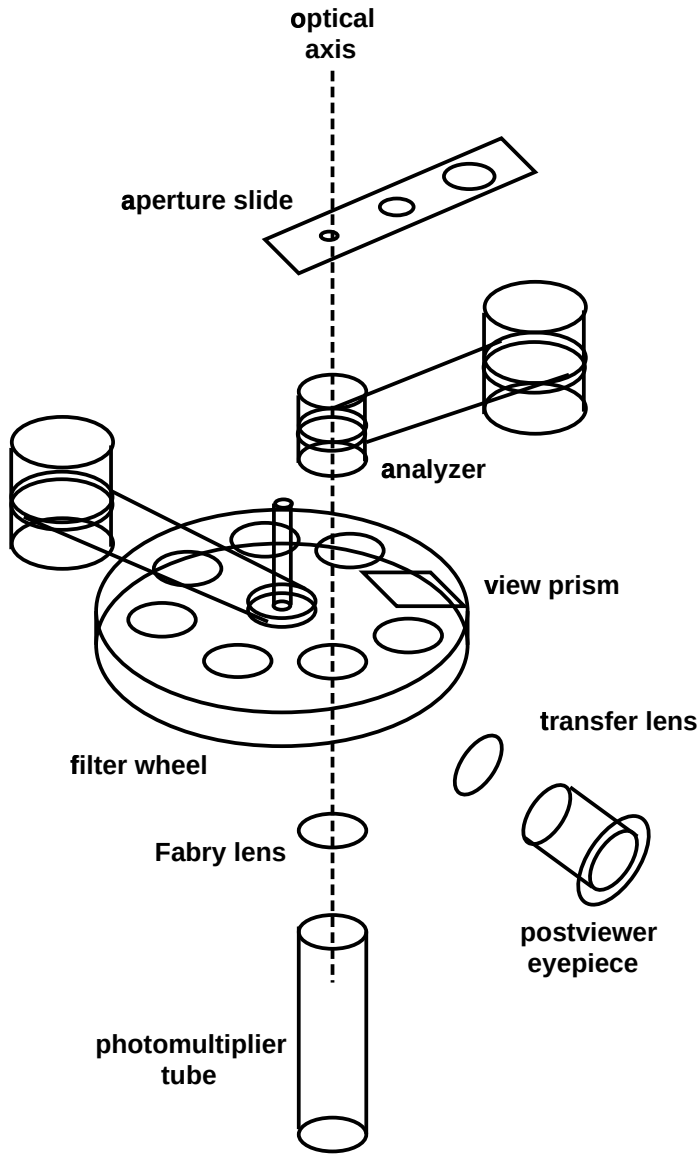

Fig. 2.— Exploded diagram of the polarimeter head.

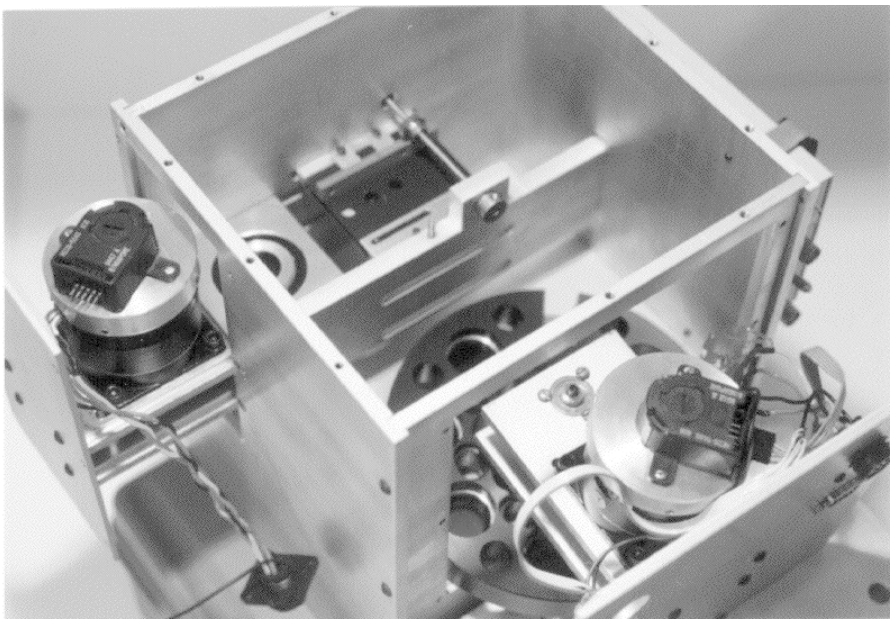

Fig. 3.— Inside the polarimeter head.

2.2. Optical

The polarimeter was designed to be mounted on the 0.4 m telescope at Limber Observatory, which has f/12 classical Cassegrain optics. The entrance hole to the instrument is 2.0 in in diameter, and the aperture slide is located at the optimal focal plane, 3.25 in behind the external surface of the tailpiece. It has three available apertures with angular diameters of $4'$ (for finding), $1'$ (for centering), and $30''$ (for measurement). The material used for the slide is black acrylite, to block both infrared and ultraviolet light and to avoid spurious polarization from metallic edges. The apertures are backlit by a pair of red LEDs.

The analyzer is a Glan-Taylor prism, rotated continuously at 10 Hz to modulate the intensity of the incoming light according to the degree of polarization. Following it in the same cylindrical mounting cell is a Lyot depolarizer, to eliminate any polarization dependent response of the rest of the optical system.

The filter wheel carries a set of *UBVRI* filters which closely match the Johnson-Cousins system when used with a photomultiplier with the standard S-20 response curve. This color system was chosen to match by prescription the color system which had been previously used for monitoring Be stars with the Breger polarimeter at McDonald Observatory. The filter materials and bandpasses of the system are shown in Table 1. One of the 8 positions in the filter wheel holds a right angle prism through which the apertures may be seen for finding and centering with the postviewer eyepiece via a transfer lens.

Fig. 4.— The polarization analyzer assembly.

An image of the telescope objective is focused as a spot of 2 mm diameter on the cathode of the photomultiplier by a fused silica plano-convex Fabry lens. Due to the beam deviation of the spinning Glan-Taylor prism, this spot moves in a small circle of diameter ~ 0.02 mm on the nonuniform surface of the photocathode, causing a sinusoidal intensity modulation of less than 1% at the rotation frequency of the analyzer. This effect, known as "tilt" since it could be caused by a deviation from normal incidence of the light on the photocathode, is easily separable from the actual modulation due to polarization, which has double the frequency.

2.3. Electronic

The analyzer and the filter wheel are driven by identical size 23 double shafted stepper motors with 4 windings rated at 2.6 A DC, wired in a bipolar parallel configuration as 2 pairs of parallel windings to generate the least possible heat. They have 200 steps per revolution and are operated by optically isolated bipolar choppers at 10 microsteps per step, with 28 V DC, 4 A power supplies. Each motor carries an incremental optical shaft encoder with a resolution of 500 parts and one index pulse per revolution. The chopper opto-isolators and the encoders are powered by 5 V DC from an exernal power

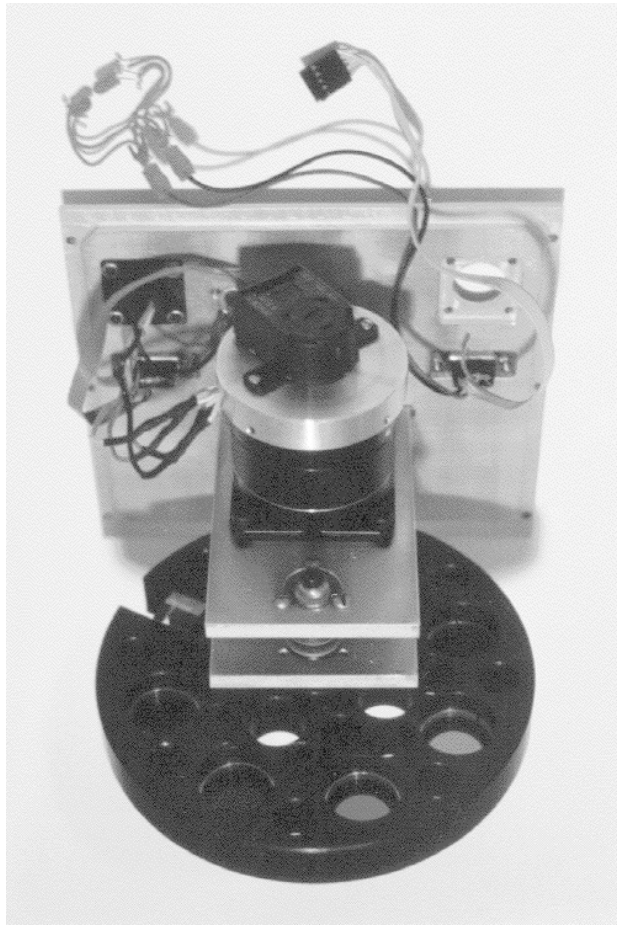

Fig. 5.— The filter wheel assembly.

supply.

The photomultiplier tube is an end-window type with an S-20 photocathode (extended red spectral response). It is operated in a grounded anode configuration with -1000 V DC applied to the cathode from an external high voltage power supply. The output of the tube is converted to a stream of 10 ns TTL pulses by a signal conditioning unit which includes a pulse amplifier, discriminator, and pulse shaper.

2.4. Control/Data Acquisition

The polarimeter is controlled by a C program running on a 66 MHz 486 DOS PC with a stepper motor interface card and a multichannel scaler card. A virtual control panel constructed with a graphical widget set allows point-and-click selection of operating parameters and functions, including analyzer rotation start/stop, filter setting, integration

time, target identification, star or background sky mode, count rate, ratio of the current count rate to that at the beginning of the integration, output data file, and abort (Figure 6). There are also two macro buttons that start preprogrammed observing sequences of either one set of *UBVRI* filter measurements or 3 repeated measurements in a single filter.

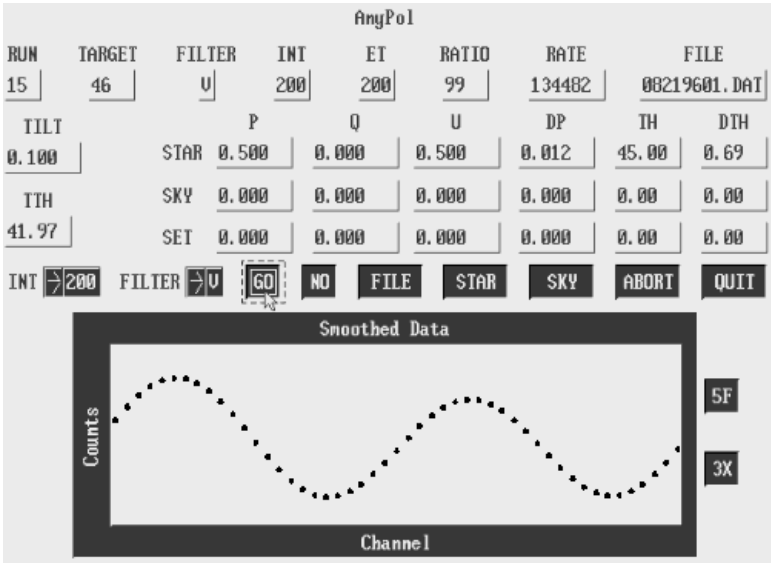

Fig. 6.— The AnyPol computer control panel.

The specified integration time is divided into the appropriate number of 10 s counting loops, with the analyzer spinning at 10 Hz. For each 10 s loop, the multichannel scaler accumulates signal pulses for 100 revolutions of the analyzer in 50 channels per revolution as triggered by the encoder index pulse. After each 10 s loop the total pulse count per channel is updated and a graph of the cumulative data buffer $cnt(i)$ is displayed. After removal of the tilt by subtracting a least squares fit to a sine wave,

Table 1. Filter System Parameters

Filter	Schott Glass Components	Effective Wavelength (Å)	Bandpass (fwhm) (Å)
U	UG2(2mm) + BG18(2mm)	3650	700
B	BG12(2mm) + GG385(2mm)	4400	1000
V	GG495(2mm) + BG18(2mm)	5500	900
R	OG570(2mm) + KG3(2mm)	6400	1500
I	RGN9(3mm)	7900	1500

a least squares fit to a double sine wave is made to determine the normalized Stokes parameters q and u, the degree of polarization p, and the polarization position angle θ, according to

$$q = \frac{2}{25}\sum_{i=0}^{24}[(c(i)/m - 1)\cos\beta(i)], \tag{A1}$$

$$u = \frac{2}{25}\sum_{i=0}^{24}[(c(i)/m - 1)\sin\beta(i)], \tag{A2}$$

$$p = \sqrt{q^2 + u^2}, \tag{A3}$$

and

$$\theta = \frac{1}{2}\arctan\frac{u}{q}, \tag{A4}$$

where

$$c(i) = cnt(i) + cnt(i + 25), \tag{A5}$$

$$m = \frac{1}{25}\sum_{i=0}^{24} c(i), \tag{A6}$$

and

$$\beta(i) = \frac{2\pi i}{25}. \tag{A7}$$

The instrumental error in q, u, and p is estimated by the variance of the double sine wave fit:

$$dp^2 = \frac{2}{250}\sum_{i=0}^{24}[(c(i)/m - 1)^2 - q^2 - u^2]. \tag{A8}$$

The error in θ (in degrees) is then estimated as

$$d\theta = 28.65\frac{dp}{p}. \tag{A9}$$

After these calculations are completed, the control panel display is updated with the latest cumulative results and another 10 s loop is started. This process repeats until

the end of the integration time. A record of the data is then written to a disk file for further reduction off line.

3. Performance

On the 0.4 m telescope at Limber Observatory the photon count rates are comparable to those obtained with the 0.9 m telescope at McDonald Observatory with a neutral density filter of 10% transmission which was necessary for the bright stars ($V = 2$–5) in the Be star monitoring program. Observational error estimates are derived from the repeatability of multiple independent measurements, and they are in general agreement with checks based on the residuals in the fit to the modulated signal and the uncertainty derived from photon counting statistics. Typical errors are on the order of 0.05% in the degree of polarization and 2° in position angle. One of the main sources of error is a slight variation in the speed of the motor driving the analyzer, which becomes significant at the level of a few hundredths of a percent in the degree of polarization. All observations are corrected for an instrumental polarization on the order of 0.10%, tracked by repeated observations of unpolarized standard stars from the list of Serkowski (1974). The position angle is calibrated by observing polarized standard stars from the list of Hsu & Breger(1982).

One individual measurement consists of 3 cycles through all 5 filters with a 200 s integration time on each filter. If there is a bright Moon, a sky cycle is taken to correct for the background polarization. The result for each single filter is taken to be the mean and standard deviation of the 3 integrations in that filter. (The standard deviation is a more conservative error estimate than the standard deviation of the mean, but it may be more realistic because 3 measurements is a very small sample.)

It is interesting to compare the Limber Observatory system with the system used previously at McDonald Observatory. For this purpose Table 13 of McDavid (1994) is reproduced here as Table 2, and Table 15 of McDavid (1999) is reproduced here as Table 3. In both tables, q/dq, u/du, p/dp, and $\theta/d\theta$ are the mean and standard deviation over four annual observing runs. Quantities in angled brackets are similar four-year means, including dpi and $d\theta i$, which are estimates of the internal precision of a single measurement. The grand averages, denoted by GAV, are averages of these data over all 5 filters.

These observations of polarized standard stars show very clearly that the two systems match extremely well. The only outstanding difference is the typical precision of a single observation, which is higher in the McDonald system. This is readily understood since the McDonald estimates were based on theoretical photon counting statistics, while the Limber estimates are based on experimental scatter in repeated measurements. With a larger value for the error in a single observation, the Limber system is sometimes a less sensitive detector of variability, but it may also give more realistic results.

Table 2. Polarized Standard Star Summary (Limber)

Star Filter	q/dq (%)	<dq> (%)	u/du (%)	<du> (%)	p/dp (%)	<dp> (%)	$\theta/d\theta$ (°)	<$d\theta$> (°)	<dpi> (%)	<$d\theta i$> (°)
2H Cam										
U	-1.83/0.09	0.04	-2.41/0.06	0.04	3.03/0.07	0.03	116.5/ 0.8	0.5	0.09	1.1
B	-1.95/0.08	0.07	-2.65/0.06	0.05	3.29/0.02	0.06	116.8/ 0.9	0.6	0.06	0.6
V	-2.05/0.02	0.06	-2.75/0.04	0.06	3.43/0.02	0.06	116.7/ 0.4	0.6	0.06	0.6
R	-1.98/0.02	0.05	-2.66/0.04	0.06	3.32/0.02	0.05	116.7/ 0.3	0.6	0.05	0.5
I	-1.79/0.03	0.07	-2.37/0.09	0.06	2.96/0.06	0.08	116.4/ 0.6	0.7	0.09	0.8
GAV	0.05	0.06	0.06	0.06	0.04	0.06	0.6	0.6	0.07	0.7
o Sco										
U	1.06/0.14	0.18	2.35/0.05	0.23	2.59/0.10	0.25	33.0/ 1.3	1.7	0.19	2.7
B	1.41/0.11	0.07	3.09/0.06	0.06	3.40/0.04	0.08	32.8/ 1.0	0.5	0.08	0.8
V	1.73/0.16	0.08	3.76/0.05	0.08	4.15/0.05	0.08	32.7/ 1.1	0.5	0.10	0.8
R	1.83/0.16	0.07	4.00/0.06	0.07	4.40/0.04	0.08	32.8/ 1.1	0.4	0.09	0.6
I	1.74/0.15	0.07	3.93/0.10	0.05	4.30/0.05	0.05	33.1/ 1.2	0.5	0.14	1.0
GAV	0.14	0.10	0.06	0.10	0.06	0.11	1.1	0.7	0.12	1.2

Table 3. Polarized Standard Star Summary (McDonald)

Star Filter	q/dq (%)	<dq> (%)	u/du (%)	<du> (%)	p/dp (%)	<dp> (%)	$\theta/d\theta$ (°)	<$d\theta$> (°)	<dpi> (%)	<$d\theta i$> (°)
2H Cam										
U	-1.83/0.05	0.11	-2.41/0.03	0.07	3.03/0.01	0.08	116.5/ 0.6	1.1	0.09	0.8
B	-1.97/0.05	0.07	-2.60/0.09	0.07	3.26/0.07	0.05	116.3/ 0.6	0.7	0.04	0.4
V	-2.07/0.06	0.07	-2.73/0.01	0.07	3.43/0.03	0.07	116.4/ 0.5	0.5	0.04	0.4
R	-1.97/0.07	0.05	-2.66/0.05	0.06	3.31/0.04	0.05	116.8/ 0.7	0.4	0.03	0.3
I	-1.75/0.06	0.09	-2.36/0.05	0.06	2.94/0.05	0.08	116.8/ 0.7	0.8	0.05	0.6
GAV	0.06	0.08	0.05	0.07	0.04	0.07	0.6	0.7	0.05	0.5
o Sco										
U	1.35/0.21	0.20	2.51/0.12	0.25	2.85/0.12	0.28	30.9/ 2.0	1.6	0.20	2.1
B	1.40/0.12	0.09	3.07/0.14	0.08	3.39/0.10	0.07	32.7/ 1.3	0.9	0.06	0.5
V	1.81/0.25	0.12	3.74/0.12	0.08	4.16/0.01	0.10	32.1/ 1.9	0.7	0.05	0.3
R	1.91/0.23	0.07	3.96/0.10	0.08	4.41/0.03	0.05	32.1/ 1.6	0.6	0.04	0.2
I	1.76/0.19	0.07	3.88/0.06	0.06	4.26/0.06	0.07	32.8/ 1.3	0.4	0.05	0.3
GAV	0.20	0.11	0.11	0.11	0.06	0.11	1.6	0.9	0.08	0.7

I wish to thank Michel Breger and Santiago Tapia for introducing me to the art of stellar polarimetry and Paul Krueger for his valuable design advice and excellent machine work.

REFERENCES

Breger, M. 1979, ApJ, 233, 97

Hsu, J.C. & Breger, M. 1982, ApJ, 262, 732

McDavid, D. 1994, PASP, 106, 949

McDavid, D. 1999, PASP, 111, 494

Serkowski, K. 1974, in IAU Coll. 23, Planets, Stars, and Nebulae Studied with Photopolarimetry, ed. Gehrels, T. (Tucson: University of Arizona), 135

Slettebak, A. 1988, PASP, 100, 770

Appendix B

Publications in Refereed Journals

Clarke, D., McDavid, D., Henrichs, H.F., & Smith, R.A. 2001, "On the polarimetric variability of bright O-type stars", Astronomy & Astrophysics, submitted

McDavid, D. 2001, "A Useful Approximation for Computing the Continuum Polarization of Be Stars", Astrophysical Journal, in press

Floquet, M., Hubert, A.M., Hirata, R., McDavid, D., Zorec, J., Gies, D., Hahula, M., Janot-Pacheco, E., Kambe, E., Leister, N.V., Stefl, S., Tarasov, A., & Neiner, C. 2000, "Stellar and circumstellar activity in the Be star EW Lacertae from the 1993 multi-site campaign", Astronomy & Astrophysics, 362, 1020

McDavid, D. 2000, "A Search for Intrinsic Polarization in O Stars with Variable Winds", Astronomical Journal, 119, 352

McDavid, D. 1999, "Multicolor Polarimetry of Selected Be Stars: 1995-1998", Publications of the Astronomical Society of the Pacific, 111, 494

Kaper, L., Henrichs, H.F., Fullerton, A.W., Ando, H., Bjorkman, K.S., Gies, D.R., Hirata, R., Kambe, E., McDavid, D., and Nichols, J.S. 1997, "Coordinated ultraviolet and H-alpha spectroscopy of bright O-type stars", Astronomy & Astrophysics, 327, 281

Bozic, H., Harmanec, P., Horn, J., Koubsky, P., Scholz, G., McDavid, D., Hubert, A.-M., & Hubert, H. 1995, "Toward a Consistent Model of the B0.5IVe + sdO Binary Phi Persei", Astronomy & Astrophysics, 304, 235

McDavid, D. 1994, "Multicolor Polarimetry of Selected Be Stars: 1990-93", Publications of the Astronomical Society of the Pacific, 106, 949

Gies, D.R., Willis, C.Y., Penny, L.R., & McDavid, D. 1993, "The He I 6678 Emission Line of Phi Persei: New Evidence of the Companion Star", Publications of the Astronomical Society of the Pacific, 105, 281

Howarth, I.D., Bolton, C.T., Crowe, R.A., Ebbets, D.C., Fieldus, M.S., Fullerton, A.W., Gies, D.R., McDavid, D., Prinja, R.K., Reid, A.H.N., Shore, S.N., and Smith, K.C. 1993, "Time-Series Observations of O Stars. III. IUE and HST Spectroscopy of Zeta Ophiuchi and Implications for the Photospheric Connection", Astrophysical Journal, 417, 338

Reid, A.H.N., Bolton, C.T., Crowe, R.A., Fieldus, M.S., Fullerton, A.W., Gies, D.R., Howarth, I.D., McDavid, D., Prinja, R.K., and Smith, K.C. 1993, "Time-Series Observations of O Stars. II. Optical Observations of Zeta Ophiuchi", Astrophysical Journal, 417, 320

Prinja, R.K., Balona, L.A., Bolton, C.T., Crowe, R.A., Fieldus, M.S., Fullerton, A.W., Gies, D.R., Howarth, I.D., McDavid, D., and Reid, A.H.N. 1992, "Time Series Observations of O Stars. I. IUE Observations of Variability in the Stellar Wind of Zeta Puppis", Astrophysical Journal, 390, 266

McDavid, D. 1990, "Multicolor Polarimetry of Selected Be Stars: 1986-89", Publications of the Astronomical Society of the Pacific, 102, 773

McDavid, D. 1986, "Multicolor Polarimetry of Selected Be Stars: A Long-Term Analysis", Publications of the Astronomical Society of the Pacific, 98, 572

McDavid, D. 1984, "The Role of the Galactic Magnetic Field in the Evolution of a Dark Globular Filament in Cygnus", Astrophysical Journal, 284, 141

D. Nelson Limber Memorial Observatory was built in the summer of 1979 in the Texas Hill Country near San Antonio as a private observatory and residence. It is named in memory of a distinguished faculty member of the University of Virginia Department of Astronomy.